

Remarks

Claims 1-9 and 21-38 are under examination, claims 10-20 and 39-47 having been withdrawn from consideration.

Applicants had provisionally elected Group V (claims 21-32), with traverse. In the current office action, Examiner has decided to rejoin Group I, comprising claims 1-9 and 33-38 drawn to pharmaceutical compositions comprising compounds of structure I, with elected Group V.

Claim 29 has been amended herein by adding a comma between the terms “hydroxy” and -OCOR₄. This amendment merely corrects a typographical error which was kindly pointed out by the Examiner at page 3 of the Office Action.

Claims 48-50 are new. Claim 48 depends from the method of independent claim 21, which encompasses a method for treating a disease or condition. Claim 48 recites “wherein the disease is a neoplastic disease”. Support for claim 48 is found throughout the specification as filed and in the claims as filed. See in particular, page 7, lines 13-33, Examples 4 and 5, page 40, line 25 to page 41, line 15, Fig. 4, Fig. 7, and Fig. 8. Furthermore, the Examiner admits at page 3 of the office action that the specification is enabling for the treatment of tumors or cancers. As described below, the data provided in the specification disclose that the compounds of the invention are effective on breast cancer, prostate cancer, and sarcomas. Additionally, at page 7, lines 12 to 33, the specification provides support for many different kinds of tumors and cancer. New Claims 49 and 50 depend from new claim 48, and recite the cancers listed on page 7, lines 23-33, and which are disclosed in the Examples.

Response to Specification Objection

Examiner objects to the disclosure, asserting that Applicants filed a WIPO document instead of an abstract. Applicants are unsure what the Examiner is referring to, because this application was filed under 35 U.S.C. 371 and no WIPO document was filed by Applicant when this application entered national stage in the U.S. Applicants assert that the abstract was a part of the PCT application from which this application claims priority and from which it was nationalized in the U.S.

Response to “Priority: Statement by Examiner

At page 3 of the Office Action, Applicants note that the Examiner has incorrectly stated the priority claim to which the application is entitled, in that the Examiner only references the two provisional applications which this application claims priority to, and does not recite the PCT application from which this application entered national stage in the U.S. That is, the Examiner failed to note the priority claim as recited in the Preliminary Amendment filed December 29, 2004 in which the specification was amended to state that the application claims priority to the PCT application from which it entered national stage in the U.S. The amendment states, and Applicants assert that:

This application is a national stage filing of International Application No. PCT/US03/18734, filed on June 12, 2003, which claims benefit under 35 U.S.C. §119(e) to US Provisional Application Serial Nos. 60/388,006, filed June 12, 2002, and 60/449,553, filed February 24, 2003, the entire disclosures of which are incorporated herein by reference.

Applicants request that the Examiner acknowledge the priority claim as recited in the Preliminary Amendment filed December 29, 2004.

Response to Claim Objection

At page 3 of the Office Action, Examiner points out that in claim 29 a comma should be inserted between the terms “hydroxyl” and “-OCOR₄”. Applicants have amended claim 29 by inserting a comma between the terms “hydroxyl” and “-OCOR₄”.

Response to Claim Rejections under 35 U.S.C. § 112, first paragraph, enablement

Claims 21-24 stand rejected as allegedly lacking enablement under 35 U.S.C. § 112, first paragraph. Applicants traverse the rejection of claims 21-24.

The Examiner admits that the specification is enabling for the treatment of some particular and specific neoplastic tumors or cancers. However, the Examiner asserts that the

specification does not reasonably provide enablement for the treatment of any other disease or conditions characterized by inappropriate activity.

The Examiner then cites a series of Wands factors. At page 4, the Examiner asserts that claim 21 is drawn to a method of treatment of a disease or a condition characterized by inappropriate Rsk activity comprising the step of administering to a human or a mammal in need thereof a composition comprising a compound represented by general structure III. The Examiner then asserts that the breadth of the claim is seen to include some diseases, including ones not yet discovered.

The Examiner asserts that the prior art (citing Bjorbaek et al., WO 0066721) discloses treatment of weight gain, obesity, reducing fat, leptin levels and increasing oxygen consumption by regulating the activity of Rsk.

The Examiner asserts that there is a level of unpredictability and that there is not sufficient data to substantiate that any disease or condition characterized by inappropriate Rsk activity can be treated by administration of the claimed compound, asserting that there is unpredictability in the pharmaceutical art, citing *In re Fisher*, 427 F.2d 833, 166 USPQ 18 (CCPA 1970). It is also the view of the Examiner that one of ordinary skill in the art cannot fully describe the genus based on a few species. Applicants do not know whether the Examiner is referring to compounds or diseases, but will address both below.

The Examiner then lists Wands factors and asserts that one of ordinary skill in the art would have to engage in undue experimentation regarding the embodiments of any known and unknown compounds having those functions encompassed in the instant claims and to test all compounds encompassed by the instant claims.

The Examiner also asserts that there is not enough guidance in the specification to enable the treatment of any disease characterized by inappropriate Rsk activity and further asserts that there is not an enabling disclosure for treatment as claimed. Lastly, the Examiner asserts that one of ordinary skill in the art would have to engage in undue experimentation “to test all compounds encompassed by the instant claims and their combinations employed in the claimed compositions to be administered to a host, with no assurance of success”.

It is well-settled that applicant need not have actually reduced the invention to practice prior to filing in order to satisfy the enablement requirement under 35 U.S.C. §112, first

paragraph. MPEP §2164.02 (citing *Gould v. Quigg*, 822 F.2d 1074 (Fed. Cir. 1987)). Indeed, the invention need not contain a single example if the invention is otherwise disclosed in such manner that one skilled in the art will be able to practice it without an undue amount of experimentation (*In re Borkowski*, 422 F.2d at 908), and “representative samples are not required by the statute and are not an end in themselves” (*In re Robins*, 429 F.2d 452, 456-57, 166 USPQ 552, 555 (CCPA 1970)). Thus, 35 U.S.C. § 112, first paragraph, enablement does not require any working examples.

The test of enablement is not whether any experimentation is necessary, but whether, if experimentation is necessary, it is undue. MPEP §2164.01 (citing *In re Angstadt*, 537 F.2d 498, 504 (C.C.P.A. 1976)). The fact that experimentation may be complex does not necessarily make it undue if the art typically engages in such experimentation. *Id.* Further, the specification need not disclose what is well-known to those skilled in the art and preferably omits that which is well-known to those skilled and already available to the public. MPEP §2164.05(a) (citing *In re Buchner*, 929 F.2d 660, 661 (Fed. Cir. 1991)). Therefore, under current law, enablement does not require a working example and experimentation is allowed so long as it is not undue.

Under the present patent law, claims 21-24, are enabled under 35 U.S.C. §112, first paragraph. The specification as filed amply supports these claims because the skilled artisan, armed with the methods disclosed in the specification, the compounds described therein, the methods of making the compounds, the assays as disclosed or known in the art, the diseases and conditions as disclosed or known in the art, would have been able to isolate and characterize, through routine experimentation, other compounds having the disclosed biological and biochemical activities as recited by the claims, and to practice the invention commensurate with the scope of the claims without undue experimentation.

Applicants respectfully point out that the phrase “inappropriate Rsk activity” is in the preamble of claim 21, which preamble is further limited by the element “administering to a human or other mammal in need thereof” and by the element “an amount effective for specifically inhibiting Rsk activity”. One of ordinary skill in the art would understand that the phrase “administering to a human or other mammal in need thereof” specifically limits the claim to those humans and other mammals in which such diseases or conditions can be treated as claimed, not just any disease or condition. One of ordinary skill in the art would also appreciate

that the element “an amount effective for specifically inhibiting Rsk activity” further limits and defines the claim.

At page 8, line 30, to page 9, line 2, of the specification, “Rsk specific inhibitor” is described as including “any compound or condition that inhibits Rsk kinase activity . . without substantially impacting the activity of other kinases. Such inhibitory effects may result from directly or indirectly interfering with the protein’s ability to phosphorylate its substrate, or may result from inhibiting the expression (transcription and/or translation) of Rsk.”

The description of “inappropriate Rsk activity” at page 28 of the specification referred to by the Examiner (see below) states “The inappropriate Rsk activity may constitute overexpression of Rsk protein, excessive Rsk kinase activity or it may represent the expression of Rsk activity in tissues that normally do not express Rsk activity.” (see page 28, lines 5-9). Applicants point out that the paragraph begins with an introduce sentence which states that one embodiment of the present invention provides “a method for inhibiting Rsk kinase activity . . as a means of treating an illness associated with inappropriate Rsk activity” (emphasis added). That introductory sentence is then followed by a description of inappropriate activity. Thus, the inappropriate activity refers to overexpression of Rsk (meaning greater than normal expression), excessive kinase activity of Rsk (which means that the activity of the Rsk is greater than normal, but one of ordinary skill in the art would understand that it could mean both an increase in the activity level of Rsk without an increase in the actual amount of Rsk, or that the increased activity could be due to more Rsk protein itself), or that there is expression of Rsk activity where there is normally no such activity.

At the time this application was filed, it was known in the art that several disease states were suggested to involve such inappropriate Rsk activity or elevated activity of the immediate upstream RSK activator, p42/p44 MAPK resulting in inappropriate RSK activity. A series of journal articles is submitted herewith which describes these activities in various diseased states. The articles are summarized in the following table:

Alzheimer's Disease	Journal of Neuroscience, 2001, 21:4125-33 Mechanisms of Aging and Development, 2001, 123:39-46
Atherosclerosis	Arteriosclerosis, Thrombosis, and Vascular Biology, 2000, 20:18-26
Asthma	British Journal of Pharmacology, 2002, 135:1915-26
Cardiomyopathy	Cardiovascular Research, 2002, 53:131-37
Drug Addiction	Journal of neuroscience, 2000 20:8701-09
Inflammation-induced pain	Journal of neuroscience, 2002 22:478-85
Lead poisoning	Journal of Pharmacology and Experimental Therapeutics, 2002, 300:818-23
Nephritis	Journal of American Society of Nephrology, 2002, 13:1473-80
Parkinson's Disease	Journal of Neurochemistry, 2001, 77:1058-66 Brain Research, 2002, 935:32-39
<i>Helicobacter pylori</i> -induced Ulcers	Biochemical and Biophysical Research Communications 2002, 294:220-24
Viral-induced myocarditis and Borna disease	Journal of Clinical Investigation, 2002, 109:1561-69 Journal of Virology, 2001, 75:4871-77

Prior to the current application, it was reported that enhanced p42/p44 MAPK was sufficient to drive proliferation of cancer cells. The present application demonstrated that the physiological response to elevated p42/p44 MAPK activity is the activation of RSK (see Examples). The present application further demonstrated that pharmacological inhibition of RSK activity stops the growth of the cancer cells even in the presence of elevated p42/p44 MAPK activity. Thus, the present application demonstrated that RSK activity was essential for the neoplastic diseased state. Because the current invention demonstrates that inhibition of RSK is sufficient to reverse a diseased state previously attributed to p42/p44 MAPK activity, one of ordinary skill in the art would understand that, as in the case for cancer, the role of p42/p44 MAPK in the above-mentioned diseases is to drive increase RSK activity or levels. The MAPK pathway was known, *inter alia*, to be involved in growth, differentiation, inflammation, and apoptosis (see page 1, lines 13 and 14). Therefore, pharmacological inhibition of RSK would relieve the symptoms or reverse the diseased state. Various diseases and conditions were also specifically referred to in the application as filed. See, for example, "tumors as well as neurological disease states such as epilepsy" (page 1, lines 18-19). The data also demonstrated various kinds of cancer cells such as viral-oncogene transformed fibroblasts (sarcomas), breast cancer cells, and prostate cancer cells, relative to their normal counterparts (see Examples 4 and 5: pages 35-41). The present specification included a method for inhibiting RSK kinase activity as a means of treating illness (such as cancer, neurological diseases and viral infection; see page

7, lines 3-33; page 13, lines 23-25) associated with inappropriate activity (page 16, lines 11-13). However, the examiner has concluded that the term “inappropriate” is too broad and does not make clear what is intended by inappropriate activity.

Additionally, the present specification discloses that a variety of types of molecules can inhibit or reduce Rsk activity, Rsk levels, or cancer cell proliferation, including compounds such as SL0101-1, SL0101-2, SL0101-3 (see figures) and siRNA (see page 36, lines 29-33). The invention further provides for other inhibitors, such as compounds comprising the general structures of the compounds of Formulas I and III, short hairpin RNA (page 19, lines 9-18), and antibodies directed against Rsk (see page 22).

Further, one of skill in the art would also be able to treat a disease or condition by administering an Rsk inhibitor of the invention following the teachings set forth in the specification as filed and/or as known in the art based upon the disclosure provided in the specification without undue experimentation. That is, the crucial teachings of the invention, *inter alia*, discovery of a compound which inhibits Rsk and the role of increased Rsk activity in disease, and the methods for making such compounds and treating disease, are amply disclosed in the specification as filed (see, e.g., Examples, and Figures). Therefore, the application merely omits that which is well-known to those skilled in the art and already available to the public, i.e., specific diseases and the methods that a skilled artisan would use to treat such a disease. Moreover, such compounds are routinely screened in the art and administered and the practice of such methods is routine in the art and should not be considered an undue burden.

There is no requirement under the current law of enablement that each embodiment be reduced to practice. *Amgen Inc. v. Chugai Pharm. Co.*, 18 USPQ2d 1016, 1027 (Fed. Cir. 1991). *Amgen v. Chugai* made clear that that enablement does not require working examples for each species encompassed by a claim under 35 U.S.C. §112, first paragraph. *Accord In re Robbins*, 166 USPQ 552 (CCPA 1970).

Regarding Examiner’s comment as to Bjorbaek and the state of the art, the Bjorbaek application speculates that inhibiting **normal** Rsk activity may reduce weight gain. The current specification teaches the inhibition of Rsk activity to treat diseases characterized by “inappropriate Rsk activity” or over expression of Rsk activity compared to that observed in the non-diseased tissue or expression of Rsk activity in tissues that normally do not express Rsk

activity in which the disease or the symptoms can be ameliorated by inhibition of Rsk catalytic activity. Additionally, Bjorbaek provides no evidence that inhibition of Rsk activity will alter the rate of weight gain, nor does Bjorbaek disclose “inappropriate Rsk activity”. Bjorbaek merely makes a naked assumption based on the evidence that deletion of the RSK2 gene reduces the weight gain of the genetically altered mouse. Expression of a mutant RSK that has no catalytic activity can effect transcription of some genes. The effect on weight gain may require complete elimination of the RSK2 protein by means other than a RSK-specific inhibitor such as described in the current specification. Additionally, deletion of a gene product often results in compensation for the loss of the gene product. It is possible that the effect of RSK2 deletion on weight gain of the genetically altered mouse results from the compensatory signaling events that occur during the development of the genetically altered fetus. The compensatory signaling events may not develop during pharmacological inhibition of Rsk activity. In this event, inhibition of Rsk activity would have no effect on weight gain. Therefore, there is no basis in Bjorbaek to even assert that inhibition of RSK2 activity alone would be sufficient to alter the rate of weight gain.

Additionally, the present application discloses that Rsk activity is required for proliferation of cancer cells. The present application further provides the first small molecule inhibitor of Rsk activity and shows that the inhibitor functions to halt the growth of the cancer cells, but not normal cells. Thus, the Rsk inhibitor induces the desired physiological response and can therefore be used to treat diseases characterized by over expression of Rsk or over expression of Rsk activity compared to that observed in the non-diseased tissue or expression of Rsk activity in tissues that normally do not express Rsk activity. The teachings embodied in this application were not part of the state of the art at the time of filing.

Regarding the Examiner’s statement that that there is unpredictability in the pharmaceutical art, citing *In re Fisher*, 427 F.2d 833, 166 USPQ 18 (CCPA 1970), Applicants assert that Fisher must be used in context and that it does not stand for pharmaceutical art unpredictability. In fact, according to MPEP 2164.01(b) “As long as the specification discloses at least one method for making and using the claims invention that bears a reasonable correlation to the entire scope of the claim, then the enablement requirement of 35 U.S.C. 112 is satisfied. *In re Fisher*, 427 F.2d 833, 839, 166 USPQ 18, 24 (CCPA 1970)”. MPEP 2164.08 further states

that enablement must only bear a “reasonable correlation” to the scope of the claims, citing *In re Fisher*. Additionally, at MPEP 2164.03, it is stated that “[t]he amount of guidance or direction needed to enable the invention is inversely related to the amount of knowledge in the state of the art as well as the predictability of the art. *In re Fisher*, 427, F.2d 833, 839, 166 USPQ 18, 24 (CCPA 1970). It can be seen that Fisher does not state that the pharmaceutical arts are unpredictable. Furthermore, *In re Fisher* merely contrasted mechanical and electrical elements with chemical reaction and physiological activity and does not go against the other court decisions cited herein and the examples described herein.

Further, it is clear that the level of skill in the art would allow an artisan to easily query numerous compounds and to treat various disease based on the known biological activity disclosed in the specification as filed, to identify and prepare candidate compounds capable of specifically inhibiting Rsk activity as claimed and as defined and disclosed by Applicants. One skilled in the art of preparing and testing compounds for those possessing a desired biological activity typically engaged in this type of experimentation at the time the application was filed. This is important since the present case law regarding enablement under 35 U.S.C. §112, first paragraph, allows significant experimentation without finding it undue if the art typically engages in such experimentation.

Those of skill in the art of treating disease are also skilled in doing so based on data derived from in vitro experiments. For example, the specification as filed teaches that 100 μ M compound III (SL0101-01) completely inhibits RSK activity in the tumor cell line, MCF-7, and the normal cell line, MCF-10A (see Example 4). The present application further discloses that at 100 μ M, compound III halts the proliferation of the tumor cell lines, MCF-7 and LNCaP (Figure 8), but not normal cells. In fact, at 50 μ M compound III is sufficient to halt the proliferation of the cancer cells (See Figure 8). Therefore, the teachings embodied in the specification do provide sufficient direction to anyone skilled in the art as to the exact concentration of compound III required to inhibit RSK in both cancer cells and normal cells regardless of the disease that one is treating with the RSK inhibitor. One of ordinary skill in the art would be able to use these data and determine how to apply it to any disease with inappropriate Rsk activity where such a compound is used to inhibit Rsk activity as claimed.

Under the present law of enablement, claims reciting large numbers of species are allowable without disclosure of every species so long as the art engages in experimentation to identify the operative species encompassed by the generic claim. In *In re Vaeck*, 20 USPQ2d 1438, 1445 (Fed. Cir. 1991), reviewing an enablement rejection of a broad claim reciting methods for producing insect proteins in cyanobacteria, the Court of Appeals for the Federal Circuit discussed enablement in the context of generic species claims:

we do not imply that patent applicants in art areas currently denominated as "unpredictable" must never be allowed generic claims encompassing more than the particular species disclosed in their specification. It is well settled that patent applicants are not required to disclose every species encompassed by their claims, even in an unpredictable art. *In re Angstadt*, 537 F.2d 498, 502-03, 190 USPQ 214, 218 (CCPA 1976). However, there must be sufficient disclosure, either through illustrative examples or terminology, to teach those of ordinary skill how to make and how to use the invention as broadly as it is claimed. This means that the disclosure must adequately guide the art worker to determine, without undue experimentation, which species among all those encompassed by the claimed genus possess the disclosed utility.

In re Vaeck, 20 USPQ2d at 1445 (emphasis added). Thus, not every species need be disclosed where one skilled in the art would be able, without undue experimentation, to determine which species possess the disclosed utility. *See also In re Druey*, 145 USPQ 219, 221 (Bd. Pat. App. & Int. 1965) ("The fact that not all possible substituents encompassed by the generic language are illustrated does not preclude appellants from asserting the genus when no reasons have been advanced by the examiner to rebut appellants' assertion that all the compounds embraced by the genus will in fact have the properties ascribed to them.").

The MPEP at § 2164.08(b), discussing inoperative subject matter, states:

The presence of inoperative embodiments within the scope of a claim does not necessarily render a claim non-enabled. The standard is whether a skilled person could determine which embodiments that were conceived, but not yet made, would be inoperative or operative with expenditure of no more effort than is normally required in the art. *Atlas Powder Co. v. E.I. du Pont de Nemours & Co.*, 224 USPQ 409, 414 (Fed. Cir. 1984) (prophetic examples do not make the disclosure nonenabling).

. . . A disclosure of a large number of operable embodiments and the identification of a single inoperative embodiment did not

render a claim broader than the enabled scope because undue experimentation was not involved in determining those embodiments that were operable. *In re Angstadt*, 190 USPQ 214, 218 (CCPA 1976).

Thus, inoperative embodiments do not necessarily render a claim nonenabled as long as the experimentation required to identify the operative species is not undue.

In the landmark enablement case of *In re Wands*, 8 USPQ2d 1400 (Fed. Cir. 1988), which was cited by the Examiner, the court discussed the adequacy of disclosure with regard to a patent disclosing an immunoassay method for the detection of hepatitis B antigen using monoclonal antibodies. The *Wands* Court noted that of 143 hybridomas produced, only nine were assayed and, of those, only four hybridomas secreted IgM antibodies and exhibited a binding affinity constant for the HBsAg determinants of at least 10^9 M^{-1} , a “respectable 44 percent rate of success.” *In re Wands*, 8 USPQ2d at 1406. Finding the claims were enabled, the *Wands* Court stated:

Wands' disclosure provides considerable direction and guidance on how to practice their invention and presents working examples.

There was a high level of skill in the art at the time when the application was filed, and all of the methods needed to practice the invention were well known.

The nature of monoclonal antibody technology is that it involves screening hybridomas to determine which ones secrete antibody with desired characteristics. Practitioners of this art are prepared to screen negative hybridomas in order to find one that makes the desired antibody. No evidence was presented by either party on how many hybridomas would be viewed by those in the art as requiring undue experimentation to screen.

In re Wands, 8 USPQ2d at 1406 (emphasis added). Therefore, where, as here, the art typically makes and screens compounds for the desired activity and/or properties, *e.g.*, capable of inhibiting Rsk, where the specification discloses several such compounds (*see, e.g.*, Examples), demonstrating extensive reduction to practice, one skilled in the art would not require undue experimentation to produce the claimed method use utilizing a compound having the desired biological function and be able to perform the desired methods. Thus, where one skilled in the art routinely screens compounds for the desired activity, having to do so is not the undue

experimentation proscribed by 35 U.S.C. § 112, first paragraph, under the reasoning of *In re Wands*.

In *In re Angstadt*, 190 USPQ 214 (CCPA 1976), the court addressed the level of experimentation in an unpredictable art, *i.e.*, the chemical arts, where the claimed invention involved a method of catalytically producing hydroperoxides where the specification admitted that not all disclosed complexes produced the hydroperoxides. The *Angstadt* Court, holding that the invention as claimed was enabled, reasoned:

We note that many chemical processes, and catalytic processes particularly, are unpredictable. . . .

Appellants have apparently not disclosed every catalyst which will work; they have apparently not disclosed every catalyst which will not work. The question, then, is whether in an unpredictable art, section 112 requires disclosure of a test with every species covered by a claim. To require such a complete disclosure would apparently necessitate a patent application or applications with “thousands” of examples or the disclosure of “thousands” of catalysts along with information as to whether each exhibits catalytic behavior resulting in the production of hydroperoxides. More importantly, such a requirement would force an inventor seeking adequate patent protection to carry out a prohibitive number of actual experiments. This would tend to discourage inventors from filing patent applications in an unpredictable area since the patent claims would have to be limited to those embodiments which are expressly disclosed. A potential infringer could readily avoid “literal” infringement of such claims by merely finding another analogous catalyst complex which could be used in “forming hydroperoxides.”

In re Angstadt, 190 USPQ at 218 (emphasis added) (citations omitted). Similarly, in *In re Bundy*, 209 USPQ 48, 52 (CCPA 1981), the court noted the public policy reasons mitigating against imposing a requirement that each compound be tested before a generic species claim would be allowed:

Early filing of an application with its disclosure of novel compounds which possess significant therapeutic use is to be encouraged. Requiring specific testing of the thousands of prostaglandin analogs encompassed by the present claim in order to satisfy the how-to-use requirement of § 112 would delay disclosure and frustrate, rather than further, the interests of the public.

Thus, where methods for assessing whether a compound having the utility of the claimed compound are well-known in the art and/or disclosed in the specification, it would not be undue experimentation to screen such compounds which have the disclosed utility where the art typically engages in such experimentation.

More recently, in *Ex parte Mark*, 12 USPQ2d 1904 (Bd. Pat. App. & Int. 1989), the Board reversed the Examiner's rejection for lack of enablement under 35 U.S.C. § 112, first paragraph, with regard to an application involving admittedly "innumerable" muteins comprising a non-essential cysteine which exhibit biological activity after modification to substitute the cysteine. In reversing the Examiner, the *Mark* Court stated:

To the extent that the examiner is concerned that undue experimentation would be required to determine other proteins suitable for use in the present invention, we find [an applicant]'s declaration to be persuasive that only routine experimentation would be needed for one skilled in the art to practice the claimed invention for a given protein. The fact that a given protein may not be amenable for use in the present invention in that the cysteine residues are needed for the biological activity of the protein does not militate against a conclusion of enablement. One skilled in the art is clearly enabled to perform such work as needed to determine whether the cysteine residues of a given protein are needed for retention of biological activity.

Ex parte Mark, 12 USPQ2d at 1907. Therefore, where one skilled in the art routinely assays the compounds (e.g., chemical compounds; see Examples 6-9 for specific synthetic schemes, and Examples for specific assays, as well as the rest of the specification other assays and schemes) for the asserted utility (e.g., inhibiting Rsk), it is not undue experimentation for them to do so.

Thus, where one skilled in the art would have routinely produced and assessed compounds, including derivatives thereof, based on a known structure and synthetic scheme (See Examples 6-9) and methods to assay such compounds, following the teachings of the disclosure provided in the specification as filed, such experimentation would not have been undue even if it was complex and even if it entailed "fishing" out the pertinent molecules from among non-pertinent molecules. Armed with the teachings of the instant invention, including that the

pertinent compounds are inhibitors of Rsk, and given the knowledge and skill of one skilled in the art, the routineer would not have had to engage in any undue experimentation to practice the invention commensurate with the scope of claims 21-24, and these claims are therefore enabled under 35 U.S.C. §112, first paragraph.

Applicants also submit that newly added claims 48-50, which depend from claim 21, are also enabled and supported by the specification as filed. Claim 48 recites “wherein the disease is a neoplastic disease”. Support for claim 48 is found throughout the specification as filed and in the claims as filed. See in particular, page 7, lines 13-33, Examples 4 and 5, page 40, line 25 to page 41, line 15, Fig. 4, Fig. 7, Fig. 8. Furthermore, the Examiner admits at page 3 of the office action that the specification is enabling for the treatment of tumors or cancers. As described below, the data provided in the specification disclose that the compounds of the invention are effective on breast cancer, prostate cancer, and sarcomas. Additionally, at page 7, lines 12 to 33, the specification provides support for many different kinds of tumors and cancer. New Claims 49 and 50 depend from new claim 48, and recite the cancers listed on page 7, lines 23-33, and which are disclosed in the Examples.

Applicants submit that claims 21-24 are enabled and request that the rejection as to these claims be reconsidered and withdrawn. Applicants also submit that claims 21-24 and new claims 48-50 are in condition for allowance.

Response to Claim Rejections under 35 U.S.C. § 112, second paragraph, indefinite

Claims 21-32 stand rejected as allegedly indefinite under 35 U.S.C. § 112, second paragraph. The Examiner specifically refers to claims 21 and 25 (each of which are independent claims) as reciting “inappropriate Rsk activity”. The Examiner then admits that page 28 of the specification recites what inappropriate activity may be, but asserts that it is not clear what applicants intend by inappropriate activity. The Examiner then asserts that in the absence of a recitation of the specific activity the claims are indefinite and that for the purpose of prosecution the claims are examined as drawn to any disease or condition wherein Rsk activity is involved. Applicants respectfully submit that the phrase “inappropriate Rsk activity” as defined and used is not indefinite and traverse the rejection for the following reasons.

Applicants point out that although each of the two independent claims (21 and 25) recite “inappropriate Rsk activity” in the preamble, the last element of each of those claims recites either “inhibiting Rsk activity” (claim 21) or using “a Rsk specific inhibitor” (claim 25). Thus, each of these two independent claims, and their dependent claims, recite inhibiting Rsk or its activity.

At page 8, line 30, to page 9, line 2, of the specification, “Rsk specific inhibitor” is described as including “any compound or condition that inhibits Rsk kinase activity . . without substantially impacting the activity of other kinases. Such inhibitory effects may result from directly or indirectly interfering with the protein’s ability to phosphorylate its substrate, or may result from inhibiting the expression (transcription and/or translation) of Rsk.”

The description of “inappropriate Rsk activity” at page 28 of the specification referred to by the Examiner states “The inappropriate Rsk activity may constitute overexpression of Rsk protein, excessive Rsk kinase activity or it may represent the expression of Rsk activity in tissues that normally do not express Rsk activity.” (see page 28, lines 5-9). Applicants point out that the paragraph begins with an introduce sentence which states that one embodiment of the present invention provides “a method for inhibiting Rsk kinase activity . . . as a means of treating an illness associated with inappropriate Rsk activity” (emphasis added). That introductory sentence is then followed by a description of inappropriate activity. It can be seen that the inappropriate activity refers to overexpression of Rsk (meaning greater than normal expression), excessive kinase activity of Rsk (which means that the activity of the Rsk is greater than normal, but one of ordinary skill in the art would understand that it could mean both an increase in the activity level of Rsk without an increase in the actual amount of Rsk, or that the increased activity could be due to more Rsk protein itself), or that there is expression of Rsk activity where there is normally no such activity.

One of ordinary skill in the art would understand that the description refers to more Rsk, or to more Rsk activity, and that the method refers to inhibiting Rsk activity, regardless of whether the activity is due to increased Rsk levels or increase Rsk kinase activity. Therefore, Applicants submit that there is ample written description in the specification to support claims 21-32. Applicants further submit that new claims 48-50, which depend from claim 21, are

supported by the specification as described above. For these reasons, Applicants request that the rejection as to claims 21-32 be withdrawn.

Response to Claim Rejections under 35 U.S.C. § 102, anticipation by Matthes

Claims 1 and 4-9 stand rejected under 35 U.S.C. 102(b) as allegedly anticipated by Matthes et al. (Phytochemistry, 1980, 19:2643). It is the view of the Examiner that Matthes discloses a compound of structural formula 7, wherein two of the three hydroxyl groups on the sugar moiety are acetylated (citing page 2645). The Examiner then asserts that this compound is structurally the same as the compound claims in instant claims 1 and 4-9. The Examiner further asserts that Matthes discloses that the compound has an extinction coefficient of $c= 0.13$ in ethanol (EtOH; citing page 2647, lines 22-24).

It is well settled that "[a] claim is anticipated only if each and every element as set forth in the claim is found, either expressly or inherently described, in a single prior art reference." See *In re Bond*, 15 USPQ2d 1566, 1567 (Fed. Cir. 1990) and also MPEP §2131 (quoting *Verdegaal Bros. v. Union Oil Co. of Calif.*, 2 USPQ2d 1051, 1053 (Fed. Cir. 1987)). "The identical invention must be shown in as complete detail as is contained in the . . . claim." *Id.* (quoting *Richardson v. Suzuki Motor Co.*, 9 USPQ2d 1913, 1920 (Fed. Cir. 1989)). Absence of any claim element from the reference "negates anticipation." *Kloster Speedsteel AB v. Crucible, Inc.*, 230 USPQ 81, 84 (Fed. Cir. 1986); *Rowe v. Dror*, 42 USPQ2d 1550, 1552 (Fed. Cir. 1992). Therefore, Matthes must describe each and every element of amended claims 1 and 4-9 in order to anticipate these claims under Section 102(b), and this reference does not.

Applicants respectfully point out that the present claims recite a pharmaceutical composition, while Matthes does not disclose a "pharmaceutical composition" as recited in claim 1 and its dependent claims, e.g., claims 4-9 and therefore does not teach each element of claims 1 and 4-9. Because Matthes does not teach each and every element of claims 1 and 4-9 it cannot anticipate these claims.

For these reasons, Applicants respectfully request that the rejection as to claims 1 and 4-9 be withdrawn.

Response to Rejection of Claim 25-27 under 35 U.S.C. § 102, anticipation by Bjorbaek

Examiner asserts that Bjorbaek teaches a method of modulating body weight, fat content, leptin levels or oxygen consumption by altering or modulating Rsk activity using nucleic acid constructs expressing Rsk2 or a biologically active fragment thereof. The Examiner relates this to treatment of disease/condition characterized by inappropriate Rsk activity. The Examiner further asserts that the compounds of Bjorbaek can be used in the form of compositions.

Applicants traverse the rejection for the following reasons.

Applicants respectfully point out that Bjorbaek only has data using Rsk2 knockout mice and looked at parameters and characteristics of those mice. Nowhere does Bjorbaek treat the knockout mice with agents, nor does Bjorbaek treat normal mice with any compound or agent which might affect Rsk activity. Any comments by Bjorbaek otherwise have no factual basis and are merely a hope and a wish and speculation.

Claims 25-27 of the present invention encompass “method for treating a disease or condition characterized by inappropriate Rsk activity, said method comprising the step of administering to a patient in need thereof a composition comprising a Rsk specific inhibitor” (claims 25), wherein the Rsk specific inhibitor comprises a compound selected from the group consisting of an anti-sense oligonucleotide and an interfering oligonucleotide (claim 26), and wherein the Rsk specific inhibitor comprises an interfering oligonucleotide directed against Rsk1, Rsk2, Rsk3 or Rsk4 (claim 27). Applicants assert that Bjorbaek does not anticipate any of these claims.

Applicants respectfully point out that Bjorbaek does not teach or even contemplate “inappropriate Rsk activity”. The discussion provided above as to the meaning and use of the terms “inappropriate Rsk activity”, “Rsk specific inhibitor”, “a patient in need thereof”, and “disease or condition” applies with equal force here. The discussion provided above as to Bjorbaek also applies here.

Additionally, Rsk4 was not known at the time of Bjorbaek and the oligonucleotide sequence directed against Rsk 4 disclosed herein is novel. Therefore, Bjorbaek has no relevance at all to Rsk4.

Claim 25 of the current specification concerns a method for treating a disease or condition characterized by over expression of Rsk or over expression of Rsk activity compared to that observed in the non-diseased tissue or the expression of Rsk activity in tissues that

normally do not express Rsk activity in which the disease or the symptoms can be ameliorated by inhibition of RSK catalytic activity, said method comprising the step of administering to a patient in need thereof a composition comprising a Rsk-specific inhibitor. Bjorbaek merely speculates that inhibiting **normal** Rsk activity may reduce weight gain. Bjorbaek does not teach inappropriate Rsk activity. The current specification teaches the inhibition of Rsk activity to treat diseases caused by or exacerbated by over expression of Rsk or over expression of Rsk activity compared to that observed in the non-diseased tissue or the expression of RSK activity in tissues that normally do not express Rsk activity. Additionally, as detailed above, Bjorbaek had absolutely no evidence that inhibition of Rsk activity will alter the rate of weight gain. This is merely an assumption based on the evidence that deletion of RSK2 reduces the weight gain of the genetically altered mouse. Therefore, it cannot be determined from Bjorbaek that inhibition of RSK2 activity alone would alter the rate of weight gain. The current specification discloses that Rsk activity is required for proliferation of the cancer cells. This specification identifies the first small molecule inhibitor of Rsk activity and shows that the inhibitor functions to halt the growth of the cancer cells. Thus, the Rsk inhibitor induces the desired physiological response and can therefore be used to treat diseases characterized by “inappropriate Rsk activity”, i.e., over expression of Rsk or over expression of RSK activity compared to that observed in the non-diseased tissue or expression of RSK activity in tissues that normally do not express RSK activity. Therefore, the teachings embodied claims 25-27 are not found in the application of Bjorbaek et al.

Applicants request that the anticipation rejection of claims 25-27 as to Bjorbaek be reconsidered and withdrawn.

Response to 35 U.S.C. § 103 Rejection

Claims 2-3 and 33-38 stand rejected under 35 U.S.C. § 103(a) as allegedly obviousness over Matthes et al. (Phytochemistry, 1980, 19:2643) in combination with Bjorbaek et al. (WO 00/66721), Marks et al. (U.S. Pat. No. 5,910,583) and Kuijpers et al. (U.S. Pat. No. 5,733,523).

The Examiner sets forth *Graham v. John Deere Co.* factors for the rejection (*Graham v. John Deere Co.*, 383 U.S. 1, 148 USPQ 459 (1966)).

Examiner asserts that Matthes discloses a compound of structural formula 7, wherein two of the three hydroxyl groups on the sugar moiety are acetylated (citing page 2645). The Examiner asserts that this compound is structurally the same as the compound of instant claims 1 and 4-9. The Examiner then asserts that the measurement of the extinction coefficient of compound 7 in ethanol represents a pharmaceutical composition (citing page 2647, lines 22-24, second column). The Examiner then asserts that Matthes teaches that the extract from the roots of *Zingiber zerumbet* was tested against a rat neoplastic liver cell strain and found to be cytotoxic (citing page 2643, left column, second sentence of "Results and Discussion"). The Examiner then admits that even though Matthes teaches a compound that shows cytotoxicity toward neoplastic cells and a composition, Matthes does not teach a composition comprising compound 7 and an anti-tumor agent, an antisense oligonucleotide or an interfering nucleotide.

Examiner asserts that Bjorbaek teaches a method of modulating body weight, fat content, leptin levels, or oxygen consumption by altering or modulation Rsk activity using nucleic acid construct expressing Rsk2 or a biologically active fragment thereof (citing page 2, lines 1-13; page 21, lines 1-7; and pages 24-31). The Examiner then asserted that the compounds of Bjorbaek can be used in the form of compositions (citing page 23, line 8 through page 24, line 20). The Examiner then admits the Bjorbaek does not teach a composition comprising the nucleic acid constructs and an anti-tumor agent.

The Examiner then asserts that Kuijpers teaches the general use of antisense oligonucleotides and their pharmaceutical compositions for the treatment of tumors (citing the abstract, column 1, lines 26-40).

It is the view of the Examiner that Marks teaches in general a variety of uses for oligonucleotide formulations, including treatment of tumors (citing column 5, lines 9-25).

The Examiner then asserts that based on the teachings of the cited art that it would have been obvious to one of ordinary skill in the art at the time the invention was made to make a composition comprising an Rsk specific inhibitor and an antitumor agent including extracts from *Zingiber zerumbet* as instantly claimed because pharmaceutical compositions comprising such active agents are individually taught in the prior art to have the same utility.

The Examiner then asserted that the instant situation is amenable to the type of analysis set forth in *In re Kerkhoven*, 205 USPQ 1069 (CCPA 1980) wherein the court held that it is

prima facie obvious to combine two compositions, each of which is taught by the prior art to be useful for the same purpose, in order to form a third composition to be used for the very same purpose, since the idea of combining them flows logically from their having been individually taught in the prior art.

It is the view of the Examiner, that applying the *In re Kerkhoven* logic to the instant claims, given the teachings of the prior art of a composition for the use in the treatment of tumors, it would have been obvious to make a composition containing an Rsk specific inhibitor as taught by Bjorbaek and oligonucleotides and antisense oligonucleotides as instantly claimed, because the idea of doing so would have logically followed from their having been individually taught in the prior art.

Applicants respectfully submit that the combination of Matthes et al. (Phytochemistry, 1980, 19:2643) in combination with Bjorbaek et al. (WO 00/66721), Marks et al. (U.S. Pat. No. 5,910,583) and Kuijpers et al. (U.S. Pat. No. 5,733,523) does not render any of the present claims *prima facie* obvious under 35 U.S.C. § 103(a) for the following reasons:

Preliminarily, the three-prong test which must be met for a reference or a combination of references to establish a *prima facie* case of obviousness has not been satisfied in the instant matter. The MPEP states, in relevant part:

To establish a *prima facie* case of obviousness, three basic criteria must be met. First, there must be some suggestion or motivation, either in the references themselves or in the knowledge generally available to one of ordinary skill in the art, to modify the reference or to combine reference teachings. Second, there must be a reasonable expectation of success. Finally, the prior art reference (or references when combined) must teach or suggest all of the claim limitations. MPEP § 2142.

Additionally, MPEP § 2143.01 provides: “The mere fact that references can be combined or modified does not render the resultant combination obvious unless the prior art also suggests the desirability of the combination. *In re Mills*, 916 F.2d 680, 16 USPQ2d 1430 (Fed. Cir. 1990)” (emphasis added).

None of these criteria have been met here.

The present application discloses that inhibition of Rsk catalytic activity halts the growth of tumor cells. Therefore, the specification as filed provides the first evidence that inhibition of Rsk catalytic activity alone results in a physiological response that would affect a diseased state.

The present invention discloses the first evidence that the physiological response to Rsk inhibition is the reversal of the diseased state. The present application disclosed that a compound such as Matthes' compound 7 was an Rsk-specific inhibitor and that Rsk played a role in cancer cell growth. The present application also disclosed that inhibition of Rsk activity would inhibit the growth of cancer cells.

Applicants assert that, contrary to the opinion of the Examiner regarding Matthes, measurement of the extinction coefficient of compound 7 in ethanol does not represent a pharmaceutical composition. A pharmaceutical composition must be suitable for administration to a subject. A pharmaceutical composition is not a solution used for measurement of physical characteristics of an extract. Furthermore, Matthes teaches that compounds 4, 5, and 6 are "highly cytotoxic", but that compound 7 was "slightly cytotoxic". Applicants assert that these results teach away from the use of compound 7, and that one of ordinary skill in the art would be motivated to use compounds such as 4, 5, or 6, instead of 7. In fact, Matthes demonstrated that at least nine different compounds were 3 to 4 fold more cytotoxic than compound 7 (see Table 1 of Matthes).

Matthes does not disclose, suggest, teach, or even contemplate, compositions or methods useful for treating diseases or condition wherein the composition is an Rsk specific inhibitor, wherein it is a compound as in claim 1, wherein a compound as in claim 1 is further combined with an additional antitumor agent (claim 2) or chemotherapeutic (claim 3), or a composition comprising an Rsk specific inhibitor in combination with an anti-tumor agent (claim 33), or where the inhibitor is an anti-sense oligonucleotide or an interfering oligonucleotide (claim 34), or is an interfering RNA directed against Rsk1, 2, 3, or 4, or the inhibitor is a plant extract, or a compound comprising the structure of compound II (claims 35-38).

Matthes does not teach that compound 7 was an Rsk-specific inhibitor, nor does Matthes contemplate such. That such compounds can act as Rsk inhibitors was disclosed in the present application. As described above, the present invention provides for the use of an Rsk-inhibitor (like compound 7 or derivatives) to treat a disease or condition characterized by over expression

of Rsk or over expression of Rsk activity compared to that observed in the non-diseased tissue or the expression of Rsk activity in tissues that normally do not express Rsk activity in which the disease or the symptoms can be ameliorated by inhibition of Rsk catalytic activity. Thus, because Matthes provides neither evidence that compound 7 is an Rsk-specific inhibitor nor that Rsk-specific inhibition stops the growth of tumor cells, it would not be obvious to apply Matthes' teachings of a compound "with no anti-HIV or anti-tumor activity" for use as a pharmacological inhibitor of Rsk and an anti-tumor agent.

For these reasons, there would be no motivation to use compound 7 as claimed in the present application. Additionally, there is no motivation or suggestion provided in Matthes to modify Matthes or to combine the teachings of Matthes with the other references cited by the Examiner, particularly since the teachings of Matthes would instead suggest the use of compounds 4, 5, or 6.

Applicants also assert that additional studies were later published by the National Cancer Institute, which indicated that compound 7 of Matthes, which is also called 3",4"-O-Deacetylafzelin by Matthes, has no anti-HIV activity and no antitumor activity (Dai et al., 1997, Natural Product Letters, 10:115-118; a copy of which is provided herewith). In fact, Dai discloses that none of the afzelins were active in either assay (see abstract). These data are also published at the National Cancer Institute website for Molecular Targets Development Program, which provides the afzelin structure and indicates that it is a natural product **without** anti-HIV and antitumor activity. That listing also cites Dai. The URL for the National Cancer Institute website page is <http://home.ncicrf.gov/mtdp/Catalog/compounds/703082.html>. The compound is also labeled as NSC 703082. A copy of the website page is also provided herewith.

The disclosure of Dai, as well as the listing at the National Cancer Institute database, teaches away from the use of the compounds of claim 1 of the present invention, as does the data of Matthes which shows little activity for their compound 7, relative to their other compounds such as 4, 5, and 6. Therefore, the art at the time this application was filed taught away from the use of such compounds as claimed. Because Matthes and similar art taught away from the present invention, there would be no motivation or suggestion to combine Matthes with other references, nor would there be a reasonable expectation of success.

Regarding Bjorbaek, it does not correct the deficiencies of Matthes, and the discussion of Bjorbaek as provided above applies with equal force here. As stated above, contrary to the assertion of the Examiner, Bjorbaek merely measured characteristics of mice with a deletion of the Rsk2 gene. Bjorbaek provided no data regarding regulation of Rsk. Bjorbaek merely speculated regarding Rsk regulation and weight control.

Bjorbaek does not disclose, suggest, teach, or even contemplate, compositions or methods useful for treating diseases or condition wherein the composition is an Rsk specific inhibitor, wherein it is a compound as in claim 1, wherein a compound as in claim 1 is further combined with an additional antitumor agent (claim 2) or chemotherapeutic (claim 3), or a composition comprising an Rsk specific inhibitor in combination with an anti-tumor agent (claim 33), or where the inhibitor is an anti-sense oligonucleotide or an interfering oligonucleotide (claim 34), or is an interfering RNA directed against Rsk1, 2, 3, or 4, or the inhibitor is a plant extract, or a compound comprising the structure of compound II (claims 35-38).

Bjorbaek did not address inappropriate Rsk activity, nor discuss anything other than possibly regulating Rsk activity. Bjorbaek made no distinction between inappropriate Rsk activity and normal Rsk activity. Furthermore, Bjorbaek only addressed Rsk2, and not other Rsk, as taught and claimed herein (for example, see claim 35). As discussed above, Rsk4 was not even known at the time, and the antisense sequence directed against Rsk4 disclosed in the present application is novel. At page 2, as cited by the Examiner, Bjorbaek merely speculates about “regulating” Rsk. Bjorbaek does not even speculate about inhibiting Rsk. Furthermore, at page 21, lines 1-7, cited by the Examiner, Bjorbaek specifically speculates about methods to “increase” the activity of Rsk (see page 21, line 1). The method claims of the present application all encompass “inhibiting” or decreasing Rsk activity, not increasing the activity as suggested by Bjorbaek. Therefore, Bjorbaek at page 21 lines 1-7 teaches away from the present invention.

Applicants assert that Kuijpers does not correct the deficiencies of Matthes, nor does it correct the deficiencies of Bjorbaek. Kuijpers encompasses radioactively labeled oligonucleotides useful for directly targeting these radioactive molecules to a location for uses such as radiation therapy. Kuijpers does not teach specific sequences useful for inhibiting activity, much less teach antisense oligonucleotides directed against Rsk. Kuijpers does not

address Rsk activity, nor disease or conditions which can be treated with inhibitors of Rsk activity.

Kuijpers does not disclose, suggest, teach, or even contemplate, compositions or methods useful for treating diseases or condition wherein the composition is an Rsk specific inhibitor, wherein it is a compound as in claim 1, wherein a compound as in claim 1 is further combined with an additional antitumor agent (claim 2) or chemotherapeutic (claim 3), or a composition comprising an Rsk specific inhibitor in combination with an anti-tumor agent (claim 33), or where the inhibitor is an anti-sense oligonucleotide or an interfering oligonucleotide (claim 34), or is an interfering RNA directed against Rsk1, 2, 3, or 4, or the inhibitor is a plant extract, or a compound comprising the structure of compound II (claims 35-38).

Kuijpers provides no motivation or suggestion to modify the teachings therein or to combine the teachings therein with other art, including the art cited by the Examiner to arrive at the present invention. Furthermore, even if Matthes and Bjorbaek were combined, and Kuijpers were also combined with these references, the result would not be the present invention as claimed.

Applicants also assert that Marks does not correct the deficiencies of Matthes, Bjorbaek, or Kuijpers. Marks is directed to antisense oligonucleotides directed against the ERBB2 oncogene. Marks does not disclose, suggest, teach, or even contemplate, compositions or methods useful for treating diseases or condition wherein the composition is an Rsk specific inhibitor, wherein it is a compound as in claim 1, wherein a compound as in claim 1 is further combined with an additional antitumor agent (claim 2) or chemotherapeutic (claim 3), or a composition comprising an Rsk specific inhibitor in combination with an anti-tumor agent (claim 33), or where the inhibitor is an anti-sense oligonucleotide or an interfering oligonucleotide (claim 34), or is an interfering RNA directed against Rsk1, 2, 3, or 4, or the inhibitor is a plant extract, or a compound comprising the structure of compound II (claims 35-38).

Marks provides no motivation or suggestion to combine the teachings therein with the teachings of Matthes, Bjorbaek, or Kuijpers. Furthermore, it would not be obvious to combine the teachings of Matthes, Bjorbaek, Kuijpers, or Marks for the reasons discussed above. Additionally, it would not be obvious to modify Matthes in view of Bjorbaek, Kuijpers, and Marks for the reasons discussed above. First, none of the references discloses that inappropriate

Rsk activity is involved in diseases and conditions, particularly cancer. Therefore, there would be no motivation to use inhibitors of Rsk to treat inappropriate Rsk activity, because inappropriate Rsk activity was not contemplated to be associated with a disease or condition in any of the four references. Additionally, none of the compounds presently claimed were known to be Rsk inhibitors. Bjorbaek merely speculated about inhibiting Rsk, but did not disclose inappropriate Rsk activity or actually make or use any Rsk inhibitors. Therefore, there would be no motivation to combine any of the compounds of the invention, such as the compounds of claim 1, which are claimed to be Rsk specific inhibitors, with any other agent, regardless of what type of agent it is.

Furthermore, as described above, it is evident that even if the cited references were combined, the result is not the invention as claimed, because the references do not teach or disclose each and every element of the claims.

Additionally, as discussed above, the art, (i.e., Matthes, Dai, and the National Cancer Institute) taught away from the use of compounds such as those of claim 1 (from which claims 2 and 3 depend), or a similar compound as in claim 37. Thus, there would be no motivation to combine these Rsk specific inhibitors with other agents as recited in claims 2-3, 37 and 38, nor would there be a reasonable expectation of success.

Applicants assert that *In re Kerkhoven*, cited by the Examiner, is inapposite to the rejected claims. As stated in MPEP 2144.06, it is *prima facie* obvious to combine two compositions each of which is taught by the prior art to be useful for the same purpose. Applicants note that the Examiner does not indicate which “two” compositions of the prior art are being combined. Examiner merely refers to “an Rsk specific inhibitor” as taught by Bjorbaek, in combination with the oligonucleotides and antisense oligonucleotides as instantly claimed. Examiner does not refer to other known compositions. Applicants submit that in order for the Examiner to assert *In re Kerkhoven*, the Examiner must show that two known compositions are combined. Examiner did not do so here. Therefore, *In re Kerkhoven* as applied by the Examiner is inapposite to the present claims.

Applicants submit that claims 2-3 and 33-38 are not obvious for the reasons provided above and request that the rejection as to these claims be reconsidered and withdrawn.

Conclusion

If the Examiner believes that personal communication will expedite prosecution of this application, the Examiner is invited to telephone the undersigned at (434) 243-6103.

Respectfully submitted,

Date: June 20, 2006

Rodney L. Sparks

Rodney L. Sparks
Registration No. 53,625
University of Virginia Patent Foundation
250 West Main Street, Suite 300
Charlottesville, VA 22902
Telephone: (434) 243-6103
Fax: (434) 924-2493

β -Amyloid Activates the Mitogen-Activated Protein Kinase Cascade via Hippocampal $\alpha 7$ Nicotinic Acetylcholine Receptors: *In Vitro* and *In Vivo* Mechanisms Related to Alzheimer's Disease

Kelly T. Dineley,¹ Marcus Westerman,³ Duy Bui,¹ Karen Bell,¹ Karen Hsiao Ashe,^{2,3} and J. David Sweatt¹

¹Division of Neuroscience, Baylor College of Medicine, Houston, Texas 77030, and Departments of ²Neurology and

³Neuroscience, University of Minnesota, Minneapolis, Minnesota 55455

Alzheimer's Disease (AD) is the most common of the senile dementias, the prevalence of which is increasing rapidly, with a projected 14 million affected worldwide by 2025. The signal transduction mechanisms that underlie the learning and memory derangements in AD are poorly understood. β -Amyloid (A β) peptides are elevated in brain tissue of AD patients and are the principal component of amyloid plaques, a major criterion for postmortem diagnosis of the disease. Using acute and organotypic hippocampal slice preparations, we demonstrate that A β peptide 1–42 (A β 42) couples to the mitogen-activated protein kinase (MAPK) cascade via $\alpha 7$ nicotinic acetylcholine receptors (nAChRs). *In vivo* elevation of A β , such as that exhibited in an animal model for AD, leads to the upregulation of $\alpha 7$ nAChR protein. $\alpha 7$ nAChR upregulation occurs concomitantly

with the downregulation of the 42 kDa isoform of extracellular signal-regulated kinase (ERK2) MAPK in hippocampi of aged animals. The phosphorylation state of a transcriptional mediator of long-term potentiation and a downstream target of the ERK MAPK cascade, the cAMP-regulatory element binding (CREB) protein, were affected also. These findings support the model that derangement of hippocampus signal transduction cascades in AD arises as a consequence of increased A β burden and chronic activation of the ERK MAPK cascade in an $\alpha 7$ nAChR-dependent manner that eventually leads to the downregulation of ERK2 MAPK and decreased phosphorylation of CREB protein.

Key words: Alzheimer's disease; MAPK; nicotinic receptor; amyloid; kinase; hippocampus; learning; memory

Alzheimer's Disease (AD) clinically presents itself as impaired memory formation, yet despite intensive study the mechanisms underlying AD-related memory dysfunction remain mysterious. The discovery that soluble β -amyloid (A β) peptides are elevated in the brains of AD patients raises the issue of whether these molecules play a causative role in AD (Kuo et al., 1996). A β peptides are generated from amyloid precursor protein (APP) via endo-proteolytic cleavage by β - and γ -secretases (Selkoe, 1998). In normal individuals A β 40 comprises the majority of the A β population; a far smaller fraction is made up of A β 42 (Kuo et al., 1996). A β 42 is highly fibrillogenic and exhibits trophic and toxic effects on neurons (Lambert et al., 1998; Hartley et al., 1999; Dodart et al., 2000).

Early onset AD is associated with several risk factors, the best correlated being age and the inheritance of specific genes that result in the increased production of A β peptides. Thus several laboratories are seeking to gain insights into AD by studying the effects of A β *in vitro* and *in vivo* (Hsiao, 1998; Dodart et al., 2000). Studies on transgenic animals that express the human genes linked to early onset familial AD (FAD) have shown that aber-

rant A β production leads to many pathological features of AD (Borchelt, 1998; Hsiao, 1998). One transgenic strain (Tg2576) exhibits several pathological features of AD, including elevated A β production with subsequent hippocampus-dependent learning and memory deficits, age-dependent accumulation of A β fibrils, and plaque formation (Hsiao et al., 1996; Irizarry et al., 1997a; Chapman et al., 1999). The Tg2576 mouse strain at 9 months of age exhibits learning deficits without neuronal cell loss or A β deposition into plaques (Irizarry et al., 1997b). Therefore, the impairments leading to this phenotype are likely in the normal cellular signaling cascades involved in learning and memory.

Using this rationale, we investigated A β 42 activation of the extracellular signal-regulated kinase (ERK2) isoform of the ERK mitogen-activated protein kinase (MAPK) cascade, because activation of this kinase in hippocampus is required for contextual and spatial memory formation in mammals (Atkins et al., 1998; Blum et al., 1999; Schafe et al., 1999; Selcher et al., 1999). In addition, we evaluated the phosphorylation state of a downstream target of ERK MAPK in hippocampus, the cAMP-regulatory element binding (CREB) protein, also a necessary component for hippocampus-dependent memory formation in mammals (Bourtchuladze et al., 1994).

The $\alpha 7$ nicotinic acetylcholine receptor (nAChR) is expressed in brain regions particularly susceptible to the ravages of AD, and the functional location of $\alpha 7$ nAChRs in hippocampus indicates a role for these receptors in memory formation (Perry et al., 1995; Frazier et al., 1998; McQuiston and Madison, 1999). Recent studies have shown that A β 42 coimmunoprecipitates with the $\alpha 7$ nAChR in samples from postmortem AD hippocampus, and $\alpha 7$ nAChR antagonists compete for A β 42 peptide binding to heterologously expressed $\alpha 7$ nAChRs (Wang et al., 2000). Further-

Received Feb. 1, 2001; revised March 13, 2001; accepted March 14, 2001.

This work was supported by awards to J.D.S. from the National Institute on Aging (NIA), National Institute of Mental Health, National Alliance for Research on Schizophrenia and Depression, and the Texas Advanced Technology Program; an NIA National Research Service Award to K.T.D.; and a National Institute of Neurological Disorders and Stroke award to J.W.P. We thank Drs. James W. Patrick and Daniel H. S. Lee for helpful discussions during the preparation of this manuscript.

Correspondence should be addressed to Kelly T. Dineley or J. David Sweatt, Division of Neuroscience, Room S603, Baylor College of Medicine, One Baylor Plaza, Houston, TX 77030. E-mail: kdineley@cns.bcm.tmc.edu or david@cns.bcm.tmc.edu.

Copyright © 2001 Society for Neuroscience 0270-6474/01/214125-09\$15.00/0

more, preincubation with $\text{A}\beta 42$ peptide antagonizes the activation of $\alpha 7$ nAChR-like currents in hippocampal interneurons (Pettit et al., 2001). Therefore, we tested the hypothesis that the $\alpha 7$ nAChR functions as a receptor for $\text{A}\beta 42$ in the hippocampus, coupling $\text{A}\beta 42$ to the ERK MAPK cascade. Furthermore, in an animal model of AD we evaluated the effects of chronic elevated $\text{A}\beta$ on this signal transduction cascade.

MATERIALS AND METHODS

Materials. Unless otherwise stated, chemicals and drugs were purchased from Sigma (St. Louis, MO). Synthetic rat $\text{A}\beta 42$ was purchased from Calbiochem (La Jolla, CA). $\text{A}\beta 42$ stock solutions were prepared at 100 μM in 100 mM HEPES, pH 8.5, aliquoted, and stored frozen. Anti- $\alpha 7$ nAChR antibody was purchased from Babco (Richmond, CA). Anti-ERK1/2 and anti-ERK1/2 dually phosphorylated at Thr202/Tyr204 antibodies were purchased from Cell Signaling Technologies. Anti-CREB antibody also was purchased from Cell Signaling Technologies. Anti-CREB phosphorylated at Ser133 antibody was developed and characterized in the laboratory of J. D. Sweatt. Tissue culture mediums and buffers were prepared with supplies from Life Technologies (Gaithersburg, MD).

Animal subjects. Acute hippocampal slices were obtained from mice heterozygous for the L250T $\alpha 7$ nAChR transgene (Orr-Urtreger et al., 2000). Morris water maze testing was performed on Tg2576 mice carrying a human APP transgene with the K670N-M671L mutation (Hsiao et al., 1996). This was followed by a longitudinal biochemical analysis of ERK, CREB, and $\alpha 7$ nAChR levels at 4, 13, and \sim 20 months of age. Postnatal day 7 (P7), P10, or P13 Sprague Dawley rat pups (Harlan Sprague Dawley, Indianapolis, IN) were used for hippocampal explant cultures. All animal experiments were performed in accordance with the Baylor College of Medicine Institutional Animal Care and Use Committee and with national regulations and policies.

Hippocampus dissection. Animals were decapitated, and both hippocampi were removed and placed into ice-cold cutting solution [containing (in mM) 1.25 NaH_2PO_4 , 28 NaHCO_3 , 60 NaCl, 3 KCl, 110 sucrose, 0.5 CaCl_2 , 7 MgCl_2 , 5 glucose, and 0.6 ascorbate]. For experiments that used $\alpha 7$ nAChR L250T heterozygote animals, 400 μm transverse slices were prepared (see below). For quantitative immunoblot that used samples from Tg2576 mice and age-matched control animals (most often littermates), area CA1 and dentate gyrus (DG) were subdivided from each hippocampus and prepared for quantitative immunoblot as described previously (Roberson et al., 1999). The following numbers of test subjects were used: 4 month Tg2576 animals, $n = 10$; 13 month animals, $n = 8$; 18–22 (\sim 20) month animals, $n = 20$.

Acute hippocampal slice preparation and drug treatments. Transverse hippocampal slices (400 μm) were prepared as described previously (Roberson et al., 1999) from mice heterozygote for the L250T mutation in the $\alpha 7$ nAChR (Orr-Urtreger et al., 2000). Slices were maintained in aCSF [containing (in mM) 125 NaCl, 2.5 KCl, 1.25 NaH_2PO_4 , 25 NaHCO_3 , 2 CaCl_2 , 1 MgCl_2 , and 25 glucose] for drug treatments. Slices were incubated in 500 μM nicotine for 10 min with or without pretreatment (for 30 min) with 1 μM MLA. Basal samples represent identical slices that were left untreated. Samples were subjected to quantitative immunoblot as described previously. All experiments included a 10 μM PDA treatment (for 10 min) as a positive control for ERK MAPK activation. Data that are normalized to basal samples are reported as average \pm SEM. Experimental results represent replicates of three to five slices per treatment.

Hippocampal slice culture and treatments. Hippocampal slice cultures were prepared from P7, P10, or P13 Sprague Dawley rat pups and maintained in culture according to the method of Stoppini et al. (1991). Then 24 hr before assay the cultures were rinsed and switched into serum-free culture medium (Neurobasal medium, pH 7.2, supplemented with B-27, 1% penicillin-streptomycin, 1.4% 1.8 M glucose, 0.5% 200 mM glutamine, and 0.25 $\mu\text{g}/\text{ml}$ Fungizone). After 5–11 d *in vitro* the slices were assayed for ERK MAPK activation after various treatments. Assays were performed on at least eight slices per treatment in triplicate or greater for each experiment. Basal samples represent identical cultures that were left untreated. Samples were subjected to quantitative immunoblot as described previously. Data that are normalized to basal samples are reported as average \pm SEM. Results represent at least three experimental replicates. Treatments were performed in serum-free culture medium and included (1) 500 μM nicotine (for 10 min) with or without

pretreatment (for 30 min) with 1 μM MLA; (2) 100 nM $\text{A}\beta 42$ for 2, 5, 10, 30, or 120 min; (3) 5 min incubation with 0.01, 0.1, 1.0, 10, or 100 nM $\text{A}\beta 42$; (4) 5 min incubation with 100 nM $\text{A}\beta 42$ with or without pretreatment (for 30 min) with 1 μM MLA or (for 2 hr) with 100 μM α -BTX; (5) 500 μM nicotine (for 10 min) with or without pretreatment (for 2 hr) with 100 nM $\text{A}\beta 42$; (6) 10 μM PDA (for 10 min) with or without pretreatment (for 2 hr) with 100 nM $\text{A}\beta 42$; (7) 100 nM $\text{A}\beta 42$ with or without pretreatment (for 1 hr) with 1 μM TTX; (8) 100 nM $\text{A}\beta 42$ with or without preincubation (for 1 hr) in culture medium containing 5 mM EGTA; (9) 100 pM $\text{A}\beta 42$ treatment for 144 hr. As a positive control for ERK MAPK activation, where relevant, the experiments included a 10 μM PDA treatment (for 10 min).

Quantitative immunoblotting. Harvested brain tissue was sonicated in sonication buffer [containing (in mM) 10 HEPES, pH 7.4, 150 NaCl, 50 NaF, 1 ED/EGTA, 10 $\text{Na}_4\text{P}_2\text{O}_7$, and 1 Na_3VO_4 plus 200 nM calyculin A, 10 $\mu\text{g}/\text{ml}$ leupeptin, 2 $\mu\text{g}/\text{ml}$ aprotinin, and 1 μM microcystin-LR], and protein concentration was determined with BCA (Pierce, Rockford, IL). Samples were subjected to SDS-PAGE and transferred to Immobilon-P (Millipore, Bedford, MA), followed by immunoblotting with the appropriate primary and secondary antibodies and chemiluminescence (ECL, Amersham/Pharmacia Biotech, Piscataway, NJ). Band intensity was quantified with Scion Image software (NIH Image, Bethesda, MD) from film exposures (BioMax, Kodak, Rochester, NY) in the linear range for each antibody and normalized to basal/control level. Normalized basal/control values were determined for each immunoblot by averaging basal/control values, dividing each basal/control and test/transgenic sample density by the average of the basal/control set, and then determining the average and SEM for basal/control and test/transgenic samples.

Spatial learning task. Initially, Tg2576 mice and age-matched control animals underwent cued training for 3 d consecutively (8 trials/d), swimming to a raised black platform marked with a black and white striped pole. The platform location and start quadrant were varied pseudorandomly in each trial. Hidden platform training was performed over 9 d consecutively (4 trials/d), wherein mice were required to locate within 60 sec a platform submerged 1.5 cm beneath the surface of opaque water. Once the platform was reached in hidden platform training, the mice were allowed to remain on the platform for 30 sec. Mice who failed to reach the platform within 60 sec were led to the platform with a retrieval scoop. At 16–24 hr after the 12th, 24th, and 36th training trials, probe trials were run in which mice swam for 60 sec in the pool with no platform. Trials were monitored by a ceiling-mounted camera above the pool and analyzed with the HVS tracking system (HVS Image Ltd., Hampton, UK). Further analysis was done with Wintrack (kindly provided by Dr. David Wolfer, University of Zurich, Switzerland).

Exclusion criteria omitted mice with obvious swimming difficulties, such as persistent floating, sinking, or abnormal swimming patterns. Mice exhibiting an escape latency >2 SD longer than the age-matched Tg2576 mean during the last four cued trials and mice that consistently failed to orient to or follow the retrieval scoop by the end of the testing period also were excluded from data analysis.

Statistical methods. Student's *t* test or one-way ANOVA was performed on quantitative immunoblot results, followed by *post hoc* analysis with the method of Tukey.

RESULTS

We first tested whether $\alpha 7$ nAChRs could mediate activation of the ERK2 MAPK cascade by treating hippocampal slices with nicotine and assaying for a resultant increase in ERK2 MAPK phosphorylation, a direct indicator of kinase activation (Sturgill et al., 1988; Payne et al., 1991). Because the wild-type $\alpha 7$ nAChR receptor rapidly desensitizes, the slices in these experiments were prepared from the hippocampi of heterozygote transgenic (L250T) animals that contain a targeted mutation in the $\alpha 7$ nAChR gene that renders the expressed $\alpha 7$ nAChRs resistant to desensitization (Revah et al., 1991; Orr-Urtreger et al., 2000). Nicotine activates the 42 kDa ERK2 isoform of MAPK in hippocampi from L250T animals (Fig. 1*a*). Stimulation of ERK2 activity is dependent on $\alpha 7$ nAChR function because an $\alpha 7$ -selective antagonist, methyllycaconitine (MLA), attenuates nicotine-induced activation of ERK2 MAPK in the L250T hippocampal slices. In addition, wild-type rat hippocampal slices

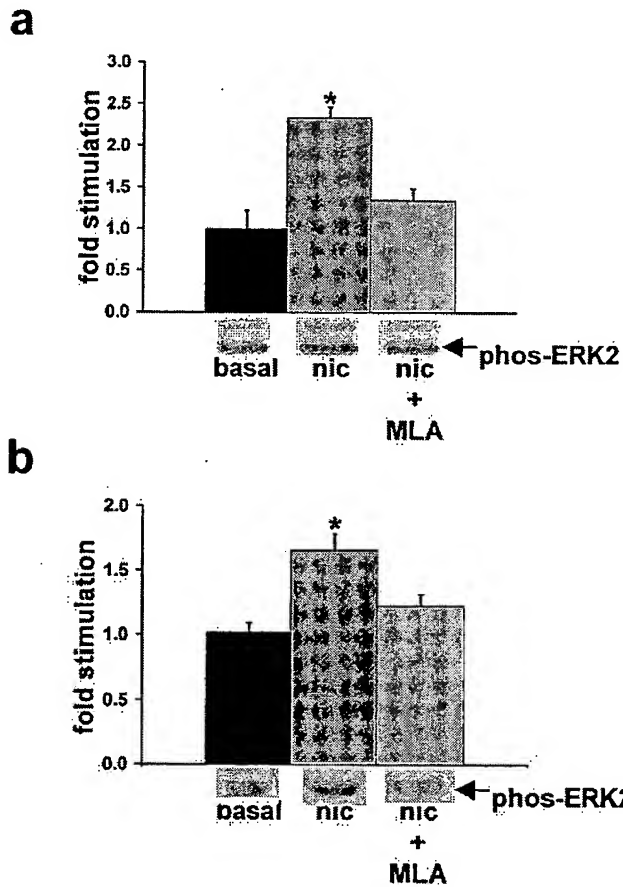


Figure 1. Nicotine activation of ERK2 in hippocampal slices is mediated by $\alpha 7$ nAChRs. *a*, Quantitative immunoblot demonstrates that 500 μM nicotine stimulated ERK2 MAPK activity, which is antagonized by 1 μM MLA in hippocampal slices from mice heterozygous for the L250T $\alpha 7$ nAChR transgene. Basal, 1.00 \pm 0.22; nicotine (nic), 2.33 \pm 0.13; MLA + nicotine, 1.34 \pm 0.14. *Significant difference from basal level; $p < 0.01$, *post hoc* Tukey multiple comparison test. Representative immunoblot results are depicted below the response histogram. ERK1 (top band) activation paralleled that of ERK2; however, absolute levels of phospho-ERK1 were far below ERK2 and were not quantified. Slices from wild-type animals did not exhibit significant ERK2 MAPK activation with nicotine treatment, likely because of the rapid desensitization kinetics of wild-type $\alpha 7$ nAChRs precluding biochemical detection of ERK2 MAPK activation (Seguila et al., 1995). *b*, Quantitative immunoblot demonstrates that ERK2 MAPK activation by nicotine in cultured rat hippocampal slices is blocked by 1 μM MLA. Basal, 1.01 \pm 0.08; nicotine, 1.66 \pm 0.13; MLA + nicotine, 1.22 \pm 0.09. *Denotes nicotine stimulation is significantly different from basal level; $p < 0.001$, *post hoc* Tukey multiple comparison test. Representative immunoblot results are depicted below the response histogram.

maintained in culture exhibit activation of ERK2 MAPK with nicotine treatment that is blocked by MLA pretreatment (Fig. 1b). These results demonstrate that $\alpha 7$ nAChR activation is capable of stimulating ERK2 MAPK in hippocampus.

Hippocampal slice culture technique was used to evaluate whether $\alpha 7$ nAChRs mediate $\text{A}\beta 42$ stimulation of the ERK MAPK cascade. $\text{A}\beta$ activates several kinase systems in cultured cells (Saitoh et al., 1993; Kosik et al., 1996), including the ERK MAPK cascade in cultured primary cortical and hippocampal neurons (Ekinci et al., 1999; Rapoport and Ferreira, 2000). The $\text{A}\beta$ preparations used in these previous studies varied vis-à-vis the aggregation state and length of the synthetic peptides that

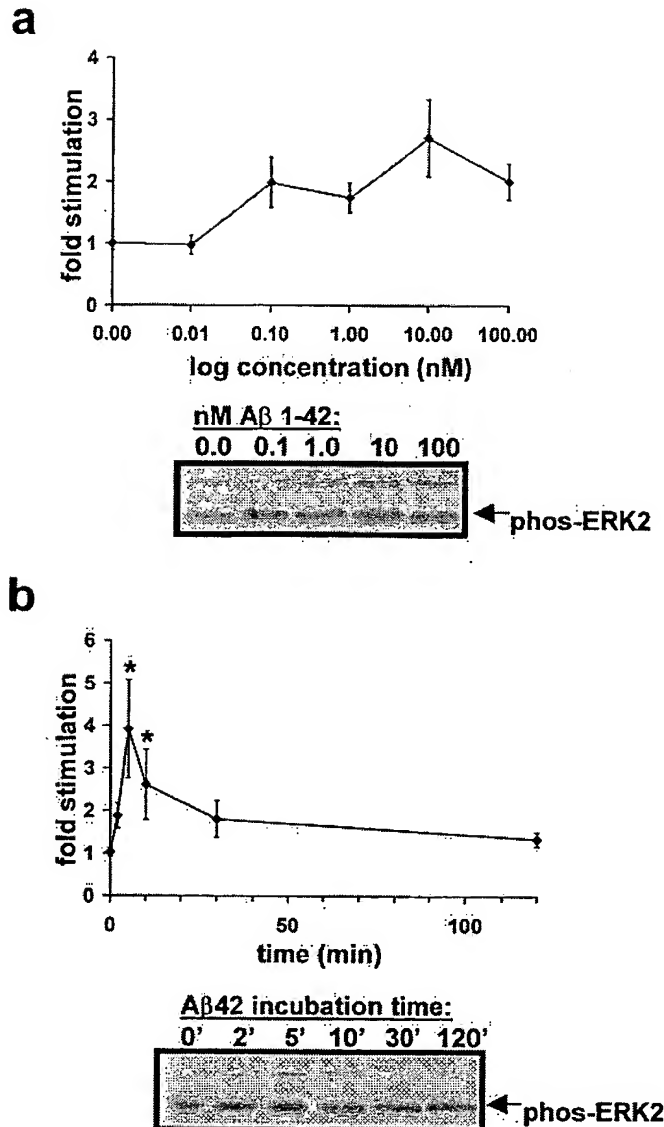
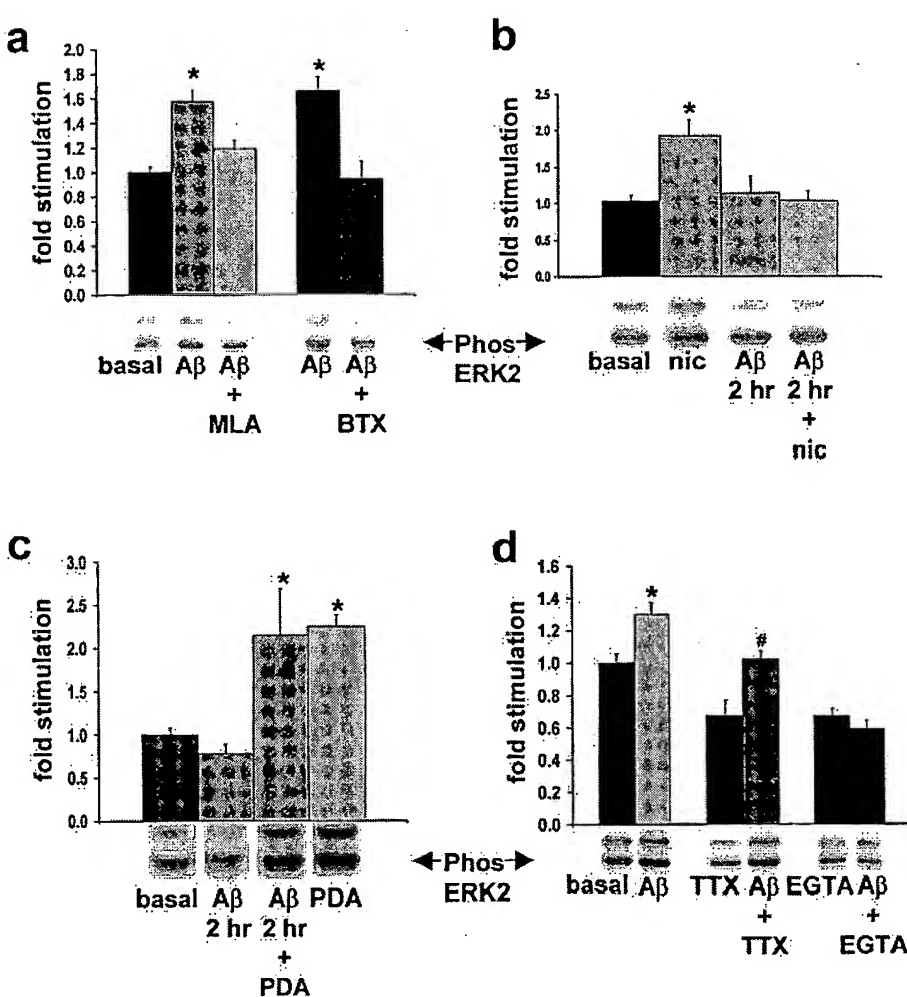


Figure 2. Time course and concentration dependence of $\text{A}\beta 42$ activation of ERK2 MAPK in cultured rat hippocampal slices. *a*, $\text{A}\beta 42$ activates ERK MAPK in the picomolar to nanomolar range. Data points are as follows: 0 nM (1.00 \pm 0.15), 0.01 (0.98 \pm 0.16), 0.1 (1.98 \pm 0.48), 1.0 (1.74 \pm 0.25), 10 (2.70 \pm 0.62), and 100 (2.01 \pm 0.30) nM $\text{A}\beta 42$ for 5 min. Representative immunoblot results are depicted below the response curve. *b*, The 100 nM $\text{A}\beta 42$ rapidly activates ERK2 MAPK in rat hippocampal slice cultures. Peak response occurs at 5 min $\text{A}\beta 42$ and returns to baseline within 2 hr. Data points are as follows: 2 (1.88 \pm 0.30), 5 (3.92 \pm 1.15), 10 (2.61 \pm 0.83), 30 (1.81 \pm 0.44), and 120 (1.34 \pm 0.17) min. *Significant difference from basal level (1.06 \pm 0.12); $p < 0.05$, Student's *t* test with Welch's correction because variances differ significantly according to Bartlett's test. Representative immunoblot results are depicted below the response curve.

were used. Our work used $\text{A}\beta 42$ peptide that was prepared under conditions to promote solubility and to retard aggregation (Burdick et al., 1992; Garzon-Rodriguez et al., 1997). We tested our $\text{A}\beta 42$ preparations for aggregation in a Congo red assay. At the concentrations used and under the incubation conditions tested, none of the $\text{A}\beta 42$ preparations significantly pelleted out of solution with Congo red dye at 2.5 or 25 μM (Brining, 1997) (data not shown). We found that synthetic $\text{A}\beta 42$ activates ERK2 MAPK in

Figure 3. $\alpha 7$ couples $\text{A}\beta 42$ activation of ERK2 MAPK in cultured rat hippocampal slices. *a*, Quantitative immunoblot demonstrates that ERK2 MAPK activation by 100 nm $\text{A}\beta 42$ is blocked by 1 μM MLA and 100 μM BTX. Basal, 1.00 ± 0.04 ; $\text{A}\beta 42$ (light-shaded bar), 1.58 ± 0.09 ; $\text{A}\beta 42$ (dark-shaded bar), 1.19 ± 0.07 ; $\text{A}\beta 42 + \text{MLA}$, 1.67 ± 0.11 ; $\text{A}\beta 42 + \text{BTX}$, 0.94 ± 0.14 . *Significant difference from basal ERK2 MAPK activity; $p < 0.0001$, Student's *t* test with Welch's correction because variances differ significantly according to Bartlett's test. Representative immunoblot results are depicted below the response histogram. *b*, $\text{A}\beta 42$ (100 nm) desensitizes the nicotine-induced (500 μM) activation of ERK2 MAPK. Basal, 1.05 ± 0.14 ; nicotine (nic), 1.94 ± 0.22 ; $\text{A}\beta 42$ (at 2 hr), 1.14 ± 0.24 ; $\text{A}\beta 42 + \text{nicotine}$ (at 2 hr), 1.03 ± 0.13 . *Significant difference from basal ERK2 MAPK activity; $p < 0.001$, *post hoc* Tukey multiple comparison test. Representative immunoblot results are depicted below the response histogram. *c*, $\text{A}\beta 42$ (100 nm) does not desensitize the PDA-induced (10 μM) activation of ERK2 MAPK. Basal, 1.00 ± 0.08 ; $\text{A}\beta 42$ (at 2 hr), 0.78 ± 0.11 ; $\text{A}\beta 42 + \text{PDA}$ (at 2 hr), 2.15 ± 0.54 ; PDA, 2.25 ± 0.13 . *Significant difference from basal ERK2 MAPK activity; $p < 0.01$, *post hoc* Tukey multiple comparison test. Representative immunoblot results are depicted below the response histogram. *d*, The 100 nm $\text{A}\beta 42$ activation of ERK2 MAPK is not blocked by TTX and exhibits Ca^{2+} dependency. Basal, 1.00 ± 0.06 ; $\text{A}\beta 42$, 1.30 ± 0.07 ; TTX, 0.67 ± 0.10 ; $\text{A}\beta 42 + \text{TTX}$, 1.02 ± 0.05 ; EGTA, 0.59 ± 0.04 ; $\text{A}\beta 42 + \text{EGTA}$, 0.65 ± 0.05 . *Significant difference from basal-induced ERK2 MAPK activity. #, Significant difference from TTX-induced ERK2 MAPK activity; $p < 0.001$, *post hoc* Tukey multiple comparison test.



cultured hippocampal slices at concentrations typically found in the CSF and brains of AD patients and in animal models of AD (Hsiao et al., 1996; Andreasen et al., 1999a,b; Tapiola et al., 2000) (Fig. 2a). Furthermore, ERK2 MAPK activation occurs rapidly and decreases with prolonged exposure to $\text{A}\beta 42$, indicative of receptor or MAPK cascade desensitization (Fig. 2b).

Stimulation of ERK2 MAPK activity with $\text{A}\beta 42$ in cultured rat hippocampal slices is blocked by the $\alpha 7$ nAChR antagonists MLA and α -bungarotoxin (BTX), demonstrating that $\alpha 7$ nAChR function is necessary for $\text{A}\beta 42$ coupling to the ERK MAPK cascade (Fig. 3a). This was also the case for acute hippocampal slices prepared from L250T animals and exposed to identical drug treatments (data not shown). Cross-desensitization is one way to test the possibility that two different agonists couple via the same receptor type. Pretreatment of cultured hippocampal slices with $\text{A}\beta 42$ blocked nicotine stimulation of ERK MAPK activity, evidence that nicotine and $\text{A}\beta 42$ mediate their effects on ERK2 MAPK via the same receptor type (Fig. 3b). $\text{A}\beta 42$ pretreatment of cultured slices did not interfere with the ability of phorbol 12,13-dibutyrate (PDA) to activate ERK MAPK, demonstrating that the MAPK cascade was not desensitized by $\text{A}\beta 42$ treatment, evidence in support of $\alpha 7$ nAChRs mediating this $\text{A}\beta 42$ effect (Fig. 3c). We tested whether action potential generation is necessary for the ERK2 MAPK activation by $\text{A}\beta 42$ by including

tetrodotoxin (TTX) in the assay medium. TTX alone decreased the basal level of ERK MAPK activation, indicating that endogenous synaptic transmission in the hippocampal slice cultures contributes to basal ERK2 MAPK activity level. $\text{A}\beta 42$ in the presence of TTX results in significant ERK2 MAPK activation as compared with cultures treated with TTX alone (Fig. 3d). Because $\alpha 7$ nAChRs are highly permeable to Ca^{2+} (Seguela et al., 1993), we tested the Ca^{2+} dependency of $\text{A}\beta 42$ -induced ERK MAPK activation. Depleting the assay system of external Ca^{2+} by including EGTA in the culture medium blocks $\text{A}\beta 42$ -induced activation of ERK2 MAPK (Fig. 3d). Overall, our experiments show that $\text{A}\beta 42$ rapidly activates ERK2 MAPK in hippocampus for which $\alpha 7$ nAChR function is necessary. This activation uses extracellular Ca^{2+} (likely via $\alpha 7$ nAChRs directly and $\alpha 7$ nAChR-dependent depolarization) and is action potential-independent; the ability of $\text{A}\beta 42$ to activate ERK2 MAPK exhibits desensitization without inhibiting phorbol ester activation of the cascade. Furthermore, ERK MAPK activation occurs in response to picomolar and nanomolar concentrations of $\text{A}\beta 42$.

As a complement to these *in vitro* experiments, we investigated the effects of elevated $\text{A}\beta$ *in vivo*. We used Tg2576 animals to evaluate the long-term effects of elevated $\text{A}\beta$ on hippocampal $\alpha 7$ nAChR expression level and ERK2 MAPK activity. A typical consequence of chronic exposure to nAChR agonist is nAChR

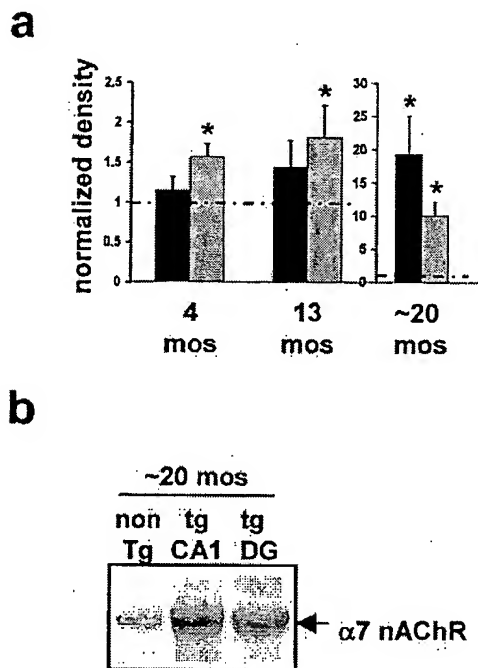


Figure 4. $\alpha 7$ nAChR is upregulated in hippocampus and DG of Tg2576 mice. *a*, Quantitative immunoblot of area CA1 and DG from 4, 13, and \sim 20 month Tg2576 hippocampus reveals upregulation of $\alpha 7$ nAChR protein as early as 4 months. *Significantly higher $\alpha 7$ nAChR level than age-matched control animals ($p < 0.03$) by Student's *t* test. Dashed line represents normalized control animal level; note the change in scale for \sim 20 month animals. Filled bar, CA1; shaded bar, DG. *b*, Representative immunoblot for $\alpha 7$ nAChR level in Tg2576 and age-matched control animals.

upregulation (Marks et al., 1983; Fenster et al., 1999). We therefore hypothesized that $\alpha 7$ nAChRs would be upregulated in Tg2576 hippocampus as a consequence of chronic exposure to $\text{A}\beta$. We found an age-dependent increase in $\alpha 7$ nAChR protein in the hippocampi of these animals as compared with age-matched controls (Fig. 4*a,b*). This increase is detected as early as 4 months of age in dentate gyrus (DG). With age, $\alpha 7$ nAChR protein continues to increase in the DG as well as in area CA1. As a control, we measured the level of another subtype of nAChR subunit, the $\alpha 4$ subunit, and found no significant increase in $\alpha 4$ nAChR protein in the hippocampi of Tg2576 animals (data not shown). Thus our data demonstrate a selective age-dependent upregulation of $\alpha 7$ nAChR in the hippocampus of Tg2576 mice. An explanation for these data in light of our findings *in vitro* is that $\alpha 7$ nAChRs in the hippocampi of Tg2576 animals are stimulated chronically by $\text{A}\beta$, leading to desensitization and upregulation of $\alpha 7$ nAChRs.

Given the necessity for ERK2 MAPK activity in certain forms of learning and memory, the finding that $\text{A}\beta 42$ activates ERK MAPK via $\alpha 7$ nAChRs, and the observation that $\alpha 7$ nAChRs are upregulated in $\text{A}\beta$ -overexpressing mice, we determined whether the ERK MAPK cascade is disrupted in Tg2576 hippocampus. Quantitative immunoblot reveals that ERK2 phosphorylation is increased significantly in Tg2576 hippocampus as compared with controls (Fig. 5*a,c*, Table 1). In area CA1 at 13 months and in DG at 4 and 13 months, ERK2 MAPK hyperactivation is detected. These results correlate with elevated $\alpha 7$ nAChR protein in these brain regions as was described above. By 20 months of age ERK2 MAPK is downregulated; the hyperactivation detected at earlier

ages is absent in DG and is below control animal levels in area CA1. At this age total ERK2 MAPK protein is unchanged in DG, whereas in area CA1 both total ERK2 MAPK protein and activity are downregulated by 22 and 27%, respectively. Previous evidence suggests that this level of reduction in ERK2 MAPK activity in hippocampus can lead to learning and memory impairments. For example, Selcher et al. (1999) have shown that partial inhibition of ERK2 MAPK activity in hippocampus blocks two forms of hippocampus-dependent learning in the mouse.

Because ERK MAPK is altered in the hippocampi of Tg2576 animals, it is of interest to learn whether downstream targets of this kinase cascade also are affected. CREB is phosphorylated at Ser133 by rsk2, a kinase that is activated by ERK MAPK phosphorylation (Xing et al., 1996). We evaluated the phosphorylation state and total protein level of CREB protein in CA1 and DG of Tg2576 hippocampi by quantitative immunoblotting (Fig. 5*b,d*, Table 1). In Tg2576 hippocampus, CREB phosphorylation is elevated at 13 months, followed by downregulation by 20 months of age. In area CA1, CREB phosphorylation fluctuates with ERK2 MAPK activity, consistent with CREB phosphorylation being coupled to the ERK MAPK cascade (Roberson and Sweatt, 1996; Impey et al., 1998; Watabe et al., 2000). CREB protein level was not altered significantly in area CA1. These data demonstrate that, in area CA1, derangements of the ERK MAPK cascade occur in conjunction with dysregulation of a downstream target, the transcriptional regulator CREB. In DG, however, CREB protein level is elevated at 13 and 20 months of age, indicative of differential regulation of CREB in DG versus area CA1. Furthermore, the correlated CREB phosphorylation with ERK2 activation was not observed in DG, although coupling between ERK MAPK activity and CREB phosphorylation at Ser133 in this region has been demonstrated (Davis et al., 2000).

Tg2576 animals exhibit long-term potentiation (LTP) and working memory deficits by 9 months of age and a spatial learning impairment that is evident at 6 months, which deteriorates further at 20–26 months of age (M. Westerman and K. H. Ashe, personal communication). We tested whether the increased $\alpha 7$ nAChR protein we observed correlated with behavioral learning defects in these animals. Before biochemical analysis, Tg2576 and control animals were trained and tested in the Morris water maze. A scatter plot of the $\alpha 7$ nAChR levels of individual animals versus the percentage of time spent in the target quadrant during a third probe trial in the Morris water maze illustrates a negative correlation ($R^2 = -0.283$ and -0.193 ; $p \leq 0.05$, for CA1 and DG, respectively) between $\alpha 7$ nAChR level and Morris water maze performance (Fig. 6). These data do not indicate a simple linear correlation between $\alpha 7$ nAChR protein levels and Morris water maze performance. However, these observations are consistent with the idea that $\alpha 7$ nAChR upregulation in hippocampus may serve as a biochemical marker for the synaptic plasticity derangement and learning and memory deficits in Tg2576 animals.

We further tested the hypothesis that chronic exposure to $\text{A}\beta 42$ leads to $\alpha 7$ nAChR upregulation in hippocampus by incubating cultured hippocampal slices with 100 pM $\text{A}\beta 42$ for 6 d. After 144 hr of $\text{A}\beta$ exposure, $\alpha 7$ nAChR protein was increased by over twofold (Fig. 7). Treated slices had the same appearance as control slices after 9 d in culture. These data demonstrate that prolonged exposure *in vitro* to a concentration of $\text{A}\beta$ found in the brains of AD patients and Tg2576 animals leads to $\alpha 7$ nAChR upregulation in hippocampal tissue.

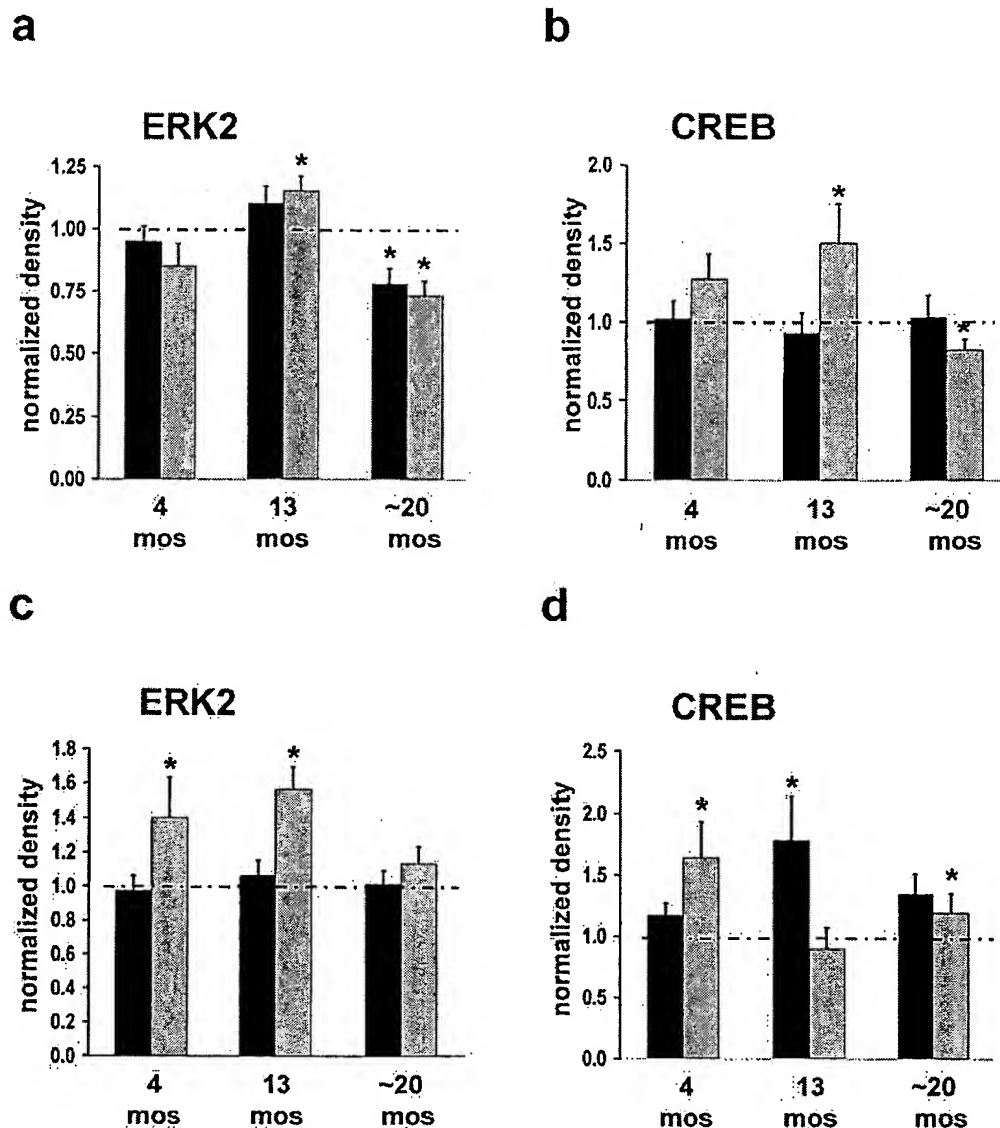


Figure 5. Downstream targets of $\alpha 7$ nAChR activation in Tg2576 hippocampus exhibit dysregulation. ERK2 and CREB proteins undergo hyperactivation, followed by downregulation, as compared with age-matched control animals. Differences between Tg2576 and age-matched control animals were detected by quantitative immunoblot of area CA1 and DG from 4, 13, and \sim 20 month Tg2576 hippocampus. Samples were evaluated for total and phospho-ERK2 MAPK (*a*, *c*) and total and phospho-CREB (*b*, *d*) levels in CA1 and DG, respectively. *Significant difference from age-matched control animal level ($p \leq 0.05$) by Student's *t* test. Dashed line represents normalized control animal level. Filled bar, Total; shaded bar, phospho.

DISCUSSION

We have demonstrated that the $\alpha 7$ nAChR couples $\text{A}\beta 42$ to the ERK2 MAPK cascade in hippocampus, uses Ca^{2+} , and is independent of action potential propagation. We found that, *in vitro*, concentrations of $\text{A}\beta 42$ that occur in the CSF and brain of AD patients rapidly activate hippocampal ERK2 MAPK and lead to $\alpha 7$ nAChR upregulation with chronic exposure. The experiments performed in this study do not address directly whether the $\alpha 7$ nAChR is a receptor for $\text{A}\beta 42$. However, the following observations are consistent with this idea: (1) extended exposure of cultured rat hippocampal slices to $\text{A}\beta 42$ blocks subsequent $\alpha 7$ nAChR agonist activation of ERK2 MAPK (under these conditions the ERK MAPK cascade is not desensitized to activation by phorbol ester); (2) both MLA and BTX block $\text{A}\beta 42$ activation of ERK2 MAPK; (3) TTX does not block $\text{A}\beta 42$ activation of ERK2 MAPK. Furthermore, ERK2 MAPK activation by $\text{A}\beta 42$ requires

Ca^{2+} influx, which is consistent with the model that Ca^{2+} influx via $\alpha 7$ nAChRs and $\alpha 7$ nAChR-dependent depolarization-induced Ca^{2+} influx leads to ERK2 MAPK activation. We favor the interpretation that $\text{A}\beta 42$ is an agonist for $\alpha 7$ nAChRs in hippocampus and that prolonged exposure to $\text{A}\beta$ can elicit $\alpha 7$ nAChR upregulation as a result of chronic receptor stimulation, a typical phenomenon after chronic nAChR agonist exposure (Marks et al., 1983; Fenster et al., 1999). In turn, we hypothesize that prolonged exposure of $\alpha 7$ nAChRs to $\text{A}\beta$ leads to chronic stimulation of ERK2 MAPK.

As predicted by our *in vitro* findings, we observed effects on $\alpha 7$ nAChR and ERK2 MAPK in the hippocampus of a transgenic mouse line that overproduces $\text{A}\beta$ peptides (Hsiao et al., 1996). In the hippocampi of these animals $\alpha 7$ nAChR protein increases in an age-dependent manner, whereas the basal activation state of ERK2 MAPK exhibits an age-dependent hyperactivation fol-

Table 1. Data summary for the parameters measured in hippocampi of Tg2576 mice at different ages as compared with age-matched control animals

Protein detected	Age (months)		
	4	13	~20
CA1			
ERK2 MAPK	0.95 ± 0.06 (ns)	1.10 ± 0.07 (ns)	0.78 ± 0.06 (0.017)
Phospho-ERK2 MAPK	0.85 ± 0.09 (ns)	1.15 ± 0.06 (0.03)	0.73 ± 0.06 (0.001)
CREB	1.02 ± 0.11 (ns)	0.93 ± 0.13 (ns)	1.03 ± 0.14 (ns)
Phospho-CREB	1.27 ± 0.16 (ns)	1.50 ± 0.25 (0.041)	0.82 ± 0.07 (0.015)
$\alpha 7$ nAChR	1.15 ± 0.17 (ns)	1.45 ± 0.33 (ns)	19.17 ± 5.89 (0.002)
DG			
ERK2 MAPK	0.97 ± 0.09 (ns)	1.06 ± 0.09 (ns)	1.01 ± 0.08 (ns)
Phospho-ERK2 MAPK	1.40 ± 0.23 (0.05)	1.56 ± 0.13 (0.001)	1.13 ± 0.10 (ns)
CREB	1.17 ± 0.10 (ns)	1.78 ± 0.35 (0.025)	1.35 ± 0.16 (0.03)
Phospho-CREB	1.64 ± 0.29 (0.015)	0.90 ± 0.17 (ns)	1.19 ± 0.16 (ns)
$\alpha 7$ nAChR	1.57 ± 0.16 (0.005)	1.82 ± 0.40 (0.028)	10.00 ± 2.08 (<0.001)

Relative densities are measured from immunoblots as described. Mean normalized densities are reported ± SEM. In parentheses below each mean value are Student's *t* test results. ns, Not significant.

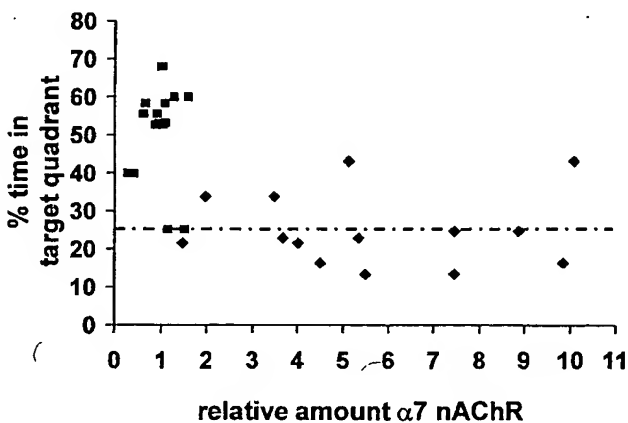


Figure 6. Animals with elevated $\alpha 7$ nAChR level fail to perform to criteria in the Morris water maze. Scatter plot of the third probe trial performance of individual ~20-month-old Tg2576 and control animals versus $\alpha 7$ nAChR protein levels in CA1 and DG. Dashed line indicates performance criterion. Filled squares, Control; filled diamonds, Tg.

lowed by downregulation. ERK2 MAPK hyperactivation is coincident with $\alpha 7$ nAChR upregulation at young ages; one interpretation of these data is that, in these animals, $\text{A}\beta$ chronically stimulates the ERK MAPK cascade via $\alpha 7$ nAChRs. Likewise, the phosphorylation state of CREB, a downstream effector of the ERK MAPK cascade in area CA1, parallels the changes measured in ERK2 MAPK in this region. Thus, in Tg2576 animals and, we hypothesize in AD as well, elevated $\text{A}\beta$ has profound

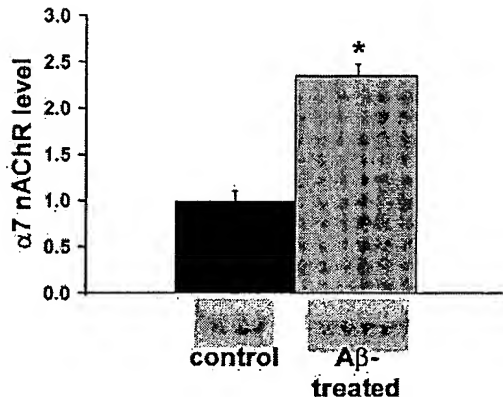


Figure 7. Chronic exposure to $\text{A}\beta 42$ leads to increased $\alpha 7$ nAChR protein in hippocampal slice cultures. Cultured rat hippocampal slices were exposed to 100 pm $\text{A}\beta 42$ for 144 hr, and $\alpha 7$ nAChR protein was quantified by immunoblot. The data that are expressed are normalized to the $\alpha 7$ nAChR protein level in cultures that were left untreated. Representative immunoblot results are shown below the histogram. *Significant difference from control level ($p < 0.0001$) by Student's *t* test. Basal, 1.00 ± 0.11; $\text{A}\beta 42$ -treated, 2.35 ± 0.13.

effects on an $\text{A}\beta$ receptor ($\alpha 7$ nAChR) and a signal transduction cascade (ERK MAPK) to which it is coupled. In older Tg2576 animals the pronounced upregulation of $\alpha 7$ nAChRs is associated with the downregulation of ERK2 MAPK.

Exposure of hippocampal slices to $\text{A}\beta 42$ triggers signal transduction events that are important for hippocampal synaptic plasticity and learning and memory; activation of the ERK2 MAPK cascade *in vitro* by $\text{A}\beta 42$ requires $\alpha 7$ nAChR function. These findings are consistent with the concept that $\alpha 7$ nAChR is an $\text{A}\beta 42$ receptor. There is an emerging literature implicating the $\alpha 7$ nAChR in AD pathophysiology and memory loss. Evidence complementing our data that $\text{A}\beta 42$ signals via the $\alpha 7$ nAChR includes the previous observations that (1) $\alpha 7$ nAChRs coimmunoprecipitate from postmortem human AD hippocampus; (2) $\text{A}\beta$ peptides compete $\alpha 7$ agonist and antagonist binding to SK-N-MC cells; (3) 20-fold more $\alpha 7$ nAChR protein immunoprecipitates with $\text{A}\beta 42$ from AD hippocampus as compared with control; (4) preincubation with $\text{A}\beta 42$ antagonizes an $\alpha 7$ nAChR-like current in hippocampal interneurons; and (5) nicotine protects SK-N-MC cells from neurotoxicity induced by prolonged exposure to $\text{A}\beta 42$ (Kihara et al., 1997; Wang et al., 2000). These last two observations are akin to the cross-desensitization of $\text{A}\beta 42$ and nicotine demonstrated in this study. It must be emphasized, however, that additional $\text{A}\beta$ receptors that play important roles in AD etiology are likely (Yan et al., 1996).

What then are the consequences of $\alpha 7$ nAChR coupling $\text{A}\beta 42$ to the ERK MAPK cascade in AD? Our findings suggest that early AD etiology involves chronic activation of the ERK MAPK cascade as a consequence of elevated $\text{A}\beta$ binding to and activating this signaling cascade via $\alpha 7$ nAChRs and that these events are concomitant with $\alpha 7$ nAChR upregulation and derangement of ERK2 MAPK signaling. $\text{A}\beta$ burden is emerging as an early indicator of cognitive decline in AD in that total $\text{A}\beta$ (nonaggregate and aggregates in diffuse or mature senile plaques combined) in the brains of elderly patients correlates with recent premorbid Clinical Dementia Rating scale values, even in the absence of severe dementia (Cummings and Cotman, 1995; Cummings et al., 1996; Naslund et al., 2000). Moreover, CSF $\text{A}\beta$ is elevated to nanomolar level in patients with short disease dura-

tion and mild cognitive impairment (Nakamura et al., 1994; Tapiola et al., 2000). These findings support the idea that extracellular $\text{A}\beta$ levels are elevated in at-risk individuals before gross plaque deposition and severe cognitive impairment. According to our findings, one consequence of nanomolar $\text{A}\beta$ in the extracellular milieu of AD brain is the (chronic) activation of the ERK2 MAPK cascade via $\alpha 7$ nAChRs, leading to upregulation of this receptor type. In fact, we have demonstrated *in vitro* that chronic exposure to $\text{A}\beta 42$ leads to increased $\alpha 7$ nAChR protein in hippocampus. An interesting implication of this hypothesis is that $\alpha 7$ nAChR-selective radioimaging techniques may be useful as a diagnostic test for early AD or risk for AD (Nordberg, 1999; Scheffel et al., 2000).

The ERK2 MAPK cascade is known to play a critical role in hippocampus synaptic plasticity and learning. In area CA1 of the rodent hippocampus ERK2 MAPK is necessary for the expression of a late phase of LTP (English and Sweatt, 1997; Impey et al., 1998; Selcher et al., 1999) and is an important pathway through which neurotransmitters modulate LTP induction (Roberson et al., 1999; Winder et al., 1999; Watabe et al., 2000). Furthermore, ERK2 MAPK activation is necessary for both contextual fear conditioning and escape training in the Morris water maze, both hippocampus-dependent associative learning paradigms (Atkins et al., 1998; Blum et al., 1999; Selcher et al., 1999). Tg2576 animals, in which $\text{A}\beta$ production is elevated, exhibit deficits in hippocampus LTP, working memory, and escape training in the Morris water maze (Hsiao et al., 1996; Chapman et al., 1999). On the basis of our findings, we propose a mechanism linking $\text{A}\beta$ overproduction to memory dysfunction; specifically, our data suggest that memory deficits occur in part via $\text{A}\beta 42$ eliciting downstream derangements in ERK MAPK signaling. $\text{A}\beta 42$ impinging on the ERK MAPK cascade suggests a molecular basis for the disruptions in memory formation accompanying AD, because the proper functioning of the ERK MAPK cascade is critical for certain types of memory formation.

Our model for the signal transduction events underlying AD etiology posits that elevated $\text{A}\beta$, such as occurs in humans genetically predisposed to the disease, chronically stimulates the ERK MAPK cascade via $\alpha 7$ nAChRs. Chronic exposure to $\text{A}\beta$ leads to upregulation of $\alpha 7$ nAChRs and hyperactivation, followed by downregulation of ERK2 MAPK as well as perturbed functionality of downstream targets of this kinase. This derangement of the ERK MAPK signaling cascade may underlie the learning and memory deficits attributed to hippocampal dysfunction in AD. An additional site of action is likely to be disruption of the normal function of the hippocampal circuit, specifically the altered excitability of pyramidal neurons because $\alpha 7$ nAChRs located on GABAergic interneurons can regulate hippocampal pyramidal neuron excitability (Freund et al., 1988, 1990; Frazier et al., 1998). Modifications of GABAergic signaling to area CA1 pyramidal neurons in the hippocampi of animals in which $\text{A}\beta$ production is either enhanced or genetically knocked-out have been demonstrated (Fitzjohn et al., 2000; Zaman et al., 2000). Overall, these findings highlight a potential therapeutic target for AD: the $\alpha 7$ nAChR.

In addition to assuaging the MAPK signaling derangement we have described, $\alpha 7$ nAChR antagonist therapy might benefit other aspects of AD etiology such as the selective loss of cholinergic inputs to the hippocampus and cortex as well as effects on $\text{A}\beta$ production itself. The cholinergic input to the hippocampus and cortex is a particularly vulnerable neural circuit in AD, and $\alpha 7$ nAChRs are expressed on these projection neurons from the

basal forebrain (Arendt et al., 1985; Breese et al., 1997). Our data suggest the possibility that $\text{A}\beta 42$ binding to presynaptic $\alpha 7$ nAChRs may elicit cholinergic fiber loss, and $\alpha 7$ nAChR antagonism might delay this aspect of neurodegeneration in AD.

Finally, although the molecular basis for $\text{A}\beta$ overproduction that is a consequence of FAD-linked gene inheritance is not understood, the ERK MAPK cascade has been implicated in regulating $\text{A}\beta$ production in neurons (Mills et al., 1997). One of the effects of downregulated ERK2 MAPK activity may be the setting up of a positive feedback loop for $\text{A}\beta$ accumulation; blocking the derangement of MAPK signaling via the $\alpha 7$ nAChR thus may alleviate one stimulant of $\text{A}\beta$ production. Overall, the findings presented here provide insights into the molecular basis of $\text{A}\beta$ -induced pathology and advance the possibilities for treatment targets in AD.

REFERENCES

- Andreasen N, Hesse C, Davidsson P, Minthon L, Wallin A, Winblad B, Vanderstichele H, Vanmechelen E, Blennow K (1999a) Cerebrospinal fluid β -amyloid (1–42) in Alzheimer disease: differences between early- and late-onset Alzheimer disease and stability during the course of disease [see comments]. *Arch Neurol* 56:673–680.
- Andreasen N, Minthon L, Vanmechelen E, Vanderstichele H, Davidsson P, Winblad B, Blennow K (1999b) Cerebrospinal fluid tau and $\text{A}\beta 42$ as predictors of development of Alzheimer's disease in patients with mild cognitive impairment. *Neurosci Lett* 273:5–8.
- Arendt T, Bigl V, Tennstedt A, Arendt A (1985) Neuronal loss in different parts of the nucleus basalis is related to neuritic plaque formation in cortical target areas in Alzheimer's disease. *Neuroscience* 14:1–14.
- Atkins CM, Selcher JC, Petraitis JJ, Trzaskos JM, Sweatt JD (1998) The MAPK cascade is required for mammalian associative learning. *Nat Neurosci* 1:602–609.
- Blum S, Moore AN, Adams F, Dash PK (1999) A mitogen-activated protein kinase cascade in the CA1/CA2 subfield of the dorsal hippocampus is essential for long-term spatial memory. *J Neurosci* 19:3535–3544.
- Borchelt DR (1998) Inherited neurodegenerative diseases and transgenic models. *Lab Anim Sci* 48:604–610.
- Bourchuladze R, Frenguelli B, Blendy J, Cioffi D, Schutz G, Silva AJ (1994) Deficient long-term memory in mice with a targeted mutation of the cAMP-responsive element binding protein. *Cell* 79:59–68.
- Breese CR, Adams C, Logel J, Drebing C, Rollins Y, Barnhart M, Sullivan B, Demasters BK, Freedman R, Leonard S (1997) Comparison of the regional expression of nicotinic acetylcholine receptor $\alpha 7$ mRNA and [^{125}I]- α -bungarotoxin binding in human postmortem brain. *J Comp Neurol* 387:385–398.
- Brining SK (1997) Predicting the *in vitro* toxicity of synthetic β -amyloid (1–40). *Neurobiol Aging* 18:581–589.
- Burdick D, Soreghan B, Kwon M, Kosmoski J, Knauer M, Henschen A, Yates J, Cotman C, Glabe C (1992) Assembly and aggregation properties of synthetic Alzheimer's $\alpha 4/\beta$ -amyloid peptide analogs. *J Biol Chem* 267:546–554.
- Chapman PF, White GL, Jones MW, Cooper-Blacketer D, Marshall VJ, Irizarry M, Younkin L, Good MA, Bliss TV, Hyman BT, Younkin SG, Hsiao KK (1999) Impaired synaptic plasticity and learning in aged amyloid precursor protein transgenic mice. *Nat Neurosci* 2:271–276.
- Cummings BJ, Cotman CW (1995) Image analysis of β -amyloid load in Alzheimer's disease and relation to dementia severity. *Lancet* 346:1524–1528.
- Cummings BJ, Pike CJ, Shankle R, Cotman CW (1996) β -Amyloid deposition and other measures of neuropathology predict cognitive status in Alzheimer's disease [see comments]. *Neurobiol Aging* 17:921–933.
- Davis S, Vanhoutte P, Pages C, Caboche J, Laroche S (2000) The MAPK/ERK cascade targets both Elk-1 and cAMP response element-binding protein to control long-term potentiation-dependent gene expression in the dentate gyrus *in vivo*. *J Neurosci* 20:4563–4572.
- Dodart JC, Mathis C, Ungerer A (2000) The β -amyloid precursor protein and its derivatives: from biology to learning and memory processes. *Rev Neurosci* 11:75–93.
- Ekinci FI, Malik KU, Shea TB (1999) Activation of the L voltage-sensitive calcium channel by mitogen-activated protein (MAP) kinase following exposure of neuronal cells to β -amyloid. MAP kinase mediates β -amyloid-induced neurodegeneration. *J Biol Chem* 274:30322–30327.
- English JD, Sweatt JD (1997) A requirement for the mitogen-activated protein kinase cascade in hippocampal long-term potentiation. *J Biol Chem* 272:19103–19106.

Fenster CP, Whitworth TL, Sheffield EB, Quick MW, Lester RA (1999) Upregulation of surface $\alpha 4\beta 2$ nicotinic receptors is initiated by receptor desensitization after chronic exposure to nicotine. *J Neurosci* 19:4804–4814.

Fitzjohn SM, Morton RA, Kuenzi F, Davies CH, Seabrook GR, Collingridge GL (2000) Similar levels of long-term potentiation in amyloid precursor protein: null and wild-type mice in the CA1 region of picrotoxin-treated slices. *Neurosci Lett* 288:9–12.

Frazier CJ, Rollins YD, Breese CR, Leonard S, Freedman R, Dunwiddie TV (1998) Acetylcholine activates an α -bungarotoxin-sensitive nicotinic current in rat hippocampal interneurons, but not pyramidal cells. *J Neurosci* 18:1187–1195.

Freund RK, Jungschaffer DA, Collins AC, Wehner JM (1988) Evidence for modulation of GABAergic neurotransmission by nicotine. *Brain Res* 453:215–220.

Freund RK, Luntz-Leybman V, Collins AC (1990) Nicotine interferes with GABA-mediated inhibitory processes in mouse hippocampus. *Brain Res* 527:286–291.

Garzon-Rodriguez W, Sepulveda-Becerra M, Milton S, Glabe CG (1997) Soluble amyloid $\text{A}\beta$ (1–40) exists as a stable dimer at low concentrations. *J Biol Chem* 272:21037–21044.

Hartley DM, Walsh DM, Ye CP, Diehl T, Vasquez S, Vassilev PM, Teplov DB, Selkoe DJ (1999) Protofibrillar intermediates of amyloid- β protein induce acute electrophysiological changes and progressive neurotoxicity in cortical neurons. *J Neurosci* 19:8876–8884.

Hsiao K (1998) Transgenic mice expressing Alzheimer amyloid precursor proteins. *Exp Gerontol* 33:883–889.

Hsiao K, Chapman P, Nilsen S, Eckman C, Harigaya Y, Younkin S, Yang F, Cole G (1996) Correlative memory deficits, $\text{A}\beta$ elevation, and amyloid plaques in transgenic mice [see comments]. *Science* 274:99–102.

Impey S, Obriean K, Wong ST, Poser S, Yano S, Wayman G, Deloulme JC, Chan G, Storm DR (1998) Cross talk between ERK and PKA is required for Ca^{2+} stimulation of CREB-dependent transcription and ERK nuclear translocation. *Neuron* 21:869–883.

Izarry MC, McNamara M, Fedorchak K, Hsiao K, Hyman BT (1997a) APPS^w transgenic mice develop age-related $\text{A}\beta$ deposits and neuropil abnormalities, but no neuronal loss in CA1 [see comments]. *J Neuropathol Exp Neurol* 56:965–973.

Izarry MC, Soriano F, McNamara M, Page KJ, Schenk D, Games D, Hyman BT (1997b) $\text{A}\beta$ deposition is associated with neuropil changes, but not with overt neuronal loss, in the human amyloid precursor protein V717F (PDAPP) transgenic mouse. *J Neurosci* 17:7053–7059.

Kihara T, Shimohama S, Sawada H, Kimura J, Kume T, Kochiyama H, Maeda T, Akaike A (1997) Nicotinic receptor stimulation protects neurons against β -amyloid toxicity. *Ann Neurol* 42:159–163.

Kosik KS, Qiu WQ, Greenberg S (1996) Cellular signaling pathways and cytoskeletal organization. *Ann NY Acad Sci* 777:114–120.

Kuo YM, Emmerling MR, Vigo-Pelfrey C, Kasunic TC, Kirkpatrick JB, Murdoch GH, Ball MJ, Roher AE (1996) Water-soluble $\text{A}\beta$ (N-40, N-42) oligomers in normal and Alzheimer disease brains. *J Biol Chem* 271:4077–4081.

Lambert MP, Barlow AK, Chromy BA, Edwards C, Freed R, Liosatos M, Morgan TE, Rozovsky I, Trommer B, Viola KL, Wals P, Zhang C, Finch CE, Kraft GA, Klein WL (1998) Diffusible, nonfibrillar ligands derived from $\text{A}\beta$ 1–42 are potent central nervous system neurotoxins. *Proc Natl Acad Sci USA* 95:6448–6453.

Marks MJ, Burch JB, Collins AC (1983) Effects of chronic nicotine infusion on tolerance development and nicotinic receptors. *J Pharmacol Exp Ther* 226:817–825.

McQuiston AR, Madison DV (1999) Nicotinic receptor activation excites distinct subtypes of interneurons in the rat hippocampus. *J Neurosci* 19:2887–2896.

Mills J, Laurent Charest D, Lam F, Beyreuther K, Ida N, Pelech SL, Reiner PB (1997) Regulation of amyloid precursor protein catabolism involves the mitogen-activated protein kinase signal transduction pathway. *J Neurosci* 17:9415–9422.

Nakamura T, Shoji M, Harigaya Y, Watanabe M, Hosoda K, Cheung TT, Shaffer LM, Golde TE, Younkin LH, Younkin SG (1994) Amyloid- β protein levels in cerebrospinal fluid are elevated in early-onset Alzheimer's disease. *Ann Neurol* 36:903–911.

Naslund J, Haroutunian V, Mohs R, Davis KL, Davies P, Greengard P, Buxbaum JD (2000) Correlation between elevated levels of amyloid β -peptide in the brain and cognitive decline [see comments]. *JAMA* 283:1571–1577.

Nordberg A (1999) PET studies and cholinergic therapy in Alzheimer's disease. *Rev Neurol (Paris)* 155:S53–S63.

Orr-Urtreger A, Broide RS, Kasten MR, Dang H, Dani JA, Beaudet AL, Patrick JW (2000) Mice homozygous for the L250T mutation in the $\alpha 7$ nicotinic acetylcholine receptor show increased neuronal apoptosis and die within 1 day of birth. *J Neurochem* 74:2154–2166.

Payne DM, Rossomando AJ, Martino P, Erickson AK, Her JH, Shabanowitz J, Hunt DF, Weber MJ, Sturgill TW (1991) Identification of the regulatory phosphorylation sites in pp42/mitogen-activated protein kinase (MAP kinase). *EMBO J* 10:885–892.

Perry EK, Morris CM, Court JA, Cheng A, Fairbairn AF, McKeith IG, Irving D, Brown A, Perry RH (1995) Alteration in nicotine binding sites in Parkinson's disease, Lewy body dementia, and Alzheimer's disease: possible index of early neuropathology. *Neuroscience* 64:385–395.

Pettit DL, Shao Z, Yakel JL (2001) β -Amyloid 1–42 peptide directly modulates nicotinic receptors in the rat hippocampal slice. *J Neurosci* 21:RC120.

Rapoport M, Ferreira A (2000) PD98059 prevents neurite degeneration induced by fibrillar β -amyloid in mature hippocampal neurons. *J Neurochem* 74:125–133.

Revah F, Bertrand D, Galzi JL, Devillers-Thiery A, Mulle C, Hussy N, Bertrand S, Ballivet M, Changeux JP (1991) Mutations in the channel domain alter desensitization of a neuronal nicotinic receptor. *Nature* 353:846–849.

Roberson ED, Sweatt JD (1996) Transient activation of cyclic AMP-dependent protein kinase during hippocampal long-term potentiation. *J Biol Chem* 271:30436–30441.

Roberson ED, English JD, Adams JP, Selcher JC, Kondratowicz C, Sweatt JD (1999) The mitogen-activated protein kinase cascade couples PKA and PKC to cAMP response element binding protein phosphorylation in area CA1 of hippocampus. *J Neurosci* 19:4337–4348.

Saitoh T, Horsburgh K, Masliah E (1993) Hyperactivation of signal transduction systems in Alzheimer's disease. *Ann NY Acad Sci* 695:34–41.

Schafe GE, Nadel NV, Sullivan GM, Harris A, LeDoux JE (1999) Memory consolidation for contextual and auditory fear conditioning is dependent on protein synthesis, PKA, and MAP kinase. *Learn Mem* 6:97–110.

Scheffel U, Hortsch AG, Koren AO, Ravert HT, Banta JP, Finley PA, London ED, Dannals RF (2000) 6-[¹⁸F]fluoro-A-85380: an *in vivo* tracer for the nicotinic acetylcholine receptor. *Nucl Med Biol* 27:51–56.

Seguela P, Wadiche J, Dineley-Miller K, Dani JA, Patrick JW (1993) Molecular cloning, functional properties, and distribution of rat brain $\alpha 7$: a nicotinic cation channel highly permeable to calcium. *J Neurosci* 13:596–604.

Selcher JC, Atkins CM, Trzaskos JM, Paylor R, Sweatt JD (1999) A necessity for MAP kinase activation in mammalian spatial learning. *Learn Mem* 6:478–490.

Selkoe DJ (1998) The cell biology of β -amyloid precursor protein and presenilin in Alzheimer's disease. *Trends Cell Biol* 8:447–453.

Stoppini L, Buchs PA, Muller D (1991) A simple method for organotypic cultures of nervous tissue. *J Neurosci Methods* 37:173–182.

Sturgill TW, Ray LB, Erikson E, Maller JL (1988) Insulin-stimulated MAP-2 kinase phosphorylates and activates ribosomal protein S6 kinase II. *Nature* 334:715–718.

Tapiola T, Pirttila T, Mikkonen M, Mehta PD, Alafuzoff I, Koivisto K, Soininen H (2000) Three-year follow-up of cerebrospinal fluid tau, β -amyloid 42 and 40 concentrations in Alzheimer's disease. *Neurosci Lett* 280:119–122.

Wang HY, Lee DH, D'Andrea MR, Peterson PA, Shank RP, Reitz AB (2000) β -Amyloid (1–42) binds to $\alpha 7$ nicotinic acetylcholine receptor with high affinity. Implications for Alzheimer's disease pathology. *J Biol Chem* 275:5626–5632.

Watabe AM, Zaki PA, O'Dell TJ (2000) Coactivation of β -adrenergic and cholinergic receptors enhances the induction of long-term potentiation and synergistically activates mitogen-activated protein kinase in the hippocampal CA1 region. *J Neurosci* 20:5924–5931.

Winder DG, Martin KC, Muzzio IA, Rohrer D, Chruscinski A, Kobilka B, Kandel ER (1999) ERK plays a regulatory role in induction of LTP by theta frequency stimulation and its modulation by β -adrenergic receptors. *Neuron* 24:715–726.

Xing J, Ginty DD, Greenberg ME (1996) Coupling of the RAS–MAPK pathway to gene activation by RSK2, a growth factor-regulated CREB kinase. *Science* 273:959–963.

Yan SD, Chen X, Fu J, Chen M, Zhu H, Roher A, Slattery T, Zhao L, Nagashima M, Morser J, Migheli A, Nawroth P, Stern D, Schmidt AM (1996) RAGE and amyloid- β peptide neurotoxicity in Alzheimer's disease [see comments]. *Nature* 382:685–691.

Zaman SH, Parent A, Laskey A, Lee MK, Borchelt DR, Sisodia SS, Malinow R (2000) Enhanced synaptic potentiation in transgenic mice expressing presenilin 1 familial Alzheimer's disease mutation is normalized with a benzodiazepine. *Neurobiol Dis* 7:54–63.



Differential activation of neuronal ERK, JNK/SAPK and p38 in Alzheimer disease: the 'two hit' hypothesis

Xiongwei Zhu ^a, Rudolph J. Castellani ^a, Atsushi Takeda ^b,
Akihiko Nunomura ^c, Craig S. Atwood ^a, George Perry ^a,
Mark A. Smith ^{a,*}

^a *Institute of Pathology, Case Western Reserve University, 2085 Adelbert Road, Cleveland,
OH 44106, USA*

^b *Department of Neurology, Tohoku University School of Medicine, Sendai 980-8574, Japan*

^c *Department of Psychiatry and Neurology, Asahikawa Medical College, Asahikawa 078-8510, Japan*

Abstract

There are multiple lines of evidence showing that oxidative stress and aberrant mitogenic signaling play an important role in the pathogenesis of Alzheimer disease. However, the chronological relationship between these and other events associated with disease pathogenesis is not known. Given the important role that mitogen-activated protein kinase (MAPK) pathways play in both mitogenic signaling (ERK) and cellular stress signaling (JNK/SAPK and p38), we investigated the chronological and spatial relationship between activated ERK, JNK/SAPK and p38 during disease progression. While all three kinases are activated in the same susceptible neurons in mild and severe cases (Braak stages III–VI), in non-demented cases with limited pathology (Braak stages I and II), both ERK and JNK/SAPK are activated but p38 is not. However, in non-demented cases lacking any sign of pathology (Braak stage 0), either ERK alone or JNK/SAPK alone can be activated. Taken together, these findings indicate that MAPK pathways are differentially activated during the course of Alzheimer disease and, by inference, suggest that both oxidative stress and abnormalities in mitotic signaling can independently serve to initiate, but both are necessary to propagate, disease pathogenesis. Therefore, we propose that both 'hits', oxidative stress and mitotic alterations, are necessary for the progression of Alzheimer disease. © 2001 Elsevier Science Ireland Ltd. All rights reserved.

Abbreviations: AD, Alzheimer disease; DAB, 3,3'-diaminobenzidine; JNK/SAPK, c-Jun N-terminal kinase/stress activated protein kinase; NGS, normal goat serum; TBS, Tris-buffered saline.

* Corresponding author. Tel.: +1-216-368-3670; fax: +1-216-368-8964.

E-mail address: mas21@po.cwru.edu (M.A. Smith).

Keywords: Alzheimer disease; MAPK mitogen; Oxidative stress

1. Introduction

Mitogen-activated protein kinase (MAPK) pathways are the central mediators that propagate extracellular signals from the membrane to the nucleus. The three best-known MAPK pathways are extracellular signal-regulated kinase (ERK), c-Jun N-terminal kinase/stress activated protein kinase (JNK/SAPK) and p38 pathways. While the ERK pathway is primarily activated by mitogenic stimuli, JNK/SAPK and p38 pathways are generally activated by cellular stressors such as oxidative stress (Robinson and Cobb, 1997; Cobb, 1999). Consistent with a pathogenic role for mitogenic stimulation (Raina et al., 2000) and oxidative stress (Markesberry, 1997; Perry et al., 1998) in Alzheimer disease (AD), these three pathways are all activated in susceptible neuronal populations in individuals with AD (Perry et al., 1999; Hensley et al., 1999; Zhu et al., 2000, 2001a,b; Shoji et al., 2000). Nonetheless, the temporal and spatial relationship of these kinases to one another, their relationship to potential disease-initiating factors as well as their relation to more downstream events, is unclear. However, given that these pathways are differentially activated by cellular stress (JNK/SAPK and p38) and mitogenic stimuli (ERK), a greater understanding of these pathways would, by inference, indicate the temporal properties of pathogenic events in AD. One obvious and important question is the relationship of oxidative stress and cell cycle abnormalities to each other and to the two pathological hallmarks of AD, namely the neurofibrillary tangles (NFT), composed of highly phosphorylated τ , and amyloid- β containing senile plaques (reviewed in Smith, 1998). Indeed, while oxidative stress and cell cycle progression are known to influence the phosphorylation state of τ protein (Raina et al., 2000; Busciglio et al., 1995; Takeda et al., 2000) as well as regulate amyloid- β production (Yan et al., 1995; Raina et al., 2000), the precise mechanisms by which these events occur in AD are not completely understood. To further address this, as well as the chronological sequence of events in individual neurons, in this study, we investigated the differential activation of the MAPK pathways in susceptible neuronal population in AD cases of different disease severity and non-demented control cases of various ages.

2. Materials and methods

2.1. Brain tissue

Hippocampal, frontal cortical and cerebellar brain tissue obtained postmortem was fixed in methacarn (methanol/chloroform/acetic acid, 6:3:1) at 4 °C for 16 h, dehydrated in ascending ethanol, embedded in paraffin and 6- μ m thick consecutive serial adjacent sections prepared on silane-coated slides (Sigma, St. Louis, MO) for

immunocytochemistry. Cases used in this study were chosen randomly and included control cases (patients with no evidence of neurodegenerative disease during life or following neuropathological examination) ranging from no pathology (Braak stage 0; $n = 7$, age = 17–81) to control cases with limited pathology (Braak stages I and II; $n = 6$, age = 62–89) and AD cases ranging from mild cases (Braak stages III and IV; $n = 4$, age = 79–90) to severe cases (Braak stages V and VI; $n = 7$, age = 60–91).

2.2. Immunocytochemical procedures

Immunocytochemistry was performed by the peroxidase anti-peroxidase protocol essentially as described previously (Sternberger, 1986; Perry et al., 1999; Zhu et al., 2000, 2001a,b). Briefly, following immersion in xylene, hydration through graded ethanol solutions and elimination of endogenous peroxidase activity by incubation in 3% hydrogen peroxide in methanol for 30 min, sections were incubated for 30 min at room temperature in 10% normal goat serum (NGS) in Tris-buffered saline (TBS; 50 mM Tris–HCl, 150 mM NaCl, pH 7.6) to reduce non-specific binding. After rinsing briefly with 1% NGS/TBS, adjacent sections were sequentially incubated overnight at 4 °C with either (i) immunoaffinity purified rabbit polyclonal antibody to phospho-ERK (Promega, Madison, WI), which only recognizes ERK activated by dual phosphorylation at Thr 202 and Tyr204; or (ii) immunoaffinity purified rabbit polyclonal antibody to phospho-JNK (New England Biolabs, Inc., Beverly, MA), which only recognizes JNK activated by dual phosphorylation at Thr183 and Tyr185; or (iii) immunoaffinity purified rabbit polyclonal antibody to phospho-p38 (New England Biolabs, Inc., Beverly, MA), which only recognizes p38 activated by dual phosphorylation at Thr180 and Tyr182; or (iv) mouse monoclonal AT8 antibody (Endogen, Woburn, MA) to phosphorylated cytoskeletal τ protein. The specificity of these antibodies was demonstrated previously by absorption and immunoblot analysis (Perry et al., 1999; Hensley et al., 1999; Zhu et al., 2000, 2001a,b). Following incubation with antibody, sections were briefly rinsed with 1% NGS-TBS and then sections were sequentially incubated in either goat anti-rabbit (ICN, Costa Mesa, CA) or goat anti-mouse (ICN, Costa Mesa, CA) antisera, followed by species-specific peroxidase anti-peroxidase complex (Sternberger Monoclonals Inc. and ICN, Cappel). 3,3'-Diaminobenzidine (DAB) was used as a chromagen.

3. Results

In control cases without any pathology (Braak stage 0), we observed two different patterns of MAPK activation in susceptible neuronal populations in both hippocampal and cortical regions. Either we found activated ERK in nuclei and diffusely in the cytoplasm with no evidence of activated phospho-JNK/SAPK or phospho-p38 (Fig. 1a–c) or, in other such control cases, we found phospho-JNK/SAPK in nuclei and diffusely in the cytoplasm but there was no evidence for

activated phospho-ERK and phospho-p38 (Fig. 1d–f). However, in control cases with limited pathology (Braak stages I and II), both phospho-ERK and phospho-JNK/SAPK were always detected in the nuclei and, more so, in the cytosol of susceptible neurons (not shown), including those with or without neuronal pathology demarcated by phospho-tau. Neurons containing phospho-p38 were either absent or rare in control cases with limited pathology.

In mild cases of AD (Braak stages III and IV), in addition to neurofibrillary pathology, phospho-ERK and phospho-JNK/SAPK also localized to nuclei and cytoplasm in areas with little pathology, although to a lesser extent, nuclear staining of phospho-p38 was sometimes also observed in these areas. In severe cases of AD (Braak stages V and VI), phospho-ERK localized to neurofibrillary pathology with a cytosolic punctate pattern being most prominent, while the distribution of phospho-JNK/SAPK and phospho-p38 was almost identical, namely, it was exclusively associated with the neurofibrillary tangles, senile plaque neurites, granulovacuolar degeneration and neuropil threads. In many neurons, phospho-ERK, phospho-JNK/SAPK and phospho-p38 were all co-localized (Fig. 2a–c). There was no apparent activation of these three MAPKs in cerebellar tissue in any of the AD

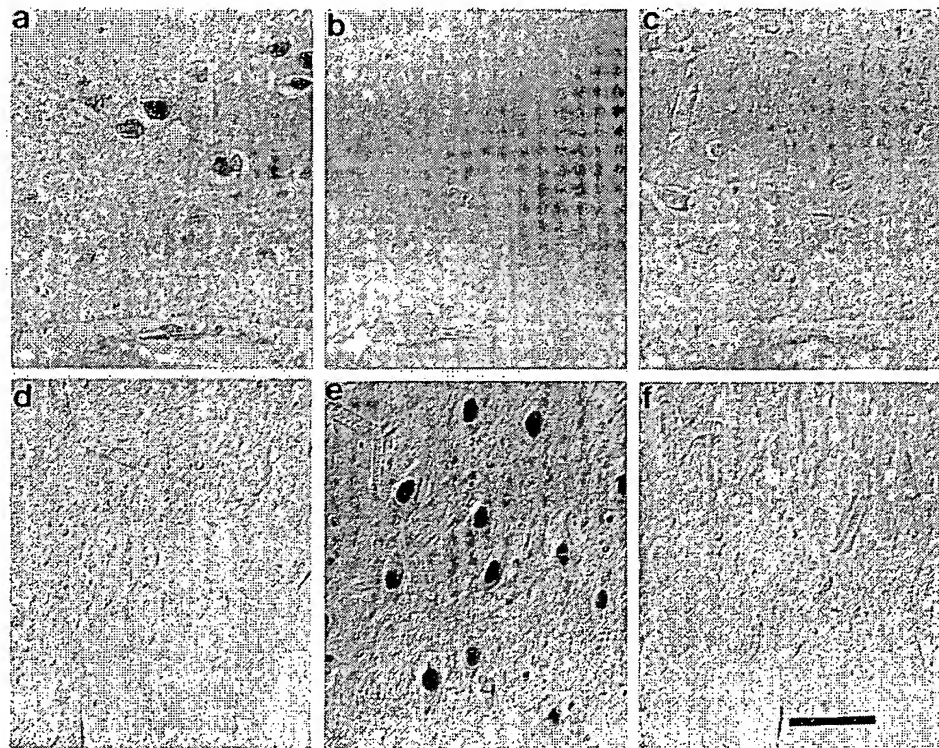


Fig. 1. In some control cases without any pathology (Braak stage 0) ERK (a) is activated while JNK/SAPK (b) and p38 (c) are not. In contrast, in some other control cases, JNK/SAPK (e) is activated while ERK (d) and p38 (f) are not. Scale bar: 50 μ m.

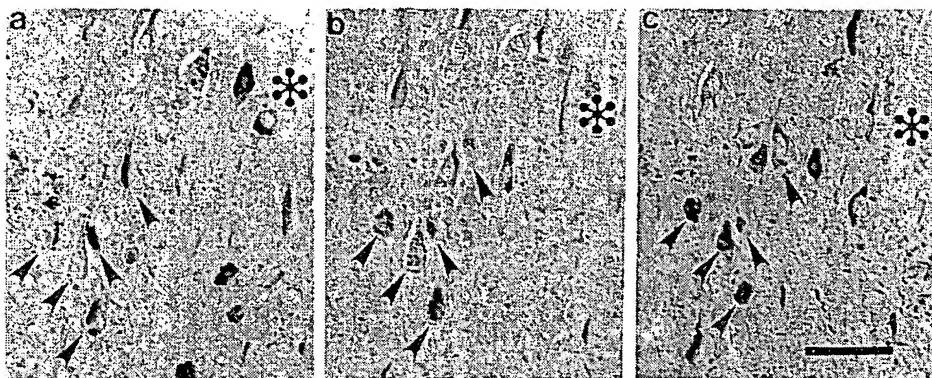


Fig. 2. Colocalization of phospho-ERK, phospho-JNK/SAPK and phospho-p38 in the very same neurons in AD can be appreciated in these serial adjacent sections. This is a representative result from a severe AD cases (Braak stages V and VI): (a) phospho-ERK, (b) phospho-JNK/SAPK, (c) phospho-p38. The arrows show representative neurons that contain phospho-ERK, phospho-JNK/SAPK and phospho-p38. * indicates landmark vessel in adjacent sections. Scale bar: 50 μ m.

or control cases examined indicating a regional specificity that parallels neuronal vulnerability.

4. Discussion

In this study, we provide evidence of the sequential activation of ERK, JNK/SAPK and p38 in susceptible neurons in control cases and individuals with AD. In control cases without any pathology (Braak stage 0) either ERK alone or JNK alone, where present, show almost exclusive activation in the nuclear compartment, whereas in those controls with limited pathology (Braak stages I and II), both ERK and JNK are simultaneously activated especially in the cytosol whereas p38 is not. Given that controls with pathology (Braak stages I and II) have a high tendency to develop AD (Petersen et al., 1999), it is likely that the simultaneous or co-activation of ERK and JNK represents one of the earliest events in disease pathogenesis that precipitates further alterations. Indeed, once a clinical diagnosis is apparent, i.e. Braak stages III–VI, all three kinases are activated in the same neurons in AD cases. This chronological activation of MAPK indicates that these kinases are sequentially activated and that p38 activation is a relatively later event than ERK and JNK/SAPK activation during the pathophysiology of AD. Notably, since each of these kinases can phosphorylate tau in vitro (Roder et al., 1993; Reynolds et al., 1997; Goedert et al., 1997) and co-localize or co-immunoprecipitate with phosphorylated tau in vivo (Perry et al., 1999; Zhu et al., 2000, 2001a,b), our result supports the role of the MAPK family members in the phosphorylation of tau in AD brain and the subsequent appearance of pathology.

While both oxidative stress and aberrant mitotic signaling are proposed to play an important role in the pathogenesis of AD (Perry et al., 1998; Zhu et al., 1999; Raina et al., 2000), their relation to each other is still debatable. Given that the activation of ERK is generally thought of as a response to mitotic signaling, whereas the activation of JNK/SAPK and p38 is associated with a response to oxidative stress, the present study sheds some light on the chronological relation between these events. Indeed, the activation of ERK and JNK/SAPK in control cases with limited pathology indicates that at least both events (aberrant mitotic signaling and oxidative stress) as well as both activation of ERK and JNK/SAPK are required for the manifestation of cellular pathology of AD. These data also suggest that although both mitotic signaling and oxidative stress can exist as 'single hit', only with 'two hits' can the disease process be initiated (Fig. 3). Given that MAPK pathways are tightly regulated, the persistent activation of JNK/SAPK and ERK throughout the disease process indicates that neurons in AD are subject to chronic or 'repeated hits' from both oxidative and mitotic sources. In fact, the essentially identical staining pattern for phospho-JNK/SAPK and phospho-p38 in severe AD cases suggests that JNK/SAPK and p38 is activated by the same signal with the earlier activation of JNK/SAPK reflecting great sensitivity to oxidative insults (Bhat and Zhang, 1999). In further support of 'multiple hits', it is notable

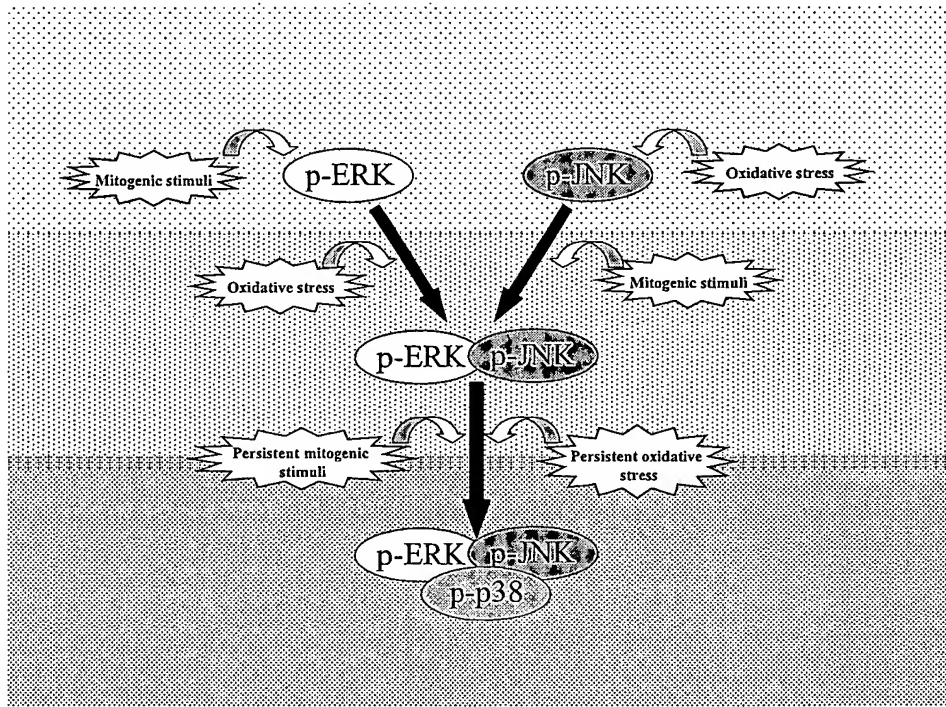


Fig. 3. Proposed chronological sequence of MAPK activation during the initiation and subsequent progression of AD.

that abnormal cell cycle markers re-expression and oxidative damage are both prominent features of susceptible neurons in AD brain. While this 'two hit' model might appear inconsistent at first glance with the recent one-hit model of cell death in neurodegenerative disease, this latter model was based on the presence of a mutation (Clarke et al., 2000), the presence of which rendered neurons vulnerable to a single hit. In our study, only sporadic, i.e. non-familial, cases were examined and since a mutation might also be considered a 'hit', as in the cancer field, the 'one hit' should really be considered a 'two hit' model as proposed here. In this regard, it will be interesting to determine the pattern of MAPK activation in familial cases of AD in future studies.

Aside from the limitation always inherent in placing static images in temporal sequence, the chronological scheme indicated above (Fig. 3) has inherent bias because it represents the cells that we can observe, that is those that survive AD. It may be that those neurons not expressing activated ERK, JNK/SAPK and p38 die while those neurons that respond to whatever stimuli by activating these kinases live longer. In this regard, a recent study showed that NFT-bearing neurons could survive for decades (Morsch et al., 1999) and neurons bearing NFT show a dramatic decrease in the relative level of 8OHG, an oxidative damage marker (Nunomura et al., 2001). Therefore, when facing cellular stress, the activation of MAPKs in susceptible neurons, by mobilizing cellular defenses and by phosphorylating tau protein (Takeda et al., 2000), may delay imminent neuronal death, although in compensation of functional loss and eventual cell death.

Acknowledgements

This work was supported through funding from the National Institutes of Health (NS38648) and the Alzheimer's Association (Stephanie B. Overstreet Scholars—IIRG-00-2163 and ZEN-99-1789). We thank Sandra L. Siedlak for technical assistance and Bethany Kumar for the assistance in preparing the manuscript.

References

- Bhat, N.R., Zhang, P., 1999. Hydrogen peroxide activation of multiple mitogen-activated protein kinases in an oligodendrocyte cell line: role for extracellular signal-regulated kinase in hydrogen peroxide induced cell death. *J. Neurochem.* 72, 112–119.
- Busciglio, J., Lorenzo, A., Yeh, J., Yankner, B.A., 1995. β -Amyloid fibrils induce tau phosphorylation and loss of microtubule binding. *Neuron* 14, 879–888.
- Clarke, G., Collins, R.A., Leavitt, B.R., Andrews, D.F., Hayden, M.R., Lumsden, C.J., McInnes, R.R., 2000. A one-hit model of cell death in inherited neuronal degenerations. *Nature* 406, 195–199.
- Cobb, M.H., 1999. MAP kinase pathways. *Prog. Biophys. Mol. Biol.* 71, 479–500.
- Goedert, M., Hasegawa, M., Jakes, R., Lawler, S., Cuenda, A., Cohen, P., 1997. Phosphorylation of microtubule-associated protein tau by stress-activated protein kinases. *FEBS Lett.* 409, 57–62.
- Hensley, K., Floyd, R.A., Zheng, N.-Y., Nael, R., Robinson, K.A., Nguyen, X., Pye, Q.N., Stewart, C.A., Geddes, J., Markesberry, W.R., Patel, E., Johnson, G.V.W., Bing, G., 1999. p38 kinase is activated in Alzheimer's disease brain. *J. Neurochem.* 72, 2053–2058.

Markesberry, W.R., 1997. Oxidative stress hypothesis in Alzheimer's disease. *Free Radical Biol. Med.* 23, 134–147.

Morsch, R., Simon, W., Coleman, P.D., 1999. Neurons may live for decades with neurofibrillary tangles. *J. Neuropathol. Exp. Neurol.* 58, 188–197.

Nunomura, A., Perry, G., Aliev, G., Hirai, K., Takeda, A., Balraj, E.K., Jones, P.K., Ghanbari, H., Wataya, T., Shimohama, S., Chiba, S., Atwood, C.S., Petersen, R.B., Smith, M.A., 2001. Oxidative damage is the earliest event in Alzheimer's disease. *J. Neuropathol. Exp. Neurol.* 60, 759–767.

Perry, G., Castellani, R.J., Hirai, K., Smith, M.A., 1998. Reactive oxygen species mediate cellular damage in Alzheimer disease? *J. Alzheimer's Dis.* 1, 45–55.

Perry, G., Roder, H., Nunomura, A., Takeda, A., Friedlich, A.L., Zhu, X., Raina, A.K., Holbrook, N., Siedlak, S.L., Harris, P.L.R., Smith, M.A., 1999. Activation of neuronal extracellular receptor kinase (ERK) in Alzheimer disease links oxidative stress to abnormal phosphorylation. *Neuroreport* 10, 2411–2415.

Petersen, R.C., Smith, G.E., Waring, S.C., Ivnik, R.J., Tangalos, E.G., Kokmen, E., 1999. Mild cognitive impairment: clinical characterization and outcome. *Arch. Neurol.* 56, 303–308.

Raina, A.K., Zhu, X., Rottkamp, C.A., Monteiro, M., Takeda, A., Smith, M.A., 2000. Cyclin' toward dementia: cell cycle abnormalities and abortive oncogenesis in Alzheimer disease. *J. Neurosci. Res.* 61, 128–133.

Reynolds, C.H., Nebreda, A.R., Gibb, G.M., Utton, M.A., Anderson, B.H., 1997. Reactivating kinase/p38 phosphorylates τ protein in vitro. *J. Neurochem.* 69, 191–198.

Robinson, M.J., Cobb, M.H., 1997. Mitogen-activated protein kinase pathways. *Curr. Opin. Cell. Biol.* 9, 180–186.

Roder, H.M., Eden, P.A., Ingram, V.M., 1993. Brain protein kinase PK40erk converts tau into a PHF-like form as found in Alzheimer's disease. *Biochem. Biophys. Res. Commun.* 193, 639–647.

Shoji, M., Iwakami, N., Takeuchi, S., Waragai, M., Suzuki, M., Kanazawa, I., 2000. JNK activation is associated with intracellular β -amyloid accumulation. *Mol. Brain Res.* 85, 221–233.

Smith, M.A., 1998. Alzheimer disease. In: Bradley, R.J., Harris, R.A. (Eds.), *International Review of Neurobiology*, vol. 42. Academic Press, San Diego, pp. 1–54.

Sternberger, L.A., 1986. *Immunocytochemistry*, 3rd ed. Wiley, New York.

Takeda, A., Perry, G., Abraham, N.G., Dwyer, B.E., Kutty, R.K., Laitinen, J.T., Petersen, R.B., Smith, M.A., 2000. Overexpression of heme oxygenase in neuronal cells, the possible interaction with tau. *J. Biol. Chem.* 275, 5395–5399.

Yan, S.D., Yan, S.F., Chen, X., Fu, J., Chen, M., Kuppusamy, P., Smith, M.A., Perry, G., Godman, G.C., Nawroth, P., Zweier, J.L., Stern, D., 1995. Non-enzymatically glycated tau in Alzheimer's disease induces neuronal oxidant stress resulting in cytokine gene expression and release of amyloid β -peptide. *Nat. Med.* 1, 693–699.

Zhu, X., Raina, A.K., Smith, M.A., 1999. Cell cycle events in neurons: proliferation or death? *Am. J. Pathol.* 155, 327–329.

Zhu, X., Rottkamp, C.A., Boux, H., Takeda, A., Perry, G., Smith, M.A., 2000. Activation of p38 kinase links tau phosphorylation, oxidative stress and cell cycle-related events in Alzheimer disease. *J. Neuropathol. Exp. Neurol.* 59, 880–888.

Zhu, X., Raina, A.K., Rottkamp, C.A., Aliev, G., Perry, G., Boux, H., Smith, M.A., 2001a. Activation and redistribution of c-Jun N-terminal kinase/stress activated protein kinase in degenerating neurons in Alzheimer's disease. *J. Neurochem.* 76, 435–441.

Zhu, X., Rottkamp, C.A., Boux, H., Perry, G., Smith, M.A., 2001b. Activation of MKK3/6, an upstream activator of p38, in Alzheimer disease. *J. Neurochem.*, in press.

Arteriosclerosis, Thrombosis, and Vascular Biology

JOURNAL OF THE AMERICAN HEART ASSOCIATION

American Heart
Association®



Learn and LiveSM

Hyperexpression and Activation of Extracellular Signal-Regulated Kinases (ERK1/2) in Atherosclerotic Lesions of Cholesterol-Fed Rabbits

Yanhua Hu, Hermann Dietrich, Bernhard Metzler, Georg Wick and Qingbo Xu
Arterioscler. Thromb. Vasc. Biol. 2000;20:18-26

Arteriosclerosis, Thrombosis, and Vascular Biology is published by the American Heart Association.
7272 Greenville Avenue, Dallas, TX 75214
Copyright © 2000 American Heart Association. All rights reserved. Print ISSN: 1079-5642. Online
ISSN: 1524-4636

The online version of this article, along with updated information and services, is
located on the World Wide Web at:
<http://atvb.ahajournals.org/cgi/content/full/20/1/18>

Subscriptions: Information about subscribing to Arteriosclerosis, Thrombosis, and Vascular Biology is online at
<http://atvb.ahajournals.org/subscriptions/>

Permissions: Permissions & Rights Desk, Lippincott Williams & Wilkins, 351 West Camden Street, Baltimore, MD 21202-2436. Phone 410-5280-4050. Fax: 410-528-8550. Email:
journalpermissions@lww.com

Reprints: Information about reprints can be found online at
<http://www.lww.com/static/html/reprints.html>

Hyperexpression and Activation of Extracellular Signal-Regulated Kinases (ERK1/2) in Atherosclerotic Lesions of Cholesterol-Fed Rabbits

Yanhua Hu, Hermann Dietrich, Bernhard Metzler, Georg Wick, Qingbo Xu

Abstract—A hallmark of hyperlipidemia-induced atherosclerosis is altered gene expression that initiates cell proliferation and (de)differentiation in the intima of the arterial wall. The molecular signaling that mediates this process *in vivo* has yet to be identified. Extracellular signal-regulated kinases (ERKs) are thought to play a pivotal role in transmitting transmembrane signals required for cell proliferation *in vitro*. The present studies were designed to investigate the activity, abundance, and localization of ERK1/2 in atherosclerotic lesions of cholesterol-fed rabbits. Immunofluorescence analysis revealed abundant and heterogeneous distribution of ERK1/2, mainly localized in the cap and basal regions of atheromas. A population of ERK-enriched cells was identified as α -actin-positive smooth muscle cells (SMCs). ERK1 and 2 were heavily phosphorylated on tyrosyl residues and coexpressed with proliferating cell nuclear antigen in atherosclerotic lesions. ERK1/2 protein levels in protein extracts from atherosclerotic lesions were 2- to 3-fold higher than the vessels of chow-fed rabbits, and their activities were elevated 3- to 5-fold over those of the normal vessel. SMCs derived from atherosclerotic lesions had increased migratory/proliferative ability and higher ERK activity in response to LDL stimulation compared with cells from the normal vessel. Inhibition of ERK activation by PD98059, a specific inhibitor of mitogen-activated protein kinase kinases (MEK1/2), abrogated LDL-induced SMC proliferation *in vitro*. Taken together, our findings support the proposition that persistent activation and hyperexpression of ERK1/2 may be a critical element to initiate and perpetuate cell proliferation during the development of atherosclerosis. (*Arterioscler Thromb Vasc Biol*. 2000;20:18-26.)

Key Words: atherosclerosis ■ animal models ■ MAP kinases ■ ERK ■ signal transduction

Mitogen-activated protein (MAP) kinase-mediated signal transduction pathways contribute to cell growth and differentiation.¹⁻³ The MAP kinase isoforms of 42 and 44 kDa, so-called extracellular signal-regulated kinases (ERK1/2), are expressed in most, if not all, mammalian cell types. ERK1 and 2 were initially identified as 2 protein kinases that became phosphorylated on tyrosine in response to growth factors.⁴ ERK-mediated signal pathways are a multistep phosphorylation cascade that transmits signals from the cell surface to cytosolic nuclear targets, which are responsible for the activation and phosphorylation of a number of other regulatory proteins, including p90^{rsk}, cPLA₂, and transcription factors needed for the expression of genes involved in cell proliferation.⁵⁻⁷ In addition, the activation of the cascade is also required for passing through certain checkpoints in the cell cycle, eg, G₁/S and G₂/M, in proliferating cells *in vitro*.⁸⁻¹⁰ Therefore, MAP kinase-mediated signal pathways play a key role in initiating cell proliferation and differentiation.

A high concentration of circulating cholesterol or LDLs is believed to be a major risk factor for atherosclerosis. The

main pathophysiological role of LDL is to deliver cholesterol to vascular smooth muscle cells (SMCs) and macrophages, which form foam cells in the development of atherosclerosis.¹¹ In addition to lipid transport, LDL can effectively stimulate SMC proliferation, a key event in the formation of atherosclerosis.¹²⁻¹⁴ There is evidence that LDL induces gene expression of platelet-derived growth factor (PDGF), PDGF receptors, c-fos, and egr-1,^{14,15} which are essential transcription factors for SMC proliferation. However, the precise signal transduction pathways that link to hypercholesterolemia and quantitative changes in gene expression in the pathogenesis of atherosclerotic lesions are largely unknown.

Most of our knowledge concerning the activation and function of ERK1/2 has come from studies on cultured cells; little is known about their activation *in vivo* and their relevance to atherogenesis in animal models. We examined ERK1/2 expression, localization, and activation in atherosclerotic lesions of cholesterol-fed rabbits and provide the first evidence of ERK overexpression and activation in lesions.

Received February 26, 1999; revision accepted July 28, 1999.

From the Institute for General and Experimental Pathology (Y.H., H.D., G.W.) and Division of Cardiology, Department of Internal Medicine (B.M.), University of Innsbruck Medical School, and the Institute for Biomedical Aging Research (G.W., Q.X.), Austrian Academy of Sciences, Innsbruck, Austria.

Correspondence to Dr Qingbo Xu, Institute for Biomedical Aging Research, Austrian Academy of Sciences, Rennweg 10, A-6020 Innsbruck, Austria. E-mail: qingbo.xu@oeaw.ac.at

© 2000 American Heart Association, Inc.

Arterioscler Thromb Vasc Biol is available at <http://www.atvbaha.org>

Moreover, we demonstrate that the increased migratory/proliferative ability of SMCs derived from the lesions correlates with ERK1/2 activities, which are induced by LDL from chow- and cholesterol-fed rabbits.

Methods

Rabbit Model for Atherosclerosis

Twenty New Zealand White male rabbits weighing between 1800 and 2200 g were obtained from Charles River (Kisslegg, Germany). All animals were selected for serum cholesterol levels <100 mg/dL and were individually housed in wire-bottomed cages at 22°C with a relative humidity of 55%. All received water ad libitum and were fed either a normal standard chow diet (T775; Tagger & Co) or a cholesterol-enriched diet (0.2% wt/wt) for 16 weeks, as described previously.^{16,17} Animals were killed by heart puncture under ketamine (25 mg/kg) and xylazine (5 to 10 mg/kg) anesthesia. Serum was collected for cholesterol assays and LDL isolation. The aortas were carefully removed intact from the aortic arch to the iliac bifurcation, immediately placed into cold PBS (4°C), and prepared for histological analysis, tissue culture, and protein extractions. For conventional histology, tissue fragments were fixed in 4% buffered (pH 7.2) formaldehyde, embedded in paraffin, and sectioned for hematoxylin-eosin staining.

Blood Cholesterol

Blood (1 to 2 mL) was taken from the central ear artery of rabbits that had been fasted for 16 hours. Serum total cholesterol values were measured every 2 or 4 weeks by an enzymatic procedure (Sigma). Briefly, 10 µL serum was added to 1 mL solution of cholesterol test kit and incubated for 18 minutes at room temperature followed by photometer measurement at 500-nm excitation wavelength (Dynatech Laboratories Inc).

Immunohistochemical and Immunofluorescence Double Staining

The procedure used for immunohistochemical staining was similar to that described elsewhere.^{16,17} Briefly, serial 4-µm-thick frozen sections were overlaid with mouse monoclonal antibodies against α-actin (Sigma), macrophages (RAM11; Dako), or CD3⁺ T cells (L11/135; ATCC; catalogue No. TIB188); incubated with rabbit anti-mouse Ig conjugated with peroxidase (Dako); and developed for 20 minutes at room temperature with a substrate solution.

For immunofluorescent staining, a mouse monoclonal antibody against ERK1/2 (Transduction) was added to the sections. After 3 washes with PBS, the sections were incubated with a rabbit anti-mouse Ig-TRITC conjugate (Dako) for 30 minutes. For double staining, sections were incubated with a monoclonal antibody against phosphorylated ERK1/2 conjugated with FITC (Santa Cruz Biotechnology Inc), rinsed, and stained with a mouse monoclonal antibody against α-actin-Cy3 conjugate (Sigma) or biotin-labeled antibody against proliferating cell nuclear antigen (PCNA) developed with streptavidin-TRITC (Dako). For visualization of nuclei, sections were counterstained with the DNA stain Hoechst 33258 (1 µg/mL PBS; Lambda Probes) for 1 minute. Sections were mounted in Gelvatol/PBS and examined in a epi-illumination immunofluorescence microscope equipped with appropriate filter combinations for the 3-wavelength method (Leitz).

Protein Extraction

The procedure used for protein extracts was similar to that described previously,¹⁸ with a slight modification. Briefly, the atherosclerotic intima and media with lesions were dissected from the remaining adventitia on ice with tweezers and scissors. Tissues were frozen in liquid nitrogen and homogenized in a Polytron homogenizer in buffer A containing 20 mmol/L HEPES (pH 7.4), 50 mmol/L β-glycerophosphate, 2 mmol/L EGTA, 1 mmol/L DTT, 1 mmol/L Na₃VO₄, 1% Triton X-100, 10% glycerol, 1 µg/mL leupeptin, 400 µmol/L PMSF, and 1 µg/mL aprotinin. The homogenate was incubated on ice for 15 minutes. After centrifugation at 17 000g for

30 minutes, the supernatant was collected, and protein concentration was measured with Bio-Rad protein assay reagent.

Western Blot Analysis

Protein extracts (50 µg/lane) prepared from the arterial tissues described above were separated by electrophoresis through a 10% SDS-polyacrylamide gel and transferred to an Immobilon-P transfer membrane.¹⁹ The membranes were processed with the monoclonal antibody against ERK1/2 or phosphorylated ERK1/2 (Santa Cruz Biotechnology). Specific antigen-antibody complexes were then detected with the ECL Western Blot Detection Kit (Amersham). The blots were stripped for 30 minutes at 70°C in the buffer containing 60 mmol/L Tris, 2% SDS, and 100 mmol/L 2-mercaptoethanol; labeled with a monoclonal antibody against β-actin (Sigma); and developed as described above. Graphs of blots were obtained in the linear range of detection and were quantified and normalized to the level of actin by scanning laser densitometry (Power-Look II, UMAX Data System Inc) of graphs.

Kinase Assay

Supernatant (0.5 mL) containing 0.5 mg proteins was incubated with 10 µL of goat anti-ERK2 antibodies (Santa Cruz Biotechnology) for 2 hours at 4°C with rotation. Subsequently, 40 µL of protein G-agarose suspension (Santa Cruz Biotechnology) was added, and rotation continued for 1 hour at 4°C. The immunocomplexes were precipitated by centrifugation and washed 2 times with buffers A, B (500 mmol/L LiCl, 100 mmol/L Tris, 1 mmol/L DTT, 0.1% Triton X-100; pH 7.6), and C (20 mmol/L MOPS, 2 mmol/L EGTA, 10 mmol/L MgCl₂, 1 mmol/L DTT, 0.1% Triton X-100; pH 7.2), respectively. ERK2 activities in the immunocomplexes were measured as described previously.^{18,19} Briefly, immunocomplexes were incubated with 35 µL of buffer C supplemented with myelin basic protein (MBP; 6 µg; Upstate Biotechnology), [γ -³²P]ATP (5 µCi), and MgCl₂ (50 mmol/L) for 20 minutes at 37°C, with vortexing every 5 minutes. To stop the reaction, 15 µL of 4× Laemmli buffer was added, and the mixture was boiled for 5 minutes. Proteins in the kinase reaction were resolved by SDS-PAGE (15% gel) and subjected to autoradiography.

Cell Culture and Proliferation Assays

Rabbit vascular SMCs were cultivated from their aortas by a modification of the procedure described by Ross and Kariya.^{20,21} In short, thoracic aortas of chow- and cholesterol-fed rabbits were removed and washed with RPMI 1640 medium (Gibco). Intima with lesions and normal media were carefully dissected from the vessel, cut into pieces (\approx 1 mm³), and explanted onto a 0.02% gelatin-coated plastic bottle (Falcon). The bottle was incubated upside-down at 37°C in a humidified atmosphere of 95% air/5% CO₂ for 3 hours, resulting in firm attachment of the explanted tissues, and then medium supplemented with 20% FCS, penicillin (100 U/mL), and streptomycin (100 µg/mL) was slowly added. The outgrowths of SMCs from the explants were counted at days 5, 10, and 15 under the microscope. The percentage of the outgrowth was determined by counting positive tissue explants with cell growth over all explanted tissue segments (50 to 100 pieces per bottle). Cells were passaged by treatment with 0.05% trypsin/0.02% EDTA solution. Experiments were conducted on SMCs between passages 5 and 10 that had just achieved confluence. The purity of SMCs was routinely confirmed by immunostaining with antibodies against α-actin.

For proliferation assays, SMCs (1×10^4) cultured in 96-well plates in medium containing 10% FCS at 37°C for 24 hours were serum-starved for 2 days. SMCs were treated with PD 98059 (Calbiochem) for 30 minutes, and then LDL (100 µg/mL) in 2% serum was added and incubated at 37°C for 24 hours. [³H]thymidine was added 6 hours before cell harvest. Radiation activities were measured.

LDL Isolation

EDTA plasma was collected from normocholesterolemic and hypercholesterolemic rabbits fasted overnight. Lipoproteins were prepared by differential centrifugation with solid KBr to adjust the density as described previously.^{22,23} LDLs were obtained in the fraction between 1.020 and 1.050 g/mL. The sample was dialyzed against

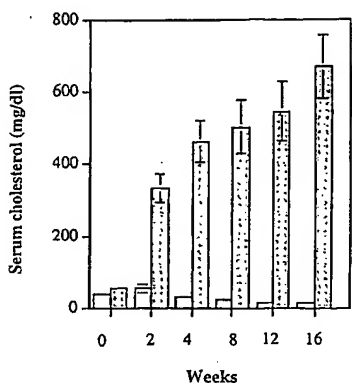


Figure 1. Serum cholesterol levels in rabbits. The values of serum cholesterol were measured every 2 or 4 weeks by an enzymatic procedure. Serum cholesterol levels in rabbits fed a 0.2% cholesterol diet (shaded bars) were significantly higher than in those (open bars) receiving the chow diet.

150 mmol/L NaCl with 0.1 mmol/L EDTA, sterilized through a 0.2- μ m Millipore membrane, and stored at 4°C up to 3 weeks. No oxidation of LDL was observed at least 3 weeks after LDL isolation, as determined by measurement of malondialdehyde by the thiobarbituric acid method. Endotoxin contents of freshly isolated LDL and LDL after 3 weeks of storage at 4°C were both below the detection limit (<1 ng/mL, Endotoxin Kit, Sigma). Concentrations of LDL

were determined gravimetrically by aliquot weight after drying, and quantities of lipoproteins were expressed as total weights.^{22,23}

Statistical Analysis

ANOVA was performed for multiple comparisons. The Mann-Whitney *U* test was used for comparison between 2 groups. A value of *P*<0.05 was considered statistically significant.

Results

Atherosclerotic Lesions in Hypercholesterolemic Rabbits

Blood cholesterol levels in rabbits receiving a 0.2% cholesterol diet were significantly elevated and reached 350 mg/dL at 2 weeks and >600 mg/dL at 16 weeks. Animals in the control group (chow diet) had blood cholesterol levels <100 mg/dL (Figure 1). To verify atherosclerotic lesions in cholesterol-fed rabbits, aortas were examined morphologically and immunohistologically 16 weeks after cholesterol feeding. Areas with lesions in the surface of aortic intima covered 50% to 80% of intima in cholesterol-fed rabbits. Figure 2A and 2B depicts the histological appearance of vessel walls of rabbits that received chow and cholesterol diets, respectively. Intima of normal vessel walls constituted a monolayer endothelium and a little connective tissue, but aortic lesions of rabbits fed

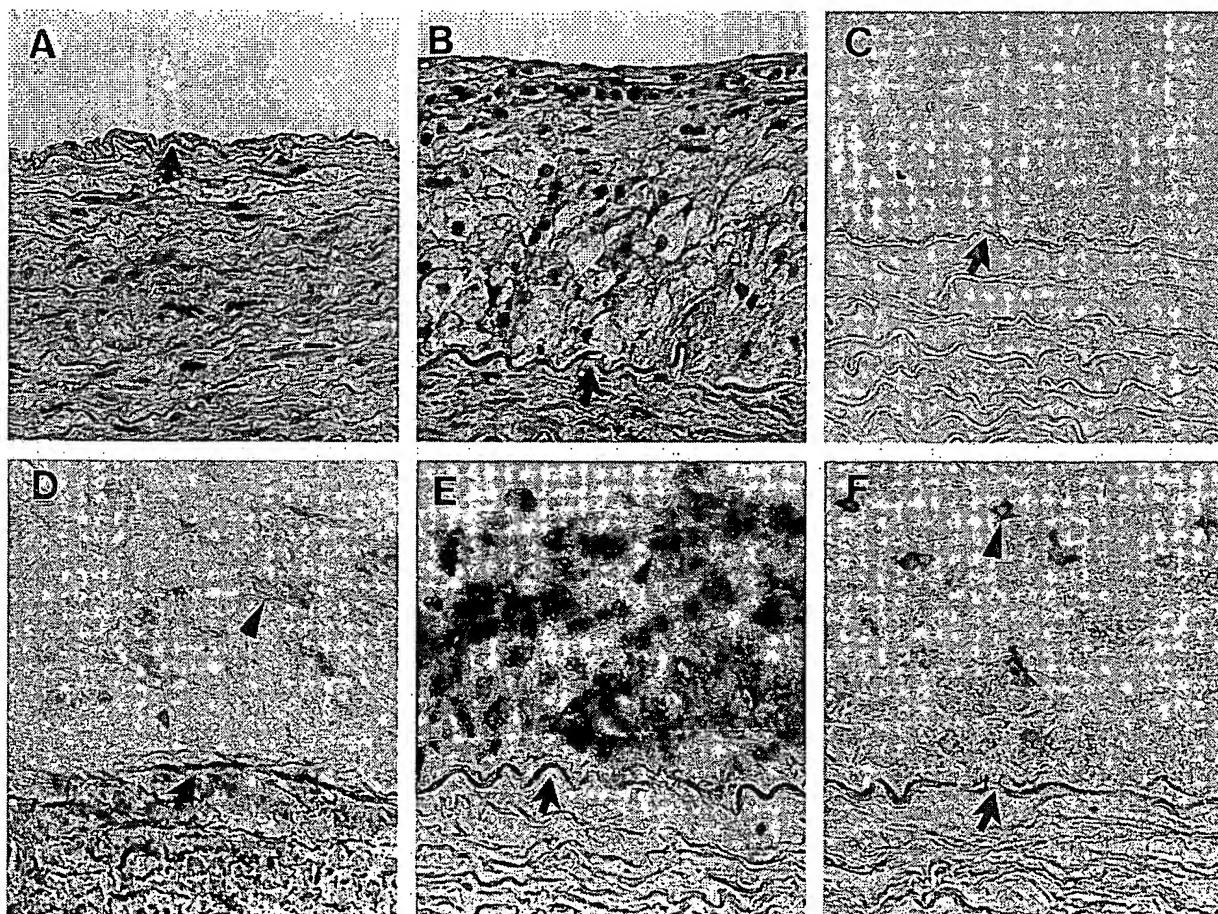


Figure 2. Cell compositions in atherosclerotic lesions. Rabbits receiving a chow or cholesterol-enriched diet for 16 weeks were killed, and aortic tissue fragments were frozen in liquid nitrogen or fixed in 4% buffered (pH 7.2) formaldehyde, embedded in paraffin, sectioned, and stained with hematoxylin-eosin (A and B). Cryostat sections from aortic segments of rabbits fed a 0.2% cholesterol diet for 16 weeks (C through F) were labeled with normal mouse Ig as a negative control (C) or monoclonal antibodies against α -actin (D), macrophages (E; RAM11), or T lymphocytes (F; L11/135) and visualized with the peroxidase system. Note the presence of positive staining (dark) in lesions. Arrows indicate internal elastic lamina; arrowheads point to examples of positive-stained cells. Magnification $\times 250$.

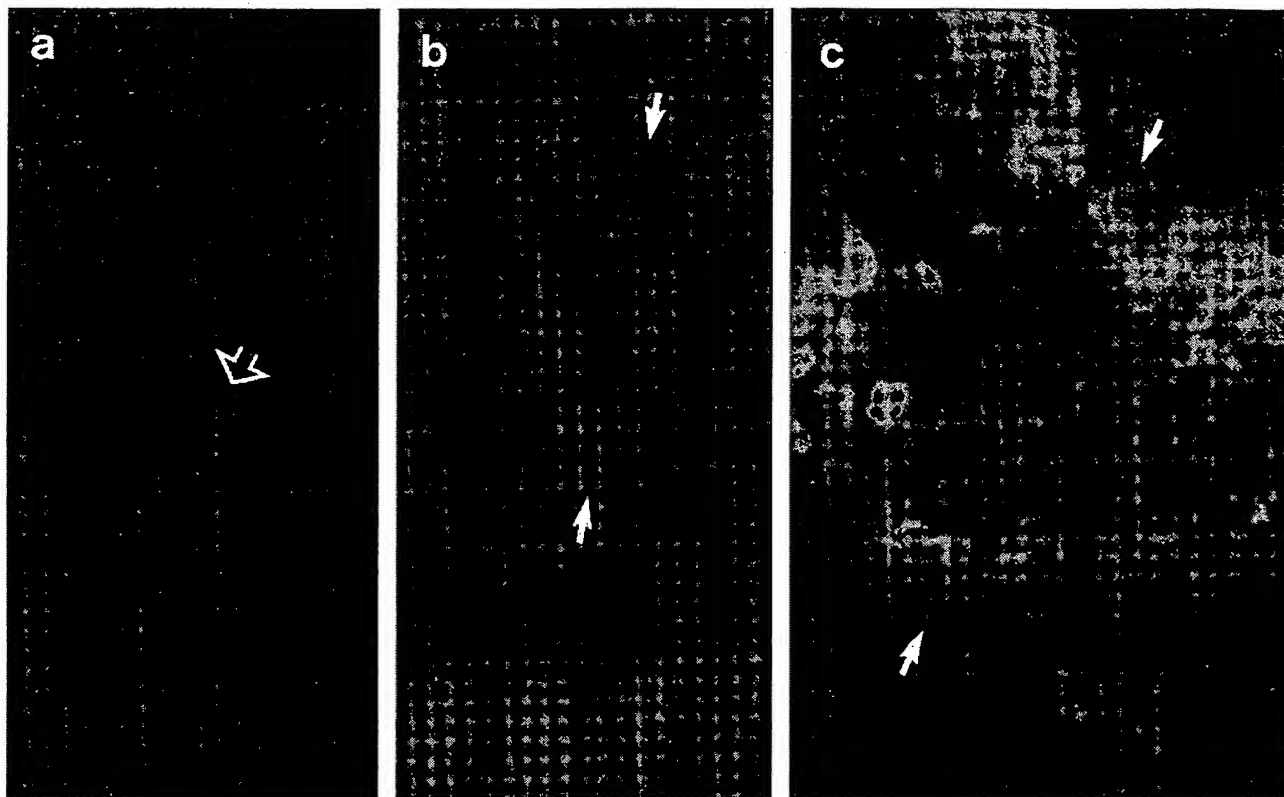


Figure 3. Immunofluorescence labeling of ERK1/2 in atherosclerotic lesions. Cryostat sections from aortic tissues of rabbits that received normal (a) or cholesterol-enriched (b and c) diet were fixed with cold 5% acetone/methanol for 30 minutes, air-dried, incubated with normal mouse serum (b) or a mouse monoclonal antibody against ERK1/2 (a and c) for 30 minutes at room temperature, and visualized by anti-mouse Ig-TRITC-conjugated rabbit Ig. Open arrow indicates surface of endothelium; solid arrows indicate lesions. Magnification $\times 250$.

a cholesterol-enriched diet were characterized by cell proliferation, foam cell accumulation, and lipid deposition in the intima (Figure 2B). To identify the main cellular components in atherosclerotic lesions, serial sections of the vessels were incubated with a battery of antibodies to specific cell markers. α -Actin-positive SMCs appeared in various stages of lesions, most frequently in advanced lesions (Figure 2D). Cells expressing the macrophage antigen identified by the RAM11 antibody²⁴ were observed in all atherosclerotic lesions (Figure 2E), including early and advanced stages, most appearing as foam cells. Finally, T lymphocytes identified by monoclonal antibody L11/135 were frequently observed, especially in advanced lesions (Figure 2F).

ERK Hyperexpression and Activation in Atherosclerotic Lesions

From each group, 5 aortic specimens were immunohistologically stained with a monoclonal antibody against mammalian ERK1/2. Normal artery showed very weak staining, if any (Figure 3a). Nonspecific reactivity was minimal in the negative control labeled with normal mouse serum (Figure 3b), whereas the lesion-covered areas in intima from rabbits receiving a cholesterol-rich diet showed increased immunostaining intensity (Figure 3c). In the small lesions, some areas within the intima became positively stained, whereas fatty streaks displayed elevated ERK1/2 content in subendothelial regions. Heterogeneity of ERK1/2 staining became more evident in atherosclerotic plaques. Sites of increased ERK1/2

were mainly within the cap and base regions of the atherosclerotic plaque (Figure 3c).

Both ERK1 and ERK2 kinases are activated by dual phosphorylation of tyrosine and threonine residues in response to mitogenic or stress stimuli.^{1,4} In addition, tissues derived from atherosclerotic lesions are heterogeneous with respect to cell types (Figure 2). Therefore, we performed immunofluorescence double staining to identify the cells expressing activated ERK1/2 in lesions. Figure 4a through 4c shows data representing double staining with antibodies against phosphorylated ERK1/2 (a; green), α -actin (b; red), and counterstaining with Hoechst 33258 (c; blue). Typical double-positive cells are indicated by arrows, demonstrating a population of SMCs in lesions expressing activated ERK1/2. In addition, some macrophages were also positively stained with phosphorylated ERK1/2, indicating an activated or proliferating state.

There is evidence that ERK activation is required for passing through certain checkpoints in the cell cycle in proliferating cells *in vitro*.⁸⁻¹⁰ We performed experiments with immunofluorescence double staining with antibodies against phosphorylated ERK1/2 (a; green), PCNA (b; red), and counterstaining with Hoechst 33258 (c; blue). Figure 5 shows that the most PCNA-positive cells had higher levels of phosphorylated ERK1/2.

To further show that ERK1/2 proteins were increased in atherosclerotic lesions, protein extracts from tissues of normal intima/media and intima and media with lesions were analyzed by Western blot analysis. Abundant ERK1/2 pro-

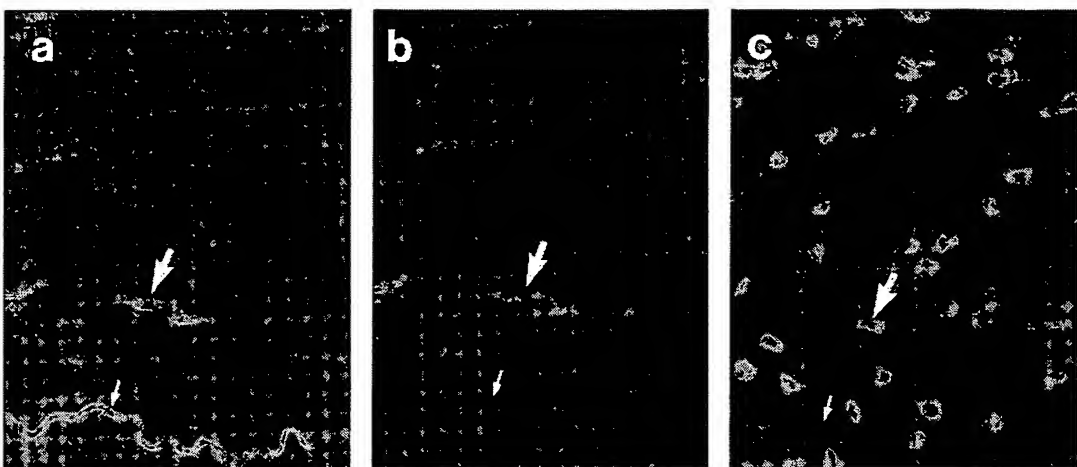


Figure 4. Immunofluorescence double labeling of phosphorylated-ERK1/2 and SMCs in atherosclerotic lesions. Cryostat sections from rabbit aortic tissues 16 weeks after administration of cholesterol-rich diet were incubated with a mouse monoclonal antibody against phosphorylated ERK1/2 conjugated with FITC (a) for 30 minutes. After a washing, sections were incubated with a monoclonal antibody against α -actin conjugated with Cy3 (b) and stained with Hoechst 33258 (1 μ g/mL) for 3 minutes (c). Small arrows indicate internal elastic lamina; large arrows point to examples of double positive-stained cells. Magnification $\times 250$.

teins in atherosclerotic lesions were observed (Figure 6A). ERK proteins in intima with lesions were significantly higher than intima/media of control animals and media of cholesterol-fed rabbits (Figure 6A, bottom) when they were normalized with respect to actin levels of the same blots.

Western blot analysis using protein extracts from the arterial tissues and the antibody recognizing the phosphorylated ERK1/2 was also performed. The activated (phosphorylated) forms of p42 and p44 were identified, which showed marked increases in protein extracts of atherosclerotic lesion tissues (Figure 6B). These results demonstrated that ERK phosphorylation is present in lesions. Furthermore, ERK1/2 activity of protein extracts was also measured with MBP used as a substrate. Figure 6C shows the results of an experiment examining ERK1/2 activities in the vessel wall. Obviously,

ERK1/2 activities were found at low levels in control vessels and media of cholesterol-fed rabbits but increased 3- to 5-fold in atherosclerotic lesions (Figure 6C).

Increased ERK Activities in Lesion-Derived SMCs

To compare cell proliferation and ERK activation between SMCs from atherosclerotic lesions and normal vessels, tissues were explanted onto gelatin-coated bottles, and SMC migration and/or proliferation from the tissues was evaluated microscopically. Data shown in Figure 7 are percentages of outgrowth SMCs around the tissue fragments. The results indicate that the migration/proliferation ability of SMCs from lesions was significantly higher than that of normal vessels.

To compare ERK activities in different types of SMCs, cellular protein extracts containing similar amounts of actin

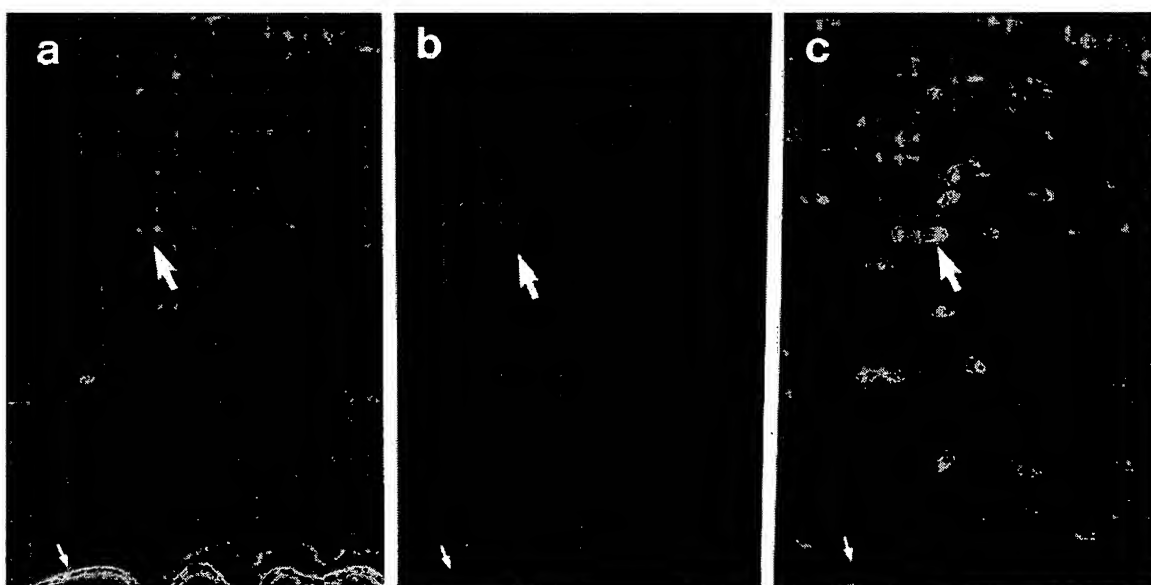


Figure 5. Immunofluorescence double labeling of phosphorylated ERK1/2 and PCNA in atherosclerotic lesions. Cryostat sections from rabbit aortic tissues 16 weeks after administration of cholesterol-rich diet were incubated with a mouse monoclonal antibody against phosphorylated ERK1/2 conjugated with FITC (a) for 30 minutes. After a washing, sections were incubated with a biotin-labeled monoclonal antibody against PCNA (b), visualized with streptavidin-TRITC, and stained with Hoechst 33258 (1 μ g/mL) for 3 minutes (c). Small arrows indicate internal elastic lamina; large arrows point to examples of double positive-stained cells. Magnification $\times 250$.

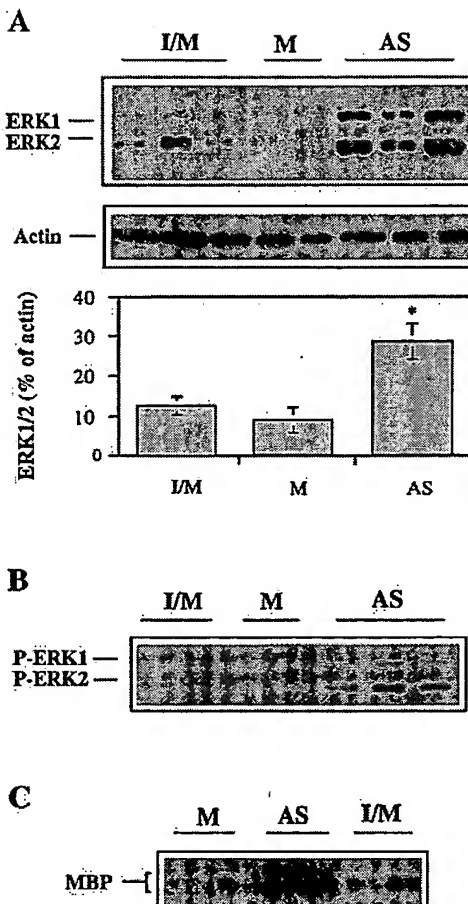


Figure 6. Elevated ERK proteins and activities in atherosclerotic lesions. Animals were killed 16 weeks after receiving a chow or cholesterol diet, and aortas were harvested. Intima and media (I/M) from chow-fed rabbits and the atherosclerotic intima (AS) and media (M) with lesions from cholesterol-fed rabbits were dissected from the remaining adventitia on ice with tweezers and scissors. Tissues were frozen in liquid nitrogen and homogenized in a Polytron homogenizer. Protein extracts (50 μ g/lane) were separated on 10% SDS-polyacrylamide gel, transferred onto membrane, and probed with the antibody against ERK1/2 (A, top) or antibody to phosphorylated-ERK1/2 (P-ERK; B). Immunocomplexes were visualized by a Western blot detection kit. To label β -actin, the blots were stripped and restained with a monoclonal antibody to actin and developed with the detection kit (A, middle). For the kinase assay, ERK2 proteins were immunoprecipitated from the protein extractions, and their kinase activities (C) were measured on the basis of phosphorylation of MBP substrate. Each lane represents an individual. A, Bottom, Graph of pan-ERK1/2 (mean \pm SD) obtained from 6 rabbits per group, which were normalized with respect to actin of corresponding blots by measurement of optical densities. *Significant difference from control, $P < 0.05$.

were used for immunoprecipitation with the specific antibody against ERK2, and kinase activities were measured on the basis of phosphorylation of basic myelin protein as a substrate. When lesion-derived SMCs were stimulated with LDL of normocholesterolemic or hypercholesterolemic rabbits, ERK2 activation was induced by both types of LDL at similar magnitudes (Figure 8A). However, ERK2 activities in lesion-derived SMCs stimulated with hypercholesterolemic LDL, PDGF, and serum were higher than those of SMCs derived from normocholesterolemic rabbits (Figure 8B). Taken to-

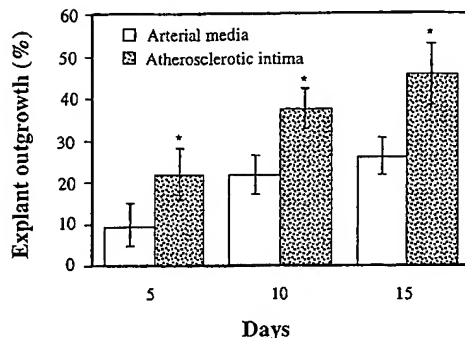


Figure 7. Percentage of SMC outgrowth in cultured explant arterial fragments. The intima with lesions from cholesterol-fed rabbits and the intima and inner half of media from chow-fed rabbits were carefully dissected from the vessel, cut into pieces (~ 1 mm 3), explanted onto a gelatin-coated plastic bottle, and incubated at 37°C in medium. The outgrowths of SMCs from the explants were counted at days 5, 10, and 15 under the microscope. Data are mean \pm SD from 3 independent experiments. *Significant difference from controls, $P < 0.05$.

gether, these observations support the notion that alterations in ERK activation in the development of atherosclerosis of cholesterol-fed rabbits are due to changed sensitivity of SMCs to LDL and mitogen stimulation.

Inhibition of ERK Activation and SMC Proliferation

Because ERK-mediated signal pathways are crucial in mediating cell migration and proliferation, the effects of PD98059, a MAP kinase kinase 1/2 inhibitor, on LDL-stimulated ERK activation and SMC proliferation were investigated. A marked activation of ERK1/2 by LDL was found, which was inhibited by PD98059 in a concentration-dependent manner (Figure 9A); ERK2 kinase phosphorylation was completely abolished by 50 μ mol/L PD98059. We had observed, by measuring [3 H]thymidine incorporation, that LDL effectively induced SMC DNA synthesis. Figure 9B depicts PD98059 inhibition of SMC proliferation stimulated by LDL. A concentration of 50 μ mol/L for treatment of SMCs completely abrogated SMC proliferation. Thus, blocking ERK-mediated signaling inhibits SMC proliferation induced by LDL.

Discussion

Activation of ERK kinase cascades is one of the major pathways for the regulation of proliferation and cell growth in various cultured cells.^{1-4,25,26} Reversible protein phosphorylation is the established mechanism of regulation of ERK kinases,²⁷ an activity controlled by a family of dual-specificity protein kinases and a complex upstream cascade.⁴ A transient kinase activation or attenuation is seen in most *in vitro* cultured cells in response to chronic stimulation. In the present studies, we have demonstrated that *in vivo*, ERK activation is sharply elevated in lesions, which cannot be ascribed solely to phosphorylation of the proteins. Immunoblotting revealed a marked increase in the amount of ERK1/2 proteins from atherosclerotic lesions compared with normal vessel tissues or aortic media of cholesterol-fed rabbits. Sustained expression and activation of ERK kinases in ERK-transfected fibroblasts resulted in oncogenicity associated with cell proliferation.²⁸ Hyperexpression and activation

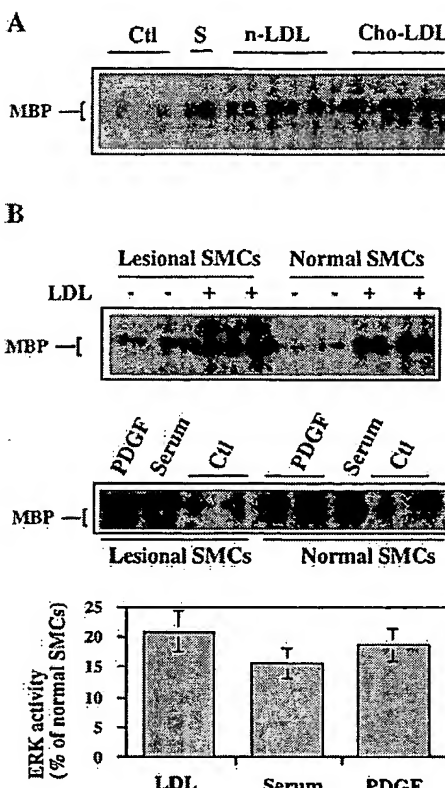


Figure 8. Enhanced ERK activation in lesional SMCs. A, Lesional SMCs were serum-starved for 2 days, exposed to normocholesterolemic (n-LDL; 200 μ g/mL) or hypercholesterolemic (Chol-LDL; 200 μ g/mL) LDL for 10 minutes, and harvested for protein extracts. B, Both normal and lesional SMCs were serum-starved for 2 days; stimulated with hypercholesterolemic LDL (200 μ g/mL), PDGF-AB (100 ng/mL), or serum (10% FCS) for 10 minutes; and harvested for protein extracts. For the kinase assay, ERK2 proteins were immunoprecipitated from the protein extractions, and their kinase activities were measured on the basis of phosphorylation of MBP substrate. Graph in B shows ERK2 kinase activities (mean \pm SD) of lesional SMCs normalized to normal SMCs (zero in y-axis indicates 100%). S indicates FCS treatment as a positive control; Ctl, negative controls.

of these kinases may play a main role in regulation of cell proliferation in the pathogenesis of atherosclerosis.

Chamley-Campbell et al²⁹ hypothesized that 2 distinct SMC phenotypes, contractile and synthetic, exist in the vessel wall and that SMCs in the atherosclerotic plaque differ from those in the normal tunica media.³⁰ It has been established that SMCs in intimal lesions display increased levels of genes for growth factors,¹⁴ tumor necrosis factors,³¹ class II histocompatibility antigens,³² vascular cell adhesion molecule-1,³³ and intercellular adhesion molecule-1.^{34,35} On the basis of these observations, Libby and Li³⁶ called them "activated" SMCs. Our findings of selective or differential hyperexpression and activation of ERK protein kinases in atherosclerotic SMCs support the concept that the ERK level and activity in SMCs reflect a situation of gene expression, activation, and replication of this SMC population. These higher ERK activities from lesional SMCs can be maintained even in *in vitro* culture for longer periods of time, further supporting the notion that SMCs from atherosclerotic lesions have been selected and differ from those from normal vessels.

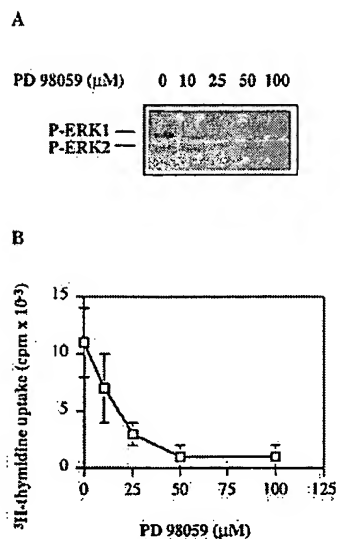


Figure 9. PD 98059 inhibited ERK activation and SMC proliferation. A, Quiescent SMCs were pretreated with PD 98059 for 30 minutes. Aortic SMCs derived from normal rabbits were exposed to LDL for 10 minutes and harvested for protein extracts. The results of Western blot analysis showed LDL-induced (200 μ g/mL) ERK1/2 phosphorylation (P-ERK) inhibited by PD 98059 in a concentration-dependent manner. B, For proliferation assays, SMCs (1×10^4) cultured in a 96-well plate in medium containing 10% FCS at 37°C for 24 hours were serum-starved for 2 days and treated with PD 98059, and LDL (200 μ g/mL) in 2% serum was added and incubated at 37°C for 24 hours. [³H]thymidine was added 6 hours before cells were harvested. Radiation activities were measured. Data are mean \pm SD of 3 experiments.

Proliferation of vascular SMCs is a hallmark in the pathogenesis of atherosclerosis.¹⁴ LDL and oxidized LDL are mitogenic to cultured SMCs and have been demonstrated to activate ERK signal pathways in cultured cells *in vitro*.³⁷⁻⁴⁰ In the present study, we provide the first evidence that hypercholesterolemia can stimulate ERK expression and activation in the intima but not media or tissues (Figures 3 and 6) from other organs, including liver, kidney, brain, and heart (data not shown). Previously, we demonstrated that acute elevation in blood pressure induced by restraint or hypertensive agents resulted in MAP kinase activation in the media of the arterial wall.⁴¹ In the present experiments, we minimized the effect of animal handling on blood pressure fluctuation by daily conditioning of rabbits with intramuscular saline injection for 1 week before their death. This treatment was shown to be effective because kinase activities of the vessel wall from control rabbits and media from cholesterol-fed rabbits were of similar, and lower, levels. Such tissue-specific activation of ERK kinases induced by hypercholesterolemia may explain why the lesion is localized only in the arterial intima and may be due to different responses of various types of cells to lipids or LDL stimulation, ie, hypercholesterolemia induces atherosclerosis but not kidney or heart sclerosis. Thus, our findings could significantly enhance our understanding of the pathogenesis of atherosclerosis during hyperlipidemia.

Recent studies have focused on the signaling events in cultured cells from cardiovascular tissue, including myocytes and SMCs, which may provide a new strategy for therapeutic

intervention.^{3,25,42,43} Depletion of MAP kinases with an antisense oligodeoxynucleotide downregulates the phenylephrine-induced hypertrophic response in rat cardiac myocytes.⁴⁴ Accumulating evidence indicates that MAP kinase phosphatase (MKP-1) specifically inhibits mitogen-induced activation of MAP kinases in cell lines.⁴⁵⁻⁴⁷ Lai et al⁴⁸ reported a reduction of MKP-1 expression in rat carotid arteries in response to balloon injury, which may be responsible for sustained activation of ERK2 during restenosis of the injured artery.⁴⁹ In the present study, we demonstrate that inhibition of the ERK kinase activation by PD98059 abrogates SMC proliferation. The therapeutic effect of ERK antagonist or inhibitor on lesion formation should be addressed in future studies. Thus, understanding of the mechanisms serving to regulate MAP kinase activities could lead to new strategies for prevention or therapeutic intervention for atherosclerosis.

Acknowledgment

This work was supported by grants P-12568-MED and P-13099-BIO (to Q. Xu) from the Austrian Science Fund and 6286 (to Q. Xu) from the Jubiläumsfonds of the Austrian National Bank. Dr Hu is a recipient of an APART Stipend from the Austrian Academy of Sciences. We thank A. Jenewein, E. Rainer, and G. Sturm for excellent technical assistance and T. Öttl for the preparation of photographs.

References

1. Davis RJ. The mitogen-activated protein kinase signal transduction pathway. *J Biol Chem.* 1993;268:14553-14556.
2. Seger R, Krebs EG. The MAPK signaling cascade. *FASEB J.* 1995;9:726-735.
3. Zou Y, Hu Y, Metzler B, Xu Q. Signal transduction in arteriosclerosis: mechanical stress-activated MAP kinases in vascular smooth muscle cells. *Int J Mol Med.* 1998;1:827-834.
4. Ray LB, Sturgill TW. Characterization of insulin-stimulated microtubule-associated protein kinase: rapid isolation and stabilization of a novel serine/threonine kinase from 3T3-L1 cells. *J Biol Chem.* 1988;263:12721-12727.
5. Sturgill TW, Ray LB, Erikson E, Maller JL. Insulin-stimulated MAP-2 kinase phosphorylates and activates ribosomal protein S6 kinase II. *Nature.* 1988;334:715-718.
6. Lin L-L, Wartmann M, Lin AY, Knopf JL, Seth A, Davis RJ. cPLA2 is phosphorylated and activated by MAP kinase. *Cell.* 1993;72:269-278.
7. Chen R-H, Abate C, Blenis J. Phosphorylation of the c-fos transcription domain by MAP kinase and 90-kDa S6 kinase. *Proc Natl Acad Sci U S A.* 1993;90:10952-10956.
8. Tamemoto H, Kadowaki T, Tobe K, Ueki K, Izumo T, Chatani Y, Kohno M, Yazaki Y, Akanuma Y. Biphasic activation of two mitogen-activated protein kinases during cell cycle in mammalian cells. *J Biol Chem.* 1992;267:20293-20297.
9. Lane HA, Fernandez A, Lamb NJC, Thomas G. p70⁶⁵ * function is essential for G1 progression. *Nature.* 1993;363:170-172.
10. Pages G, Lenormand P, L'Allemand G, Chambard J-C, Meloche S, Pouysségur J. Mitogen-activated protein kinases p42^{mapk} and p44^{mapk} are required for fibroblast proliferation. *Proc Natl Acad Sci U S A.* 1993;90:8319-8323.
11. Brown SM, Goldstein LJ. A receptor-mediated pathway for cholesterol homeostasis. *Science.* 1986;232:34-37.
12. Libby P, Miao P, Ordovas JM, Schäfer EJ. Lipoproteins increase growth of mitogen stimulated arterial smooth muscle cells. *J Cell Physiol.* 1985;124:1-8.
13. Scott-Burden T, Resink TJ, Hahn AW, Baur U, Box RJ, Buchler FR. Induction of growth-related metabolism in human vascular smooth muscle cells by low density lipoprotein. *J Biol Chem.* 1989;264:12582-12589.
14. Ross R. The pathogenesis of atherosclerosis: a perspective for the 1990s. *Nature.* 1993;362:801-809.
15. Sachinidis A, Ko Y, Wieczorek A, Weisser B, Locher R, Vetter W, Vetter H. Lipoproteins induce expression of the early growth response gene-1 in vascular smooth muscle cells from rat. *Biochem Biophys Res Commun.* 1993;192:794-799.
16. Xu Q, Dietrich H, Steiner HJ, Gown AM, Mikuz G, Kaufmann SHE, Wick G. Induction of arteriosclerosis in normocholesterolemic rabbits by immunization with heat shock protein 65. *Arterioscler Thromb.* 1992;12:789-799.
17. Xu Q, Kleindienst R, Waitz W, Dietrich H, Wick G. Increased expression of heat shock protein 65 coincides with a population of infiltrating T lymphocytes in atherosclerotic lesions of rabbits specifically responding to heat shock protein 65. *J Clin Invest.* 1993;91:2693-2702.
18. Hu Y, Metzler B, Xu Q. Discordant activation of stress-activated protein kinases or c-Jun NH₂-terminal protein kinases in tissues of heat-stressed mice. *J Biol Chem.* 1997;272:9113-9119.
19. Hu Y, Böck G, Wick G, Xu Q. Activation of PDGF receptor α in vascular smooth muscle cells by mechanical stress. *FASEB J.* 1998;12:1135-1142.
20. Ross R, Kariya B. Smooth muscle cells in culture. In: Bohr DF, Somlyo AP, and Sparks HV, eds. *Handbook of Physiology: Circulation, Vascular Smooth Muscle.* Bethesda, Md: American Physiological Society; 1980: 69-91.
21. Xu Q, Hu Y, Kleindienst R, Wick G. Nitric oxide induces heat-shock protein 70 expression in vascular smooth muscle cells via activation of heat shock factor 1. *J Clin Invest.* 1997;100:1089-1097.
22. Jürgens G, Xu Q, Huber LA, Böck G, Howanietz H, Wick G, Traill KN. Promotion of lymphocyte growth by high density lipoproteins (HDL): physiological significance of the HDL binding site. *J Biol Chem.* 1989;264:8549-8556.
23. Xu Q, Jürgens G, Huber LA, Böck G, Wolf H, Wick G. Lipid utilization by human lymphocytes is correlated with high-density-lipoprotein binding site activity. *Biochem J.* 1992;285:105-112.
24. Tsukada T, Rosenfeld M; Ross R, Gown AM. Immunocytochemical analysis of cellular components in lesions of atherosclerosis in the Watanabe and fat-fed rabbit using monoclonal antibodies. *Arteriosclerosis.* 1986;6:601-613.
25. Force T, Bonventre JV. Growth factors and mitogen-activated protein kinases. *Hypertension.* 1998;31:152-161.
26. Robinson MJ, Cobb MH. Mitogen-activated protein kinase pathways. *Curr Opin Cell Biol.* 1997;9:180-186.
27. Blenis J. Signal transduction via MAP kinase: proceed at your own RSK. *Proc Natl Acad Sci U S A.* 1994;90:5889-5892.
28. Brunet A, Pages G, Pouysségur J. Constitutively active mutants of MAP kinase kinase induce growth factor-relaxation and oncogenicity when expressed in fibroblasts. *Oncogene.* 1994;9:3379-3387.
29. Chamley-Campbell JH, Campbell GR, Ross R. The smooth muscle cell in culture. *Am Physiol Soc.* 1979;58:1-61.
30. Caplice NM, West MJ, Campbell GR, Campbell J. Inhibition of human vascular smooth muscle cell growth by heparin. *Lancet.* 1994;344:97-98.
31. Libby P, Hansson GK. Involvement of the immune system in human atherosclerosis: current knowledge and unanswered questions. *Lab Invest.* 1991;64:5-15.
32. Xu Q, Oberhuber G, Gruschwitz M, Wick G. Immunology of atherosclerosis: cellular composition and major histocompatibility complex class II antigen expression in aortic intima, fatty streaks, and atherosclerotic plaques in young and aged human specimens. *Clin Immunol Immunopathol.* 1990;56:344-359.
33. Cybulsky MI, Gimbrone MA Jr. Endothelial expression of a mononuclear leukocyte adhesion molecule during atherosclerosis. *Science.* 1991;251:788-791.
34. Poston RN, Haskard DO, Coucher JR, Gall NP, Johnson-Tidey RR. Expression of intercellular adhesion molecule-1 in atherosclerotic plaques. *Am J Pathol.* 1992;140:665-673.
35. Printseva O, Peclo MM, Gown AM. Various cell types in human atherosclerotic lesions express ICAM-1: further immunocytochemical and immunochemical studies employing monoclonal antibody 10F3. *Am J Pathol.* 1992;140:889-896.
36. Libby P, Li H. Vascular cell adhesion molecule-1 and smooth muscle cell activation during atherosclerosis. *J Clin Invest.* 1993;92:538-539.
37. Deigner H-P, Claus R. Stimulation of mitogen activated protein kinase by LDL and oxLDL in human U-937 macrophage-like cells. *FEBS Lett.* 1996;385:149-153.
38. Kusuhara M, Chait A, Cader A, Berk BC. Oxidized LDL stimulates mitogen-activated protein kinases in smooth muscle cells and macrophages. *Arterioscler Thromb Vasc Biol.* 1997;17:141-148.
39. Sachinidis A, Seewald S, Epping P, Seul C, Ko Y, Vetter H. The growth-promoting effect of low-density lipoprotein may be mediated by

a pertussis toxin-sensitive mitogen-activated protein kinase pathway. *Mol Pharmacol*. 1997;52:389–397.

40. Augé N, Escargueil-Blanc I, Nègre-Salvayre A, Salvayre R. Potential role for ceramide in mitogen-activated protein kinase activation and proliferation of vascular smooth muscle cells induced by oxidized low density lipoprotein. *J Biol Chem*. 1998;273:12893–12900.
41. Xu Q, Liu Y, Gorospe M, Udelsman R, Holbrook NJ. Acute hypertension activates mitogen-activated protein kinases in arterial wall. *J Clin Invest*. 1996;97:508–514.
42. Traub O, Berk BC. Laminar shear stress: mechanisms by which endothelial cells transduce an atheroprotective force. *Arterioscler Thromb Vasc Biol*. 1998;18:677–685.
43. Sugden PH, Clerk A. “Stress-responsive” mitogen-activated protein kinases (c-Jun N-terminal kinases and p38 mitogen-activated protein kinases) in the myocardium. *Circ Res*. 1998;83:345–352.
44. Glennon PE, Kaddoura S, Sale EM, Sale GJ, Fuller SJ, Sugden PH. Depletion of mitogen-activated protein kinase using an antisense oligodeoxynucleotide approach downregulates the phenylephrine-induced hypertrophic response in rat cardiac myocytes. *Circ Res*. 1996;78:954–961.
45. Sun H, Tonks NK, Bar-Sagi D. Inhibition of Ras-induced DNA synthesis by expression of the phosphatase MKP-1. *Science*. 1994;266:285–288.
46. Liu Y, Gorospe M, Yang C, Holbrook NJ. Role of mitogen-activated protein kinase phosphatase during the cellular response to genotoxic stress. *J Biol Chem*. 1995;270:8377–8380.
47. Xu Q, Fawcett TW, Gorospe G, Guyton KZ, Liu Y, Holbrook NJ. Induction of mitogen-activated protein kinase phosphatase-1 during acute hypertension. *Hypertension*. 1997;30:106–111.
48. Lai K, Wang H, Lee W-S, Jain MK, Lee M-E, Haber E. Mitogen-activated protein kinase phosphatase-1 in rat arterial smooth muscle cell proliferation. *J Clin Invest*. 1996;98:1560–1567.
49. Hu Y, Cheng L, Hochleitner B-W, Xu Q. Activation of mitogen-activated protein kinases (ERK/JNK) and AP-1 transcription factor in rat carotid arteries after balloon injury. *Arterioscler Thromb Vasc Biol*. 1997;17:2808–2816.

Regulation of IL-13 synthesis in human lymphocytes: implications for asthma therapy

*¹Andreas Pahl, ¹Meixia Zhang, ²Hildegard Kuss, ²Istvan Szelenyi & ¹Kay Brune

¹Department of Experimental and Clinical Pharmacology and Toxicology, University of Erlangen-Nürnberg, Fahrstr. 17, D-91054 Erlangen, Germany and ²Corporate Research & Development, ASTA Medica AG, Meissnerstr. 191, D-01445 Radebeul, Germany

1 IL-13 is an important mediator in inflammatory diseases such as asthma. IL-13 is mainly produced by T cells. However, signalling pathways leading to induction of this cytokine are not well-characterized. We analysed the regulation of IL-13 in human peripheral blood mononuclear cells and CD4⁺ T cells.

2 Cyclosporine (CsA) and FK-506 inhibited IL-13 synthesis, when cells were stimulated by TPA/ionomycin. However, stimulation by α -CD3/ α -CD28 led to an enhanced IL-13 synthesis.

3 NF- κ B inhibitor N-tosyl-L-lysine chloromethylketone (TLCK) inhibited IL-13 synthesis more effectively after TPA/ionomycin stimulation. After α -CD3/ α -CD28 stimulation, only 300 μ M TLCK inhibited IL-13 synthesis. Dexamethasone inhibited IL-13 equally effective after α -CD3/ α -CD28 and TPA/ionomycin stimulation.

4 p38 MAPK inhibitor SB203580 inhibited IL-13 synthesis only partially. MEK inhibitor U0126 inhibited TPA/ionomycin induced IL-13 synthesis very effectively, whereas α -CD3/ α -CD28 stimulated IL-13 induction was resistant to this drug.

5 These results were confirmed in purified CD4⁺ T cells. In difference to PBMCs α -CD3/ α -CD28 stimulated IL-13 synthesis was effectively inhibited by CsA, FK-506 and U0126.

6 Therefore U0126 was tested in an animal model of allergic asthma. We could demonstrate for the first time that inhibition of the MEK-ERK cascade is a therapeutic option for asthma. Intraperitoneal administration of 10 mg kg⁻¹ U0126 reduced lung eosinophilia in ovalbumin-challenged Brown Norway rats by 44%.

7 These results demonstrate that different signalling pathways are involved in regulating IL-13 synthesis in primary human T cells. Characterizing highly potent inhibitors of IL-13 synthesis can be exploited to identify new drugs to treat immunological diseases such as asthma.

British Journal of Pharmacology (2002) 135, 1915–1926

Keywords: IL-13; T-cell activation; cyclosporine; FK-506; dexamethasone; TLCK; U0126; SB203580

Abbreviations: BAL, bronchoalveolar lavage fluid; CsA, cyclosporine A; ERK, extracellular signal-regulated kinase; IL, interleukin; JNK, jun NH₂-terminal kinase; MAPK, mitogen-activated protein kinase; MEK, MAPK kinase; OVA, ovalbumin; PBMC, peripheral blood mononuclear cells; PKC, protein kinase C; TCR, T-cell receptor; TLCK, N-tosyl-L-lysine chloromethylketone; TPA, 12-O-tetradecanoylphorbol-13-acetate; VCAM, vascular cell adhesion molecule

Introduction

IL-13 is a cytokine that is produced in large quantities by appropriately stimulated CD4⁺ Th2 cells (Brubaker & Montaner, 2001). It has a variety of effects that are relevant to asthma and other Th2-dominated inflammatory disorders, including the ability to induce IgE production, CD23 expression, and endothelial cell VCAM-1 expression (Brombacher, 2000; Corry, 1999). IL-13 and IL-4 have overlapping effector profiles. This overlap is at least partially due to the shared use of receptor components in the multimeric IL-13 and IL-4 receptor complexes (Vita *et al.*, 1995). The IL-13 receptor complex is composed of at least three distinct components, including the IL-4 α receptor, the low-affinity binding chain IL-13R α 1, and the

high-affinity binding chain IL-13R α 2 (Brubaker *et al.*, 2001). However, recent *in vivo* studies using different infection and asthma models suggest that IL-13 possesses many important functional activities that are distinct from IL-4. These differences comprise the different ability of these cytokines to drive the differentiation of naive cord blood T cells to a Th2 phenotype, to support the *in vitro* proliferation of activated human or mouse T cells, to regulate prostaglandin biosynthesis, contribute to nematode expulsion, regulate epithelial electrolyte secretion, prolong eosinophil survival, and stimulate eosinophil chemotaxis (Endo *et al.*, 1998; Horie *et al.*, 1997; Sornasse *et al.*, 1996; Urban *et al.*, 1998; Zund *et al.*, 1996). In addition, IL-13 and IL-4 are produced by different cells and are differentially regulated by mediators such as IFN α (Kaser *et al.*, 1998) and transcription factors such as NF-AT (Feske *et al.*, 2000).

*Author for correspondence at: Institut für Pharmakologie und Toxikologie, Universität Erlangen, Fahrstr. 17, D-91054 Erlangen, Germany; E-mail: pahl@pharmakologie.uni-erlangen.de

Increased production of IL-13 is well documented in extrinsic and intrinsic asthma, atopic dermatitis, allergic rhinitis, and chronic sinusitis (Humbert *et al.*, 1997). Asthma is a disease characterized by the infiltration of eosinophils and lymphocytes into airway epithelium and subsequent epithelial damage and tissue remodelling (Busse & Lemanske, 2001). T helper (Th) 2 cells and their cytokine products play a crucial role in this process (Kay, 2001). IL-13 is one of the important Th2-type cytokines which have been implicated in asthma in which they are up-regulated (Huang *et al.*, 1995). Recent studies indicate that IL-13 can induce pathologic changes reminiscent of asthma in animals, including infiltration of eosinophils and mononuclear cells, epithelial damage, hyperplasia of goblet cells, and subepithelial fibrosis (Wills-Karp *et al.*, 1998). IL-13 probably plays important roles as a mucus-stimulating cytokine as well as in the recruitment of eosinophils. Endothelial cell expression of VCAM-1, an adhesion molecule involved in eosinophil recruitment, has been shown to be induced by IL-13 (Doucet *et al.*, 1998). A recent study reported that the inhibition of IL-13 in a mouse model leads to a reduced asthmatic response (Gruenig *et al.*, 1998).

IL-13 is mainly produced by T cells. In contrast to IL-2 and IL-4, signalling pathways leading to induction of IL-13 are poorly understood. Furthermore, most studies focusing on T-cell activation use T cell clones or transformed T cell lines, of which the signal transduction pathways may be altered and are largely uncoupled from proliferation (Hughes & Pober, 1996).

Three intracellular pathways have been demonstrated to be important for T-cell activation. Phosphorylation of the T-cell receptor complex allows the association of several 'adaptor' molecules, leading to several signalling cascades (Weiss & Littman, 1994). One of these cascades (reviewed in Crabtree & Clipstone (1994)) involves phosphorylation and activation of PLC γ 1, which cleaves phosphatidylinositol 4,5-bisphosphate to generate diacylglycerol and inositol 1,4,5-trisphosphate. The latter activate PKC and trigger an increase in the concentration of intracellular calcium respectively. The first pathway is initiated by this rapid and sustained increase in $[Ca^{2+}]_i$ resulting in the activation of the calmodulin/calcium-dependent phosphatase calcineurin; this phosphatase regulates IL-2 gene transcription by dephosphorylating the cytoplasmic form of NF-AT and allowing its translocation into the nucleus (Clipstone & Crabtree, 1992; Wesselborg *et al.*, 1996).

The second signalling pathway results in the activation of AP-1 (reviewed in Foletta *et al.* (1998)), which binds the IL-2 promoter both directly and as a component of an NF-AT complex (Jain *et al.*, 1993). AP-1 is a heterodimer of Fos and Jun family proteins (Foletta *et al.*, 1998). It has been established that regulation of *c-fos* gene transcription is mediated by the nuclear factor Elk-1, which is phosphorylated and activated by *ras*-dependent signal cascades involving ERK and JNK (Price *et al.*, 1996). On the other hand, *c-jun* is also regulated by JNK for which it appears to be a direct substrate (Derijard *et al.*, 1994). ERK1/2, JNK, and another pathway involving the kinase p38, which represent parallel kinase cascades initiated at the *ras* level, are commonly termed MAP kinase pathways (Su & Karin, 1996). In human T-cells, at least two MAP kinases, ERK-1 and ERK-2, are activated through the *ras* pathway in

response to occupancy of the TCR (Izquierdo *et al.*, 1993). Activation of ERK1/2 is induced by phosphorylation mediated by MEK-1/2 (Cobb & Goldsmith, 1995), the activity of which is itself regulated through phosphorylation by a MAP kinase kinase kinase; the serine/threonine protein kinase Raf-1, which couples p21 *ras* and interacts with MEK-1 to form a ternary signalling complex (Jelinek *et al.*, 1994), appears to be this MAP kinase kinase kinase (Leevers *et al.*, 1994). Altogether, these results provide a clear and convincing proof demonstration that MEK-1 and ERKs function in conveying stimulatory signals to the IL-2 gene.

Thirdly, activation of NF- κ B is important for T-cell activation (Liou *et al.*, 1999). This cascade is initiated by PKC. Recently, PKC θ has been identified as the prime PKC isoform in the signalling cascade after TCR activation (Bauer *et al.*, 2000; Coudronniere *et al.*, 2000; Lin *et al.*, 2000). This PKC in turn activates NF- κ B via small G-proteins *ras* and Raf-1 (Altman *et al.*, 2000).

Here we describe the regulation of IL-13 in primary human peripheral leukocytes. By using pharmacological inhibitors, we traced important signalling pathways leading to IL-13 production in primary human cells. Finally, we used a selective MAPK inhibitor to demonstrate the importance of IL-13 production in an animal model of allergic asthma.

Methods

Reagents

Oligonucleotides were synthesized by TIB Molbiol (Berlin, Germany). DMSO, TPA, ionomycin, dexamethasone, TLCK and Histopaque-1077 were from Sigma, (Deisenhofen, Germany). CsA, FK-506 and U0126 were from CALBIO-CHEM (San Diego, CA, U.S.A.). SB203580 was from BIOMOL Research Labs., Inc. (Plymouth Meeting, U.S.A.). Purified anti-human CD3 and purified anti-human CD28 were from PharMingen Becton Dickinson Co. (Heidelberg, Germany). RPMI 1640 medium was from Life Technologies (Heidelberg, Germany). CD4 $^+$ T Cell Isolation Kit was from Miltenyi Biotec (Bergisch Gladbach, Germany). Unless otherwise indicated, all other chemicals were purchased from the Sigma Chemical Co (Deisenhofen, Germany).

Preparation of PBMC

Buffy coats from healthy human volunteers were obtained from the Erlangen Blood Bank. PBMC were isolated by density gradient centrifugation over Histopaque 1077 (Sigma, Deisenhofen, Germany), washed twice in Hanks buffer (Life Technologies, Heidelberg, Germany) and resuspended in RPMI 1640 medium supplemented with 10% foetal calf serum (Boehringer Mannheim, Penzberg, Germany).

Preparation of CD4 $^+$ T cells

PBMC were incubated with hapten-antibody cocktails and MACS anti-hapten microbeads. (CD4 $^+$ T cell isolation kit, Miltenyi Biotec, Bergisch Gladbach, Germany). CD4 $^+$ T cells were isolated by negative selection on VS+ columns using high gradient magnetic cell separation system MACS

(Miltenyi Biotec, Bergisch Gladbach, Germany) according to the manufacturer's instructions. Purities of populations were assessed by flow cytometry with over 90% (FACScan, Becton Dickinson, Heidelberg, Germany). Purified CD4⁺ T cells were resuspended in RPMI 1640 medium supplemented with 10% FCS.

Cell culture

For cytokine production, PBMC were resuspended at 10⁶ cells ml⁻¹ and incubated in 500 µl aliquots in 24-well tissue culture plates (Falcon Becton Dickinson Labware, Heidelberg, Germany) at 37°C, 5% CO₂. After preincubation with test substances for 30 min, cells were stimulated with soluble α-CD3 mAb (1 µg ml⁻¹), anti-CD3 mAb (1 µg ml⁻¹) plus α-CD28 mAb (0.3 µg ml⁻¹), TPA (25 ng ml⁻¹), ionomycin (1 µM) or TPA (25 ng ml⁻¹) plus ionomycin (1 µM). At the indicated times, cells were sedimented by centrifugation, the supernatants were harvested and kept frozen at -80°C until cytokine protein determination; the cells were lysed by RLT lysis buffer (Qiagen, Hilden, Germany) and frozen at -80°C until RNA isolation.

Enzyme-linked immunosorbent assay

Cytokine measurements in culture supernatants were done by sandwich ELISA using matched antibody pairs (BD Pharmingen, Heidelberg, Germany). ELISA plates (Maxisorb, Nunc) were coated overnight with anti-IL-13 mAb in 0.1 M carbonate buffer, pH 9.5. After being washed, plates were blocked with Assay Diluent (Pharmingen, Heidelberg, Germany) for 1 h and washed again. Appropriately diluted supernatant samples and standards were distributed in duplicates and the plates were incubated for 2 h at room temperature. Plates were washed, incubated for 1 h with working detector (biotinylated anti-IL-13 Ab and Avidin-horseradish peroxidase conjugate). After washing, substrate (TMB and hydrogen peroxide) was added. The reaction was stopped by addition of 1 M H₃PO₄. Plates were read at 450 nm (reference 570 nm) in a microplate reader (Dynatech). The results were expressed as a percentage of the control level of cytokines production by cells stimulated in the presence of the vehicle of the corresponding compound.

Analysis of cytokine mRNA expression by real-time RT-PCR

RNA was prepared from frozen lysates using Rneasy (Qiagen, Hilden, Germany). One-tube RT-PCR was performed using TaqMan EZ RT-PCR Kit from PE Applied Biosystems (Weiterstadt, Germany). Expression of cytokines were determined in relation to beta-actin by real time RT-PCR using TaqMan assay on a ABI Prism 7700. Primers and probes are: β-Actin forward: 5'-CAG CGG AAC CGC TCA TTG CCA ATG G; β-Actin reverse: 5'-TCA CCC ACA CTG TGC CCA TCT ACG A; β-actin probe: 5'-(6FAM)-ATG CCC (TAMRA)T CCC CCA TGC CAT CCT GCG T; IL-13 forward: 5'-GGA GCT GGT CAA CAT CAC CC; IL-13 reverse: 5'-CGT TGA TCA GGG ATT CCA GG; IL-13 probe: 5'-(6FAM)-CCAGAAGGC-(TAMRA)-TCCGCTCTGCAATGGC.

Rat IL-13 was determined using Quantitect SYBR Green RT-PCR Kit from QIAGEN (Hilden, Germany) using the

forward primer GTGCCCTCAGGGAGCTTAT and the reverse primer CTGTCAGGTCCACGCTCCAT. Quantity of mRNA was calculated using the $\Delta\Delta C_T$ method (PE Applied Biosystems User Bulletin #2; ABI PRISM 7700 Sequence Detection System, 1997). For each RT-PCR the threshold cycle (C_T) was determined, being defined as the cycle at which the fluorescence exceeds 10 times the standard deviation of the mean baseline emission for cycles 3 to 10. IL-13 mRNA levels were normalized to the housekeeping gene β-actin according to the following formula: $\Delta C_T = C_T^{\beta\text{-actin}} - C_T^{\text{IL-13}}$. Subsequently, respective IL-13 mRNA levels were calculated using the $\Delta\Delta C_T$ method, i.e., ΔC_T values representing mRNA from cells treated with stimulus in combination with a test compound were set in relation to the ΔC_T value representing mRNA levels from cells treated with stimulus alone according to the following formula: $\Delta\Delta C_T = \Delta C_T(\text{drug}) - \Delta C_T(\text{vehicle})$. The relative mRNA level for the respective test compound was calculated as $2^{-\Delta\Delta C_T} \times 100\%$ based on the results of control experiments with an efficiency of the PCR reaction of approximately 100%.

Late phase eosinophilia

Male Brown-Norway rats weighing 180–230 g were used. Animals were purchased from Moellegaard Breeding & Research Centre A/S, Skensved, Denmark. The animals were kept under constant environmental conditions (temperature: 22±2°C, humidity: 40–60%, light cycle: 0700–1900). They had free access to standardized food pellets (purchased from Spezialdiäten GmbH, Soest, Westfalen, Germany) and tap water. All animal studies were performed in accordance with the national animal protection rules and permitted by the local governmental authority (Regierungspräsidium Dresden, Germany).

Brown-Norway (BN) rats were actively sensitized by subcutaneous injections of ovalbumin mixed with Al(OH)₃ gel and i.p. Bordetella pertussis vaccine on days 1, 14 and 21. On day 28, the animals were used for experiments. Compounds as suspension in tylose, were given intraperitoneally 2 h prior to challenge. Then the rats were exposed to an ovalbumin-containing aerosol in a nose-only inhalation system (TSE GmbH, Bad Homburg, Germany) for 1 h to provoke an influx of inflammatory cells into the airways. Vehicle-treated control animals were sensitized and exposed to saline aerosol. At the time of maximal influx of eosinophilic granulocytes into the airways (48 h later), animals were sacrificed by an urethane overdose and a bronchoalveolar lavage (BAL) was performed by three times 4 ml Hank's balanced solution. The number of eosinophils as well as the total cell number from the pooled BAL samples were counted 48 h post challenge using a haemocytometer (Technicon H1E, Bayer Diagnostics GmbH, Munich, Germany). Each group of animals treated with compounds was compared with vehicle (tylose)-treated saline-challenged and ovalbumin-challenged control groups.

Data analysis

Data are expressed as means±s.e.mean. Significant differences were statistically analysed by the unpaired Student's *t*-test and by ANOVA. IC₅₀ values were calculated using the

computer program PRISM 3.0 (GraphPad Software Inc., San Diego, CA, U.S.A.).

Results

Induction of IL-13 in human PBMCs

We compared the stimulation of human PBMCs by different mitogenic agents and antibodies directed against surface receptors all leading to the production of IL-13. For our studies, we developed a real-time RT-PCR method for accurate quantitation of IL-13 mRNA levels (see Methods). Whereas no IL-13 mRNA was detectable in unstimulated cells, each stimulus or combination thereof tested caused an increase of IL-13 mRNA levels in adult blood leukocytes (Figure 1). α -CD3 alone was a poor stimulus, whereas its combination with α -CD28 or ionomycin was much more efficient. α -CD28 alone was insufficient to induce IL-13. Similarly, TPA alone induced hardly detectable levels of IL-13, whereas the combination with ionomycin gave rise to the highest level of IL-13. Combination of two stimuli increased the mRNA levels more than the additive effect of the correspondent single stimuli. IL-13 protein levels in the supernatant correlated with the mRNA levels measured by RT-PCR (Figure 1; $r^2=0.94$, $P<0.0001$).

Time course of IL-13 induction

α -CD3/ α -CD28 as a physiologic and TPA/ionomycin as a mitogenic stimulus were chosen to study the time course of IL-13 mRNA induction. As can be seen from Figure 2, TPA/ionomycin induced mRNA levels rapidly peaking at 4 h following a rapid decline to baseline levels. Protein levels follow similar kinetics while the peak is shifted to 8 h. In contrast, IL-13 mRNA after antigen receptor stimulation increased more slowly than with TPA/ionomycin but remained close to peak levels for the whole period. Similarly, IL-13 protein levels started to increase from 24 h onwards

and reached much higher levels compared to IL-13 protein induced by TPA/ionomycin.

Effects of inhibitors of the calcium \rightarrow NF-AT pathway (CsA and FK-506)

Three intracellular pathways have been demonstrated to be important for T-cell activation. One depends on the release of intracellular calcium leading to the subsequent activation of calcineurin and NF-AT. Therefore, we raised the question as to whether IL-13 induction in human leukocytes is sensitive to CsA and FK-506, two specific calcineurin inhibitors. First, we analysed the dose response on IL-13 induced by stimulation with TPA/ionomycin. CsA inhibits mRNA as well as protein induction in the low nanomolar range (Figure 3a). The dose-response curve for mRNA is steeper than for the protein. FK-506 also inhibits IL-13 induction, but this drug is about 30 fold more potent than CsA (Figure 4a). If the cells are stimulated by α -CD3/ α -CD28, the cytokines respond quite differently (Figures 3b and 4b). Under these conditions IL-13 is stimulated by CsA and FK-506. This effect was seen for mRNA as well as for the secreted protein. Again, only 30 fold lower concentrations of FK-506 are needed to obtain similar effects compared to CsA.

Effects of NF- κ B inhibitors

The activation of NF- κ B via PKC has also been shown to be important for T cell activation (Trushin *et al.*, 1999). We therefore investigated whether the proteasome inhibitor TLCK, which has been shown to inhibit activation of NF- κ B by inhibiting the degradation of I- κ B, affects IL-13 induction. As shown in Figure 5a, TPA/ionomycin-induced IL-13 is inhibited by TLCK at low micromolar concentrations. In contrast, TLCK inhibited α -CD3/ α -CD28 induction of cytokines only at concentrations above 100 μ M (Figure 5b).

Steroids have been shown to interfere with NF- κ B activation at several stages. Therefore, we compared the

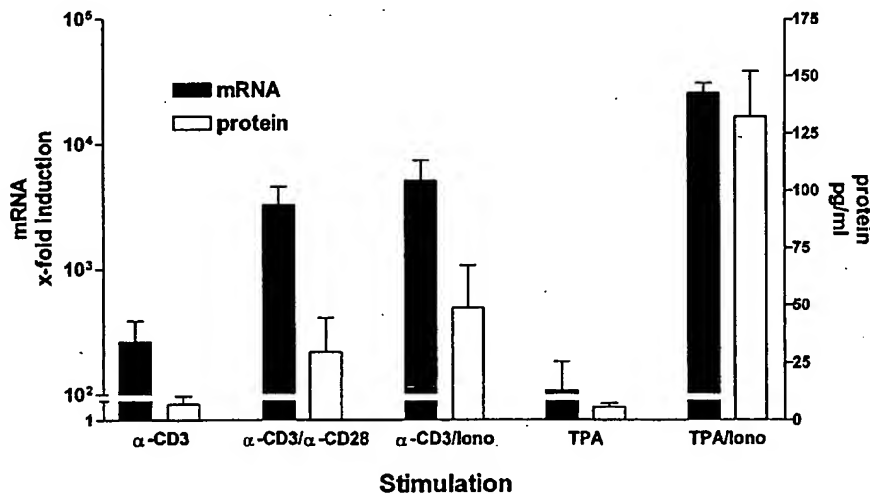


Figure 1 Induction of IL-13 in healthy donors by different stimuli. PBMCs were stimulated for 4 and 24 h. IL-13 mRNA level were determined using real-time RT-PCR after 4 h. Levels were normalized to β -actin and unstimulated cells were set to 1. IL-13 protein was determined in the supernatant by ELISA after 24 h. Each column represents mean \pm s.e.mean of three different volunteers. Similar results were obtained in three independent experiments.

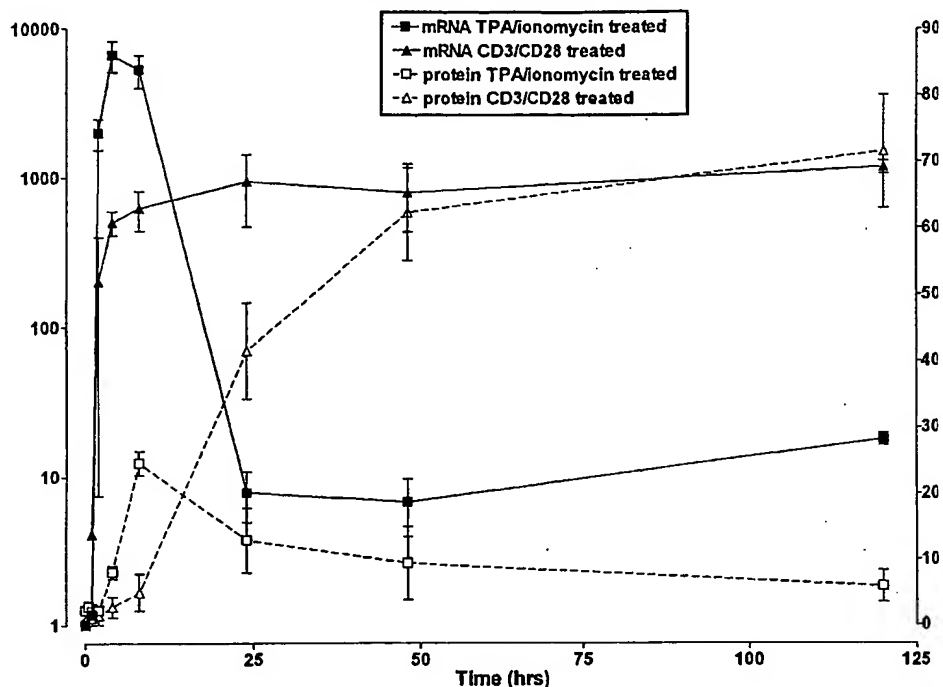


Figure 2 Time course of IL-13 induction. PBMCs were stimulated by TPA/ionomycin and α -CD3/ α -CD28 respectively and harvested after different time points. IL-13 mRNA level were determined using real-time RT-PCR. Levels were normalized to β -actin and unstimulated cells were set to 1. IL-13 protein was determined in the supernatant by ELISA. Each point and bar represents mean \pm s.e.mean of three different volunteers. Similar results were obtained in three independent experiments.

effect of dexamethasone with that of TLCK (Figure 6). It inhibited IL-13 induced by TPA/ionomycin in low nanomolar concentrations (Figure 6a). Furthermore, dexamethasone inhibited α -CD3/ α -CD28 mediated IL-13 induction with similar effectiveness (Figure 6b).

Effects of the MAPK inhibitors

It has been shown that different MAP kinases are involved in signalling events downstream of the TCR. We analysed the effects of two inhibitors of two different MAP kinases. SB 203580 is a specific inhibitor of the p38 MAP kinase pathway. It did not inhibit TPA/ionomycin-induced IL-13 synthesis at concentrations up to $10 \mu\text{M}$ (Figure 7a). Higher concentrations have been reported to cause unspecific inhibition of other kinases (Lali *et al.*, 2000). Only α -CD3/ α -CD28 induced IL-13 was inhibited to some extent at $10 \mu\text{M}$ (Figure 7b). U0126 is a specific inhibitor of the MEK-ERK pathway. It inhibited IL-13 dose dependently after stimulation by TPA/ionomycin (Figure 8a). In contrast, after stimulation with α -CD3/ α -CD 28, this compound inhibited IL-13 synthesis only at the highest concentration of $10 \mu\text{M}$.

Comparison of IC_{50} with $CD4^+$ T cells

To compare the different compounds, we calculated IC_{50} s from the experiments shown above where possible (Table 1). There was no apparent dose-dependent inhibition by SB 203580 and TLCK to calculate IC_{50} values for these compounds. The IC_{50} s for CsA and FK-506 after TPA/ionomycin stimulation are very similar for mRNA and protein. In sharp contrast, IL-13 is stimulated by these

calcineurin inhibitors after α -CD3/ α -CD28 stimulation. Dexamethasone is effective for both stimuli with similar affinity. In contrast the MAPK inhibitor, U0126 seems to inhibit the IL-13 protein release more effectively than the mRNA induction for both stimulation conditions. Since PBMC are a heterogeneous cell population, we also determined IC_{50} s for these compounds in purified human $CD4^+$ T cells. Due to the smaller amount of cells available, we focused on the mRNA level. Whereas the inhibition by CsA and FK-506 was similar for TPA/ionomycin, the stimulatory effect for α -CD3/ α -CD28 stimulation was abolished in $CD4^+$ T cells. The IC_{50} s are similar to the IC_{50} s for TPA/ionomycin stimulation. Dexamethasone showed similar IC_{50} s for PBMCs and $CD4^+$ T cells at both stimulation conditions. In contrast, for U0126 we observed at least 4 fold lower IC_{50} s in $CD4^+$ T cells after TPA/ionomycin stimulation. Furthermore, α -CD3/ α -CD28 stimulated IL-13 synthesis, resistant in PBMCs, was very effectively inhibited by U0126 in $CD4^+$ T cells.

Effect of U0126 in a rat model of asthma: late-phase eosinophilia

The finding that U0126 very effectively inhibits IL-13 in $CD4^+$ T cells prompted us to investigate whether this inhibitor may be active in an animal model of allergic asthma. Brown Norway rats were actively sensitized to ovalbumin and challenged by inhalation of ovalbumin. The inhibition by U0126 compared to CsA of the influx of eosinophils into the lung is shown in Table 2. Intraperitoneally administration of U0126 inhibited dose-dependently the accumulation of eosinophils in the tracheoalveolar lumen. The higher dose of 10 mg kg^{-1} significantly inhibited

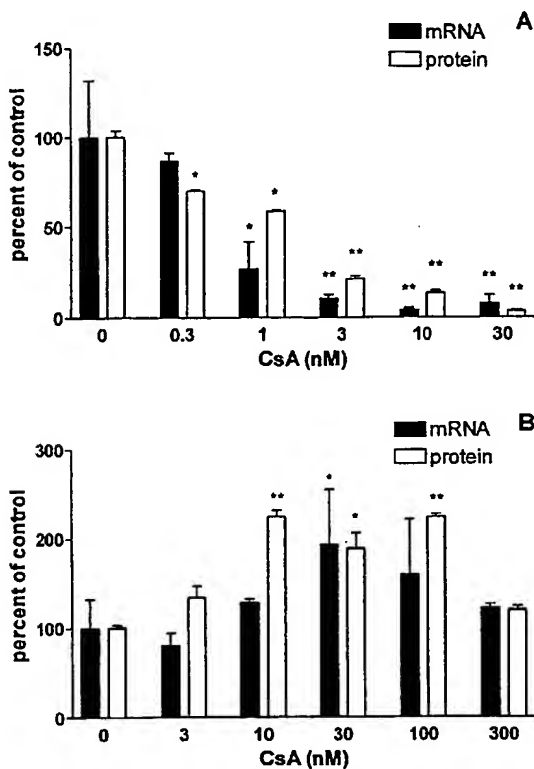


Figure 3 Effect of CsA on IL-13 induction. PBMCs were preincubated with different doses of CsA for 30 min. Then cells were stimulated either with TPA/ionomycin (a) or with α -CD3/ α -CD28 (b) for 4 h for mRNA determination and 24 h for protein determination respectively. Cytokine mRNA level were determined using real-time RT-PCR and were normalized to β -actin. Protein was determined in the supernatant by ELISA. Stimulated cells treated with DMSO were used as 100% control. Each column represents mean \pm s.e.mean of three replicate measurements of one donor. This experiment is one representative for three different donors. * P < 0.05, ** P < 0.01 (vs control).

eosinophil influx (Table 2). The reference compound CsA also reduced the presence of eosinophils in the BAL. Its IC_{50} was about 3 mg kg^{-1} . Since the reduction of eosinophils may be due to a mechanism different to the inhibition of IL-13, we analysed expression of IL-13 in BAL *in vivo*. As shown in Figure 9, BAL cells from OVA-sensitized rats produced IL-13 in response to OVA. Production of IL-13 in BAL was significantly reduced in mice treated with CsA 30 mg kg^{-1} and U0126 10 mg kg^{-1} .

Discussion

IL-13 is an important mediator of immunological diseases such as asthma. In this study, we have examined the induction and regulation of IL-13 in human PBMCs and CD4 $^{+}$ T cells. Different combinations of mitogenic and surface receptor stimulating antibodies were able to induce IL-13 synthesis. TPA/ionomycin caused most efficient stimulation of IL-13 both at mRNA and protein level. α -CD3 and α -CD28 stimulation increased IL-13 mRNA and protein more slowly than did TPA/ionomycin. We investigated the effects of pharmacological agents inhibiting three

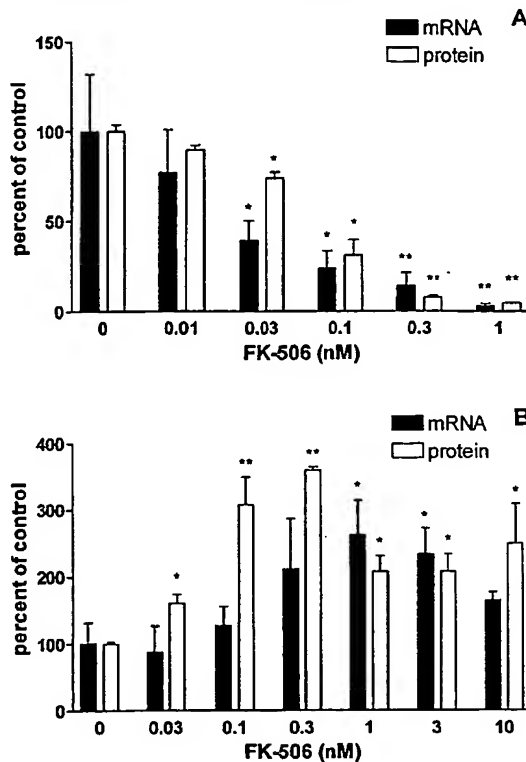


Figure 4 Effect of FK-506 on IL-13 induction. PBMCs were preincubated with different doses of FK-506 for 30 min. Then cells were stimulated either with TPA/ionomycin (a) or with α -CD3/ α -CD28 (b) for 4 h for mRNA determination and 24 h for protein determination respectively. Cytokine mRNA level were determined using real-time RT-PCR and were normalized to β -actin. Protein was determined in the supernatant by ELISA. Stimulated cells treated with DMSO were used as 100% control. Each column represents mean \pm s.e.mean of three replicate measurements of one donor. This experiment is one representative for three different donors. * P < 0.05, ** P < 0.01 (vs control).

different signalling cascades on IL-13 induced by α -CD3/ α -CD28 or TPA/ionomycin: (1) the calcineurin inhibiting immunosuppressants CsA and FK-506; (2) NF- κ B inhibitors TLCK and dexamethasone; (3) MAPK inhibitors SB 203580 and U0126. Using these drugs, we were able to elucidate signalling pathways leading to IL-13 synthesis. After comparing the effects of these drugs on PBMCs with pure human CD4 $^{+}$ T cells, we found that U0126 was at least 10 times more potent in inhibiting IL-13 in CD4 $^{+}$ T cells compared to PBMCs. Finally, we tested this drug in an animal model of asthma in which U0126 was able to reduce the influx of eosinophils into the lungs of sensitized and challenged rats.

The combination of two different stimulating agents increased the IL-13 levels more when compared to the additive effect of the corresponding single stimuli. This indicates a synergistic effect on T cell activation as has been observed for other cytokines such as IL-2 as well (Truneh *et al.*, 1985; van Lier *et al.*, 1988). IL-13 protein levels in the supernatant correlated very well ($r^2 = 0.94$) with mRNA levels excluding post-transcriptional effects during the induction of IL-13. The combination of TPA and ionomycin caused the highest level of IL-13. In contrast, TPA alone is a poor stimulus. It has been shown that TPA is also insufficient to

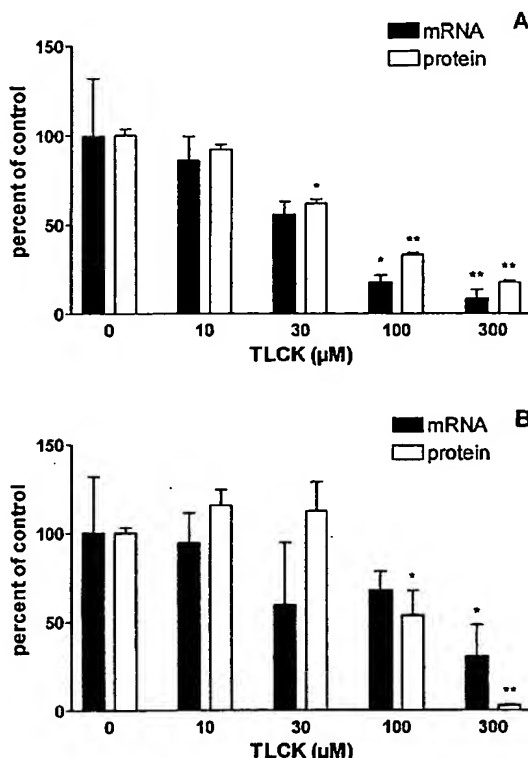


Figure 5 Effect of TLCK on IL-13 induction. PBMCs were preincubated with different doses of TLCK for 30 min. Then cells were stimulated either with TPA/ionomycin (a) or with α -CD3/ α -CD28 (b) for 4 h for mRNA determination and 24 h for protein determination respectively. Cytokine mRNA level were determined using real-time RT-PCR and were normalized to β -actin. Protein was determined in the supernatant by ELISA. Stimulated cells treated with DMSO were used as 100% control. Each column represents mean \pm s.e. mean of three replicate measurements of one donor. This experiment is one representative for three different donors. * P < 0.05, ** P < 0.01 (vs control).

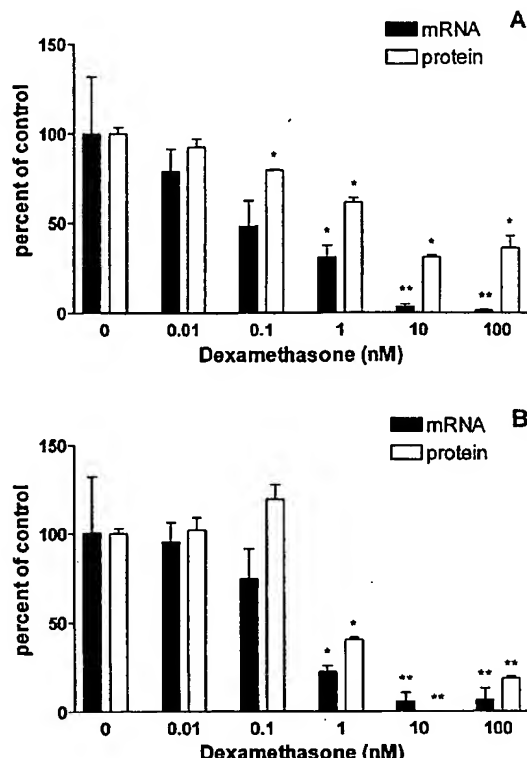


Figure 6 Effect of dexamethasone on IL-13 induction. PBMCs were preincubated with different doses of dexamethasone for 30 min. Then cells were stimulated either with TPA/ionomycin (a) or with α -CD3/ α -CD28 (b) for 4 h for mRNA determination and 24 h for protein determination respectively. Cytokine mRNA level were determined using real-time RT-PCR and were normalized to β -actin. Protein was determined in the supernatant by ELISA. Stimulated cells treated with DMSO were used as 100% control. Each column represents mean \pm s.e. mean of three replicate measurements of one donor. This experiment is one representative for three different donors. * P < 0.05, ** P < 0.01 (vs control).

stimulate IL-4 synthesis in T cells (Boothby *et al.*, 2001). In contrast, ionomycin is a very potent IL-4 inducer (Paliogianni *et al.*, 1996) whereas it was insufficient to induce IL-13 (not shown). In contrast, using ionomycin together with α -CD3 proved to be very potent, reaching similar levels to those attained by stimulation with α -CD3/ α -CD28.

Time course experiments revealed that TPA/ionomycin induced a rapid and transient increase of IL-13 mRNA and protein levels. With TPA/ionomycin, IL-13 mRNA peaked at 4 h, whereas the protein peak occurred at 8 h. Stimulation with α -CD3/ α -CD28 caused a much slower increase which remained at high levels throughout the observation period. Similar kinetics have been observed for IL-2 (Herold *et al.*, 1986).

CsA and FK-506 strongly inhibited IL-13 induced by TPA/ionomycin both at mRNA and protein level. However, these substances enhanced gene expression and protein production after stimulation with α -CD3/ α -CD28. The enhancing effect of CsA on IL-13 synthesis after this kind of stimulation has been reported earlier for a drug concentration of 100 ng ml⁻¹ (van der Pouw Kraan *et al.*, 1996). Dumont, (1997) reports a stimulatory effect of FK-506 on PBMCs stimulated by α -CD3/ α -CD28. We also observe a stimulatory effect of FK-506 at similar concentrations. Since both drugs cause the

same effect, the common target of CsA and FK-506, calcineurin, probably mediates this effect. Supporting this hypothesis, we found that rapamycin, while binding to the same receptor as FK-506, does not enhance IL-13 levels (data not shown). Surprisingly, this stimulation could not be observed in pure human CD4⁺ T cells. In these cells, CsA and FK-506 were effective inhibitors. These findings lead to the hypothesis that CD8⁺ T cells, NK cells or B cells are responsible for the induction of IL-13 after CsA or FK-506 treatment and stimulation with α -CD3/ α -CD28. In contrast, the calcium \rightarrow calcineurin \rightarrow NF-AT pathway seems to be important for induction of IL-13 in CD4⁺ T cells. IL-2 stimulation with α -CD3/ α -CD28 has been reported to be resistant to CsA (June *et al.*, 1987). IFN γ production is also enhanced by CsA after α -CD3/ α -CD28 stimulation (Rafiq *et al.*, 1998). Testing a single dose of FK-506 Dumont *et al.* (1998b) reported after α -CD3/ α -CD28 stimulation the enhancement of IFN γ , IL-5 and GM-CSF synthesis and the inhibition of IL-2, IL-3 and IL-4 synthesis by this drug. These results indicate that α -CD3/ α -CD28 stimulation activates a number of different signalling pathways of which only some are necessary for activation of cytokines such as IL-2, IFN γ and IL-13.

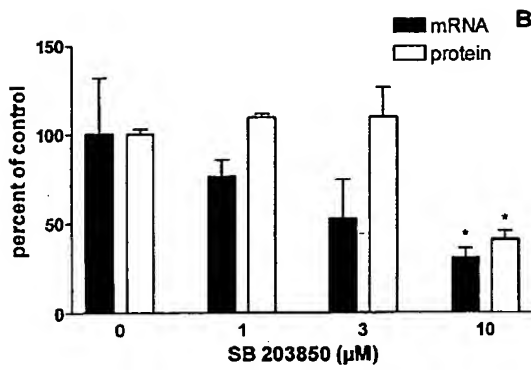
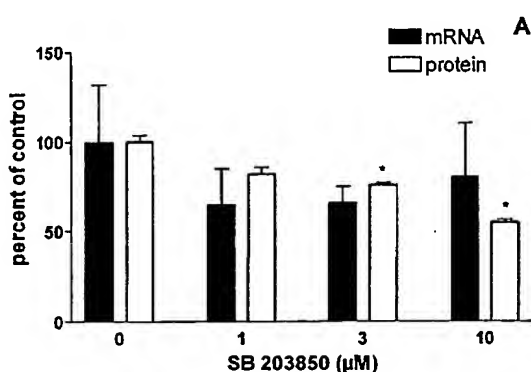


Figure 7 Effect of SB 203850 on IL-13 induction. PBMCs were preincubated with different doses of SB 203850 for 30 min. Then cells were stimulated either with TPA/ionomycin (a) or with α -CD3/ α -CD28 (b) for 4 h for mRNA determination and 24 h for protein determination respectively. Cytokine mRNA level were determined using real-time RT-PCR and were normalized to β -actin. Protein was determined in the supernatant by ELISA. Stimulated cells treated with DMSO were used as 100% control. Each column represents mean \pm s.e. mean of three replicate measurements of one donor. This experiment is one representative for three different donors. * P < 0.05, ** P < 0.01 (vs control).

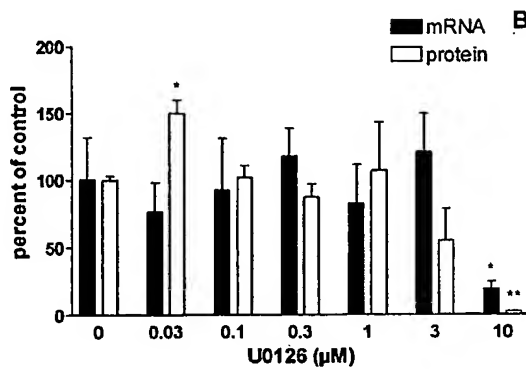
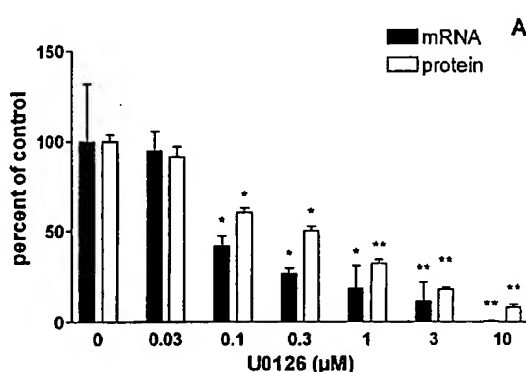


Figure 8 Effect of U0126 on IL-13 induction. PBMCs were preincubated with different doses of U0126 for 30 min. Then cells were stimulated either with TPA/ionomycin (a) or with α -CD3/ α -CD28 (b) for 4 h for mRNA determination and 24 h for protein determination respectively. Cytokine mRNA level were determined using real-time RT-PCR and were normalized to β -actin. Protein was determined in the supernatant by ELISA. Stimulated cells treated with DMSO were used as 100% control. Each column represents mean \pm s.e. mean of three replicate measurements of one donor. This experiment is one representative for three different donors. * P < 0.05, ** P < 0.01 (vs control).

Table 1 IC₅₀ values for the inhibition of IL-13 mRNA and protein synthesis by different drugs

Stimulation	PBMC		CD4 ⁺		PBMC		CD4 ⁺	
	TPA/ionomycin mRNA	TPA/ionomycin Protein	TPA/ionomycin mRNA	TPA/ionomycin mRNA	α -CD3/ α -CD28 mRNA	α -CD3/ α -CD28 Protein	α -CD3/ α -CD28 mRNA	
CsA (nM)	0.80 \pm 0.46	3.69 \pm 2.70	0.23 \pm 0.01	stimulation	stimulation	stimulation	2.18 \pm 1.28	
FK-506 (nM)	0.045 \pm 0.004	0.05 \pm 0.03	0.045 \pm 0.010	stimulation	stimulation	stimulation	0.180 \pm 0.014	
Dexamethasone (nM)	1.46 \pm 0.37	1.02 \pm 0.83	1.20 \pm 0.02	2.30 \pm 2.24	0.89 \pm 0.14	0.89 \pm 0.14	0.54 \pm 0.41	
U0126 (nM)	812 \pm 1065	515 \pm 189	200.6 \pm 100.5	> 5000	646 \pm 364	646 \pm 364	63 \pm 57	

Data shown are mean IC₅₀ \pm s.e. mean of at least three different donors.

TLCK is a proteasome inhibitor which inhibits the NF- κ B activation via the inhibition of I- κ B degradation (Kim *et al.*, 1995). It inhibited TPA/ionomycin induced IL-13 effectively but only at highest concentration after stimulation with α -CD3/ α -CD28. Our findings that TPA is an efficient IL-13 stimulus and that TLCK inhibits this induction is consistent with reports describing the activation of NF- κ B by TPA in T cells (Lin *et al.*, 2000; Sun *et al.*, 2000). Stimulation with α -CD3/ α -CD28 also activates NF- κ B at least via PKCs (Lin *et al.*, 2000; Sun *et al.*, 2000). The resistance of this kind of

stimulation to TLCK hints at activation of further signalling cascades leading to NF- κ B activation compared to stimulation by TPA/ionomycin.

Dexamethasone was also used as an NF- κ B inhibitor, because two of its major mechanisms are induction of I- κ B and direct inhibition of NF- κ B (Dumont *et al.*, 1998a). Nevertheless, other mechanisms of action have been reported (Beato & Klug, 2000). This is supported by our study: dexamethasone was able to inhibit α -CD3/ α -CD28-induced IL-13 synthesis whereas TLCK could not. Dexamethasone

Table 2 Inhibition of late phase eosinophilia in Brown-Norway rats

Substance	Dose (mg kg ⁻¹)	% Inhibition x
U0126	5	18
	10	44*
Cyclosporin A	1	12
	5	70*
	30	99*

Actively sensitized rats were challenged by ovalbumin inhalation. Compounds were given intraperitoneally 2 h prior to ovalbumin challenge. After 48 h, numbers of eosinophils in bronchoalveolar lavage were determined. Vehicle-treated animals were set to 100%, x = mean of at least five animals. *P < 0.05 as compared to vehicle-treated animals.

seems to inhibit further signalling pathways induced by this kind of stimulation. The transcription of IL-2 is inhibited by dexamethasone via the inhibition of AP-1 (Paliogianni *et al.*, 1993). Stimulation by α -CD28 has been reported to activate a CD28RE in the IL-2 promoter. Conflicting results have been published concerning transcription factors binding to this element (Harhaj & Sun, 1998; Kempf *et al.*, 1999). It is most likely that binding of transactivators to this element is inhibited by dexamethasone, which explains its inhibitory effect on both kinds of stimulation. The IC₅₀ for dexamethasone is similar for PBMCs and CD4⁺ T cells, indicating that the mechanism in the two cell systems is similar.

Three different kinds of MAPKs have been described in mammalian cells. These are ERK, JNK and p38 kinase (Su *et al.*, 1996). ERK, JNK and p38 pathways have all been shown to play a critical role in the events leading to activation and increased IL-2 production in T cells stimulated by TPA/ionomycin or α -CD3/ α -CD28 (DeSilva *et al.*, 1997; Su *et al.*, 1996; Whitehurst & Geppert, 1996). Unfortunately, no JNK inhibitor is publicly available. Previous studies of p38 MAP kinase in Jurkat human T cells line (Matsuda *et al.*, 1998), human purified T cell (Koprak *et al.*, 1999), CD4⁺ subset (Schafer *et al.*, 1999) and mouse T cell clones (Zhang *et al.*, 1999) clearly demonstrated the involvement of p38 MAP kinase in the cell activation through TCR and CD28 costimulation signal pathways. However, little is known about this MAP kinase in human primary peripheral blood leukocytes. In CD45RO⁺ T cells the p38 inhibitor SB 203580 inhibited only IL-4 production whereas IL-2 was unaffected (Schafer *et al.*, 1999). We observed that SB 203580 inhibited IL-13 gene expression by 40% in human PBMC stimulated with TPA/ionomycin or α -CD3/ α -CD28. Therefore, IL-13 production is largely p38-independent but this kinase is required for maximal expression. Koprak *et al.* (1999) reported that SB 203850 inhibited IL-13 only on protein level, but had no effect on mRNA level. This difference is most likely due to different experimental protocols and the use of a different T cell population.

U0126 is a specific MEK kinase inhibitor. MEK phosphorylates ERK and by this U0126 is a specific inhibitor of the ERK pathway. We determined the influence of this drug on IL-13 gene expression and protein production. Our results indicate that U0126 inhibited IL-13 very potently after stimulation with TPA/ionomycin. In contrast, stimulation by

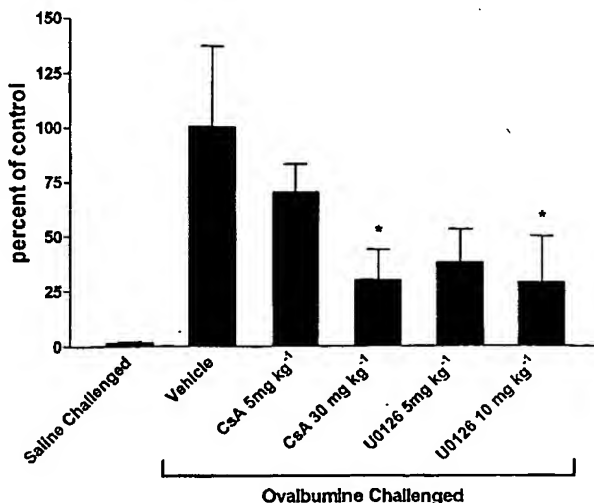


Figure 9 Effect of U0126 on IL-13 production in BAL cells. Actively sensitized rats were challenged by ovalbumin or saline inhalation. Compounds were given intraperitoneally 2 h prior to ovalbumin challenge. After 48 h, cells were recovered from bronchoalveolar lavage by centrifugation and RNA was prepared from the cell pellet. IL-13 mRNA level were determined using real-time RT-PCR and were normalized to β -actin. OVA challenged vehicle-treated animals were set to 100%. Each column represents mean \pm s.e. of at least five animals. *P < 0.05 (versus OVA challenged vehicle control).

α -CD3/ α -CD28 was resistant to U0126. Inhibition at 10 μ M may be due to non-specific actions on other kinases. Only a few studies have been published about the effect of this drug on other cytokines. At 10 μ M, it inhibited IL-2 mRNA induction in a murine T cell clone (DeSilva *et al.*, 1998). Surprisingly, investigation of pure human CD4⁺ T cells revealed that in these cells U0126 was 4 fold more effective in inhibiting IL-13 synthesis after TPA/ionomycin stimulation. Furthermore, α -CD3/ α -CD28 stimulated IL-13 synthesis, resistant in PBMCs to this drug, was highly sensitive to U0126 in these cells. These results indicate that the MEK \rightarrow ERK pathway plays a pivotal role in regulating IL-13 production after TPA/ionomycin and α -CD3/ α -CD28 stimulation in human CD4⁺ T cells. PBMCs have to contain other cells which are responsible for the resistance to this drug. Hence these cells must possess partially different IL-13 signalling pathways.

The high sensitivity of CD4⁺ T cells to U0126 in respect of IL-13 synthesis prompted us to analyse this drug in an animal model of asthma. It effectively reduced the induction of IL-13 mRNA in BAL cells and the influx of eosinophils into the lungs of sensitized and challenged rats. Only inhibitors of p38 MAPK have been analysed in asthma models so far. The effect of the p38 inhibitor SB 203580 was recently tested in the same animal model. No influence on antigen-induced airway eosinophilia could be observed (Escott *et al.*, 2000). In another study, a second generation p38 inhibitor was found to be effective (Underwood *et al.*, 2000). CsA was a little more effective in reducing airway eosinophilia, but compared to U0126 the affinity of CsA to its receptor is approximately 100 fold higher. Therefore U0126 is more effective on a molecular basis. Although there is no doubt that immunosuppressants such as FK506 and CsA are effective in asthma

treatment, they cannot find a broad practice due to their unacceptable side effects (Corrigan *et al.*, 1996; Khan *et al.*, 2000; Lock *et al.*, 1996; Mori *et al.*, 2000; Sperr *et al.*, 1997). These agents interfere with multiple T cell functions, thereby causing generalized immunosuppression. An agent capable of selectively regulating cytokine synthesis with little effect on other major T cell cytokines would provide an ideal treatment for inflammation without severe side effects including general immunosuppression.

In conclusion, regulation of IL-13 in T cells differs from that of other cytokines such as IL-2 and IL-4. The calcium→calcineurin→NF-AT pathway is important for TPA/ionomycin—as well as α -CD3/ α -CD28-induced IL-13 synthesis. NF- κ B is only important after induction by TPA/ionomycin. The MAP kinase ERK is important for both

Regulation of IL-13 in human T-cells

stimuli while p38 MAPK activation is dispensable. The different regulation can be exploited to find new specifically targeted drugs aimed for diseases where IL-13 plays an important pathophysiological role. We could demonstrate for the first time that inhibition of the MEK–ERK cascade is a therapeutic option for asthma. The specific MEK inhibitor U0126 reduced the influx of eosinophils in an animal model of asthma. The development of more specific IL-13-targeted drugs would support this approach to treating diseases such as asthma.

This study was supported by the German Ministry for Education and Research (Grant no. 0312231 and 0312241).

References

ALTMAN, A., ISAKOV, N. & BAIER, G. (2000). Protein kinase C θ : a new essential superstar on the T-cell stage. *Immunol. Today*, **21**, 567–573.

BAUER, B., KRUMBOECK, N., GHAFFARI-TABRIZI, N., KAMPFER, S., VILLUNGER, A., WILDA, M., HAMEISTER, H., UTERMANN, G., LEITGES, M., UBERALL, F. & BAIER, G. (2000). T cell expressed PKC θ demonstrates cell-type selective function. *Eur. J. Immunol.*, **30**, 3645–3654.

BEATO, M. & KLUG, J. (2000). Steroid hormone receptors: an update. *Hum. Reprod. Update*, **6**, 225–236.

BOOTHBY, M., MORA, A.L., ARONICA, M.A., YOUN, J., SHELLER, J.R., GOENKA, S. & STEPHENSON, L. (2001). IL-4 signaling, gene transcription regulation, and the control of effector T cells. *Immunol. Res.*, **23**, 179–191.

BROMBACHER, F. (2000). The role of interleukin-13 in infectious diseases and allergy. *BioEssays*, **22**, 646–656.

BRUBAKER, J.O. & MONTANER, L.J. (2001). Role of interleukin-13 in innate and adaptive immunity. *Cell. Mol. Biol. (Noisy-le-grand)*, **47**, 637–651.

BUSSE, W.W. & LEMANSKE, JR, R.F. (2001). Advances in immunology—Asthma. *N. Engl. J. Med.*, **344**, 350–362.

CLIPSTONE, N.A. & CRABTREE, G.R. (1992). Identification of Calcineurin as a Key Signalling Enzyme in Lymphocyte-T Activation. *Nature*, **357**, 695–697.

COBB, M.H. & GOLDSMITH, E.J. (1995). How MAP kinases are regulated. *J. Biol. Chem.*, **270**, 14843–14846.

CORRIGAN, C.J., BUNGRE, J.K., ASSOUI, B., COOPER, A.E., SEDDON, H. & KAY, A.B. (1996). Glucocorticoid resistant asthma: T-lymphocyte steroid metabolism and sensitivity to glucocorticoids and immunosuppressive agents. *Eur. Respir. J.*, **9**, 2077–2086.

CORRY, D.B. (1999). IL-13 in allergy: home at last. *Curr. Opin. Immunol.*, **11**, 610–614.

COUDRONNIERE, N., VILLALBA, M., ENGLUND, N. & ALTMAN, A. (2000). NF- κ B activation induced by T cell receptor/CD28 costimulation is mediated by protein kinase C- θ . *Proc. Natl. Acad. Sci. U.S.A.*, **97**, 3394–3399.

CRABTREE, G.R. & CLIPSTONE, N.A. (1994). Signal transmission between the plasma membrane and nucleus of T lymphocytes. *Annu. Rev. Biochem.*, **63**, 1045–1083.

DERIJARD, B., HIBI, M., WU, I.H., BARRETT, T., SU, B., DENG, T., KARIN, M. & DAVIS, R.J. (1994). JNK1: a protein kinase stimulated by UV light and Ha-Ras that binds and phosphorylates the c-Jun activation domain. *Cell*, **76**, 1025–1037.

DE SILVA, D.R., JONES, E.A., FAVATA, M.F., JAFFEE, B.D., MAGOLDA, R.L., TRZASKOS, J.M. & SCHERLE, P.A. (1998). Inhibition of mitogen-activated protein kinase kinase blocks T cell proliferation but does not induce or prevent anergy. *J. Immunol.*, **160**, 4175–4181.

DE SILVA, D.R., JONES, E.A., FEESER, W.S., MANOS, E.J. & SCHERLE, P.A. (1997). The p38 mitogen-activated protein kinase pathway in activated and anergic Th1 cells. *Cell. Immunol.*, **180**, 116–123.

DOUCET, C., BROUTY-BOYE, D., POTTIN-CLEMENCEAU, C., JASMIN, C., CANONICA, G.W. & AZZARONE, B. (1998). IL-4 and IL-13 specifically increase adhesion molecule and inflammatory cytokine expression in human lung fibroblasts. *Int. Immunol.*, **10**, 1421–1433.

DUMONT, A., HEHNER, S.P., SCHMITZ, M.L., GUSTAFSSON, J.A., LIDEN, J., OKRET, S., VAN DER SAAG, P.T., WISSINK, S., VAN DER BURG, B., HERRLICH, P., HAEGEMAN, G., DE BOSSCHER, K. & FIERS, W. (1998a). Cross-talk between steroids and NF- κ B: what language? *Trends Biochem. Sci.*, **23**, 233–235.

DUMONT, F.J. (1997). FK506 enhances IL-13 production by T cells activated through CD3/CD28. *Int. Arch. Allergy Immunol.*, **114**, 300–301.

DUMONT, F.J., STARUCH, M.J., FISCHER, P., DASILVA, C. & CAMACHO, R. (1998b). Inhibition of T cell activation by pharmacologic disruption of the MEK1/ERK MAP kinase or calcineurin signaling pathways results in differential modulation of cytokine production. *J. Immunol.*, **160**, 2579–2589.

ENDO, T., OGUSHI, F., KAWANO, T. & SONE, S. (1998). Comparison of the regulations by Th2-type cytokines of the arachidonic-acid metabolic pathway in human alveolar macrophages and monocytes. *Am. J. Respir. Cell. Mol. Biol.*, **19**, 300–307.

ESCOTT, K.J., BELVISI, M.G., BIRRELL, M.A., WEBBER, S.E., FOSTER, M.L. & SARGENT, C.A. (2000). Effect of the p38 kinase inhibitor, SE 203580, on allergic airway inflammation in the rat. *Br. J. Pharmacol.*, **131**, 173–176.

FESKE, S., DRAEGER, R., PETER, H.H., EICHMANN, K. & RAO, A. (2000). The duration of nuclear residence of NFAT determines the pattern of cytokine expression in human SCID T cells. *J. Immunol.*, **165**, 297–305.

FOLETTA, V.C., SEGAL, D.H. & COHEN, D.R. (1998). Transcriptional regulation in the immune system: all roads lead to AP-1. *J. Leukoc. Biol.*, **63**, 139–152.

GRUENIG, G., WARNOCK, M., WAKIL, A.E., VENKAYYA, R., BROMBACHER, F., RENNICK, D.M., SHEPPARD, D., MOHRS, M., DONALDSON, D.D., LOCKSLEY, R.M. & CORRY, D.B. (1998). Requirement for IL-13 independently of IL-4 in experimental asthma. *Science*, **282**, 2261–2263.

HARAHJ, E.W. & SUN, S.C. (1998). IkappaB kinases serve as a target of CD28 signaling. *J. Biol. Chem.*, **273**, 25185–25190.

HEROLD, K.C., LANCKI, D.W., DUNN, D.E., ARAI, K. & FITCH, F.W. (1986). Activation of lymphokine genes during stimulation of cloned T cells. *Eur. J. Immunol.*, **16**, 1533–1538.

HORIE, S., OKUBO, Y., HOSSAIN, M., SATO, E., NOMURA, H., KOYAMA, S., SUZUKI, J., ISOBE, M. & SEKIGUCHI, M. (1997). Interleukin-13 but not interleukin-4 prolongs eosinophil survival and induces eosinophil chemotaxis. *Intern. Med.*, **36**, 179–185.

HUANG, S.K., XIAO, H.Q., KLEINE-TEBBE, J., PACIOTTI, G., MARSH, D.G., LICHTENSTEIN, L.M. & LIU, M.C. (1995). IL-13 expression at the sites of allergen challenge in patients with asthma. *J. Immunol.*, **155**, 2688–2694.

HUGHES, C.C. & POBER, J.S. (1996). Transcriptional regulation of the interleukin-2 gene in normal human peripheral blood T cells. Convergence of costimulatory signals and differences from transformed T cells. *J. Biol. Chem.*, **271**, 5369–5377.

HUMBERT, M., DURHAM, S.R., KIMMITT, P., POWELL, N., ASSOUFI, B., PFISTER, R., MENZ, G., KAY, A.B. & CORRIGAN, C.J. (1997). Elevated expression of messenger ribonucleic acid encoding IL-13 in the bronchial mucose of atopic and nonatopic subjects with asthma. *J. Allergy Clin. Immunol.*, **99**, 657–665.

IZQUIERDO, M., LEEVERS, S.J., MARSHALL, C.J. & CANTRELL, D. (1993). p21ras couples the T cell antigen receptor to extracellular signal-regulated kinase 2 in T lymphocytes. *J. Exp. Med.*, **178**, 1199–1208.

JAIN, J.N., MCCAFFREY, P.G., MINER, Z., KERPPOLA, T.K., LAMBERT, J.N., VERDINE, G.L., CURRAN, T. & RAO, A. (1993). The T-Cell Transcription Factor NFAT(p) Is a Substrate for Calcineurin and Interacts with Fos and Jun. *Nature*, **365**, 352–355.

JELINEK, T., CATLING, A.D., REUTER, C.W., MOODIE, S.A., WOLFMAN, A. & WEBER, M.J. (1994). RAS and RAF-1 form a signalling complex with MEK-1 but not MEK-2. *Mol. Cell. Biol.*, **14**, 8212–8218.

JUNE, C.H., LEDBETTER, J.A., GILLESPIE, M.M., LINDSTEN, T. & THOMPSON, C.B. (1987). T-cell proliferation involving the CD28 pathway is associated with cyclosporine-resistant interleukin 2 gene expression. *Mol. Cell. Biol.*, **7**, 4472–4481.

KASER, A., MOLNAR, C. & TILG, H. (1998). Differential regulation of interleukin 4 and interleukin 13 production by interferon alpha. *Cytokine*, **10**, 75–81.

KAY, A.B. (2001). Advances in immunology—Allergy and allergic diseases—Second of two parts. *N. Engl. J. Med.*, **344**, 109–113.

KEMPIAKI, S.J., HIURA, T.S. & NEL, A.E. (1999). The Jun kinase cascade is responsible for activating the CD28 response element of the IL-2 promoter: proof of cross-talk with the I kappa B kinase cascade. *J. Immunol.*, **162**, 3176–3187.

KHAN, L.N., KON, O.M., MACFARLANE, A.J., MENG, Q., YING, S., BARNES, N.C. & KAY, A.B. (2000). Attenuation of the allergen-induced late asthmatic reaction by cyclosporine A is associated with inhibition of bronchial eosinophils, interleukin-5, granulocyte macrophage colony-stimulating factor, and eotaxin. *Am. J. Respir. Crit. Care Med.*, **162**, 1377–1382.

KIM, H., LEE, H.S., CHANG, K.T., KO, T.H., BAEK, K.J. & KWON, N.S. (1995). Chloromethyl ketones block induction of nitric oxide synthase in murine macrophages by preventing activation of nuclear factor-kappa B. *J. Immunol.*, **154**, 4741–4748.

KOPRAK, S., STARUCH, M.J. & DUMONT, F.J. (1999). A specific inhibitor of the p38 mitogen activated protein kinase affects differentially the production of various cytokines by activated human T cells: dependence on CD28 signalling and preferential inhibition of IL-10 production. *Cell Immunol.*, **192**, 87–95.

LALI, F.V., HUNT, A.E., TURNER, S.J. & FOXWELL, B.M.J. (2000). The pyridinyl imidazole inhibitor SB203580 blocks phosphoinositide-dependent protein kinase activity, protein kinase B phosphorylation, and retinoblastoma hyperphosphorylation in interleukin-2-stimulated T cells independently of p38 mitogen-activated protein kinase. *J. Biol. Chem.*, **275**, 7395–7402.

LEEVERS, S.J., PATERSON, H.F. & MARSHALL, C.J. (1994). Requirement for Ras in Raf activation is overcome by targeting Raf to the plasma membrane. *Nature*, **369**, 411–414.

LIN, X., O'MAHONY, A., MU, Y.J., GELEZUNAS, R. & GREENE, W.C. (2000). Protein kinase C-theta participates in NF-kappaB activation induced by CD3-CD28 costimulation through selective activation of IkappaB kinase beta. *Mol. Cell. Biol.*, **20**, 2933–2940.

LIOU, H.C., JIN, Z., TUMANG, J., ANDJELIC, S., SMITH, K.A. & LIOU, M.L. (1999). c-Rel is crucial for lymphocyte proliferation but dispensable for T cell effector function. *Int. Immunol.*, **11**, 361–371.

LOCK, S.H., KAY, A.B. & BARNES, N.C. (1996). Double-blind, placebo-controlled study of cyclosporin A as a corticosteroid-sparing agent in corticosteroid-dependent asthma. *Am. J. Respir. Crit. Care Med.*, **153**, 509–514.

MATSUDA, S., MORIGUCHI, T., KOYASU, S. & NISHIDA, E. (1998). T lymphocyte activation signals for interleukin-2 production involve activation of MKK6-p38 and MKK7-SAPK/JNK signalling pathways sensitive to cyclosporin A. *J. Biol. Chem.*, **273**, 12378–12382.

MORI, A., KAMINUMA, O., OGAWA, K., NAKATA, A., EGAN, R.W., AKIYAMA, K. & OKUDAIRA, H. (2000). Control of IL-5 production by human helper T cells as a treatment for eosinophilic inflammation: Comparison of in vitro and in vivo effects between selective and nonselective cytokine synthesis inhibitors. *J. Allergy Clin. Immunol.*, **106**, S58–S64.

PALIOGIANNI, F., HAMA, N., MAVROTHALASSITIS, G.J., THY-PHRONITIS, G. & BOUMPAS, D.T. (1996). Signal requirements for interleukin 4 promoter activation in human T cells. *Cell Immunol.*, **168**, 33–38.

PALIOGIANNI, F., RAPTIS, A., AHUJA, S.S., NAJJAR, S.M. & BOUMPAS, D.T. (1993). Negative transcriptional regulation of human interleukin 2 (IL-2) gene by glucocorticoids through interference with nuclear transcription factors AP-1 and NF-AT. *J. Clin. Invest.*, **91**, 1481–1489.

PRICE, M.A., CRUZALEGUI, F.H. & TREISMAN, R. (1996). The p38 and ERK MAP kinase pathways cooperate to activate Ternary Complex Factors and c-fos transcription in response to UV light. *EMBO J.*, **15**, 6552–6563.

RAFIQ, K., KASRAN, A., PENG, X.H., WARMERDAM, P.A.M., COOREVITS, L., CEUPPENS, J.L. & VAN GOOL, S.W. (1998). Cyclosporin A increases IFN-gamma production by T cells when co-stimulated through CD28. *Eur. J. Immunol.*, **28**, 1481–1491.

SCHAFFER, P.H., WADSWORTH, S.A., WANG, L.W. & SIEKIERKA, J.J. (1999). p38alpha mitogen-activated protein kinase is activated by CD28-mediated signalling and is required for IL-4 production by human CD4+CD45RO+ T cells and Th2 effector cells. *J. Immunol.*, **162**, 7110–7119.

SORNASSE, T., LARENAS, P.V., DAVIS, K.A., DE VRIES, J.E. & YSEL, H. (1996). Differentiation and stability of T helper 1 and 2 cells derived from naive human neonatal CD4+ T cells, analyzed at the single-cell level. *J. Exp. Med.*, **184**, 473–483.

SPERR, W.R., AGIS, H., SEMPER, H., VALENTE, R., SUSANI, M., SPERR, M., WILLHEIM, M., SCHEINER, O., LIEHL, E., LECHNER, K. & VALENT, P. (1997). Inhibition of allergen-induced histamine release from human basophils by cyclosporine A and FK-506. *Int. Arch. Allergy Immunol.*, **114**, 68–73.

SU, B. & KARIN, M. (1996). Mitogen-activated protein kinase cascades and regulation of gene expression. *Curr. Opin. Immunol.*, **8**, 402–411.

SUN, Z.M., ARENDT, C.W., ELLMEIER, W., SCHAEFFER, E.M., SUNSHINE, M.J., GANDHI, L., ANNES, J., PETRZILKA, D., KUPFER, A., SCHWARTZBERG, P.L. & LITTMAN, D.R. (2000). PKC-theta is required for TCR-induced NF-kappaB activation in mature but not immature T lymphocytes. *Nature*, **404**, 402–407.

TRUNEH, A., ALBERT, F., GOLSTEIN, P. & SCHMITT-VERHULST, A.M. (1985). Early steps of lymphocyte activation bypassed by synergy between calcium ionophores and phorbol ester. *Nature*, **313**, 318–320.

TRUSHIN, S.A., PENNINGTON, K.N., ALGECIRAS-SCHIMNICH, A. & PAYA, C.V. (1999). Protein kinase C and calcineurin synergize to activate IkappaB kinase and NF-kappaB in T lymphocytes. *J. Biol. Chem.*, **274**, 22923–22931.

UNDERWOOD, D.C., OSBORN, R.R., KOTZER, C.J., ADAMS, J.L., LEE, J.C., WEBB, E.F., CARPENTER, D.C., BOCHNOWICZ, S., THOMAS, H.C., HAY, D.W. & GRISWOLD, D.E. (2000). SB 239063, a potent p38 MAP kinase inhibitor, reduces inflammatory cytokine production, airways eosinophil infiltration, and persistence. *J. Pharmacol. Exp. Ther.*, **293**, 281–288.

URBAN JR., J.F., NOBEN-TRAUTH, N., DONALDSON, D.D., MADDEN, K.B., MORRIS, S.C., COLLINS, M. & FINKELMAN, F.D. (1998). IL-13, IL-4Ralpha, and Stat6 are required for the expulsion of the gastrointestinal nematode parasite *Nippostrongylus brasiliensis*. *Immunity*, **8**, 255–264.

VAN DER POUW KRAAN, T.C., BOEIJE, L.C., TROON, J.T., RUTSCHMANN, S.K., WIJDENES, J. & AARDEN, L.A. (1996). Human IL-13 production is negatively influenced by CD3 engagement. Enhancement of IL-13 production by cyclosporin A. *J. Immunol.*, **156**, 1818–1823.

VAN LIER, R.A., BROUWER, M. & AARDEN, L.A. (1988). Signals involved in T cell activation. T cell proliferation induced through the synergistic action of anti-CD28 and anti-CD2 monoclonal antibodies. *Eur. J. Immunol.*, **18**, 167–172.

VITA, N., LEFORT, S., LAURENT, P., CAPUT, D. & FERRARA, P. (1995). Characterization and comparison of the interleukin 13 receptor with the interleukin 4 receptor on several cell types. *J. Biol. Chem.*, **270**, 3512–3517.

WEISS, A. & LITTMAN, D.R. (1994). Signal transduction by lymphocyte antigen receptors. *Cell*, **76**, 263–274.

WESSELBORG, S., FRUMAN, D.A., SAGOO, J.K., BIERER, B.E. & BURAKOFF, S.J. (1996). Identification of a physical interaction between calcineurin and nuclear factor of activated T cells (NFATp). *J. Biol. Chem.*, **271**, 1274–1277.

WHITEHURST, C.E. & GEPPERT, T.D. (1996). MEK1 and the extracellular signal-regulated kinases are required for the stimulation of IL-2 gene transcription in T cells. *J. Immunol.*, **156**, 1020–1029.

WILLS-KARP, M., LUYIMBAZI, J., XU, X.Y., SCHOFIELD, B., NEBEN, T.Y., KARP, C.L. & DONALDSON, D.D. (1998). Interleukin-13: Central mediator of allergic asthma. *Science*, **282**, 2258–2261.

ZHANG, J., SALOJIN, K.V., GAO, J.X., CAMERON, M.J., BERGEROT, I. & DELOVITCH, T.L. (1999). p38 mitogen-activated protein kinase mediates signal integration of TCR/CD28 costimulation in primary murine T cells. *J. Immunol.*, **162**, 3819–3829.

ZUND, G., MADARA, J.L., DZUS, A.L., AWTREY, C.S. & COLGAN, S.P. (1996). Interleukin-4 and interleukin-13 differentially regulate epithelial chloride secretion. *J. Biol. Chem.*, **271**, 7460–7464.

(Received November 9, 2001)

Revised February 5, 2002

Accepted February 7, 2002)

Activation of mitogen-activated protein kinases and p90 ribosomal S6 kinase in failing human hearts with dilated cardiomyopathy

Yasuchika Takeishi^{a,*}, Qunhua Huang^{b,1}, Jun-ichi Abe^{b,1}, Wenyi Che^b, Jiing-Dwan Lee^c, Hisaaki Kawakatsu^d, Brian D. Hoit^a, Bradford C. Berk^b, Richard A. Walsh^a

^aDepartment of Medicine, Case Western Reserve University, Cleveland, OH 44106-5029, USA

^bCenter for Cardiovascular Research, University of Rochester, Rochester, NY 14642, USA

^cDepartment of Immunology, The Scripps Research Institute, La Jolla, CA 92037, USA

^dLung Biology Center, University of California at San Francisco, San Francisco, CA 94143, USA

Received 19 March 2001; accepted 2 August 2001

Abstract

Objective: A new member of the MAP kinase family, big MAP kinase-1 (BMK1), has been recently identified to promote cell growth and attenuate apoptosis. P90 ribosomal S6 kinase (p90RSK), one of the potentially important substrates of extracellular signal regulated kinase (ERK), regulates gene expression in part via phosphorylation of CREB and the Na^+/H^+ exchanger. Recently, we have demonstrated that the activity of BMK1, Src (the upstream regulator of BMK1) and p90RSK was increased in hypertrophied myocardium induced by pressure-overload in the guinea pig. However, the abundance and activity of these kinases in human hearts are unknown. **Methods:** In addition to the three classical MAP kinases (ERK, p38 kinase, and c-Jun NH₂-terminal kinase (JNK)), we examined the protein expression and activity of Src, BMK1, and p90RSK in explanted hearts from patients with dilated cardiomyopathy ($n=9$). Normal donor hearts, which were not suitable for transplant for technical reasons, were used as controls ($n=5$). **Results:** There were no significant differences in the levels of protein expression of these kinases between normal and failing hearts. ERK1/2 and p90RSK were activated in heart failure compared to control ($P<0.01$ and $P<0.03$, respectively), while the activity of p38 kinase was decreased ($P<0.05$) and the activity of JNK was unchanged in heart failure. By contrast, the activities of Src and BMK1 were significantly reduced in end-stage heart failure compared to normal donor hearts ($P<0.05$). **Conclusion:** These data suggest that multiple MAP kinases, p90RSK, and Src are differentially regulated in human failing myocardium of patients with idiopathic dilated cardiomyopathy and may be involved in the pathogenesis of this complex disease. © 2002 Elsevier Science B.V. All rights reserved.

Keywords: Cardiomyopathy; Heart failure; Protein kinases; Signal transduction

1. Introduction

Heart failure is an increasingly important public health problem with a high mortality rate. Although a variety of metabolic and/or neurohumoral factors are implicated in the progression of this syndrome, the precise mechanisms

responsible for this complex condition are poorly understood. Activation of the G_q signaling pathway, which includes protein kinase C (PKC), appears to play a critical role in the progression of heart failure [1]. Recently, we found that translocation of PKC isoforms from cytosolic to membranous fractions were increased in a conventional animal model of heart failure that was induced by pressure-overload [2,3] and in myocardium from patients with end-stage heart failure [4]. As downstream phosphorylation targets of PKC activation, the mitogen-activated protein (MAP) kinase family plays an important role in cardiac hypertrophy and failure [5]. Four subfamilies of

*Corresponding author. Present address: The First Department of Internal Medicine, Yamagata University School of Medicine, 2-2-2 Iida-Nishi, Yamagata 990-9585, Japan. Tel.: +81-23-628-5302; fax: +81-23-628-5305.

E-mail address: takeishi@med.id.yamagata-u.ac.jp (Y. Takeishi).

¹Yasuchika Takeishi, Qunhua Huang, and Jun-ichi Abe contributed equally to this work.

Time for primary review 29 days.

MAP kinases have been identified, including extracellular signal-regulated kinase (ERK1/2), c-Jun NH₂ terminal kinase (JNK), p38 kinase, and big MAP kinase 1 (BMK1 or ERK5) [5]. BMK1 is a recently identified MAP kinase family member, which shares the TEY activation motif with ERK1/2 but is activated by MEK5 [6]. It has been reported that oxidative stress using H₂O₂ activates ERK1/2, JNK and p38 kinase in neonatal rat cardiomyocytes [7], and ischemia followed by reperfusion activates JNK and p38 kinase in isolated coronary-perfused rat hearts [8]. In addition, we recently showed that oxidative stress activates ERK1/2 and BMK1 in coronary-perfused isolated adult guinea pig hearts [9]. Each MAP kinase subfamily may be regulated by different signal transduction pathways that modulate specific cell functions [10]. A potentially important downstream effector of ERK1/2 is p90 ribosomal S6 kinase (p90RSK), which plays a pivotal role in cell growth by activating several transcription factors as well as the Na⁺/H⁺ exchanger (NHE-1) [11].

Although there are considerable data pertaining to MAP kinases in animal models of cardiac hypertrophy and heart failure, data regarding these kinases in the failing human heart are limited, particularly for p90RSK and BMK1. Accordingly, the purpose of this study was to characterize the activity of multiple MAP kinases including BMK1 and p90RSK in explanted failing hearts from patients with idiopathic dilated cardiomyopathy. Of note, we excluded patients with ischemic cardiomyopathy from the present study, since it is known that ischemia itself activates several MAP kinases.

2. Material and methods

2.1. Patient population

Left ventricular myocardium was obtained from nine hearts explanted from patients with end-stage heart failure who were undergoing orthotopic cardiac transplantation (all men, mean age 41±15 years). All patients were diagnosed with New York Heart Association class IV congestive heart failure secondary to idiopathic dilated cardiomyopathy. Non-failing human myocardium was obtained from five donors (four men and one woman, mean age 44±19 years), who had sustained traumatic brain death; these donors had normal cardiac function (as assessed echocardiographically) and had not been prescribed cardiovascular medications. The normal donor hearts were not used for transplantation because of technical reasons, such as death of the recipient, logistic problems, signs of chest trauma after explantation, etc. The investigation conforms with the principles outlined in the Declaration of Helsinki (*Cardiovascular Research* 1997;35:2–3).

2.2. Protein preparation

Myocardial samples were immediately frozen in liquid nitrogen after dissection and were stored at -80°C until use [4,12]. The sampling conditions were identical for both failing and non-failing hearts. Fibrotic or adipose tissue, endocardium, epicardium, or great vessels were carefully excised, and remaining tissue was homogenized with 4 vols of ice-cold lysis buffer (50 mM sodium pyrophosphate, 50 mM NaF, 50 mM NaCl, 5 mM EDTA, 5 mM EGTA, 100 μM Na₃VO₄, 10 mM HEPES, pH 7.4, 1% Triton X-100, 0.1% SDS, 500 μM phenylmethanesulfonyl fluoride (PMSF), and 10 μg/ml leupeptin). The heart homogenates were centrifuged at 14 000×g (4°C for 30 min), and protein concentration was determined using the Bradford protein assay (Bio-Rad, Hercules, CA, USA) [2,9,12]. The protein expression and activity of the following kinases were examined in both failing and non-failing human myocardium: ERK1/2, P38 kinase, JNK, p90RSK, Src, and BMK1.

2.3. Immunoprecipitation and Western blot analysis

For immunoprecipitation, cell lysates were incubated with rabbit anti-human BMK1 antibody (J.D. Lee, The Scripps Research Institute, La Jolla, CA, USA) for 12 h at 4°C and then incubated with 20 μl of protein A-Sepharose CL-4B (Pharmacia Biotech, Piscataway, NJ, USA) for 1 h on a roller system (RT-50, Taitec, Koshigaya, Saitama, Japan) at 4°C [9,13]. The beads were washed two times with 1 ml lysis buffer, two times with 1 ml LiCl wash buffer (500 mM LiCl, 100 mM Tris-HCl, pH 7.6, 0.1% Triton X-100, 1 mM DTT) and two times in 1 ml washing buffer (HEPES 20 mM, pH 7.2, 2 mM EGTA, 10 mM MgCl₂, 1 mM DTT, 0.1% Triton X-100). For Western blot analysis, cell lysates or immunoprecipitates were subjected to SDS-PAGE and proteins were transferred to nitrocellulose membranes (Amersham Life Science, Arlington Heights, IL, USA) as previously described [9,13]. The membrane was blocked for 1 h at room temperature with a commercially available blocking buffer from Gibco BRL (Life Technologies, Rockville, MD, USA). To examine the protein expression, the blots were then incubated for 1 h at room temperature with anti-BMK1, ERK1, ERK2 (rabbit anti-rat, cross-reactive with human; Santa Cruz Biotechnology, Santa Cruz, CA, USA), p38 kinase (rabbit anti-human; Santa Cruz Biotechnology), JNK1, JNK2 (rabbit anti-human; Santa Cruz Biotechnology), p90RSK (goat anti-human; Santa Cruz Biotechnology), or Src (rabbit anti-human; Santa Cruz Biotechnology), followed by incubation for 1 h with secondary antibody conjugated with horse radish peroxidase (KPL laboratories, Gaithersburg, MD, USA). Immunoreactive bands were visualized using enhanced chemiluminescence (ECL, Amersham Life Science).

2.4. Activity for ERK1/2, p38 kinase and Src

To examine phosphorylation of ERK1/2 and p38 kinase, the blots were incubated for 12 h with anti phospho-specific ERK1/2 (mouse anti-human; New England Biolabs, Beverly, MA, USA) and phospho-specific p38 kinase (mouse anti-human; New England Biolabs) antibodies, respectively. We and other investigators have previously reported that immunoblotting with phospho-specific ERK1/2 antibody has a good correlation with an immune complex kinase assay [14,15]. Activity of Src was measured using anti activated-Src antibody clone 28 (H. Kawakatsu, University of California San Francisco, San Francisco, CA, USA), which recognizes only the activated form of Src [9,13].

2.5. p90RSK, JNK, and BMK1 kinase assays

p90RSK kinase activity was measured by glutathione S-transferase (GST)-NHE-1 phosphorylation and BMK1 kinase activity was measured by autophosphorylation as described previously [9]. JNK activity was measured with a commercially available kit (New England Biolabs, Beverly, MA, USA) based on phosphorylation of recombinant c-Jun [9]. We could not detect ERK1/2, p38, p90RSK, or BMK1 in c-Jun fusion protein beads immunoprecipitates, indicating that JNK is the dominant c-Jun kinase present (data not shown).

2.6. Statistical analysis

Data are reported as mean \pm S.D. Statistical analysis was performed with the StatView 4.0 package (Abacus Concepts, Berkeley, CA, USA). Differences between failing and non-failing hearts were analyzed by un-paired *t*-test. *P* values less than 0.05 were considered significant.

3. Results

3.1. ERK1/2 expression and activity: comparison with p90RSK

As determined by quantitative immunoblotting, there were no significant differences in the level of ERK1/2 protein expression between failing human hearts with end-stage dilated cardiomyopathy and non-failing human hearts (Fig. 1A). By contrast, the activity of ERK1/2 was increased in failing hearts with dilated cardiomyopathy compared to non-failing control hearts (4.2 ± 0.1 -fold, *P* < 0.01).

We also evaluated p90RSK activation in the same samples, since p90RSK is one of the important downstream substrates of ERK1/2. As shown in Fig. 1B, there was no significant difference in p90RSK protein expres-

sion between failing and non-failing hearts. However, p90RSK activity was significantly increased (2.1 ± 0.7 -fold, *P* < 0.03) in failing myocardium.

3.2. Determination of p38 kinase and JNK expression and activity

It has been reported that cellular stresses such as hyperosmotic shock, protein synthesis inhibitors (e.g. anisomycin), hypoxia/reoxygenation, and reactive oxygen species activate p38 kinase and JNK in cultured cardiomyocytes [5]. To determine the role of p38 kinase and JNK in failing human hearts with idiopathic dilated cardiomyopathy, we examined the protein expression and activity of p38 kinase and JNK. As shown in Fig. 2, although neither the protein expression of p38 kinase, JNK1, and JNK2 nor the activity of JNK were significantly different in normal and failing myocardium, the p38 kinase activity (0.4 ± 0.3 -fold, *P* < 0.05) was significantly reduced in myocardium from failing hearts.

3.3. Src and BMK1 expression and activity in human failing hearts

We previously demonstrated that Src kinase regulates BMK1 activity in part by oxidative stress in adult guinea pig hearts [8]. Since reactive oxygen species are known to be increased in failing myocardium, we also examined here Src and BMK1 kinases activity. As shown in Fig. 3, Src and BMK1 protein expression was not different between failing and non-failing myocardium. Src activity, which was evaluated by anti-activated Src-clone 28 antibody, was decreased significantly in failing human hearts (0.7 ± 0.2 -fold, *P* < 0.05). As shown in Fig. 3B, BMK1 activity was also decreased in failing human hearts compared to non-failing hearts (0.4 ± 0.2 -fold, *P* < 0.05).

4. Discussion

In the present study, we examined whether the expression and activity of multiple MAP kinases, p90RSK, and Src were altered in ventricular tissue from failed human hearts with end-stage dilated cardiomyopathy. We found no differences in protein abundance of these kinases between failing and non-failing human hearts. The mean activities of ERK1/2 and p90RSK were significantly greater in failing hearts compared to non-failing donor hearts. In contrast, p38 kinase, Src, and BMK1 activities were reduced in human myocardium with end-stage heart failure. We could not detect any significant changes in JNK activity between failing and non-failing hearts. These data suggest that the MAP kinase family activity is differentially regulated in human dilated cardiomyopathy without any alterations in protein abundance.

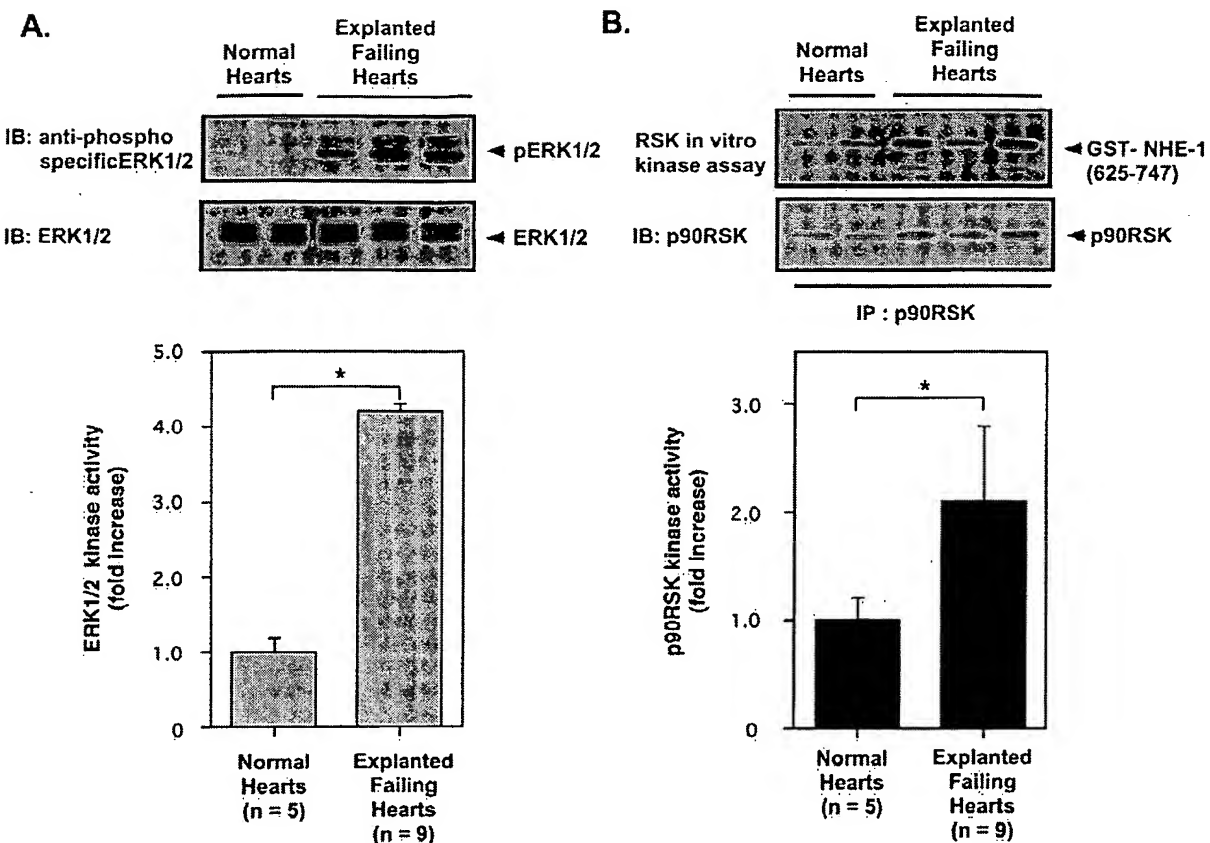


Fig. 1. ERK1/2 and p90RSK in failing and non-failing human hearts. (A) ERK1/2 activity in whole heart extracts was measured by Western blot analysis with a phospho-specific ERK antibody (upper). No difference in the amount of ERK1/2 protein was observed in lysates from any of the heart samples by Western blot analysis with anti-ERK1/2 (lower). For densitometric analysis of ERK1/2 activity, results were normalized for all experiments by arbitrarily setting the densitometry of control heart samples (non-failing hearts) to 1.0 (shown is mean \pm S.D.). (B) p90RSK activity was measured by an in vitro kinase assay using GST-NHE-1 (625–747) as a substrate. p90RSK protein level was examined by Western blot analysis with anti-p90RSK antibody. Representative autoradiogram showing p90RSK kinase activity (upper panel) and Western blot analysis showing p90RSK protein levels (lower panel). Densitometric analysis revealed that kinase activity of ERK1/2 and p90RSK was significantly increased in explanted human failing hearts compared to normal control hearts. IB, immuno-blotting; * $P < 0.05$.

Cook et al. [16] have reported that ERK1/2 activity was unchanged and p38 kinase activity was increased in failing human hearts secondary to ischemic cardiomyopathy. In our study, the patients were diagnosed as idiopathic dilated cardiomyopathy, while in that study they selected patients with heart failure secondary to ischemic cardiomyopathy. It has been reported that ischemia and ischemia/reperfusion induced multiple MAP kinase activation [5,8,9]. Therefore, it is likely that the presence of ischemia itself, in addition to LV dysfunction and heart failure, modulates the activity of multiple MAP kinases in these patients.

To our knowledge, this is the first report of p90RSK, Src and BMK1 activity in human tissues. We have reported that protein expression and activity of PKC isoforms are elevated in guinea pig model of heart failure by chronic pressure-overload [2,3] and in human explanted hearts with end-stage heart failure [4,12]. We and others have

reported that ERK1/2 and p90RSK activation are at least in part PKC-dependent [17]. ERK1/2 were the first MAP kinases described and it has been reported that ERK1/2 activation protects against apoptotic cell death [18,19]. Among the substrates of ERK, p90RSK is a versatile mediator of ERK signal transduction [11,17]. These include: (1) regulation of gene expression via phosphorylation of transcription factors including c-fos, cAMP-response element-binding protein (CREB) and CREB-binding protein, (2) regulation of protein synthesis by phosphorylation of polyribosomal proteins and glycogen synthase kinase-3, and (3) stimulation of the Na^+/H^+ exchanger by phosphorylating serine 703 of NHE-1 [10]. Recently Bonni et al. [19] and Tan et al. [20] reported that p90RSK phosphorylated the pro-apoptotic protein BAD at serine 112. Phosphorylation of BAD at serine 112 specifically suppressed BAD-mediated apoptosis. Further in-

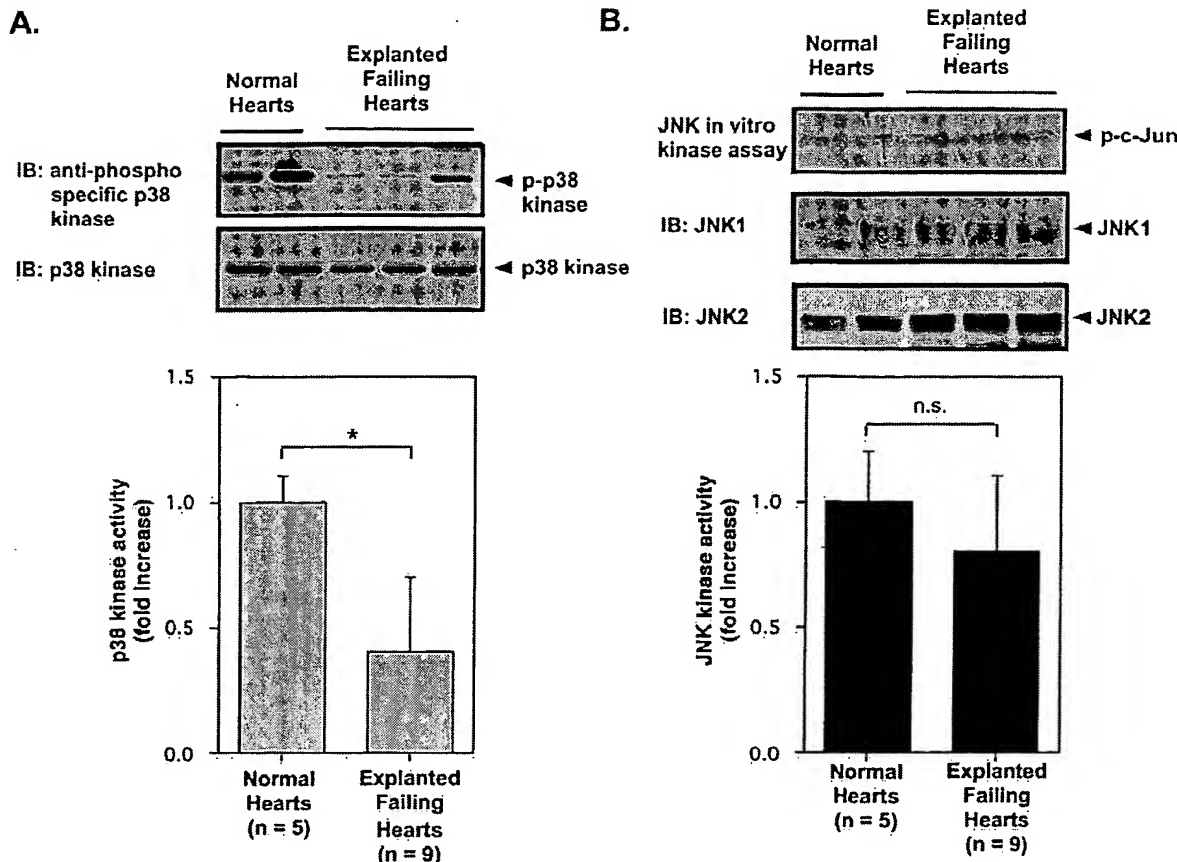


Fig. 2. p38 kinase and JNKs in failing and non-failing hearts. (A) p38 kinase activity in whole extracts was measured by Western blot analysis with a phospho-specific p38 antibody (upper). No difference in the amount of p38 kinase was observed in lysates from any of the heart samples by Western blot analysis with anti-p38 kinase antibody (lower). Densitometric analysis showed that p38 kinase activity was reduced in failing human hearts. Results were normalized for all experiments by arbitrarily setting the densitometry of control heart samples (non-failing hearts) to 1.0 (shown is mean \pm S.D.). (B) JNK activity was measured by in vitro kinase assay using c-Jun (1–89) fusion protein as a substrate. Western blots were performed with an anti phospho-specific c-Jun antibody for JNK activity assay (upper). No difference in the amount of JNK1/2 protein was observed in samples by Western blot analysis with anti-JNK (lower) and c-Jun substrate by Ponceau staining (data not shown).

vestigation is needed to define the precise role of ERK1/2 and p90RSK activation in failing human hearts.

Recently, Kato et al. [21] have reported that BMK1 activation is also protective against apoptotic cell death. BMK1 is highly expressed in cardiac myocytes and activated by reactive oxygen species in the adult guinea pig heart [8]. Recently, we have demonstrated that BMK1 is activated in hypertrophied myocardium induced by chronic pressure-overload [22]. MEK5-dependent BMK1 activation results in the phosphorylation of MEF2A and MEF2C, which are transcription factors belonging to the myocyte enhancer factor-2 (MEF2)-family [23]. Since BMK1 activation was significantly decreased in failing human hearts in the present study, it will be interesting to evaluate critically the role of this MAP kinase in diminished contractility of the failing heart.

In conclusion, multiple MAP kinases, p90RSK, and Src

were differentially regulated in human failing myocardium of patients with idiopathic dilated cardiomyopathy and may be involved in the pathogenesis of this clinical syndrome.

Acknowledgements

The authors wish to thank Dr C. Yan for their invaluable assistance and critical reading of this manuscript. This study was supported by grants from National Institutes of Health (HL44721 and HL49192 to B.C. Berk, HL52318 to R.A. Walsh, and HL66919 to J. Abe), a grant-in-aid for Scientific Research (No. 12770337 to Y.T.) from the Ministry of Education, Science, Sports and Culture, Japan, and a grant from Kanae Foundation (to Y.T.).

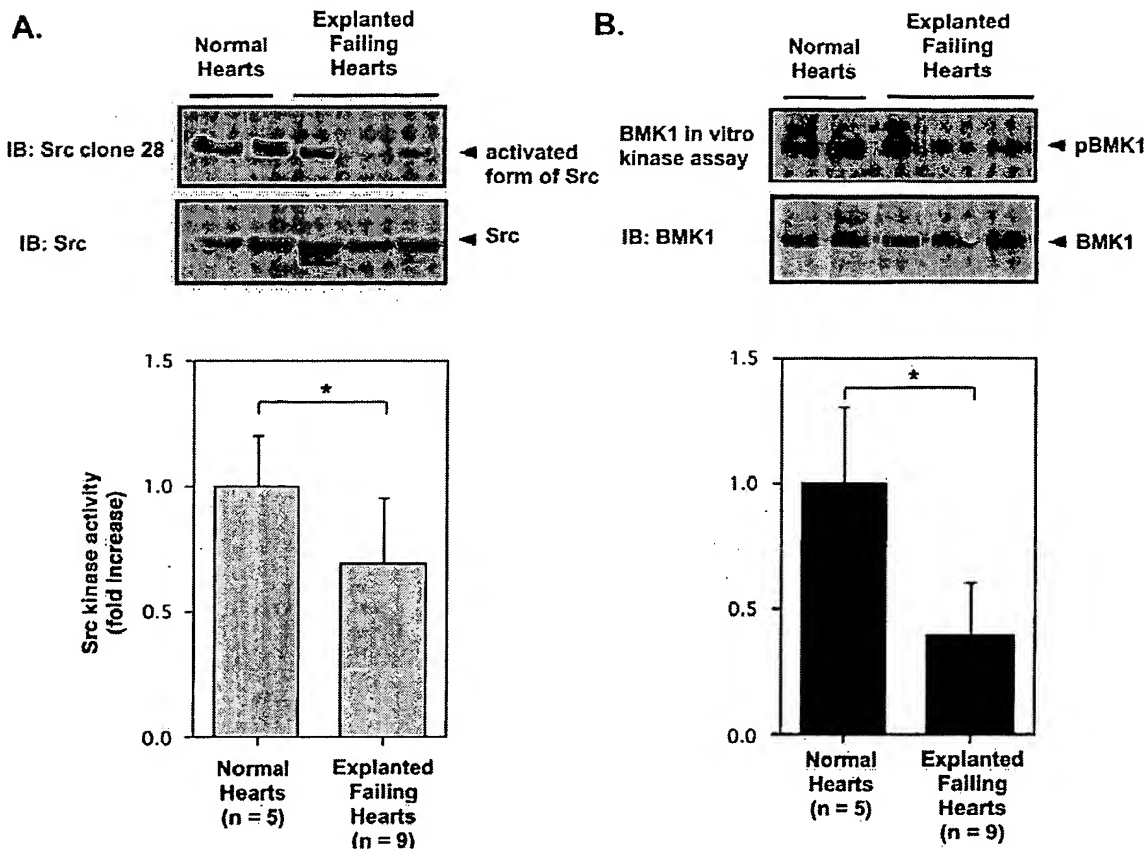


Fig. 3. Src and BMK1 in failing and non-failing hearts. (A) Src kinase activity in whole extracts was measured by Western blot analysis with a Src antibody clone 28 which recognizes the activated form of Src (upper). No difference in the amount of Src was observed in lysates from any of the heart samples by Western blot analysis with anti-Src antibody (lower). (B) BMK1 activity was analyzed by autophosphorylation in an immune complex kinase assay (upper). BMK1 protein level was assayed by Western blot analysis with anti-BMK1 antibody. No difference in the amount of BMK1 was observed in immunoprecipitates from any of the heart samples with anti-BMK1 antibody (lower). Densitometric analysis indicated that Src and BMK1 kinase activity was decreased in failing hearts compared with normal hearts (shown is mean \pm S.D.).

References

- [1] Takeishi Y, Chu G, Kirkpatrick DM et al. In vivo phosphorylation of cardiac troponin I by protein kinase C β 2 decreases cardiomyocyte calcium responsiveness and contractility in transgenic mouse hearts. *J Clin Invest* 1998;102:72–78.
- [2] Takeishi Y, Bhagwat A, Ball NA et al. Effect of angiotensin-converting enzyme inhibition on protein kinase C and SR proteins in heart failure. *Am J Physiol* 1999;276:H53–62.
- [3] Jalili T, Takeishi Y, Song G et al. PKC translocation without changes in G α q and PLC- β protein abundance in cardiac hypertrophy and failure. *Am J Physiol* 1999;277:H2298–2304.
- [4] Bowling N, Walsh RA, Song G et al. Increased protein kinase C activity and expression of Ca $^{2+}$ -sensitive isoforms in the failing human heart. *Circulation* 1999;99:384–391.
- [5] Sugden PH, Clerk A. 'Stress-responsive' mitogen-activated protein kinases (c-Jun N-terminal kinases and p38 mitogen-activated protein kinases) in the myocardium. *Circ Res* 1998;83:345–352.
- [6] Lee JD, Ulevitch RJ, Han J. Primary structure of BMK1: a new mammalian map kinase. *Biochem Biophys Res Commun* 1995;213:715–746.
- [7] Clerk A, Michael A, Sugden PH. Stimulation of multiple mitogen-activated protein kinase sub-families by oxidative stress and phosphorylation of the small heat shock protein, HSP25/27, in neonatal ventricular myocytes. *Biochem J* 1998;333:581–589.
- [8] Clerk A, Fuller SJ, Michael A, Sugden PH. Stimulation of 'stress-regulated' mitogen-activated protein kinases (stress-activated protein kinases/c-Jun N-terminal kinases and p38-mitogen-activated protein kinases) in perfused rat hearts by oxidative and other stresses. *J Biol Chem* 1998;273:7228–7234.
- [9] Takeishi Y, Abe J, Lee JD et al. Differential regulation of p90 ribosomal S6 kinase and big mitogen-activated protein kinase 1 by ischemia/reperfusion and oxidative stress in perfused guinea pig hearts. *Circ Res* 1999;85:1164–1172.
- [10] Abe J, Berk BC. Reactive oxygen species as mediators of signal transduction in cardiovascular disease. *Trends Cardiovasc Med* 1998;8:59–64.
- [11] Takahashi E, Abe J, Gallis B et al. p90RSK is a serum-stimulated NHE1 kinase: regulatory phosphorylation of serine 703 of Na $^{+}$ /H $^{+}$ exchanger isoform-1. *J Biol Chem* 1999;274:20206–20214.
- [12] Takeishi Y, Jalili T, Hoit BD et al. Alterations in Ca $^{2+}$ cycling proteins and G α q signaling after left ventricular assist device support in failing human hearts. *Cardiovasc Res* 2000;45:883–888.
- [13] Abe J, Takahashi M, Ishida M, Lee JD, Berk BC. c-Src is required for oxidative stress-mediated activation of big mitogen-activated protein kinase 1 (BMK1). *J Biol Chem* 1997;272:20389–20394.
- [14] Tseng H, Peterson TE, Berk BC. Fluid shear stress stimulates mitogen-activated protein kinase in endothelial cells. *Circ Res* 1995;77:869–878.
- [15] Griffith CE, Zhang W, Wang RL. ZAP-70-dependent and -in-

dependent activation of Erk in Jurkat T cells. Differences in signalling induced by H_2O_2 and Cd3 cross-linking. *J Biol Chem* 1998;273:10771–10776.

[16] Cook SA, Sugden PH, Clerk A. Activation of c-Jun N-terminal kinases and p38-mitogen-activated protein kinases in human heart failure secondary to ischaemic heart disease. *J Mol Cell Cardiol* 1999;1:1429–1434.

[17] Takahashi E, Abe J, Berk BC. Angiotensin II stimulates p90^{rk} in vascular smooth muscle cells. A potential Na^+/H^+ exchanger kinase. *Circ Res* 1997;81:268–273.

[18] Abe J, Baines CP, Berk BC. Role of mitogen-activated protein kinases in ischemia and reperfusion injury: the good and the bad. *Circ Res* 2000;86:607–609.

[19] Bonni A, Brunet A, West AE et al. Cell survival promoted by the Ras-MAPK signaling pathway by transcription-dependent and -independent mechanisms. *Science* 1999;286:1358–1362.

[20] Tan Y, Ruan H, Demeter MR, Comb MJ. p90(RSK) blocks bad-mediated cell death via a protein kinase C-dependent pathway. *J Biol Chem* 1999;274:34859–34867.

[21] Kato Y, Tapping RI, Huang S et al. Bmk1/Erk5 is required for cell proliferation induced by epidermal growth factor. *Nature* 1998;395:713–716.

[22] Takeishi Y, Huang Q, Abe J, et al. Differential activation of mitogen-activated protein kinase family and p90 ribosomal S6 kinase in hypertrophied myocardium induced by pressure-overload. *J Mol Cell Cardiol* 2001 (in press).

[23] Kato Y, Kravchenko VV, Tapping RI et al. BMK1/ERK5 regulates serum-induced early gene expression through transcription factor MEF2C. *EMBO J* 1997;16:7054–7066.

Involvement of the Extracellular Signal-Regulated Kinase Cascade for Cocaine-Rewarding Properties

Emmanuel Valjent,^{1,2} Jean-Christophe Corvol,³ Christiane Pagès,¹ Marie-Jo Besson,¹ Rafael Maldonado,² and Jocelyne Caboche¹

¹Laboratoire de Neurochimie-Anatomie, Institut des Neurosciences, Centre National de la Recherche Scientifique, Unité Mixte de Recherche 7624, Université Pierre et Marie Curie, 75005 Paris, ²Laboratori de Neurofarmacologia, Facultat de Ciències de la Salut i de la Vida, Universitat Pompeu Fabra, E-08003 Barcelona, Spain, and ³Institut National de la Santé et de la Recherche Médicale U 114, Chaire de Neuropharmacologie, Collège de France, 75231, Paris Cedex 05, France

A central feature of drugs of abuse is to induce gene expression in discrete brain structures that are critically involved in behavioral responses related to addictive processes. Although extracellular signal-regulated kinase (ERK) has been implicated in several neurobiological processes, including neuronal plasticity, its role in drug addiction remains poorly understood. This study was designed to analyze the activation of ERK by cocaine, its involvement in cocaine-induced early and long-term behavioral effects, as well as in gene expression. We show, by immunocytochemistry, that acute cocaine administration activates ERK throughout the striatum, rapidly but transiently. This activation was blocked when SCH 23390 [a specific dopamine (DA)-D1 antagonist] but not raclopride (a DA-D2 antagonist) was injected before cocaine. Glutamate receptors of NMDA subtypes also participated in ERK activation, as shown after injection of the NMDA receptor antagonist MK 801. The systemic injection of

SL327, a selective inhibitor of the ERK kinase MEK, before cocaine, abolished the cocaine-induced ERK activation and decreased cocaine-induced hyperlocomotion, indicating a role of this pathway in events underlying early behavioral responses. Moreover, the rewarding effects of cocaine were abolished by SL327 in the place-conditioning paradigm. Because SL327 antagonized cocaine-induced *c-fos* expression and Elk-1 hyperphosphorylation, we suggest that the ERK intracellular signaling cascade is also involved in the prime burst of gene expression underlying long-term behavioral changes induced by cocaine. Altogether, these results reveal a new mechanism to explain behavioral responses of cocaine related to its addictive properties.

Key words: cocaine; ERK; Elk-1; *c-fos* expression; striatum; dopamine receptors; reward

A central feature of psychostimulants is to produce, in rodents, a release of dopamine (DA) in the mesolimbic system (Di Chiara and Imperato, 1988) and to induce gene expression in discrete brain structures (Hope et al., 1992; Moratalla et al., 1993). These molecular events are thought to be crucial for behavioral responses related to addictive processes (for review, see Nestler and Aghajanian, 1997; Berke and Hyman, 2000). In this way, acute psychostimulant administration has been reported to induce immediate early gene (IEG) expression in the striatum, a major cerebral target of DA inputs (Graybiel et al., 1990; Young et al., 1991; Hope et al., 1992; Moratalla et al., 1993; Konradi et al., 1994; Berke et al., 1998). Although their induction is transient because most mRNAs return to baseline within a few hours to a day, some of them are thought to form the basis of initial neural plasticity as they encode transcription factors (*c-fos*, JunB). Chronic exposure desensitizes the capability of psychostimulants to induce these proteins and results instead in a gradual long-term accumulation of novel Fos-related proteins, termed chronic FRAs (Hope et al., 1994), which are associated with long-lasting changes in synaptic efficacy and structural changes (Fitzgerald et al., 1996; Kelz et al., 1999).

The role of DA-D1 receptor subtype in transient bursts of altered gene expression and behavioral responses is now well

established because both are blocked by D1 antagonists (Cabib et al., 1991; Young et al., 1991) and by the deletion of D1 receptors in knock-out mice (Xu et al., 1994a,b; Moratalla et al., 1996). By elevating intracellular cAMP levels, and thereby activating PKA, DA-D1 stimulation leads to cAMP response element-binding protein (CREB) phosphorylation, which in turn controls transcriptional expression via the cAMP and calcium response element (CRE) present in the promoter of various IEGs (such as *c-fos*, *junB*, or *zif268*) (for review, see Herdegen and Leah, 1998). However, recent evidences in PC12 and neuronal cells show that cAMP can also stimulate extracellular signal-regulated kinase (ERK) (Vossler et al., 1997; Impey et al., 1998; Vincent et al., 1998; Yao et al., 1998; York et al., 1998; Roberson et al., 1999), which is thought to play an important role in neuronal adaptive responses (English and Sweatt, 1996, 1997; Martin et al., 1997; Davis et al., 2000) as well as memory formation (Atkins et al., 1998). After activation, ERK proteins can translocate to the nucleus (Chen et al., 1992), where they phosphorylate the ternary complex factor Elk-1 (Gille et al., 1992, 1995) and thereby control *c-fos* transcription via the serum response element (SRE) (for review, see Hill et al., 1993; Marais et al., 1993; Hipskind et al., 1994a,b; Janknecht et al., 1994; Treisman, 1995; Zinck et al., 1995).

The aim of this study was to investigate whether acute cocaine administration induced ERK activation in the striatum. We report a rapid and transient activation of ERK *in vivo*, in different striatal subregions. This activation is linked to D1 receptor stimulation, with a partial contribution of D2 and NMDA receptors. Using a specific inhibitor of MEK, the dual-specific protein kinase that phosphorylates ERK, we partially antagonized cocaine-induced locomotor response and totally reversed cocaine-rewarding effects on the place preference paradigm. Furthermore, cocaine-induced *c-fos* expression and Elk-1 hyperphosphorylation were also blocked by the MEK inhibitor. This suggests that the control exerted by the

Received June 20, 2000; revised Sept. 5, 2000; accepted Sept. 11, 2000.

This work was supported by the University Pierre et Marie Curie and the Centre National de la Recherche Scientifique for J.C. and European Commission (BIOMED-2 # 98-227) for R.M. E.V. was supported by a grant from "La fondation des Treilles". We are grateful to J. M. Trzaskos, J. L. Hyrek, A. C. Tabaka, J. S. Picaré, and C. Teleha for the generous gift of SL327. We are grateful to Jean Antoine Girault for helpful discussions and support for adenyl cyclase measurements.

Correspondence should be addressed to Jocelyne Caboche, Laboratoire de Neurochimie-Anatomie, Institut des Neurosciences, Unité Mixte de Recherche 7624, Centre National de la Recherche Scientifique, Université Pierre et Marie Curie, 75005 Paris, France. E-mail: Jocelyne.Caboche@snv.jussieu.fr.

Copyright © 2000 Society for Neuroscience 0270-6474/00/208701-09\$15.00/0

ERK–Elk-1 cascade on the prime burst of gene expression in striatum plays a crucial role in some cocaine behavioral response, such as rewarding effects.

MATERIALS AND METHODS

Animals and drug. Male CD-1 mice (Charles River, France) weighing 22–24 gm were housed 10 per cage and acclimatized to the laboratory conditions (12 hr light/dark cycle, 21 ± 1°C room temperature) 1 week before the experiment. Food and water were available *ad libitum*. Behavioral tests and animal care were conducted in accordance with the standard ethical guidelines (National Institutes of Health, publication number 85-23, revised 1985; European Community Guidelines on the Care and Use of Laboratory Animals) and approved by the local ethics committee. All drugs were administered by intraperitoneal injection. Cocaine (Sigma, Arbrésle, France), *R*(+)-SCH 23390 (Sigma), *S*(-)-raclopride (Sigma), and (+)-MK 801 (Sigma) were dissolved in saline 0.9%. The MEK inhibitor SL327 was dissolved in DMSO and then diluted twice in sterile water.

Treatments. The same experimental conditions and doses were used for immunocytochemistry and behavioral assay. *R*(+)-SCH 23390 (0.1 mg/kg) and *S*(-)-raclopride (0.3 mg/kg) were injected 15 min before cocaine injection (20 mg/kg). (+)-MK 801 (0.15 mg/kg) was administered 30 min before cocaine treatment. SL327 (50 mg/kg) was injected 1 hr before cocaine administration. For the conditioned place preference experiment, SL327 and/or cocaine were administered every drug-conditioning day. For chronic treatments, cocaine (20 mg/kg) was injected once daily for 6 d. On day seven, a challenge of cocaine was performed at the same dose.

Tissue preparation for immunocytochemistry. Mice brains were fixed by intracardiac perfusion of 4% paraformaldehyde (PFA) in 0.1 M Na₂HPO₄–Na₂PO₄ buffer, pH 7.5 (phosphate buffer), delivered with a peristaltic pump at 20 ml/min for 5 min. Brains were removed and post-fixed overnight in the same fixative solution. Sections (30 µm) were cut with a vibratome (Leica, Nussloch, Germany) and then kept in a solution containing 30% ethylene glycol, 30% glycerol, 0.1 M phosphate buffer, and 0.1% diethylpyrocarbonate (DEPC; Sigma, Deisenhofen, Germany) at –20°C until they were processed for immunocytochemistry.

Antibodies. The anti-active ERK antibody was a polyclonal antibody raised against the dually phosphorylated Thr/Glu/Tyr region within the catalytic core of the active form of p44–ERK1 and p42–ERK2 (anti-phospho Thr¹⁸³–Tyr¹⁸⁵ ERKs; New England Biolabs, Beverly, MA). The anti-active Elk-1 antibody was a monoclonal antibody directed against a phospho-Ser³⁸³ peptide corresponding to residues 379–392 of Elk-1 (Santa Cruz Biotechnology, Santa Cruz, CA). The c-fos antibody was a polyclonal antibody directed against residues 3–16 of human c-fos (Santa Cruz). The dilutions used for immunostaining were 1:400 for p-ERK antiserum; 1:250 for p-Elk-1 antiserum, and 1:1000 for c-fos.

Immunocytochemistry. The immunohistochemical procedure was adapted from protocols previously described (Sgambato et al., 1998) except that for the detection of phosphorylated proteins, 0.1 mM NaF was included in all buffers and incubation solutions. Day 1: Free-floating sections were rinsed in Tris-buffered saline (TBS, 0.25 M Tris and 0.5 M NaCl, pH 7.5), incubated for 5 min in TBS containing 3% H₂O₂ and 10% methanol, and then rinsed three times for 10 min each in TBS. After a 15 min incubation in 0.2% Triton X-100 in TBS, the sections were rinsed three times in TBS. These were incubated with the primary antibody for 72 hr (cFos) or overnight (p-ERK, p-Elk-1) at 4°C. Day 2: After three rinses in TBS, the sections were incubated for 2 hr at room temperature with the secondary biotinylated antibody (anti-IgG), using a dilution twice that of the first antibody in TBS. After being washed, the sections were incubated for 90 min in avidin–biotin–peroxidase complex (ABC) solution (final dilution, 1:50; Vector Laboratories, Peterborough, UK). The sections were then washed in TBS and twice in TB (0.25 M Tris, pH 7.5) for 10 min each, placed in a solution of TB containing 0.1% 3,3'-diaminobenzidine (DAB; 50 mg/100 ml), and developed by H₂O₂ addition (0.02%). After processing, the tissue sections were mounted onto gelatin-coated slides and dehydrated through alcohol to xylene for light microscopic examination.

P-ERK positive neurons were plotted at 10× magnification using a computerized image analyzer (Biocom). Cell counts were performed for each mouse in the whole striatum divided in dorsomedial (DM), dorsolateral (DL), core, and shell. In each region, the total amount of P-ERK-positive neurons (evaluated on the basis of a cytoplasmic and nuclear staining) was counted.

Adenyl cyclase assays. Mouse brains were sectioned in 300-µm-thick slices in Ca²⁺-free artificial CSF (in mM: NaCl 125, KCl 2.4, KH₂PO₄ 0.5, Na₂SO₄ 0.5, MgCl₂ 1.93, NaHCO₃ 27, and glucose 10) using Vibroslice apparatus (Campden Instruments, Leicester, UK). Tissue microdisks were punched out from caudate putamen using a stainless steel cylinder and homogenized at 1 mg of protein per milliliter in a buffer containing 2 mM Tris-maleate, pH 7.2, 2 mM EGTA, and 300 mM sucrose using a Potter-Elvehjem apparatus. Adenyl cyclase activity was measured by the conversion of α -(³²P)-ATP into cyclic (³²P)-AMP as described previously (Bockaert et al., 1977). Adenyl cyclase activities were measured in the presence of vehicle or dopamine 10^{–4} M and various concentrations of SL327 (0.3, 3, 10, 30, 100, and 300 µM). The cyclic (³²P)-AMP formed was isolated according to Salomon et al. (1974), and dopamine response on adenyl cyclase activity was calculated in picomoles of cAMP produced

per minute and per milligram of protein and expressed as percentage increase.

Locomotor assay. Locomotor activity was measured by using locomotor activity boxes consisted in individual plastic rectangular area (9 × 20 × 11 cm; Imetronic). The boxes contained a line of photocells 2 cm above the floor to measure horizontal movements and another line located 6 cm above the floor to measure vertical activity (rearrings). Mice were individually placed in the locomotor boxes 5 min after injection of drug or saline, and locomotion was recorded for 15 min in a low luminosity environment (20–25 lux).

Conditioned place preference. Cocaine-rewarding effects were evaluated in the conditioned place preference paradigm by using an unbiased procedure, as previously described (Maldonado et al., 1997). Briefly, the protocol consists of three different phases: preconditioning, conditioning, and postconditioning phases. During preconditioning phase, mice were allowed *ad libitum* access for 18 min to the two chambers that were distinguished by different patterns on floors and walls. During conditioning phase, mice received pairing of saline or cocaine (20 mg/kg) once a day for 6 d in separate compartments using a counterbalanced design. After injection, animals were confined to a given chamber for a period of 25 min. Each mouse received three pairings each in one chamber with cocaine and other with saline. The postconditioning phase began 24 hr after last conditioning session, when animals were permitted *ad libitum* access to both chambers. Place preference was quantified in terms of time spent in drug paired side. A score was calculated for each mouse as the difference between postconditioning and preconditioning time spent in drug-paired compartment.

Statistical analysis. Data were analyzed using one-way ANOVA between subjects for immunocytochemistry, locomotion, and score values of conditioned place preference. *Post hoc* comparisons were made using the Newman–Keuls test. Preconditioning and postconditioning times spent in the drug-paired compartment were analyzed using two-way ANOVA with between (treatment) and within (phase) groups factors, followed by corresponding one-way ANOVA and *post hoc* comparisons (Newman–Keuls test). In all cases, significance was set at $p < 0.05$.

RESULTS

Acute cocaine treatment induces ERK activation throughout the striatum

After the administration of cocaine (20 mg/kg), the temporal pattern of ERK activation was analyzed *in vivo*, into the striatum, by immunocytochemistry. This activation was detected with an antiserum specifically recognizing the phosphorylated form (anti-phospho-Thr¹⁸³ and Tyr¹⁸⁵) of ERK proteins, as tested by Western blot (Sgambato et al., 1998; Davis et al., 2000). In saline-treated mice, no P-ERK immunoreactivity was found in the nucleus accumbens (NA), and only a low level was detectable in the dorsal striatum (Fig. 1A,B). By contrast, 5 and 10 min after cocaine administration, immunostaining for P-ERK increased markedly throughout the dorsal striatum and the NA (Fig. 1A,B). As exemplified in Figure 1B, P-ERK immunostaining corresponded to both P-ERK-positive neurons and neuropil. In neuronal cells, the immunolabeling was mainly present in cytoplasmic compartments (soma and dendrites) 5 min after cocaine administration, suggesting a local activation of the protein (Fig. 1C). Then, a strong nuclear staining was observed 10 min after cocaine, supporting a nuclear translocation of activated ERK proteins at this time point (Fig. 1C).

ERK activation was rapid, but transient, because a strong decrease of cocaine-induced ERK activation was found in the dorsal striatum and NA 20 min after cocaine injection (Fig. 1A,B). One hour after cocaine injection, P-ERK immunostaining returned to basal levels (data not shown). The kinetics of ERK activation was slightly modified by previous chronic administration of cocaine (20 mg/kg, 6 d, once daily), with a strong increase of P-ERK immunostaining occurring from 5 to 20 min (Fig. 1D). Noteworthy was the lack of P-ERK induction when chronic cocaine treatment was followed by saline. In summary, acute and challenge of cocaine injection after chronic treatment are both able to induce a rapid and strong activation of ERK in the different subregions of the striatum.

ERK activation induced by acute cocaine depends on dopamine receptors

We then evaluated the involvement of dopaminergic receptors in cocaine-induced ERK activation at its peak time point of activation (i.e., 10 min). One-way ANOVA (between subjects) revealed sig-

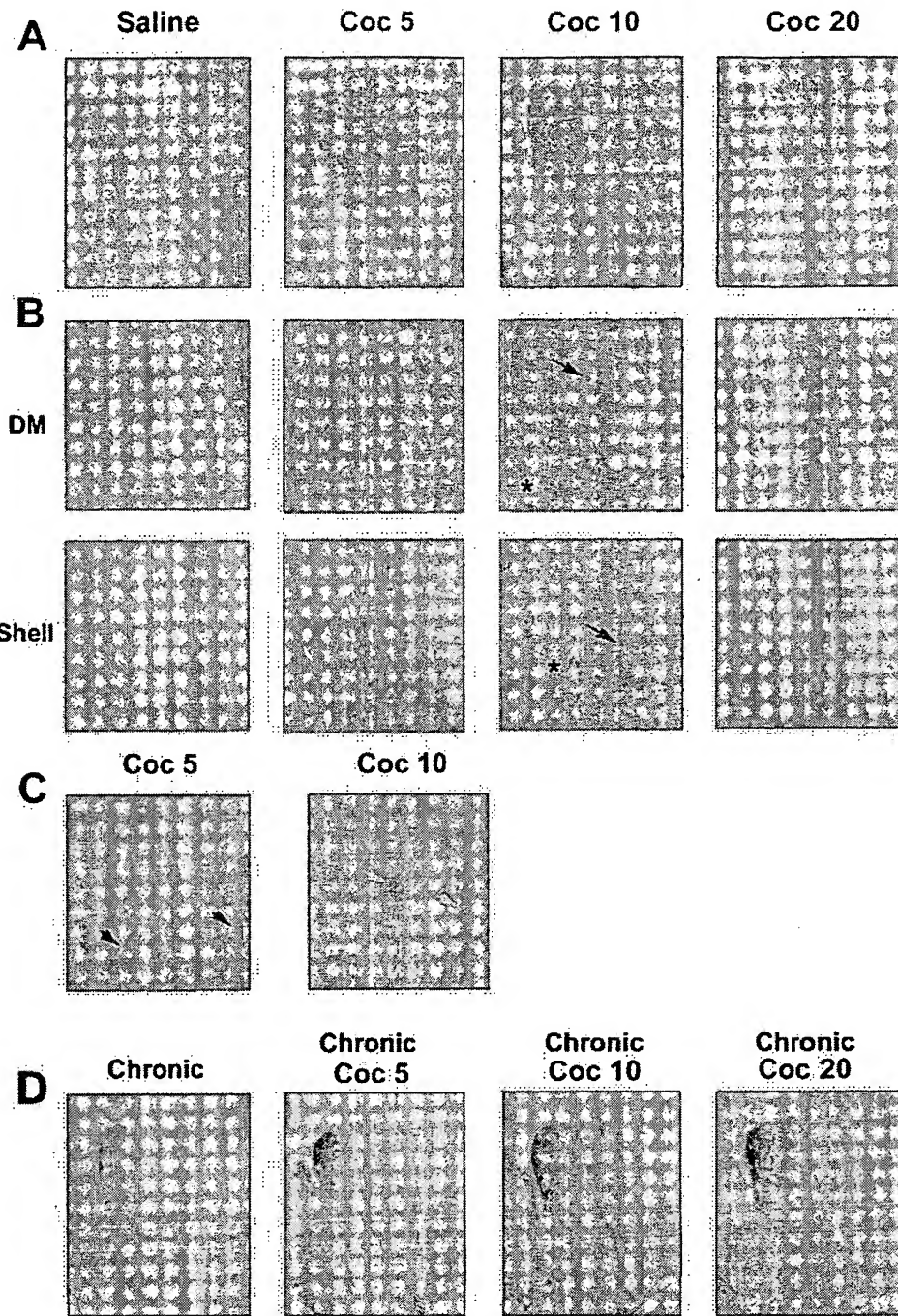


Figure 1. Acute cocaine injection activates ERK in the striatum. Immunocytochemical detection of activated ERK proteins was detected using a specific anti-active antibody, 5 (Coc 5), 10 (Coc 10), and 20 (Coc 20) min after cocaine injection (20 mg/kg, i.p.). *A*, Low magnification (50 \times) showing P-ERK immunoreactivity in the whole striatum. Note the strong immunoreactivity at Coc 5 and Coc 10 in the whole striatum and its decrease at Coc 20 (data are representative of 5 independent animals in each group). *B*, Higher magnification (200 \times) of P-ERK immunoreactivity in the dorsomedial striatum (DM) and the shell of NA. In both striatal regions, this immunoreactivity corresponds to both neuropil (asterisk) and cell bodies (arrows). *C*, Whereas at Coc 5 most of cell bodies showed a cytoplasmic (black arrows) P-ERK immunolabeling, at Coc 10, the majority of P-ERK was nuclear (white arrows). *D*, P-ERK immunoreactivity at low magnification showing ERK activation in chronically treated mice (6 d, once daily) with a challenge of cocaine (Coc 5, Coc 10, Coc 20) performed on day 7 (data are representative of 4 independent animals in each group).

nificant differences in number of P-ERK positive cells in the following striatal compartments: dorsolateral ($F_{(5,12)} = 62.8$; $p < 0.01$), dorsomedial ($F_{(5,12)} = 66.4$; $p < 0.01$), core ($F_{(5,12)} = 44.1$; $p < 0.01$), and shell ($F_{(5,12)} = 43.9$; $p < 0.01$). Post hoc comparisons (Newman–Keuls) showed a significant increase in P-ERK-immunoreactive cells after cocaine administration in dorsal striatum and NA ($p < 0.01$) (Fig. 2*A*). The blockade of D1 receptors by administration of a selective antagonist, SCH 23390 (0.1 mg/kg), resulted in a total inhibition of cocaine-induced ERK activation

throughout the dorsal striatum (dorsolateral and dorsomedial, $p < 0.01$) and NA (core and shell, $p < 0.01$) (Fig. 2*A,B*). This result shows that ERK activation was dependent on DA via D1 receptor activation. Moreover, basal P-ERK immunoreactivity found in control mice was significantly decreased by SCH 23390 in dorsomedial striatum ($p < 0.05$), implicating D1 receptors in spontaneous tonic control of ERK activity (Fig. 2*B*).

The possible involvement of D2 receptor subtype in cocaine-induced ERK activation was also analyzed. Raclopride injection

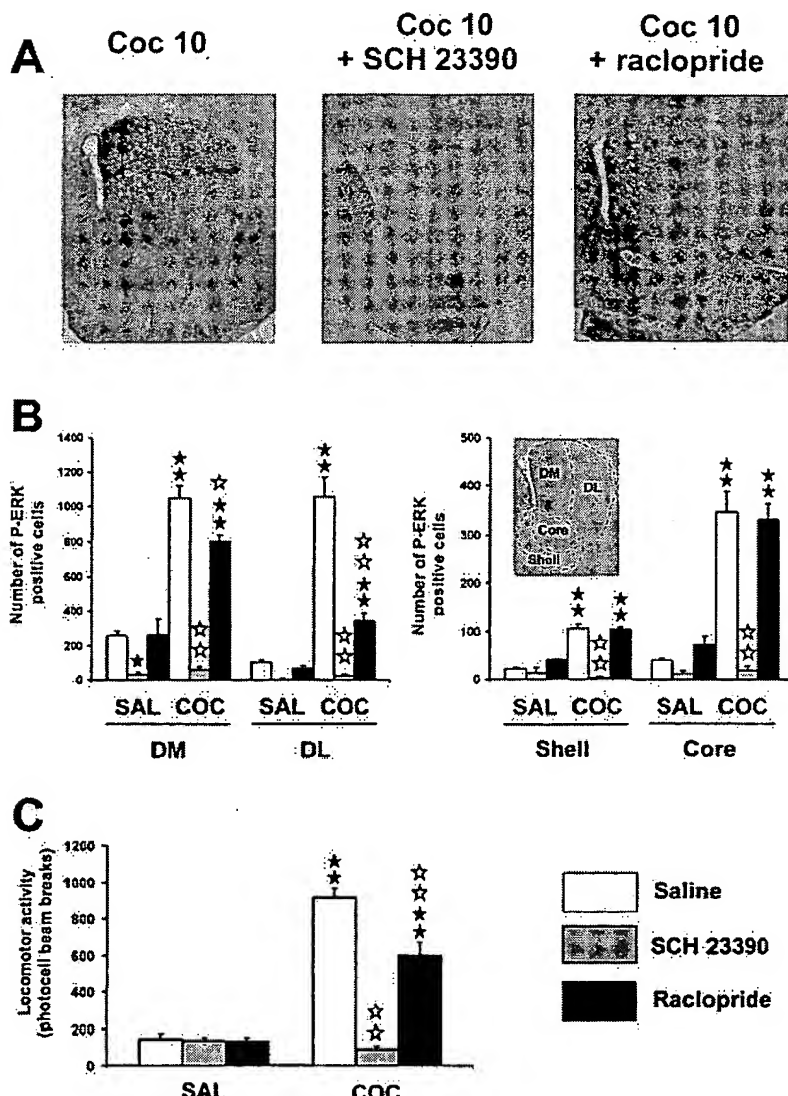


Figure 2. Cocaine-induced ERK activation depends on DA-D1 receptors. SCH 23390 (0.1 mg/kg, i.p.) or raclopride (0.3 mg/kg, i.p.) were injected 15 min before cocaine. *A*, Low magnification of P-ERK immunolabeling in the striatum in cocaine-injected mice, in the presence or not of DA antagonists. Note the total inhibition of cocaine-induced P-ERK immunolabeling by DA-D1 antagonist. *B*, P-ERK-immunoreactive cells were counted in the dorsomedial (DM) and dorsolateral (DL) striatum, core, and shell of the NA from three independent mice in each group. Data represents the total number of P-ERK-positive cells in each region, delimited as depicted in *insert*. *C*, The same doses of DA antagonists were used to analyze locomotor response induced by cocaine ($n = 8$ mice for each group). Statistical comparisons for *B* and *C*: * $p < 0.05$; ** $p < 0.01$ when comparing with saline group. \star $p < 0.05$; $\star\star$ $p < 0.01$ when comparing with cocaine group (Newman-Keuls test).

(0.3 mg/kg) alone induced a slight but not significant activation in number of P-ERK-positive neurons in the shell of NA. Raclopride failed to block cocaine-induced P-ERK immunoreactivity in the NA (core and shell) but partially decreased it in the dorsal striatum (dorsomedial, $p < 0.05$; dorsolateral, $p < 0.01$), suggesting that D2 receptors could also play some role in these cocaine effects (Fig. 2*A, B*). Taken together, these results show that cocaine-induced ERK activation critically involves D1 receptors, whereas contribution of D2 receptors seems to be restricted to dorsal striatum.

Doses of DA antagonists used above to analyze ERK activity were also tested in hyperlocomotion induced by cocaine. As revealed by one-way ANOVA, significant effects of treatment on locomotor responses are observed under these experimental conditions ($F_{(5,43)} = 87.4$; $p < 0.001$). Post hoc comparison (Newman-Keuls) showed that SCH 23390 (0.1 mg/kg) completely abolished hyperlocomotion induced by cocaine (20 mg/kg) ($p < 0.01$), whereas raclopride (0.3 mg/kg) poorly affected this response ($p < 0.01$) (Fig. 2*C*). These data are consistent with literature data (Cabib et al., 1991; Xu et al., 1994a) showing that D1 receptors are preferentially involved in cocaine-induced hyperlocomotion.

Contribution of NMDA receptor in cocaine-induced ERK activation

Because NMDA receptor activation plays a role in amphetamine-induced gene regulation (Konradi et al., 1996) and is known to activate ERK pathway (English and Sweatt, 1996), the involvement

of NMDA receptors in cocaine-induced ERK activation was studied. The noncompetitive NMDA receptor antagonist MK 801 (0.15 mg/kg) did not modify basal P-ERK immunoreactivity but decreased cocaine-induced P-ERK immunoreactivity in the striatum (Fig. 3*A*). Statistical comparisons (Fig. 3*B*) showed a significant decrease in the dorsomedial ($F_{(3,8)} = 48.5$; $p < 0.01$) and dorsolateral striatum ($F_{(3,8)} = 54.8$; $p < 0.01$), as well as in the core ($F_{(3,8)} = 26$; $p < 0.01$) and shell ($F_{(3,8)} = 19.7$; $p < 0.01$) of NA. Thus, ERK activation by cocaine involves a participation of NMDA glutamate receptor. Interestingly, the neuropil still remained highly labeled after MK801 treatment, suggesting the involvement of NMDA receptors in the control of P-ERK activation at the postsynaptic level rather than presynaptically (Fig. 3*A*). The effects of MK 801 (0.15 mg/kg) were also evaluated in cocaine-induced hyperlocomotion ($F_{(3,27)} = 39.9$; $p < 0.01$). Despite its effect on ERK activation, MK 801, at the dose used here, did not modify hyperlocomotion induced by cocaine (Fig. 3*C*).

Cocaine-induced locomotor activity is partially linked to ERK activity

Because ERK activation was completely prevented by D1 antagonist (Fig. 2*A*), we then tested whether ERK activation was involved in cocaine-induced locomotor activity. For this purpose, we assessed the effects of SL327, a selective MEK inhibitor (Atkins et al., 1998). This compound is a structural analog of the highly selective and efficient MEK inhibitor U0126 (Favata et al., 1998).

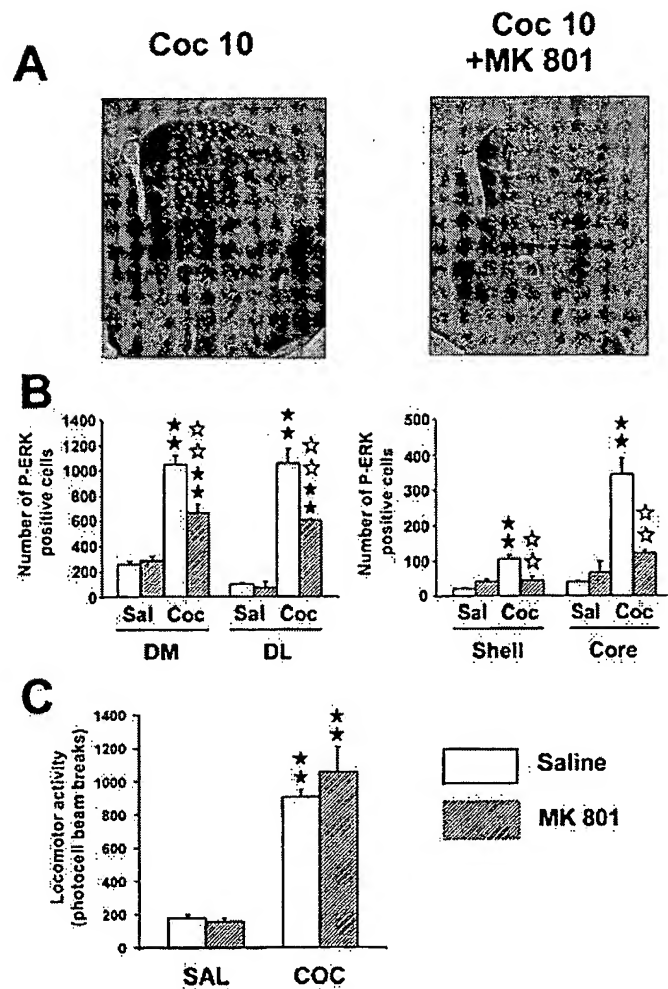


Figure 3. Partial contribution of glutamatergic NMDA receptors on cocaine-induced ERK activation. MK 801 (0.15 mg/kg, i.p.) was injected 30 min before cocaine. *A*, Low magnification of P-ERK immunolabeling in the striatum in cocaine-injected mice, in the presence or not of MK 801. Note the slight decrease of cocaine-induced P-ERK immunolabeling. *B*, P-ERK-immunoreactive cells were counted in the four striatal subregions as described Figure 3 ($n = 3$ independent mice for each group). *C*, The same dose of MK 801 was used to analyze locomotor response induced by cocaine ($n = 8$ mice for each group). Statistical comparisons for *B* and *C* were performed as described Figure 2.

Although recent studies report that this compound has no effect on a variety of other kinases, including PKA, PKC, or CamKII (Atkins et al., 1998; Selcher et al., 1999) (J. M. Trzaskos unpublished results), we analyzed whether it could have any D1 receptor blocking activity. Adenyl cyclase activity induced by dopamine (10^{-4} M) was tested from mouse brain slices in the presence of various concentrations of SL 327 (0.3, 3, 10, 30, 100 and 300 μ M). Table 1 shows that, whatever the concentration used, this compound has no effect on DA-induced cAMP production. When administered systemically, SL327 (50 mg/kg) totally abolished cocaine-induced ERK activation in the whole striatum (Fig. 4*A*). However, cocaine-induced hyperlocomotion ($F_{(3,28)} = 59.2$; $p < 0.01$) was only partially decreased, by SL327 (50 mg/kg), as shown in Figure 4*B*. We noted a complete blockade of rearing behavior induced by cocaine after SL327 administration (data not shown). These results suggest that ERK activation plays a role in the control of locomotor response induced by cocaine.

Induction of c-fos and Elk-1 hyperphosphorylation by acute cocaine is dependent on ERK activation

Hyperphosphorylation of ERK was clearly nuclear 10 min after cocaine administration (Fig. 1), suggesting a possible involvement

Table 1. Effects of SL 327 on dopamine-induced cAMP production on striatal mouse slices

Dopamine (M)	SL 327 (μ M)	% increase
10^{-4}	0	124 \pm 9
0	10	12 \pm 8
0	100	7 \pm 6
10^{-4}	0.3	129 \pm 21
10^{-4}	3	126 \pm 3
10^{-4}	10	167 \pm 42
10^{-4}	30	163 \pm 42
10^{-4}	100	143 \pm 22
10^{-4}	300	140 \pm 30

Adenyl cyclase activity stimulated by dopamine was measured in presence of increasing doses of SL327 (0.3–300 μ M). Results were calculated in picomoles of cAMP formed per minute per milligram of protein and expressed in percentage of increase when compared to the basal adenyl cyclase activity ($n = 3$ individual experiments run in triplicate). Note the lack of effects of SL327 on both the basal and dopamine-induced cAMP levels.

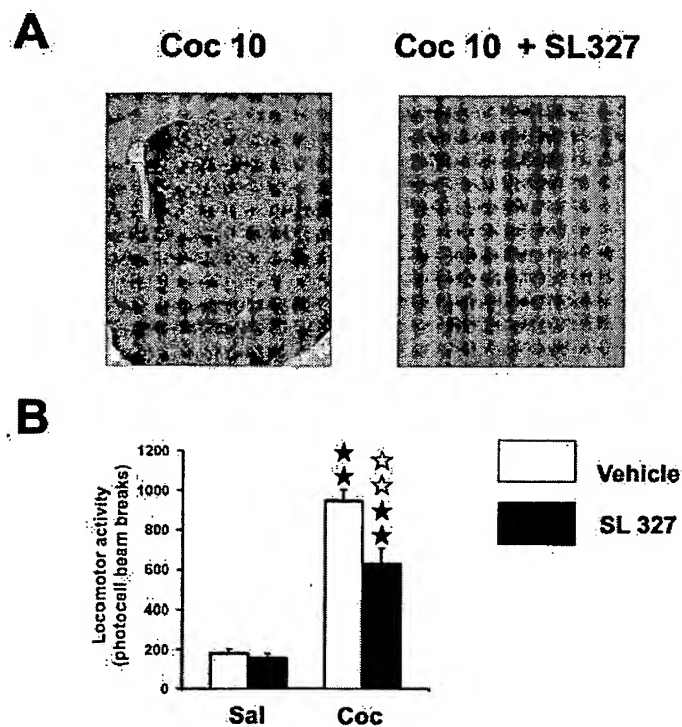


Figure 4. SL 327, an inhibitor of ERK activation, partially inhibits cocaine-induced hyperlocomotion. SL 327 (50 mg/kg, i.p.) was injected 1 hr before cocaine. *A*, Note the total inhibition of cocaine-induced P-ERK immunoreactivity by SL 327. *B*, Effect of SL 327 on cocaine-induced hyperlocomotion ($n = 8$ mice for each group). Statistical comparisons were performed as described Figure 2.

of ERK activation in IEG upregulation (for review, see Grewal et al., 1999). Because c-fos is a prime marker of gene expression after cocaine treatment, and its transcriptional regulation is critically controlled by ERK in the striatum (Sgambato et al., 1998; Vanhoutte et al., 1999), we analyzed cocaine-induced c-fos expression after inhibition of ERK by SL327 (50 mg/kg). A strong induction of c-fos expression in the dorsal striatum and the NA was found 1 hr after cocaine administration, as previously described (Graybiel et al., 1990; Moratalla et al.; 1993) (Fig. 5). When SL327 was injected before cocaine injection, c-fos immunolabeling returned to baseline levels in the dorsal striatum and strongly decreased in the shell of the NA (Fig. 5).

Although CREB activation can be linked to ERK activation in various model systems (Xing et al., 1996; Impey et al., 1998; Davis

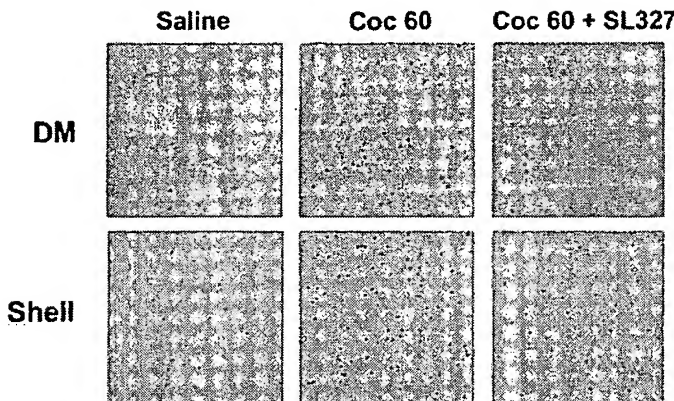


Figure 5. SL 327 inhibits c-fos induction by cocaine. c-fos expression was analyzed 1 hr after cocaine injection in the dorsomedial striatum (DM) and in the shell of the NA. SL 327 was injected as described Figure 4. Note the total inhibition of c-fos immunoreactivity in the DM and the strong but not total inhibition in the shell (data are representative of 4 independent mice for each group).

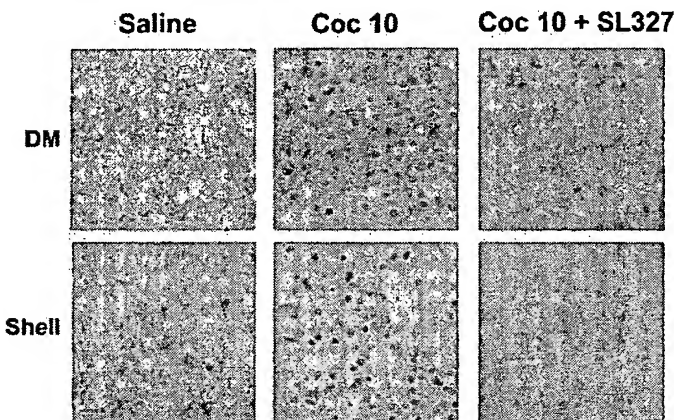


Figure 6. Cocaine-induced Elk-1 hyperphosphorylation depends on ERK activation. Elk-1 hyperphosphorylation was analyzed using an anti-active antibody (anti-phospho-Ser³⁸³-Elk-1) 10 min after cocaine injection in the absence or presence of SL 327. Note the strong induction of Elk-1 activation by cocaine in the dorsomedial striatum (DM) and in the shell of the NA. This activation is totally inhibited by SL 327 (data are representative of 4 independent mice for each group).

et al., 2000) and its involvement in cocaine responses has been reported (Carlezon et al., 1998), no data yet describes whether Elk-1, a direct nuclear target of ERKs is also activated after cocaine treatment. A hyperphosphorylation of Elk-1 was found in a strict spatiotemporal correlation with ERK activation, i.e., in both the dorsal striatum and NA 10 min after cocaine injection (Fig. 6). Furthermore, P-Elk1 immunoreactivity was prevented by SL327, demonstrating that Elk1 activation is completely dependent on ERK activation. Altogether, these data suggest that ERK activation, targeting the transcription factor Elk-1, is involved in cocaine-induced c-fos expression in the striatum.

Inhibition of ERK activity impairs rewarding properties induced by cocaine

Expression of transcription factors encoded by IEGs has been hypothesized to initiate downstream molecular events, which in turn are involved in the instantiation of cocaine-rewarding properties (for review, see Berke and Hyman, 2000). The place preference conditioning paradigm was used to assess the role of ERK activation on the rewarding effects of cocaine. Two-way ANOVA revealed a significant effect of treatment ($F_{(3,28)} = 8.079$; $p < 0.01$) and phase-treatment interaction ($F_{(3,28)} = 8.21$; $p < 0.01$) with no main effect of phase alone ($F_{(1,28)} = 3.649$; NS). Comparison of

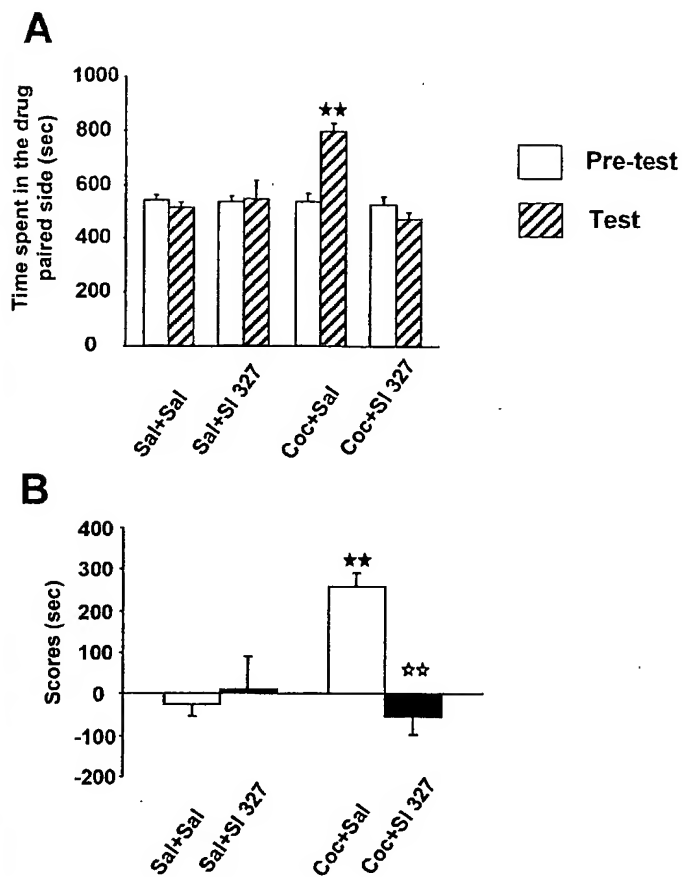


Figure 7. Lack of cocaine-induced place preference in mice injected with SL 327. *A*, Time spent in drug-associated compartment during the preconditioning (white bars) and the testing phase (hatched bars). Values represent mean \pm SEM from $n = 8$ independent mice per group. *B*, Scores calculated as the difference between postconditioning and preconditioning time spent in the compartment associated with cocaine. ★★ $p < 0.001$ when comparing with saline group. ★★ $p < 0.001$ when comparing with cocaine group (Newman-Keuls test).

preconditioning times spent in the drug-paired compartment did not reveal any significant difference between groups, indicating the unbiased characteristics of the experimental design. After conditioning, mice treated with cocaine (20 mg/kg) spent more time in the cocaine-paired compartment, revealing a clear place preference as revealed by one-way ANOVA ($F_{(3,28)} = 8.22$; $p < 0.01$) and *post hoc* comparisons ($p < 0.01$) of score values (Fig. 7*A,B*). Interestingly, pretreatment with SL 327 during the conditioning phase completely abolished the place preference induced by cocaine ($p < 0.01$) (Fig. 7*A,B*). No conditioned response or locomotor modification was observed in mice treated with SL327 alone (Fig. 7*A,B*). These results suggest a critical involvement of ERK signaling cascade on the rewarding effects of cocaine.

DISCUSSION

The ERK pathway that involves a complex intracellular signaling cascade, including the small GTP-binding protein Ras and the kinases Raf and MEK, controls various neurobiological effects, including neuronal differentiation (for review, see Seger and Krebs, 1995) and synaptic plasticity in the adult CNS (for review, see Orban et al., 1999). Initially described in response to neurotrophin receptors, the Ras-ERK pathway can also integrate second messenger systems, such as calcium, PKA, and DAG, which may explain its crucial role in activity-dependent regulation of neuronal function (for review, see Grewal et al., 1999).

This work reports that acute cocaine administration strongly activates ERK, which is rapid and transient. This activation oc-

curred in the striatum but not in the ventral tegmental area (VTA) (data not shown). We did not find any ERK activation in the striatum after chronic cocaine administration (analyzed 12 hr after the last injection), a result in agreement with previous studies (Berhow et al., 1996). In this case, authors described a specific ERK activation in the VTA, which was thought to result from stimulation of tyrosine kinase receptors by neurotrophins such as BDNF (Berhow et al., 1996) or neurotrophin-3 (Pierce et al., 1999). However, it must be noticed that ERK activation was found in the striatum when analyzed rapidly (5 min) after a challenge cocaine injection on day 7, and this activation was more sustained than after an acute injection, suggesting a sensitization of this pathway by previous chronic cocaine injection. Altogether these data suggest that ERK signaling in the striatum could be involved in the control of cocaine-induced effects.

ERK activation was critically linked to D1 receptors. Several second messengers could be responsible for the link between D1 receptors and ERK, such as the small Ras-related G protein Rap1, activated by PKA, and the subsequent activation of B Raf isoform (Vossler et al., 1997; Yao et al., 1998; York et al., 1998). Another possible intermediate between D1 receptor and ERK activation could be Calcyon, a D1 receptor-interacting protein, expressed in the striatum and stimulating intracellular calcium release (Lezcano et al., 2000), which is known to activate the Ras-ERK pathway (Lev et al., 1995). An interesting observation was the different subcellular localization of activated ERK proteins during the time course. Indeed, ERK activation was first observed in cytoplasmic compartments, suggesting an early local role of the protein at the membrane–cytoplasmic level. As a matter of fact, activated ERKs can target a number of membrane-associated proteins such as EGR receptors, phospholipase A2, or cytoskeletal proteins, including microtubule-associated proteins (MAPs) and neurofilaments (for review, see Grewal et al., 1999). The later nuclear activation suggests a second effect in gene expression (see below). Another localization of activated ERK likely corresponded to presynaptic terminals, as attested by the strong immunolabeling observed in the neuropil. This presynaptic activation could be possibly related to the facilitating role of ERK in neurotransmitter release via phosphorylation of synapsins (Jovanovic et al., 2000).

The D1 antagonist SCH 23390 completely reversed ERK activation and hyperlocomotion induced by acute cocaine. However, the MEK inhibitor only partially blocked cocaine locomotor response, although the increase observed in rearing behavior was completely abolished (data not shown). These data suggest that D1 receptors control cocaine-induced striatal activity and hyperlocomotion via both ERK-dependent and ERK-independent pathways. The ERK-dependent control of striatal synaptic activity remains to be established, however various presynaptic or postsynaptic substrates could participate in this control (Grewal et al., 1999; Jovanovic et al., 2000). Concerning the ERK-independent pathway, it is now well known that D1 receptors can regulate striatal neuronal excitability by activation of PKA and subsequent modification of the phosphorylation state of various substrates (such as L type calcium channels, DARPP 32, NMDA receptors, or electronic ion pumps) (for review, see Greengard et al., 1999).

Glutamate receptors of NMDA subtype strongly contributed to ERK activation by cocaine, in particular in the NA where MK 801 totally abolished cocaine-induced ERK activation in neurons but not in the neuropil. This result further illustrates the participation of NMDA receptors in D1-mediated intracellular events previously showed by Konradi et al. (1996). Whether this cooperation occurs at the level of neuronal circuitry or intrinsically in striatal neurons remains to be established. However, the lack of P-ERK inhibition in the neuropil after MK 801 argues for a preferential postsynaptic effect, probably through glutamatergic cortical inputs (Spencer, 1976). No modification of cocaine-induced hyperlocomotion was found after MK 801 blockade. In this regard, it must be noted that controversial results have been previously reported on the contribution of NMDA receptors in acute behavioral responses induced

by cocaine, depending on doses, animal species, and experimental conditions (Pulvirenti et al., 1991; Witkin, 1993; Wolf et al., 1994).

Cocaine-induced locomotor activity was partially inhibited by the D2 antagonist raclopride. Interestingly, raclopride also decreased ERK activation, but only in the dorsolateral striatum, a striatal region involved in the motor responses of cocaine (Canales and Graybiel, 2000). Recent evidences indicate that D2 agonists can activate ERK in striatal slices independently of $\beta\gamma$ subunits of G-proteins but via coupling of a G_q-protein to PLC β pathway and mobilization of intracellular calcium stores (Yan et al., 1999). Although D1 and D2 receptors are classically considered to be localized in distinct striatal subpopulations (Gerfen et al., 1990), our observations suggest a synergism of both D1 and D2 receptors in the same striatal subpopulation. Interestingly, recent anatomical and physiological evidences show their colocalization in striatal neurons (Aizman et al., 2000).

Activated ERKs were translocated to the nucleus 10 min after cocaine injection. A prime nuclear target of activated ERK is the ternary complex factor Elk-1, which acts as a transcriptional activator, via the SRE of various IEG, such as c-fos. Elk-1 was strongly phosphorylated after cocaine treatment, in a strict spatiotemporal correlation with ERK activation. The MEK inhibitor SL 327 totally abolished Elk-1 activation, supporting its complete dependence on ERK pathway. Although Elk-1 is a common substrate of the different MAP kinase pathways in cell model systems (Davis, 1993), neither N-terminal Jun kinase (JNK) nor p38 were activated by cocaine in this study (data not shown). The lack of JNK activation is in agreement with previous data indicating that neither dopamine nor forskolin activate JNK on striatal primary neuronal cells (Schwarzchild et al., 1997).

After nuclear translocation, activated ERK controls IEG transcription in neuronal cells (Davis et al., 2000). In agreement with this, a strong inhibition of cocaine-induced c-fos expression was found after treatment with the MEK inhibitor SL327. Because this compound has no effect on a variety of other kinases, including PKA, PKC, or CamKII (Atkins et al., 1998; Selcher et al., 1999) (Trzaskos, unpublished results), or adenylyl cyclase production, this effect on c-fos expression cannot be readily attributed to nonspecific actions of the drug. It must be noticed, however, that although total in the dorsomedial striatum, c-fos inhibition was only partial in the shell of NA. Therefore, the transcriptional regulation of c-fos seems to be under a combined control of an ERK-dependent and -independent pathway, at least in this striatal region. In this way, it is now well established that cAMP-PKA pathway directly controls CREB phosphorylation, which targets the CRE site of the c-fos promoter (Dash et al., 1991). Interestingly, consistent with our data, results from mutant mice in which the CRE response is affected indicate that this site is not sufficient to induce full expression of c-fos proteins (Robertson et al., 1995; Maldonado et al., 1996).

An important observation was the abolishment of cocaine-induced conditioned place preference after blockade of ERK by SL327. The locomotor sensitization observed in mice receiving a repeated cocaine administration during this conditioned treatment was prevented (data not show). In agreement with this, inhibition of ERK in the VTA, a brain structure closely related to drugs of abuse-induced rewarding effect (Koob, 1992), blocked cocaine-induced behavioral sensitization (Pierce et al., 1999). By controlling the expression of tyrosine hydroxylase, ERK activation in the VTA was thought to be involved in increased DA neuronal activity (Berhow et al., 1996). Thus, the ERK pathway could be involved in cocaine-induced behavioral rewarding effects via different mechanisms: (1) control of genes encoding transcription factors (such as c-fos) in the striatum, and (2) control of genes associated with DA neuronal activity after neurotrophin receptor activation.

In summary, the present results reveal that cocaine-induced ERK activation plays an important role in striatal c-fos expression and some of its behavioral responses related to the development of addiction. These findings provide a new mechanism to explain the neurobiological substrate of cocaine rewarding properties that

could be important to better understand the different neural pathways involved in its addictive properties.

REFERENCES

Aizman O, Brismar H, Uhlen P, Zettergren E, Levey AI, Forssberg H, Greengard P, Aperia A (2000) Anatomical and physiological evidence for D1 and D2 dopamine receptor colocalization in neostriatal neurons. *Nat Neurosci* 3:226–230.

Atkins CM, Selcher JC, Petraitis JJ, Trzaskos JM, Sweatt JD (1998) The MAPK cascade is required for mammalian associative learning. *Nat Neurosci* 1:602–609.

Berhow MT, Hiroi N, Nestler EJ (1996) Regulation of ERK (extracellular signal regulated kinase), part of the neurotrophin signal transduction cascade, in the rat mesolimbic dopamine system by chronic exposure to morphine or cocaine. *J Neurosci* 16:4707–4715.

Berke JD, Hyman SE (2000) Addiction, dopamine, the molecular mechanisms of memory. *Neuron* 25:515–532.

Berke JD, Paletzki RF, Aronson GJ, Hyman SE, Gerfen CR (1998) A complex program of striatal gene expression induced by dopaminergic stimulation. *J Neurosci* 18:5301–5310.

Bockaert J, Tassin JP, Thierry AM, Glowinski J, Premont J (1977) Characteristics of dopamine and beta-adrenergic sensitive adenylate cyclases in the frontal cerebral cortex of the rat. Comparative effects of neuroleptics on frontal cortex and striatal dopamine sensitive adenylate cyclase. *Brain Res* 122:71–86.

Cabib S, Castellano C, Cestari V, Filibeck U, Puglisi-Allegra S (1991) D1 and D2 receptor antagonists differently affect cocaine-induced locomotor hyperactivity in the mouse. *Psychopharmacology* 105:335–339.

Canales JJ, Graybiel AM (2000) A measure of striatal function predicts motor stereotypy. *Nat Neurosci* 3:377–383.

Carlezon Jr WA, Thome J, Olson VG, Lane-Ladd SB, Brodkin ES, Hiroi N, Duman RS, Neve RL, Nestler EJ (1998) Regulation of cocaine reward by CREB. *Science* 282:2272–2275.

Chen RH, Sarneki C, Blenis J (1992) Nuclear localization and regulation of *erk*- and *rsk*-encoded protein kinases. *Mol Cell Biol* 12:915–927.

Dash PK, Karl KA, Prywes R, Kandel ER (1991) cAMP response element-binding protein is activated by Ca^{2+} /calmodulin as well as cAMP dependent protein kinase. *Proc Natl Acad Sci USA* 88:5061–5065.

Davis RJ (1993) The mitogen-activated protein kinase signal transduction pathway. *J Biol Chem* 268:14553–14556.

Davis S, Vanhoutte P, Pages C, Caboche J, Laroche S (2000) The MAPK/ERK cascade targets both Elk-1 cAMP response element-binding protein to control long-term potentiation-dependent gene expression in the dentate gyrus *in vivo*. *J Neurosci* 20:4563–4572.

Di Chiara G, Imperato A (1988) Drugs abused by humans preferentially increase synaptic dopamine concentrations in the mesolimbic system of freely moving rats. *Proc Natl Acad Sci USA* 85:5274–5278.

English JD, Sweatt JD (1996) Activation of p42 mitogen-activated protein kinase in hippocampal long term potentiation. *J Biol Chem* 271:24329–24332.

English JD, Sweatt JD (1997) Requirement for the mitogen-activated protein kinase cascade in hippocampal long-term potentiation. *J Biol Chem* 272:19103–19106.

Favata MF, Horiuchi KY, Manos EJ, Daulerio AJ, Stradley DA, Feeser WS, Van Dyk DE, Pitts WJ, Earl RA, Hobbs F, Copeland RA, Magolda RL, Scherer PA, Trzaskos JM (1998) Identification of a novel inhibitor of Mitogen-activated Protein kinase kinase. *J Biol Chem* 273:18623–18632.

Fitzgerald LW, Ortiz J, Hamedani AG, Nestler EJ (1996) Regulation of glutamate receptor subunit expression by drugs of abuse and stress: common adaptation among cross-sensitizing agents. *J Neurosci* 16:274–282.

Gerfen CR, Engber TM, Mahan LC, Susel Z, Chase TN, Monsma Jr FJ, Sibley DR (1990) D1 and D2 dopamine receptor-regulated gene expression of striatonigral and striatopallidal neurons [see comments]. *Science* 250:1429–1432.

Gille H, Sharrocks AD, Shaw PE (1992) Phosphorylation of transcription factor p62TCF by MAP kinase stimulates ternary complex formation at c-fos promoter. *Nature* 358:414–417.

Gille H, Kortenjann M, Thoma O, Moomaw C, Slaughter C, Cobb M, Shaw PE (1995) ERK phosphorylation potentiates Elk-1-mediated ternary complex formation and transactivation. *EMBO J* 14:951–962.

Graybiel A, Moratalla R, Robertson HA (1990) Amphetamine and cocaine induce drug-specific activation of the c-fos gene in striosome-matrix compartments and limbic subdivisions of the striatum. *Proc Natl Acad Sci USA* 87:6912–6916.

Greengard P, Allen PB, Nairn AC (1999) Beyond the dopamine receptor: the DARPP-32/protein phosphatase-1 cascade. *Neuron* 23:435–447.

Grewal SS, York RD, Stork PJ (1999) Extracellular-signal-regulated kinase signalling in neurons. *Curr Opin Neurobiol* 9:544–553.

Herdegen T, Leah JD (1998) Inducible and constitutive transcription factors in the mammalian nervous system: control of gene expression by Jun, Fos and Krox, and CREB/ATF proteins. *Brain Res Brain Res Rev* 28:370–490.

Hill CS, Marais R, John S, Wynne J, Dalton S, Treisman R (1993) Functional analysis of a growth factor-responsive transcription factor complex. *Cell* 73:395–406.

Hope B, Kosofsky B, Hyman SE, Nestler EJ (1992) Regulation of immediate early gene expression and AP-1 binding in the rat nucleus accumbens by chronic cocaine. *Proc Natl Acad Sci USA* 89:5764–5768.

Hope BT, Nye HE, Kelz MB, Self DW, Iadarola MJ, Nakabepu Y, Duman RS, Nestler EJ (1994) Induction of a long-lasting AP-1 complex composed of altered Fos-like proteins in brain by chronic cocaine and other chronic treatments. *Neuron* 13:1235–1244.

Hipskind RA, Baccarini M, Nordheim A (1994a) Transient activation of RAF-1, MEK, and ERK2 coincides kinetically with ternary complex factor phosphorylation and immediate-early gene promoter activity in vivo. *Mol Cell Biol* 14:6219–6231.

Hipskind RA, Büscher D, Nordheim A, Baccarini M (1994b) Ras/MAP kinase-dependent and-independent signaling pathways target distinct ternary complex factors. *Genes Dev* 8:1803–1816.

Impey S, Obrietan K, Wong ST, Poser S, Yano S, Wayman G, Deloulme JC, Chan G, Storm DR (1998) Cross talk between ERK and PKA is required for Ca^{2+} stimulation of CREB-dependent transcription and ERK nuclear translocation. *Neuron* 21:869–883.

Janknecht R, Zinck R, Ernst WH, Nordheim A (1994) Functional dissection of the transcription factor Elk-1. *Oncogene* 9:1273–1278.

Jovanovic JN, Czernik AJ, Fienberg AA, Greengard P, Sihra TS (2000) Synapsins as mediators of BDNF-enhanced neurotransmitter release. *Nat Neurosci* 3:323–329.

Kelz MB, Chen J, Carlezon Jr WA, Whisler K, Gilden L, Bechmann AM, Steppen C, Zhang YJ, Marotti L, Self DW, Tkatch T, Baranauskas G, Surmeier DJ, Neve RL, Duman RS, Picciotto MR, Nestler EJ (1999) Expression of the transcription factor deltaFosB in the brain controls sensitivity to cocaine. *Nature* 401:272–276.

Konradi C, Cole RL, Heckers S, Hyman SE (1994) Amphetamine regulates gene expression in rat striatum via transcription factor CREB. *J Neurosci* 14:5623–5634.

Konradi C, Leveque JC, Hyman SE (1996) Amphetamine and dopamine-induced immediate early gene expression in striatal neurons depends on postsynaptic NMDA receptors and calcium. *J Neurosci* 16:4231–4239.

Koob GF (1992) Drugs of abuse: anatomy, pharmacology, and function of reward pathways. *Trends Pharmacol Sci* 13:177–184.

Lev S, Moreno H, Martinez R, Canoll P, Peles E, Musacchio JM, Plowman GD, Rudy B, Schlessinger J (1995) Protein tyrosine kinase PYK2 involved in Ca^{2+} -induced regulation of ion channel and MAP kinase functions. *Nature* 376:737–745.

Lezcano N, Mrzljak L, Eubanks S, Levenson R, Goldman-Rakic P, Bergson C (2000) Dual signaling regulated by calcyon, a D1 dopamine receptor interacting protein. *Science* 287:1660–1664.

Maldonado R, Blendy JA, Tzavara E, Gass P, Roques BP, Hanoune J, Schutz G (1996) Reduction of morphine abstinence in mice with a mutation in the gene encoding CREB [see comments]. *Science* 273:657–659.

Maldonado R, Saiardi A, Valverde O, Samad TA, Roques BP, Borrelli E (1997) Absence of opiate rewarding effects in mice lacking dopamine D2 receptors. *Nature* 388:586–589.

Marais R, Wynne J, Treisman R (1993) The SRF accessory protein Elk-1 contains a growth factor-regulated transcriptional activation domain. *Cell* 73:381–393.

Martin KC, Michael D, Rose JC, Barad M, Casadio A, Zhu H, Kandel ER (1997) MAP Kinase translocates into the nucleus of the presynaptic cell and is required for long-term facilitation in *Aplysia*. *Neuron* 18:899–912.

Moratalla R, Vickers EA, Robertson HA, Cochran BH, Graybiel AM (1993) Coordinate expression of c-fos and jun B is induced in the rat striatum by cocaine. *J Neurosci* 13:423–433.

Moratalla R, Xu M, Tonegawa S, Graybiel AM (1996) Cellular responses to psychomotor stimulant and neuroleptic drugs are abnormal in mice lacking the D1 dopamine receptor. *Proc Natl Acad Sci USA* 93:14928–14933.

Nestler EJ, Aghajanian GK (1997) Molecular and cellular basis of addiction. *Science* 278:58–63.

Orban PC, Chapman PF, Brambilla R (1999) Is the Ras-MAPK signalling pathway necessary for long-term memory formation? *Trends Neurosci* 22:38–44.

Pierce RC, Pierce-Bancroft AF, Prasad BM (1999) Neurotrophin-3 contributes to the initiation of behavioral sensitization to cocaine by activating the Ras/Mitogen-activated protein kinase signal transduction cascade. *J Neurosci* 19:8685–8695.

Pulvirenti L, Swerdlow NR, Koob GF (1991) Nucleus accumbens NMDA antagonist decreases locomotor activity produced by cocaine, heroin or accumbens dopamine, but not caffeine. *Pharmacol Biochem Behav* 40:815–845.

Roberson ED, English JD, Adams JP, Selcher JC, Kondratic C, Sweatt JD (1999) The mitogen-activated protein kinase cascade couples PKA and PKC to cAMP response element binding protein phosphorylation in area CA1 of hippocampus. *J Neurosci* 19:4337–4348.

Robertson LM, Kerolla TK, Vendrell M, Luk D, Smeley RJ, Bocchiaro C, Morgan JI, Curran T (1995) Regulation of c-fos expression in transgenic mice requires multiple interdependent transcription control elements. *Neuron* 14:214–225.

Salomon Y, Londos C, Rodbell M (1974) A highly sensitive adenylate cyclase assay. *Anal Biochem* 58:541–548.

Schwarzschild MA, Col RL, Hyman SE (1997) Glutamate, but not dopa-

mine, stimulates stress-activated protein kinase and AP-1-mediated transcription in striatal neurons. *J Neurosci* 17:3455–3466.

Seger R, Krebs EG (1995) The MAPK signaling pathway. *FASEB J* 9:726–735.

Selcher JC, Atkins CM, Trzaskos JM, Paylor R, Sweatt JD (1999) A necessity for MAP kinase activation in mammalian spatial learning. *Learn Mem* 6:478–490.

Spencer HJ (1976) Antagonism of cortical excitation of striatal neurons by glutamic acid diethylster: evidence for glutamic acid as an excitatory transmitter in the rat striatum. *Brain Res* 102:91–101.

Sgambato V, Pages C, Rogard M, Besson MJ, Caboche J (1998) Extracellular signal-regulated kinase (ERK) controls immediate early gene induction on corticostriatal stimulation. *J Neurosci* 18:8814–8825.

Treisman R (1995) Journey to the surface of the cell: Fos regulation and the SRE. *EMBO J* 14:4905–4913.

Vanhoutte P, Barnier JV, Guibert B, Pagès C, Besson MJ, Hipskind RA, Caboche J (1999) Glutamate induces phosphorylation of Elk-1 and CREB, along with c-fos activation via an extracellular signal-regulated kinase-dependent pathway in brain slices. *Mol Cell Biol* 19:136–146.

Vincent SR, Sebenn M, Dubuis A, Bockaert J (1998) Neurotransmitter regulation of MAP kinase signaling in striatal neurons in primary culture. *Synapse* 29:29–36.

Vossler MR, Yao H, York RD, Pan M-G, Rim CS, Stork PJS (1997) cAMP activates MAP kinase and Elk-1 through a B-Raf- and Rap1-dependent pathway. *Cell* 89:73–62.

Xing J, Ginty DD, Greenberg ME (1996) Coupling of the ras-MAPK pathway to gene activation by RSK2, a growth-factor-regulated CREB kinase. *Science* 273:959–963.

Xu M, Hu XT, Cooper DC, Moratalla R, Graybiel AM, White FJ, Tonegawa S (1994a) Elimination of cocaine-induced hyperactivity and dopamine-mediated neurophysiological effects in dopamine D1 receptor mutant mice. *Cell* 79:945–955.

Xu M, Moratalla R, Gold LH, Hiroi N, Koob GF, Graybiel AM, Tonegawa S (1994b) Dopamine D1 receptor mutant mice are deficient in striatal expression of dynorphin and in dopamine-mediated behavioral responses. *Cell* 79:729–742.

Yan Z, Feng J, Fienberg AA, Greengard P (1999) D(2) dopamine receptors induce mitogen-activated protein kinase and cAMP response element-binding protein phosphorylation in neurons. *Proc Natl Acad Sci USA* 96:11607–11612.

Yao H, York RD, Misra-Press A, Carr DW, Stork PJ (1998) The cyclic adenosine monophosphate-dependent protein kinase (PKA) is required for the sustained activation of mitogen-activated kinases and gene expression by nerve growth factor. *J Biol Chem* 273:8240–8247.

York RD, Yao H, Dillon T, Ellig CL, Eckert SP, McCleskey EW, Stork PJ (1998) Rap1 mediates sustained MAP kinase activation induced by nerve growth factor. *Nature* 392:622–626.

Young ST, Portnoy LJ, Iadarola MJ (1991) Cocaine induces striatal c-fos-immunoreactive proteins via dopaminergic D1 receptors. *Proc Natl Acad Sci USA* 88:1291–1295.

Witkin JM (1993) Blockade of the locomotor stimulant effects of cocaine and methamphetamine by glutamate antagonists. *Life Sci* 53:405–410.

Wolf ME, Xue CJ, White FJ, Dahlin SL (1994) MK-801 does not prevent acute stimulatory effects of amphetamine or cocaine on locomotor activity or extracellular dopamine levels in rat nucleus accumbens. *Brain Res* 15:223–231.

Zinck R, Cahill MA, Kracht M, Sachsenmaier C, Hipskind RA, Nordheim A (1995) Protein synthesis inhibitors reveal differential regulation of mitogen-activated protein kinase and stress-activated protein kinase pathways that converge on Elk-1. *Mol Cell Biol* 15:4930–4938.

ERK MAP Kinase Activation in Superficial Spinal Cord Neurons Induces Prodynorphin and NK-1 Upregulation and Contributes to Persistent Inflammatory Pain Hypersensitivity

Ru-Rong Ji, Katia Befort, Gary J. Brenner, and Clifford J. Woolf

Neural Plasticity Research Group, Department of Anesthesia and Critical Care, Massachusetts General Hospital and Harvard Medical School, Boston, Massachusetts 02129

Activation of ERK (extracellular signal-regulated kinase) MAP (mitogen-activated protein) kinase in dorsal horn neurons of the spinal cord by peripheral noxious stimulation contributes to short-term pain hypersensitivity. We investigated ERK activation by peripheral inflammation and its involvement in regulating gene expression in the spinal cord and in contributing to inflammatory pain hypersensitivity. Injection of complete Freund's adjuvant (CFA) into a hindpaw produced a persistent inflammation and a sustained ERK activation in neurons in the superficial layers (laminae I–II) of the dorsal horn. CFA also induced an upregulation of prodynorphin and neurokinin-1 (NK-1) in dorsal horn neurons, which was suppressed by intra-

thecal delivery of the MEK (MAP kinase kinase) inhibitor U0126. CFA-induced phospho-ERK primarily colocalized with prodynorphin and NK-1 in superficial dorsal horn neurons. Although intrathecal injection of U0126 did not affect basal pain sensitivity, it did attenuate both the establishment and maintenance of persistent inflammatory heat and mechanical hypersensitivity. Activation of the ERK pathway in a subset of nociceptive spinal neurons contributes, therefore, to persistent pain hypersensitivity, possibly via transcriptional regulation of genes, such as prodynorphin and NK-1.

Key words: ERK; MAP kinase; prodynorphin; neurokinin-1; spinal cord; inflammatory pain

Input to the spinal cord dorsal horn from high-threshold nociceptors induces central sensitization, a heterosynaptic facilitation that outlives the initiating stimulus for tens of minutes and that plays a major role in the generation of immediate postinjury pain hypersensitivity (Woolf, 1983). The increased neuronal excitability appears to result from post-translational regulation, such as phosphorylation, of key membrane receptors and channels (Woolf and Salter, 2000; Ji and Woolf, 2001).

Recently, we showed that ERK (extracellular signal-regulated kinase), a member of the MAPK (mitogen-activated protein kinase) family, is activated with a short latency (<1 min) in superficial dorsal horn neurons by noxious but not by innocuous stimuli. This activation contributes to short-term (<1 hr) pain hypersensitivity (Ji et al., 1999). Because the involvement of ERK activation in generating acute pain hypersensitivity can be detected well before any transcriptional change manifests, ERK activation in the spinal cord, as in the hippocampus (English and Sweatt, 1997; Impey et al., 1998, 1999; Winder et al., 1999), is likely to contribute to short-term changes in neuronal excitability by post-translational regulation.

Activated ERK is also, however, translocated to the nucleus in which it phosphorylates the transcription factor cAMP element-binding protein (CREB), via the CREB kinase Rsk2, subsequently activating cAMP response element (CRE)-mediated

gene expression (Xing et al., 1996; Impey et al., 1998; Obrietan et al., 1999). ERK activation is required for long-term potentiation and long-term memory (English and Sweatt, 1997; Atkins et al., 1998; Impey et al., 1998, 1999). However, apart from immediate early genes such as *c-fos*, the specific target genes regulated by ERK responsible for long-lasting synaptic plasticity are primarily unknown (Xia et al., 1996; Sgambato et al., 1998).

Injection of irritant chemicals into a hindpaw of the rat produces a localized tissue inflammation and inflammatory pain hypersensitivity (Stein et al., 1988; Dubner and Ruda, 1992). Peripheral inflammation results in the transcriptional activation of many genes in dorsal horn neurons (Hunt et al., 1987; Wisden et al., 1990; Dubner and Ruda, 1992; Ji et al., 1994, 1995; Mannion et al., 1999; Woolf and Costigan, 1999; Samad et al., 2001), among which, prodynorphin and the substance P receptor neurokinin-1 (NK-1) have been intensively studied (Iadarola et al., 1988; Ruda et al., 1988; Schafer et al., 1993; McCarsson and Krause, 1994; Abbadie et al., 1996). Increased prodynorphin expression after inflammation has been suggested to be involved in the inflammation-induced enhanced excitability and subsequent development of expanded dorsal horn neuronal receptive fields (Hylden et al., 1991; Dubner and Ruda, 1992). Several lines of evidence suggest that NK-1 in the dorsal horn also plays an important role in inflammatory pain hypersensitivity (Traub, 1996; De Felipe et al., 1998; Ma et al., 1998; Woolf et al., 1998).

Noxious stimulation and inflammation induce CREB phosphorylation in dorsal horn neurons (Ji and Rupp, 1997; Messer-Smith et al., 1998), as well as ERK activation (Ji et al., 1999). CRE sites are present, moreover, in the promoter regions of both the prodynorphin and NK-1 genes (Hershey et al., 1991; Cole et al., 1995). This raises the possibility that the ERK pathway may play a role in regulating expression of CRE-containing genes, such as prodynorphin and NK-1, in the dorsal horn after inflammation

Received June 22, 2001; revised Oct. 3, 2001; accepted Oct. 26, 2001.

The work was supported by National Institutes of Health Grants RO1 NS38253 (C.J.W.) and RO1 NS40698 (R.R.J.). We thank Sara Billek for technical support, Dr. Linda Kobierski (Massachusetts General Hospital) for the prodynorphin cDNA vector, and Dr. Robert Elde (University of Minnesota) for prodynorphin antibody.

Correspondence should be addressed to Dr. Ru-Rong Ji, Neural Plasticity Research Group, Department of Anesthesia and Critical Care, Massachusetts General Hospital, Harvard Medical School, 149 13th Street, Room 4309, Charlestown, MA 02129. E-mail: ji@helix.mgh.harvard.edu.

Copyright © 2002 Society for Neuroscience 0270-6474/02/220478-08\$15.00/0

and in this way contribute to altered pain sensitivity. We now investigated this.

MATERIALS AND METHODS

Animals and drugs. Adult male Sprague Dawley rats (230–300 gm) were used according to Massachusetts General Hospital Animal Care institutional guidelines. Animals were anesthetized with pentobarbital (50 mg/kg, i.p.). Complete Freund's adjuvant (CFA) (100 μ l) was injected into the plantar surface of a hindpaw. For intrathecal drug delivery, a polyethylene-10 catheter was implanted into the intrathecal space of the spinal cord at the lumbar enlargement, and 10 μ l of the MEK (MAP kinase kinase) inhibitor U0126 (1 μ g; dissolved in 10% DMSO; Calbiochem, La Jolla, CA) was administered. DMSO (10%) was injected as vehicle control. For sustained drug delivery, an Alzet osmotic pump (3 d pump, 1 μ l/hr) was filled with the MEK inhibitor U0126 (0.5 μ g/ml) in 50% DMSO, and the catheter of the pump was implanted intrathecally at least 3 hr before CFA injection. DMSO (50%) was used as vehicle control.

Immunohistochemistry. Rats were deeply anesthetized with pentobarbital (120 mg/kg, i.p.) and perfused through the ascending aorta with saline, followed by 4% paraformaldehyde with 1.5% picric acid. L4–L5 spinal cord segments were dissected and post-fixed for 2–4 hr. Transverse spinal cord sections (free floating, 30 μ m) were cut and processed for immunohistochemistry using the ABC method as described previously (Ji et al., 1995, 1999). Briefly, sections were blocked with 2% goat serum in 0.3% Triton X-100 for 1 hr at room temperature (RT) and incubated overnight at 4°C with primary antibody. The sections were then incubated for 2 hr with biotinylated secondary antibody (1:200) and 1 hr with ABC complex (1:50; Vector Laboratories, Burlingame, CA) at RT. Finally, the reaction product was visualized with 0.05% DAB–0.002% hydrogen peroxide in 0.1 M acetate buffer, pH 6.0, containing 2% ammonium nickel sulfate for 2–5 min. Some sections were processed with immunofluorescence by incubating overnight with primary antibody and 1 hr at RT with FITC-conjugated secondary antibody (1:300; Jackson ImmunoResearch, West Grove, PA). The following antibodies were used: anti-phospho-ERK (pERK) (also called anti-pMAPK; anti-rabbit, 1:500; New England Biolabs, Beverly, MA), anti-pERK (monoclonal; 1:300; New England Biolabs), anti-NK1 (anti-rabbit; 1:3000; Oncogene, Sciences, Uniondale, NY), and anti-prodynorphin (anti-guinea pig; 1:3000; kindly provided by Dr. R. Elde, University of Minnesota, Minneapolis, MN). Double immunofluorescence was performed by incubating a mixture of primary antibodies (mouse anti-pERK–rabbit anti-NK1 or rabbit anti-pERK–guinea pig anti-prodynorphin), followed by a mixture of corresponding secondary antibodies conjugated with either Cy3 or FITC.

In situ hybridization. Animals were rapidly sacrificed in a CO₂ chamber, and L4–L5 spinal cord segments were removed and cut on a cryostat at a thickness of 20 μ m. A vector (pSP65) with a 1.7 kb prodynorphin insert was kindly provided by Dr. Linda Kobierski (Harvard Medical School). Antisense RNA probe, and the corresponding sense control probe, were labeled by *in vitro* transcription using linearized DNA templates for prodynorphin and digoxigenin (DIG) labeling mixture for 2 hr at 37°C. Hybridization was processed as described previously (Ji et al., 1998). Tissue sections were air dried for 2 hr, fixed in 4% paraformaldehyde for 15 min, and acetylated in acetic anhydride (0.25%) for 10 min. Sections were prehybridized for 2 hr at RT and then incubated in hybridization buffer overnight at 60°C. After hybridization, sections were washed in decreasing concentrations of SSC (2 \times , 1 \times , and 0.2 \times) for 2 hr total. Sections were then blocked with 2% goat serum for 1 hr and incubated overnight at 4°C with alkaline phosphatase-conjugated anti-DIG antibody (1:5000; Boehringer Mannheim, Indianapolis, IN). Finally, the sections were visualized in 75 μ g/ml nitroblue-tetrazolium-chloride, 50 μ g/ml 5-bromo-4-chloro-3-indolyl-phosphate, and 0.24 mg/ml levamisole for 2–24 hr.

RNA protection. Dynorphin cDNA was generated by reverse transcription-PCR from rat DRG total RNA, using primers 5'-TGGAAAAGC-CCAGCTCTAGACCT-3' and 5'-TTCTCGTGGGCTTGAAGT-GTAAA-3' and cloned into pCRII (Invitrogen, San Diego, CA). The plasmid was linearized with EcoRV, and an antisense probe was synthesized using Sp6 RNA polymerase and labeled with [³²P]UTP (800 Ci/mmol; NEN, Boston, MA). RNA protection assays (RPAs) were performed using the RPA III (Ambion, Austin, TX) protocol, as reported previously (Samad et al., 2001). Briefly, 10 μ g of RNA samples were hybridized with labeled probe overnight at 42°C and then digested with RNase A/RNase T1 mix in RNase digestion buffer for 30 min at 37°C.

Finally, samples were separated on denaturing acrylamide gel and exposed to x-ray films. A β -actin probe was used for each sample as loading controls.

Western blot. Animals were sacrificed, and dorsal horns of the L4–L5 spinal segments were rapidly removed and homogenized with a hand-held pellet pestle in lysis buffer containing a cocktail of phosphatase inhibitors (100 \times) and proteinase inhibitors (25 \times ; Sigma, St. Louis, MO). For NK-1 protein, the dorsal horns were directly homogenized in boiling SDS sample buffer (100 mM Tris, pH 6.8, 2% SDS, 20% glycerol, 10% β -mercaptoethanol, and 0.1% bromophenol blue). Protein samples were separated on SDS-PAGE gel (4–15% gradient gel; Bio-Rad, Hercules, CA) and transferred to polyvinylidene difluoride filters (Millipore, Bedford, MA). The filters were blocked with 3% milk and incubated overnight at 4°C with polyclonal anti-pERK (1:1000; New England Biolabs) or anti-NK-1 (1:5000; Oncogene Sciences) primary antibody. The blots were incubated for 1 hr at RT with HRP-conjugated secondary antibody (1:3000; Amersham Biosciences, Arlington Heights, IL) and visualized in ECL solution (NEN, Boston, MA) for 1 min and exposed onto hyperfilms (Amersham Biosciences) for 1–30 min. The blots were then incubated in stripping buffer (67.5 mM Tris, pH 6.8, 2% SDS, and 0.7% β -mercaptoethanol) for 30 min at 50°C and reprobed with polyclonal anti-ERK or anti-CREB antibody (1:3000; New England Biolabs) as loading controls.

Behavioral analysis. Animals were habituated to the testing environment daily for 2 d before baseline testing. Except for the heat test, all of the animals were placed on an elevated wire grid. For mechanical allodynia, the plantar surface of the hindpaw was stimulated with a series of von Frey hairs. The threshold was taken as the lowest force that evokes a brisk withdrawal response. For heat hyperalgesia, the plantar surface of a hindpaw was exposed to a beam of radiant heat through a transparent Perspex surface (Hargreaves et al., 1988). The withdrawal latency was recorded, with a maximum 15 sec as cutoff. The withdrawal latency was averaged over three trials.

Quantification and statistics. Eight nonadjacent sections from the L4–L5 lumbar spinal cord were randomly selected, and the numbers of immunoreactive or mRNA-positive neuronal profiles in the superficial laminae and/or deep laminae of the dorsal horn in each section were counted (under a 20 \times objective field) by an observer blind to the treatment. The values from the eight sections were averaged for each animal. The data are represented as mean \pm SEM. For RNase protection and Western blots, each experiment was repeated at least twice, and, in all cases, the same results were obtained. The density of specific bands was measured with a computer-assisted imaging analysis system (IP Lab software) and normalized against a loading control. Differences between groups were compared using Student's *t* test or ANOVA, followed by Fisher's PLSD. For nonparametric data, Mann–Whitney *U* test was applied. The criterion for statistical significance was *p* < 0.05.

RESULTS

ERK activation by peripheral inflammation

To investigate whether ERK is activated by peripheral inflammation, we injected 100 μ l of CFA into the plantar surface of a hindpaw under pentobarbital anesthesia (50 mg/kg, i.p.). This produced an area of localized swelling, erythema, and hypersensitivity to mechanical and thermal stimuli, which persisted for the duration of the experiment (48 hr). The inflammation induced by the CFA injection resulted in the induction of pERK in neurons in the medial superficial dorsal horn on the ipsilateral side of the lumbar enlargement (Fig. 1*a,b*). No induction was found in the contralateral spinal cord (Fig. 1*a*). Intraplantar injection of saline (100 μ l) only induced a very weak pERK induction (data not shown). The CFA-induced pERK was found only in neurons; all pERK cells expressed neuronal-specific nuclear protein, a marker for neuronal cells (data not shown). The pERK-labeled neurons were predominantly localized in laminae I–IIo, and the pERK was present in the nucleus, cytoplasm, and dendrites, as reported previously (Ji et al., 1999). The number of pERK neurons peaked at 10 min but remained elevated with a slow decline for 48 hr (Fig. 1*c*). This temporal pattern differs substantially from the transient (<2 hr) ERK activation evoked by intraplantar capsaicin (Ji et al.,

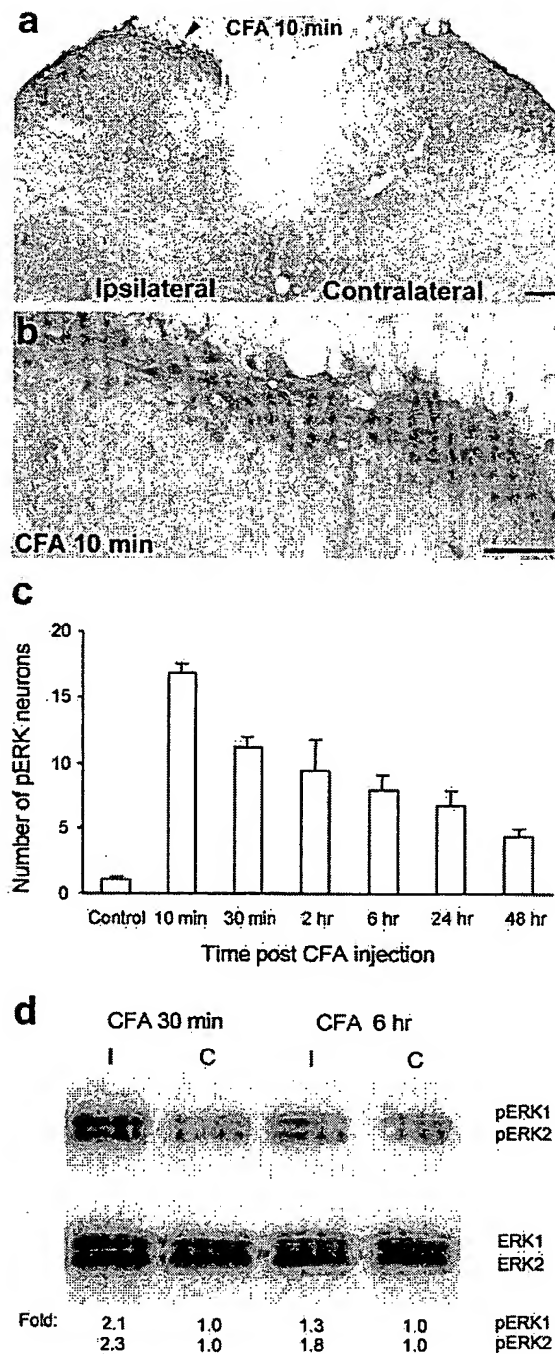


Figure 1. CFA induces a sustained activation of ERK. *a*, A low-magnification image showing induction of ERK phosphorylation in laminae I–IIo neurons of the ipsilateral spinal cord (indicated with an arrowhead) 10 min after CFA injection into a hindpaw. Scale bar, 200 μ m. *b*, A high-magnification image of *a*, showing ERK activation in the medial superficial dorsal horn of the ipsilateral spinal cord 10 min after CFA injection. Scale bar, 50 μ m. *c*, Time course of pERK induction after CFA administration measured by the number of pERK-positive neurons in the superficial (I–IIo) layers of the ipsilateral dorsal horn. Data are represented as mean \pm SEM ($n = 3$). *d*, Western blot showing increased ERK phosphorylation of both ERK1 (44 kDa) and ERK2 (42 kDa) in the ipsilateral (*I*) dorsal horn compared with contralateral (*C*) side, 30 min and 6 hr after CFA injection. The bottom panel indicates levels of total ERK1 and ERK2, as loading controls. *Fold* represents comparative levels over the corresponding contralateral side after normalizing for loading.

1999). ERK activation by CFA was confirmed by Western blot analysis. The phosphorylation level of both ERK1 (44 kDa) and ERK2 (42 kDa) increased in the ipsilateral dorsal horn compared with the contralateral side at 30 min and 6 hr (Fig. 1*d*). Because ERK is only activated in a small subset of dorsal horn neurons, Western blot is less sensitive than immunohistochemistry in detecting ERK activation in the superficial dorsal horn.

Because pERK reached a peak level very rapidly (10 min) after the CFA injection, we tested whether the CFA also produced hyperalgesia at this time. CFA (100 μ l) injected into the plantar surface of hindpaw in awake rats produced both immediate erythema and a rapid heat hyperalgesia. The paw-withdrawal latency (in seconds) decreased by 60% (from 10.8 ± 0.4 to 4.3 ± 0.7 ; $p < 0.01$; *t* test; $n = 3$) and 50% (from 9.7 ± 1.2 to 4.9 ± 1.3 ; $p < 0.05$) at 10 and 30 min, respectively. Saline-injected rats did not show any heat hypersensitivity.

Prodynorphin induction by inflammation

To investigate changes in the expression of prodynorphin in response to inflammation, we used RPA, *in situ* hybridization, and immunohistochemistry. The peripheral inflammation resulted in a substantial upregulation of prodynorphin mRNA in the ipsilateral spinal dorsal horn 24 and 48 hr after CFA injection, as detected by the RPA (Fig. 2*a*). With the *in situ* hybridization, many strongly labeled prodynorphin mRNA-labeled neurons were found both in the superficial and deep layers of the ipsilateral dorsal horn 24 hr after CFA injection, whereas on the contralateral side, only a few weakly labeled neurons were detected (Fig. 2*b*). An increase in the number of prodynorphin peptide immunoreactive neurons was also found in the superficial and deep dorsal horn 48 hr after the CFA-induced inflammation (Fig. 2*c*).

ERK activation and prodynorphin expression

We then investigated whether prodynorphin mRNA expression in the dorsal horn is regulated by ERK activation. A specific and potent MEK inhibitor, U0126 (Favata et al., 1998), was intrathecally injected twice (1 μ g), 30 min before and 6 hr after intraplantar CFA injection. This reduced the CFA-induced prodynorphin mRNA increase in the ipsilateral dorsal horn, as detected by the RPA (Fig. 3*a*). The CFA-evoked increase in the number of prodynorphin mRNA-positive neurons in the superficial dorsal horn was also decreased by U0126 (2 \times 1 μ g) without any effect on the number of labeled neurons in the deep laminae, as detected by *in situ* hybridization (Fig. 3*b,c*).

ERK activation and NK-1 expression

In agreement with previous studies (Abbadie et al., 1996, 1997), we observed increased NK-1 immunoreactivity in the superficial dorsal horn after CFA-induced inflammation using both immunohistochemistry and Western blot analysis (Fig. 4*a,c*). However, in contrast to the previous studies (Abbadie et al., 1997; Honore et al., 1999), we found more NK-1-expressing cells after inflammation compared with our control (Fig. 4*a,b*). This discrepancy is attributable to the different detection thresholds for NK-1-positive neurons; our quantification, based on standard DAB staining, did not include weakly stained cells in control animals. These cells would be detected with confocal microscopy (Abbadie et al., 1997; Honore et al., 1999). The increase in NK-1-immunoreactive neurons we detected in lamina I (Fig. 4*a*) reflects the increase in staining intensity seen by others (Abbadie et al., 1997; Honore et al., 1999) in this lamina. To explore whether ERK activation is involved in the NK-1 upregulation, the MEK

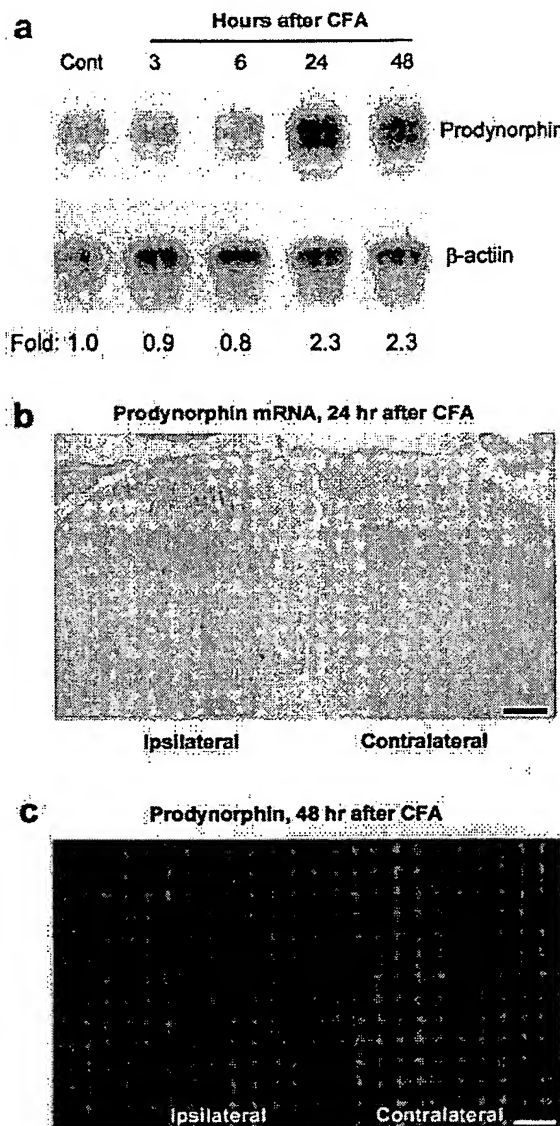


Figure 2. CFA induces prodynorphin upregulation in the dorsal horn. *a*, An RNase protection assay reveals an increase in prodynorphin mRNA in the ipsilateral dorsal horn 24 and 48 hr after CFA injection. *Fold* represents comparative levels over control after normalizing for loading. *b*, *In situ* hybridization indicates an increased expression of prodynorphin mRNA in ipsilateral superficial and deep dorsal horn neurons 24 hr after CFA. Scale bar, 50 μ m. *c*, Increased number of prodynorphin-immunoreactive neurons was induced in the ipsilateral superficial and deep dorsal horn by CFA injection at 48 hr. Scale bar, 50 μ m.

inhibitor U0126 was delivered intrathecally before the induction of inflammation via an osmotic pump ($0.5 \mu\text{g} \cdot \mu\text{l}^{-1} \cdot \text{hr}^{-1}$ for 2 d). MEK inhibition suppressed the CFA-induced elevation of NK-1-immunoreactive neurons in the superficial dorsal horn (Fig. 4*a,b*). A Western blot analysis confirmed this (Fig. 4*c*). The NK-1 antibody recognized a single band of ~ 46 kDa, which corresponds to the predicted molecular weight of cloned NK-1 receptor (Hershey and Krause, 1990).

To test whether the pERK-positive neurons and prodynorphin–NK-1-expressing neurons belong to same subset of dorsal horn cells, we performed double immunofluorescence for pERK–prodynorphin and for pERK–NK-1. Almost all prodynorphin-

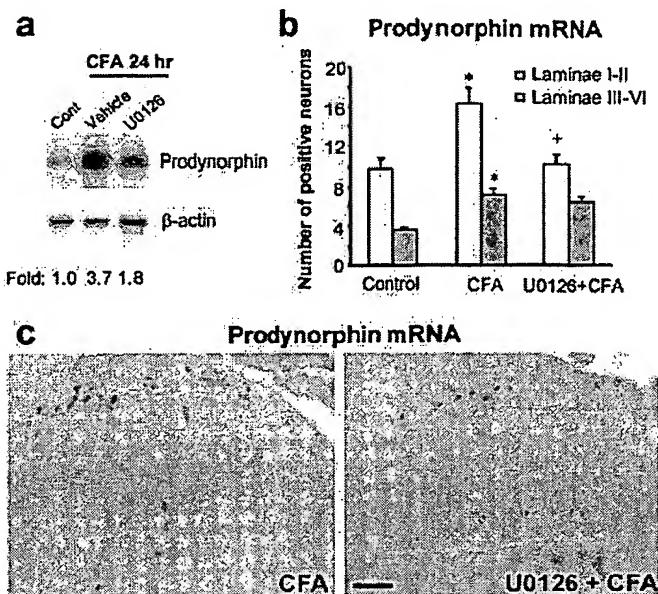


Figure 3. ERK activation regulates prodynorphin expression. *a*, Partial suppression of the CFA-induced increase in prodynorphin mRNA in the dorsal horn at 24 hr by U0126 (1 μg , intrathecally injected 30 min before and 6 hr after CFA). *Fold* represents comparative levels over control after normalizing for loading. *b*, Quantification of prodynorphin mRNA-positive neurons in laminae I–II and III–VI of the ipsilateral dorsal horn 24 hr after CFA injection. * $p < 0.001$, compared with control; + $p < 0.001$, compared with CFA ($n = 4$). *c*, *In situ* hybridization showing an inhibition of the CFA-induced increase in prodynorphin mRNA-labeled neurons in the superficial dorsal horn by U0126 24 hr after CFA injection. Scale bar, 50 μ m.

and NK-1-positive neurons in the superficial dorsal horn also express pERK 24 hr after CFA injection (Fig. 5).

ERK activation and persistent inflammatory pain

To examine the functional consequences of ERK activation and its downstream effects on prodynorphin and NK-1 upregulation, we tested whether inhibition of ERK activation modified inflammatory pain hypersensitivity. Intrathecal administration of U0126 (1 μg) into non-inflamed animals, like another MEK inhibitor PD 98059 (Ji et al., 1999), produced no significant change in basal pain sensitivity measured in terms of mechanical withdrawal threshold (108% of the vehicle control) and heat withdrawal latency (113% of vehicle control), when tested 30 min after the administration. However, intrathecal administration of U0126 via an osmotic pump ($0.5 \mu\text{g} \cdot \mu\text{l}^{-1} \cdot \text{hr}^{-1}$), started before the CFA injection and maintained for 48 hr, significantly reduced the inflammation-induced heat and mechanical hypersensitivity measured at 24 and 48 hr (Fig. 6*a,b*).

Acute pain hypersensitivity (10–60 min after an intraplantar formalin injection) is reduced by inhibition of ERK activation, presumably by preventing post-translational changes (Ji et al., 1999). ERK activation by CFA could conceivably contribute to inflammatory pain hypersensitivity by either maintaining ongoing post-translational changes or inducing transcription of genes, such as prodynorphin and NK-1. In the former case, blocking ERK activation in established inflammation would be expected to reduce the pain hypersensitivity within tens of minutes as the substrates were dephosphorylated. If the contribution of ERK activation were through transcription, however, inhibiting ERK activation would be expected to have no immediate effect but

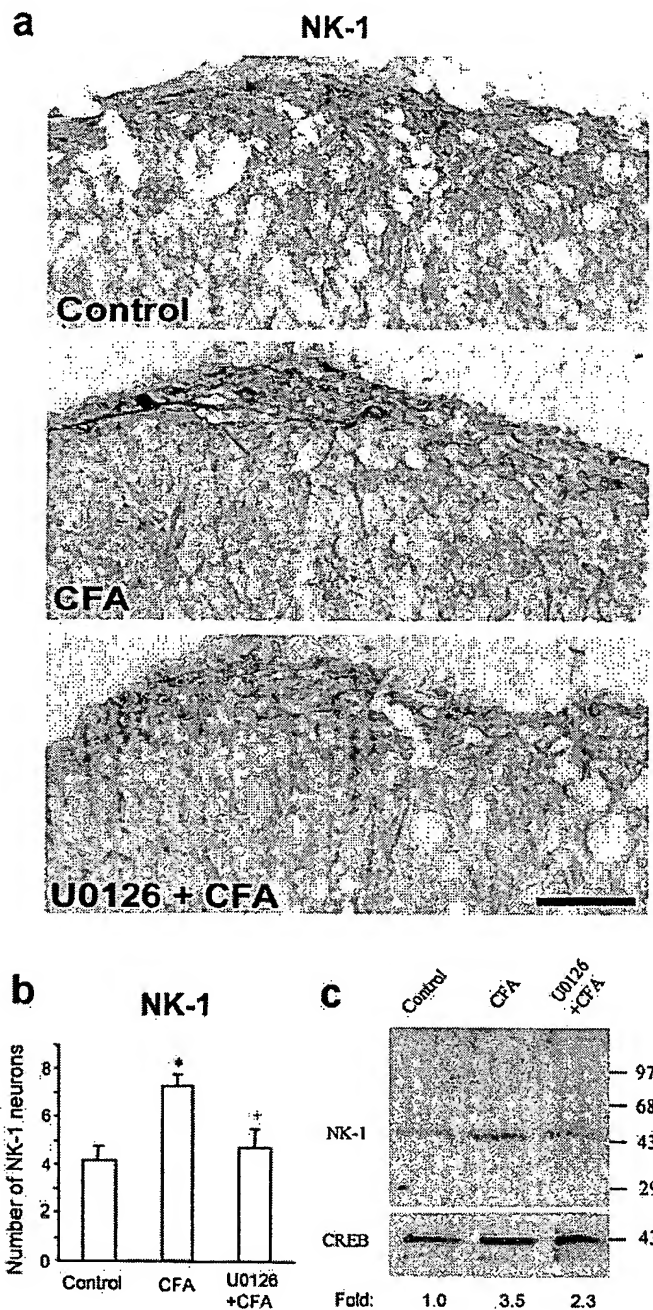


Figure 4. ERK activation regulates NK-1 expression. *a*, Suppression of the CFA-induced increase in NK-1 immunoreactivity in the medial superficial dorsal horn at 48 hr by U0126 delivered via an osmotic pump. Scale bar, 50 μ m. *b*, Quantification of the numbers of NK-1 neurons in laminae I–IIo of the ipsilateral dorsal horn 48 hr after CFA injection. * p < 0.001, compared with control; + p < 0.001, compared with CFA (n = 5). *c*, Western blot indicates that the CFA-induced NK-1 increase in the dorsal horn at 24 hr is inhibited by U0126 (1 μ g, intrathecally injected 30 min before and 6 hr after CFA injection). CREB, a constitutively expressed protein, was used as a loading control. *Fold* represents comparative levels over control after normalizing for loading.

rather a delayed effect. To test this, we intrathecally injected U0126 (1 μ g) in rats with established inflammation (24 hr after CFA injection) and tested pain hypersensitivity 30 min, 6 hr, and 24 hr after the U0126 injection. Neither heat hyperalgesia nor

mechanical allodynia was significantly affected by such post-treatment when tested at 30 min (Fig. 7*a,b*). However, the post-treatment decreased heat hyperalgesia at 24 hr and mechanical allodynia at 6 hr (Fig. 7*a,b*), indicating a long-latency contribution of ERK activation to the maintenance of persistent inflammatory pain.

DISCUSSION

ERK activation in nociceptive dorsal horn neurons

Peripheral inflammation induced, after a short latency, a persistent activation of ERK in laminae I–IIo neurons of the ipsilateral superficial dorsal horn. Inhibition of this activation, using an MEK inhibitor, blocked elevation of prodynorphin and NK-1 expression in this particular subset of dorsal horn neurons, as well as reduced inflammatory pain hypersensitivity. pERK was induced by CFA in the same subset of dorsal horn neurons that express prodynorphin and NK-1. Many NK-1- and dynorphin-expressing neurons in lamina I are projection neurons (Nahin et al., 1989; Marshall et al., 1996). Projection neurons in lamina I exhibit an enlargement of their receptive fields after CFA-induced inflammation (Dubner and Ruda, 1992). A targeted loss of NK-1-expressing neurons in lamina I has been shown to abolish inflammatory pain (Nichols et al., 1999). These studies indicate a critical role for the aforementioned superficial neurons in the reaction of the CNS to inflammation. A particular subset of C-nociceptor fibers, those that are NGF-responsive, and TrkA- and neuropeptide-expressing, terminate in laminae I and IIo, in an area overlapping the neurons that show ERK activation. Another subset of C-fibers, those that respond to the glial cell line-derived neurotrophic factor family of growth factors and are characterized by selective binding of the IB4 lectin, terminate in lamina IIo (Averill et al., 1995; Molliver et al., 1997). The neurons these fibers contact, many of which contain PKC γ (Malmberg et al., 1997), do not show ERK activation after capsaicin or CFA injection (R.-R. Ji et al., unpublished observations). The role of ERK in regulating pain hypersensitivity is, therefore, restricted to a particular subset of nociceptive dorsal horn neurons, only those located in laminae I–IIo, and this activation is likely to reflect activation only of TrkA-expressing C-fibers.

Transcriptional regulation in response to ERK activation

pERK was found in the nucleus of neurons after CFA injection (Fig. 1*a*), pointing to a possible transcriptional role for the activated kinase. Unlike the transient activation (lasting <2 hr) induced after capsaicin injection (Ji et al., 1999), CFA produced persistent ERK activation (Fig. 1*c*). The sustained ERK activation after CFA injection is associated with persistent upregulation of prodynorphin mRNA (lasting >48 hr) (Fig. 2*a*), whereas the transient pERK induced by capsaicin is associated with a shorter-lasting upregulation of prodynorphin mRNA (<6 hr; R.-R. Ji and C. J. Woolf, unpublished observation). ERK activation is likely to regulate the expression of prodynorphin and NK-1, both of which are CRE-containing genes, via CREB phosphorylation. CREB is required for dopamine-induced expression of prodynorphin in striatal neurons (Cole et al., 1995) and is phosphorylated in NK-1 receptor-expressing neurons after noxious stimulation (Anderson and Seybold, 2000). Interestingly, a CRE site has been shown to mediate a long-term sensitization of nociceptive neurons in *Aplysia* (Lewin and Walters, 1999).

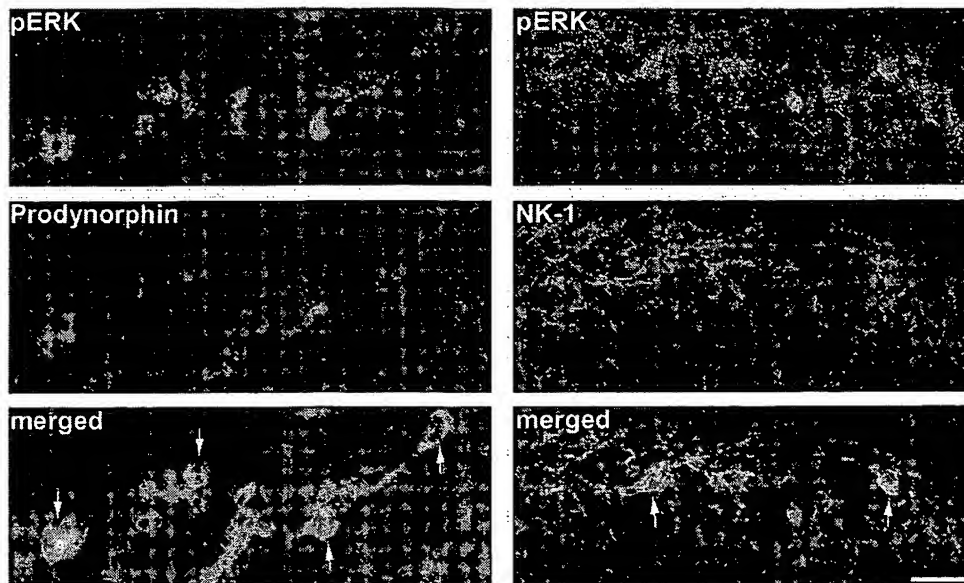


Figure 5. ERK is activated in a subset of prodynorphin- and NK-1-expressing neurons. pERK (red) is primarily colocalized with prodynorphin (green; left) and NK-1 (green; right) in the medial superficial dorsal horn 24 hr after CFA injection. Arrows indicate double-labeled neurons. Scale bar, 20 μ m.

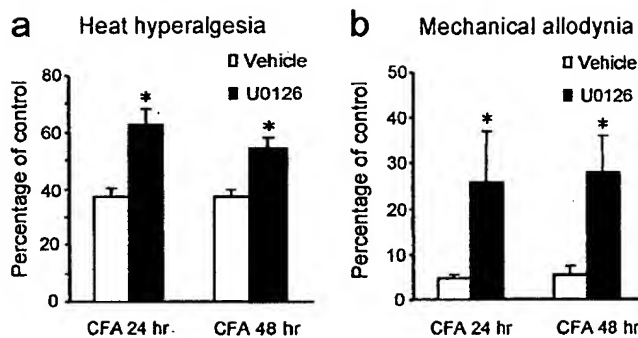


Figure 6. Sustained infusion of an MEK inhibitor reduces CFA-induced inflammatory pain. The MEK inhibitor U0126 delivered by osmotic pump ($0.5 \mu\text{g} \cdot \mu\text{l}^{-1} \cdot \text{hr}^{-1}$) before CFA injection reduces thermal hyperalgesia (a) and mechanical allodynia (b) 24 and 48 hr after CFA injection. These were measured by paw-withdrawal latency and paw-withdrawal threshold, respectively, and expressed as percentage of pre-CFA baseline measurements of vehicle control (50% DMSO). * $p < 0.01$, compared with corresponding vehicle control ($n = 8$).

ERK activation and inflammatory pain hypersensitivity

U0126 is a potent and selective MEK inhibitor (Favata et al., 1998), achieving inhibition of ERK activation even in the face of strong activators, such as phorbol esters, whereas other major signal transduction pathways are not affected (Roberson et al., 1999). This inhibitor has not only been used in *in vitro* studies (Roberson et al., 1999) but also in *in vivo* studies (Han and Holtzman, 2000; Kuroki et al., 2001). At the dose we used, we did not find obvious toxicity of this inhibitor, animals behaved normally, and locomotion was unaffected. Although basal pain sensitivity was not affected by the inhibitor, persistent inflammatory pain was reduced. This could conceivably result from either preventing some post-translational change mediated by the ERK signal transduction pathway, as for acute pain hypersensitivity (Ji et al., 1999), or a reduction in transcription of target genes, such as prodynorphin and NK-1. The involvement suggested by a number of different studies, of both the NK-1 receptor and prodynorphin in pain mechanisms, together with their regulation by ERK activation, is compatible with a hypothesis that ERK

activation after inflammation contributes to pain hypersensitivity by regulating gene transcription. The temporal profile of the effect of blocking ERK activation represents additional support. The acute pain hypersensitivity established within minutes of intraplantar formalin can be reduced by preventing ERK activation (Ji et al., 1999), an effect that is too quick (<1 hr) to be mediated by an inhibition of transcription and is likely therefore to represent some post-translational change downstream of the activated ERK. At present, it is not clear what the substrate for such post-translational change is, but it may well be an ion channel or receptor, such as the NMDA or AMPA receptor (Woolf and Salter, 2000). Such post-translational changes underlie the induction and maintenance of central sensitization, a use-dependent plasticity that outlasts its initiating stimulus by tens of minutes (Woolf, 1983; Woolf and Wall, 1986). If inflammatory hypersensitivity were a manifestation only of a central sensitization maintained by ongoing afferent input from the inflamed tissue, then blocking the initiation of central sensitization, by inhibiting an ERK-mediated phosphorylation, should reduce the hypersensitivity over a period of tens of minutes as the key proteins were dephosphorylated. The fact that MEK inhibition during established inflammation had no immediate effect, but rather only reduced mechanical and thermal hypersensitivity 6–24 hr later, argues that the role of ERK activation may well be via transcriptional regulation.

Dynorphin and NK-1 contribute to inflammatory pain hypersensitivity

A temporal correlation has been shown previously between the expression of prodynorphin and NK-1 and development of inflammatory pain hypersensitivity (Iadarola et al., 1988; Abbadié et al., 1996). Unlike other opioid peptides, intrathecal injection of dynorphin does not produce analgesia (Laughlin et al., 1997). Dynorphin has actually been found to be pronociceptive in some pathological pain states. For example, dynorphin A antiserum reduces the pain hypersensitivity after nerve injury (Nichols et al., 1997; Wegert et al., 1997; Malan et al., 2000), and neuropathic pain does not persist in prodynorphin knock-out mice (Wang et al., 2001). The pronociceptive action of dynorphin appears to be the result of its nonopiod actions (Laughlin et al., 1997), includ-

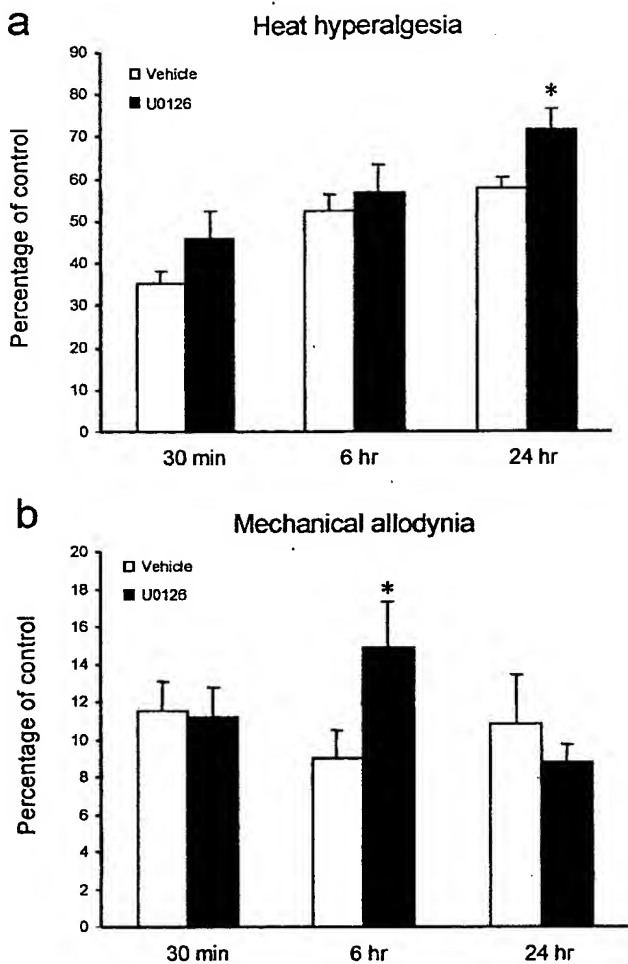


Figure 7. Post-treatment with an MEK inhibitor has a delayed effect on inflammatory pain. U0126 (1 μ g) or vehicle (10% DMSO) was intrathecally administered 24 hr after CFA injection. Heat hyperalgesia (a) and mechanical allodynia (b) were tested 30 min, 6 hr, and 24 hr after the administration of the U0126. * p < 0.05, compared with corresponding vehicle control (n = 10). The data are expressed as percentage of pre-CFA baseline measurements of vehicle control.

ing an activation of NMDA receptors sufficient to induce excitotoxicity (Dubner and Ruda, 1992).

Inflammation induces NK-1 receptor upregulation in dorsal horn neurons and upregulation of its ligand, the neuropeptide substance P, in primary afferent neurons (Noguchi et al., 1988; Abbadie et al., 1996) (also see Woolf et al., 1998). NK-1 antagonists have been shown to reduce inflammatory pain (both hyperalgesia and mechanical allodynia) in several different animal models (Neumann et al., 1996; Ren et al., 1996; Traub, 1996; Ma et al., 1998; Woolf et al., 1998; Trafton and Basbaum, 2000), including NK-1 knock-out mice (De Felipe et al., 1998). The increased amount and internalization of the NK-1 receptor on the dendrites of dorsal horn neurons in response to noxious and innocuous stimuli after inflammation indicates that this receptor is activated by substance P in response to peripheral stimuli (Abbadie et al., 1997).

Conclusion

ERK activation has two roles in nociceptive plasticity in the dorsal horn: a short-latency contribution to acute noxious

stimulus-induced central sensitization and an involvement in the induction and maintenance of inflammatory pain. The involvement of pERK in peripheral inflammatory pain hypersensitivity may be contributed to by its regulation of prodynorphin and NK-1 expression, as well as other target genes. ERK activation plays, therefore, a pivotal role in the functional plasticity and chemical phenotype of a group of neurons in the superficial dorsal horn, determining the activation of particular effector responses to divergent inputs, which in turn contribute to altered sensibility.

REFERENCES

Abbadie C, Brown JL, Mantyh PW, Basbaum AI (1996) Spinal cord substance P receptor immunoreactivity increases in both inflammatory and nerve injury models of persistent pain. *Neuroscience* 70:201–209.

Abbadie C, Trafton J, Liu H, Mantyh PW, Basbaum AI (1997) Inflammation increases the distribution of dorsal horn neurons that internalize the neurokinin-1 receptor in response to noxious and non-noxious stimulation. *J Neurosci* 17:8049–8060.

Anderson LE, Seybold VS (2000) Phosphorylated cAMP response element binding protein increases in neurokinin-1 receptor-immunoreactive neurons in rat spinal cord in response to formalin-induced nociception. *Neurosci Lett* 283:29–32.

Atkins CM, Selcher JC, Petraitis JJ, Trzaskos JM, Sweatt JD (1998) The MAPK cascade is required for mammalian associative learning. *Nat Neurosci* 1:602–609.

Averill S, McMahon SB, Clary DO, Reichardt LF, Priestley JV (1995) Localization of trkB receptors in chemically identified subgroups of adult rat sensory neurons. *Eur J Neurosci* 7:1484–1494.

Cole RL, Konradi C, Douglass J, Hyman SE (1995) Neuronal adaptation to amphetamine and dopamine: molecular mechanisms of prodynorphin gene regulation in rat striatum. *Neuron* 14:813–823.

De Felipe C, Herrero JF, O'Brien JA, Palmer JA, Doyle CA, Smith AJ, Laird JM, Belmonte C, Cervero F, Hunt SP (1998) Altered nociception, analgesia and aggression in mice lacking the receptor for substance P. *Nature* 392:394–397.

Dubner R, Ruda MA (1992) Activity-dependent neuronal plasticity following tissue injury and inflammation. *Trends Neurosci* 15:96–103.

English JD, Sweatt JD (1997) A requirement for the mitogen-activated protein kinase cascade in hippocampal long term potentiation. *J Biol Chem* 272:19103–19106.

Favata M, Horiuchi KY, Manos EJ, Daulerio AJ, Stradley DA, Feeser WS, Van Dyk DE, Pitts WJ, Earl RA, Hobbs F, Copeland RA, Magolda RL, Scherle PA, Trzaskos JM (1998) Identification of a novel inhibitor of mitogen-activated protein kinase kinase. *J Biol Chem* 273:18623–18632.

Han BH, Holtzman DM (2000) BDNF protects the neonatal brain from hypoxic-ischemic injury in vivo via the ERK pathway. *J Neurosci* 20:5775–5781.

Hargreaves K, Dubner R, Brown F, Flores C, Joris J (1988) A new and sensitive method for measuring thermal nociception in cutaneous hyperalgesia. *Pain* 32:77–88.

Hershey AD, Krause JE (1990) Molecular characterization of a functional cDNA encoding the rat substance P receptor. *Science* 247:958–962.

Hershey AD, Dykema PE, Krause JE (1991) Organization, structure and expression of the gene encoding the rat substance P receptor. *J Biol Chem* 266:4366–4374.

Honore P, Menning PM, Rogers SD, Nichols ML, Basbaum AI, Besson JM, Mantyh PW (1999) Spinal substance P receptor expression and internalization in acute, short-term, and long-term inflammatory pain states. *J Neurosci* 19:7670–7678.

Hunt SP, Pini A, Evan G (1987) Induction of c-fos-like protein in spinal cord neurons following sensory stimulation. *Nature* 328:632–634.

Hylden JL, Nahin RL, Traub RJ, Dubner R (1991) Effects of spinal kappa-opioid receptor agonists on the responsiveness of nociceptive superficial dorsal horn neurons. *Pain* 44:187–193.

Iadarola MJ, Brady LS, Draisce G, Dubner R (1988) Enhancement of dynorphin gene expression in spinal cord following experimental inflammation: stimulus specificity, behavioral parameters and opioid receptor binding. *Pain* 35:313–326.

Impey S, Obrietan K, Wong ST, Poser S, Yano S, Wayman G, Deloulme JC, Chan G, Storm DR (1998) Cross talk between Erk and PKA is required for Ca^{2+} stimulation of CREB-dependent transcription and Erk nuclear translocation. *Neuron* 21:869–883.

Impey S, Obrietan K, Storm DR (1999) Making new connections: role of ERK/MAP kinase signaling in neuronal plasticity. *Neuron* 23:11–14.

Ji RR, Rupp F (1997) Phosphorylation of transcription factor CREB in rat spinal cord after formalin-induced hyperalgesia: relationship to c-fos induction. *J Neurosci* 17:1776–1785.

Ji RR, Woolf CJ (2001) Neuonal plasticity and signal transduction in nociceptive neurons: Implications for the initiation and maintenance of pathological pain. *Neurobiol Dis* 8:1–10.

Ji RR, Zhang X, Wiesenfeld-Hallin Z, Hokfelt T (1994) Expression of neuropeptide Y and neuropeptide Y (Y1) receptor mRNA in rat spinal cord and dorsal root ganglia following peripheral tissue inflammation. *J Neurosci* 14:6423–6434.

Ji RR, Zhang X, Nilsson S, Wiesenfeld-Hallin Z, Hokfelt T (1995) Central and peripheral response to galanin induced by inflammation. *Neuroscience* 68:563–576.

Ji RR, Schlaepfer TE, Aizenman CD, Qiu D, Hung JC, Rupp F (1998) Repetitive transcranial magnetic stimulation activates specific neural regions. *Proc Natl Acad Sci USA* 95:15635–15640.

Ji RR, Baba H, Brenner G, Woolf CJ (1999) Nociceptive-specific activation of ERK in spinal neurons contributes to pain hypersensitivity. *Nat Neurosci* 2:1114–1119.

Kuroki Y, Fukushima K, Kanda Y, Mizuno K, Watanabe Y (2001) Neuroprotection by estrogen via extracellular signal-regulated kinase against quinolinic acid-induced cell death in the rat hippocampus. *Eur J Neurosci* 13:472–476.

Laughlin TM, Vanderah TW, Lashbrook J, Nichols ML, Ossipov M, Porreca F, Wilcox GL (1997) Spinally administered dynorphin A produces long-lasting allodynia: involvement of NMDA but not opioid receptors. *Pain* 72:253–260.

Lewin MR, Walters ET (1999) Cyclic GMP pathway is critical for inducing long-term sensitization of nociceptive sensory neurons. *Nat Neurosci* 2:18–23.

Ma QP, Allochorne AJ, Woolf CJ (1998) Morphine, the NMDA receptor antagonist MK801 and tachykinin NK1 receptor antagonist RP67580 attenuate the development of inflammation-induced progressive tactile hypersensitivity. *Pain* 77:49–57.

Malan TP, Ossipov MH, Gardell LR, Ibrahim M, Bian D, Lai J, Porreca F (2000) Extraterritorial neuropathic pain correlates with multisegmental elevation of spinal dynorphin in nerve-injured rats. *Pain* 86:185–194.

Malmborg AB, Chen C, Susumu T, Basbaum AI (1997) Preserved acute pain and reduced neuropathic pain in mice lacking PKC gamma. *Science* 278:279–283.

Mannion RJ, Costigan M, Decosterd I, Amaya F, Ma QP, Holstege JC, Ji RR, Acheson A, Lindsay RM, Wilkinson GA, Woolf CJ (1999) Brain-derived neurotrophic factor-a centrally acting modulator of tactile stimulus-induced inflammatory pain hypersensitivity. *Proc Natl Acad Sci USA* 96:9385–9390.

Marshall GE, Shehab SA, Spike RC, Todd AJ (1996) Neurokinin-1 receptors on lumbar spinothalamic neurons in the rat. *Neuroscience* 72:255–263.

McCarsson KE, Krause JE (1994) NK-1 and NK-3 type tachykinin receptor mRNA expression in the rat spinal cord dorsal horn is increased during adjuvant or formalin-induced nociception. *J Neurosci* 14:712–720.

Messersmith DJ, Kim DJ, Iadarola MJ (1998) Transcription factor regulation of prodynorphin gene expression following rat hindpaw inflammation. *Mol Brain Res* 53:260–269.

Molliver DC, Wright DE, Leitner ML, Parsadanian AS, Doster K, Wen D, Yan Q, Snider WD (1997) IB4-binding DRG neurons switch from NGF to GDNF dependence in early postnatal life. *Neuron* 19:849–861.

Nahin RL, Hyden JL, Iadarola MJ, Dubner R (1989) Peripheral inflammation is associated with increased dynorphin immunoreactivity in both projection and local circuit neurons in the superficial dorsal horn of the rat lumbar spinal cord. *Neurosci Lett* 96:247–252.

Neumann S, Doubell TP, Leslie T, Woolf CJ (1996) Inflammatory pain hypersensitivity mediated by phenotypic switch in myelinated primary sensory neurons. *Nature* 384:360–364.

Nichols ML, Lopez Y, Ossipov MH, Bian D, Porreca F (1997) Enhancement of the antiallodynic and antinociceptive efficacy of spinal morphine by antisera to dynorphin A (1–13) or MK-801 in a nerve-ligation model of peripheral neuropathy. *Pain* 69:317–322.

Nichols ML, Allen BJ, Rogers SD, Ghilardi JR, Honore P, Luger NM, Finke MP, Li J, Lappi DA, Simone DA, Mantyh PW (1999) Transmission of chronic nociception by spinal neurons expressing the substance P receptor. *Science* 286:1558–1561.

Noguchi K, Morita Y, Kiyama H, Ono K, Tohyama MA (1988) Noxious stimulus induces the preprotachykinin-A gene expression in the rat dorsal root ganglion: a quantitative study using *in situ* hybridization histochemistry. *Brain Res* 464:31–35.

Obrietan K, Impey S, Smith D, Athos J, Storm DR (1999) Circadian regulation of cAMP response element-mediated gene expression in the suprachiasmatic nuclei. *J Biol Chem* 274:17748–17756.

Ren K, Iadarola MJ, Dubner R (1996) An isobolographic analysis of the effect of N-methyl-D-aspartate and NK1 tachykinin receptor antagonists on inflammatory hyperalgesia in the rat. *Br J Pharmacol* 117:196–202.

Roberson ED, English JD, Adams JP, Selcher JC, Kondratick C, Sweat JD (1999) The mitogen-activated protein kinase cascade couples PKA and PKC to cAMP response element binding protein phosphorylation in area CA1 of hippocampus. *J Neurosci* 19:4337–4348.

Ruda MA, Iadarola MJ, Cohen LV, Young WS (1988) *In situ* hybridization histochemistry and immunohistochemistry reveal an increase in spinal dynorphin biosynthesis in rat model of peripheral inflammation and hyperalgesia. *Proc Natl Acad Sci USA* 85:622–626.

Samad A, Moore KA, Sapirstein A, Bilezikian S, Allchorne A, Poole S, Bonventre JV, Woolf CJ (2001) An interleukin-1 β -mediated induction of Cox-2 in the central nervous system contributes to inflammatory pain hypersensitivity. *Nature* 22:471–475.

Schafer MK, Nohr D, Krause JE, Weihe E (1993) Inflammation-induced upregulation of NK1 receptor mRNA in dorsal horn neurons. *NeuroReport* 4:1007–1010.

Sgambato V, Pages C, Rogard M, Besson MJ, Caboche J (1998) Extracellular signal-regulated kinase (ERK) controls immediate early gene induction on corticostrital stimulation. *J Neurosci* 18:8814–8825.

Stein C, Millan MJ, Herz A (1988) Unilateral inflammation of the hindpaw in rats as a model of prolonged noxious stimulation: alterations in behavior and nociceptive thresholds. *Pharmacol Biochem Behav* 31:445–451.

Trafton JA, Basbaum AI (2000) The contribution of spinal cord neurokinin-1 receptor signaling to pain. *J Pain Suppl* 1:57–65.

Traub RJ (1996) The spinal contribution of substance P to the generation and maintenance of inflammatory hyperalgesia in the rat. *Pain* 67:151–161.

Wang Z, Gardell LR, Ossipov MH, Vanderah TW, Brennan MB, Hochgeschwender U, Hruby VJ, Malan Jr TP, Lai J, Porreca F (2001) Pronociceptive actions of dynorphin maintain chronic neuropathic pain. *J Neurosci* 21:1779–1786.

Wegert S, Ossipov MH, Nichols ML, Bian D, Vanderah TW, Malan TP Jr, Porreca F (1997) Differential activities of intrathecal MK-801 or morphine to alter responses to thermal and mechanical stimuli in normal or nerve-injured rats. *Pain* 71:57–64.

Winder DG, Martin KC, Muzzio IA, Rohrer D, Chruscinski A, Kobilka B, Kandel ER (1999) ERK plays a regulatory role in induction of LTP by theta frequency stimulation and its modulation by b-adrenergic receptors. *Neuron* 24:715–726.

Wisden W, Errington ML, Williams S, Dunnett SB, Waters C, Hitchcock D, Evan G, Bliss TVP, Hunt SP (1990) Differential expression of immediate early genes in the hippocampus and spinal cord. *Neuron* 4:603–614.

Woolf CJ (1983) Evidence for a central component of post-injury pain hypersensitivity. *Nature* 306:686–688.

Woolf CJ, Costigan M (1999) Transcriptional and post-translational plasticity and the generation of inflammatory pain. *Proc Natl Acad Sci USA* 96:7723–7730.

Woolf CJ, Salter MW (2000) Neuronal plasticity: increasing the gain in pain. *Science* 288:1765–1769.

Woolf CJ, Wall PD (1986) Relative effectiveness of C primary afferent fibers of different origins in evoking a prolonged facilitation of the flexor reflex in the rat. *J Neurosci* 6:1433–1442.

Woolf CJ, Mannion RJ, Neumann S (1998) Null mutations lacking substance: elucidating pain mechanisms by genetic pharmacology. *Neuron* 20:1063–1066.

Xia Z, Dudek H, Miranti CK, Greenberg ME (1996) Calcium influx via the NMDA receptor induces immediate early gene transcription by a MAPK/ERK-dependent mechanism. *J Neurosci* 16:5425–5436.

Xing J, Ginty DD, Greenberg ME (1996) Coupling of the RAS-MAPK pathway to gene activation by RSK2, a growth factor-regulated CREB kinase. *Science* 273:959–963.

Inorganic Lead Activates the Mitogen-Activated Protein Kinase Kinase-Mitogen-Activated Protein Kinase-p90^{RSK} Signaling Pathway in Human Astrocytoma Cells via a Protein Kinase C-Dependent Mechanism

HAILING LU, MARINA GUZZETTI, and LUCIO G. COSTA

Department of Environmental, University of Washington, Seattle, Washington (H.L., M.G., L.G.C.); and Department of Pharmacology and Physiology, University of Roma "La Sapienza", Roma, Italy (L.G.C.).

Received October 4, 2001; accepted November 14, 2001

This article is available online at <http://jpet.aspetjournals.org>

ABSTRACT

We have previously reported that lead acetate activates protein kinase C α (PKC α) and induces DNA synthesis in human 1321N1 astrocytoma cells. In this study, we investigated the ability of lead to activate the mitogen-activated protein kinase (MAPK) cascade. We found that exposure to lead acetate (1–50 μ M) resulted in concentration- and time-dependent activation of MAPK (extracellular signal responsive kinase 1/2), as shown by increased phosphorylation and increased kinase activity. This effect was significantly reduced by the PKC-specific inhibitor bisindolylmaleimide (GF109203X), by down-regulation of PKC with 12-O-tetradecanoyl-phorbol 13-acetate, by a pseudosubstrate to PKC α , and by selective down-regulation of PKC α by prior lead exposure.

Lead was also shown to activate MAPK kinase (MEK1/2), and this effect was mediated by PKC. Two MEK inhibitors, 2-(2'-amino-3'-methoxyphenol)-oxanaphthalen-4-one (PD98059) and 1,4-diamino-2,3-dicyano-1,4-bis[2-aminophenylthio]butadiene (UO126), blocked lead-induced MAPK activation and inhibited lead-induced DNA synthesis, as measured by incorporation of [$\text{methyl-}^3\text{H}$]thymidine into cell DNA. The 90 kDa ribosomal S6 protein kinase, p90^{RSK}, a substrate of MAPK, was also found to be activated by lead in a PKC- and MAPK-dependent manner. Stimulation of DNA synthesis by lead in astrocytoma cells may be of interest in light of the observed association between exposure to lead and an increased risk of astrocytomas.

Lead is a widespread environmental pollutant, the major health concerns of which relate to its developmental neurotoxicity (Ballinger et al., 1987). Lead is also classified by the International Agency for Research on Cancer as a group 2B carcinogen (possible human carcinogen). In animals, there is evidence of lead inducing renal adenomas, lung adenomas, and cerebral gliomas (ATSDR, 1999). Excess of renal (Steenland et al., 1992), lung (Anttila et al., 1995), and brain (particularly astrocytomas) (Anttila et al., 1996) cancers, have also been found in epidemiological studies in lead-exposed workers. As lead-induced gene mutations in mammalian cells have been usually observed only at high toxic concentrations (Zelikoff et al., 1988), such genotoxicity may not be the result of direct damage to DNA but may occur by indirect mechanisms, such as inhibition of DNA repair (Hartwig,

1994). There is, however, evidence that lead can increase proliferation of rat and mouse kidney cells (Choe and Richter, 1974), rat liver cells (Liu et al., 1997), vascular smooth-muscle cells (Fujiwara et al., 1995), and spleen cells (Razani-Boroujerdi et al., 1999), suggesting that it may act as a tumor promoter.

The established receptors for potent tumor promoters, such as the phorbol esters, are the classical and novel isozymes of protein kinase C (PKC) (Mellor and Parker, 1998). A large body of evidence exists which indicates that lead can activate PKC in different cellular systems and under different experimental conditions (reviewed in Costa, 1998). We have recently found that lead can stimulate DNA synthesis and cell cycle progression in human astrocytoma cells and that this effect is due to a selective activation of PKC α by lead (Lu et al., 2001). However, the signal transduction pathway leading from PKC α activation to DNA synthesis remains to be elucidated.

This study was supported in part by Grants ES 07033 and ES 04696 from the National Institute of Environmental Health Sciences and Grant AA 08154 from the National Institute on Alcohol Abuse and Alcoholism.

ABBREVIATIONS: PKC, protein kinase C; MAPK, mitogen-activated protein kinase; ERK, extracellular signal responsive kinase; MEK, mitogen-activated protein kinase kinase; p90^{RSK}, 90 kDa ribosomal S6 kinases; FBS, fetal bovine serum; GST, glutathione S-transferase; TPA, 12-O-tetradecanoyl-phorbol 13-acetate; GF109203X, bisindolylmaleimide; PDGF, platelet-derived growth factor; PD98059, 2-(2'-amino-3'-methoxyphenol)-oxanaphthalen-4-one; UO126, 1,4-diamino-2,3-dicyano-1,4-bis[2-aminophenylthio]butadiene; 70^{S6K}, 70 kDa ribosomal S6 kinases; PI3K, phosphatidylinositol 3-kinase; LY294002, 2-(4-morpholino)-8-phenyl-4H-1-benzopyran-4-one.

In the present study, we investigated the ability of lead to activate the MAPK cascade and the role of PKC in this signal transduction pathway. MAPKs are a family of protein kinases playing a central role in signal transduction and thought to mediate diverse processes ranging from transcription of protooncogenes to programmed cell death (Derkinderen et al., 1999; Pearson et al., 2000). The best studied MAPK are ERK1 and ERK2 (p42 and p44 MAPK), which are activated by mitogens and play a central role in cell proliferation (Ferrell, 1996). ERK1/2 are regulated upstream by a MAPK kinase (MEK1/2), which in turn is activated by Raf kinases, particularly Raf-1 (Ferrell, 1996; Derkinderen et al., 1999). PKC α has been shown to activate Raf-1 kinase, either by direct phosphorylation or by modulating its membrane association (Kolch et al., 1993; Schonwasser et al., 1998). Activated ERK1/2 translocate to the nucleus where they phosphorylate and activate other kinases, transcription factors, and other target proteins (Derkinderen et al., 1999; Pearson et al., 2000) including the family of p90 kDa ribosomal S6 kinases (p90^{RSK}), which seem to play a relevant role in cell proliferation (Frodin and Gammeltoft, 1999). The aim of the present study was, therefore, to investigate whether lead would stimulate this cascade of signal transduction events (PKC α \rightarrow Raf-1 \rightarrow MEK1/2 \rightarrow ERK1/2 \rightarrow p90^{RSK}) leading to proliferation of human astrocytoma cells.

Experimental Procedures

Materials. Dulbecco's modified Eagle's medium, fetal bovine serum (FBS), penicillin/streptomycin, and trypsin were purchased from Invitrogen (Carlsbad, CA). [*methyl*-³H]Thymidine (6.7 Ci/mmol) was purchased from PerkinElmer Life Sciences (Boston, MA). Anti-phosphoERK1/ERK2 antibody and horseradish peroxidase-conjugated donkey anti-rabbit IgG antibody were obtained from Promega (Madison, WI). Anti-phospho-Elk-1, anti-phospho-MEK1/2, anti-phospho-p90^{RSK} (Ser381), and immobilized anti-phospho-MAPK antibodies were obtained from New England Biolabs (Beverly, MA). Anti-ERK1/ERK2 antibody was purchased from Santa Cruz Biotechnology (Santa Cruz, CA). The protease inhibitor cocktail tablets were obtained from Roche Molecular Biochemicals (Indianapolis, IN). The myristoylated PKC peptide inhibitor, based on the pseudosubstrate region for classical PKC (Myr-Arg-Phe-Ala-Arg-Lys-Gly-Ala-Leu-Arg-Gln-Lys-Asn-Val), was purchased from Promega. Lead acetate and all other chemicals were purchased from Sigma Chemical Co. (St. Louis, MO). Lead acetate was dissolved in deionized water and prepared as a 2 mM stock solution.

Cell Culture. The human astrocytoma cell line 1321N1 (kindly donated by Dr. J. H. Brown, University of California at San Diego) was maintained in low-glucose Dulbecco's modified Eagle's medium, supplemented with 5% FBS, 100 U/ml penicillin G, and 100 μ g/ml streptomycin in 75-cm² flasks under a humidified atmosphere of 5% CO₂/95% air at 37°C. Cells were subcultured every 7 days, and the growth medium was changed every 3 or 4 days. Cells were seeded in 24-well plates at the density of 2.5×10^4 /ml for the proliferation experiments and in 100-mm dishes at the density of 1×10^5 /ml for Western blot experiments.

Measurement of DNA Synthesis. Incorporation of [*methyl*-³H]thymidine into cell DNA was measured as described previously (Guizzetti et al., 1996). Briefly, cells were seeded at the density of 2.5×10^4 /ml in 24-well plates. After 4 days in medium supplemented with 5% FBS, cells were switched to serum-free medium supplemented with 0.1% bovine serum albumin for 48 h, before treatment. Treatment with lead or other compounds was for 24 h. One μ Ci/well of [*methyl*-³H]thymidine was included for the last 6 h of the incubation at 37°C under an atmosphere of 5% CO₂/95% air. At the end of

the incubation, cells were washed twice with cold PBS and fixed in methanol. Unincorporated [³H]thymidine was removed by two washes with ice-cold 10% trichloroacetic acid and one wash of ice-cold 0.5% trichloroacetic acid. The monolayer was dissolved in 500 μ l of 1 M NaOH, and 250 μ l was transferred to scintillation fluid and counted for radioactivity in a Beckman LS5000 CE scintillation counter (Beckman Coulter, Inc., Fullerton, CA).

Western Blot Analyses. Cells were seeded on 100-mm dishes in medium containing 5% FBS and were switched to serum-free medium when confluent. Treatments were done after 48 h of serum starvation. After treatment, cells were harvested in buffer containing 20 mM Tris, pH 7.5, 150 mM NaCl, 1 mM EDTA, 1% Triton, 2.5 mM sodium pyrophosphate, 1 mM β -glycerol phosphate, 1 mM sodium orthovanadate, 1 μ g/ml leupeptin, and 15% final volume protease inhibitor cocktail. Proteins were quantified using the Bradford method, and a 5 \times sample buffer was added. After boiling for 5 to 10 min, samples containing 20 to 50 μ g of proteins were loaded on a 10% SDS-polyacrylamide gel. After separation, proteins were transferred to Immobilon membranes (Millipore Corporation, Bedford, MA), which were incubated with the appropriate primary antibodies overnight at 4°C and then 1 h at room temperature with horseradish peroxidase-conjugated secondary antibody (dilution 1:2000). Bands were revealed by chemiluminescent detection using an enhanced chemiluminescence kit (Amersham Biosciences, Arlington Heights, IL), and densitometrically quantified using a Millipore Image System.

Immunoprecipitation and Kinase Assay. After chemical stimulation, cells were harvested in a lysis buffer containing 20 mM Tris (pH 7.5), 150 mM NaCl, 1 mM EDTA, 1% Triton, 2.5 mM sodium pyrophosphate, 1 mM β -glycerol phosphate, 1 mM sodium orthovanadate, 1 μ g/ml leupeptin, and 15% final volume protease inhibitor cocktail. Cell extracts (100–200 μ g) were incubated with immobilized phosphospecific (Thr²⁰²/Tyr²⁰⁴) MAPK antibody overnight at 4°C. The immune complexes were washed twice with lysis buffer and then twice with kinase buffer containing 25 mM Tris, pH 7.5, 5 mM glycerol phosphate, 2 mM dithiothreitol, 0.1 mM sodium orthovanadate, and 10 mM MgCl₂. Each complex was then suspended in 25 μ l of kinase buffer with 200 μ M ATP and 1 μ g of the substrate, the GST-Elk-1 fusion protein, and incubated at 30°C for 30 min. The reactions were terminated by addition of 3 \times SDS sample buffer. The samples were analyzed by SDS-polyacrylamide gel electrophoresis and Western blot as described above. MAPK activity was measured by using a phospho-Elk-1 antibody.

Statistical Analysis. Each experiment was performed at least three times. All statistical tests were carried out using the StatView 512 program (Abacus Concepts, Berkeley, CA) or Microsoft Excel (Microsoft, Redmond, WA) on a Macintosh personal computer (Cupertino, CA). One-way analysis of variance followed by Fisher's least significant difference test was used to determine significant difference between treatments.

Results

Lead Causes MAPK (ERK1/ERK2) Activation in 1321N1 Human Astrocytoma Cells. Time course experiments showed that lead caused a rapid activation of ERK1/2 with a maximum at 15 min and a decrease to control level after 4 h (Fig. 1A). Dose-response experiments showed that lead-induced MAPK activation was concentration-dependent (Fig. 1B). Levels of phosphorylated ERK1 and ERK2 were similar in control cells as well as in cells stimulated with lead or with the phorbol ester TPA (Fig. 1C). An immunocomplex kinase assay using GST-Elk-1 as a substrate indicated that lead also increased MAPK activity (Fig. 1D). Total MAPK protein levels, measured by an anti-ERK1/2 antibody, did not change upon lead exposure (Fig. 1E). In this range of concen-

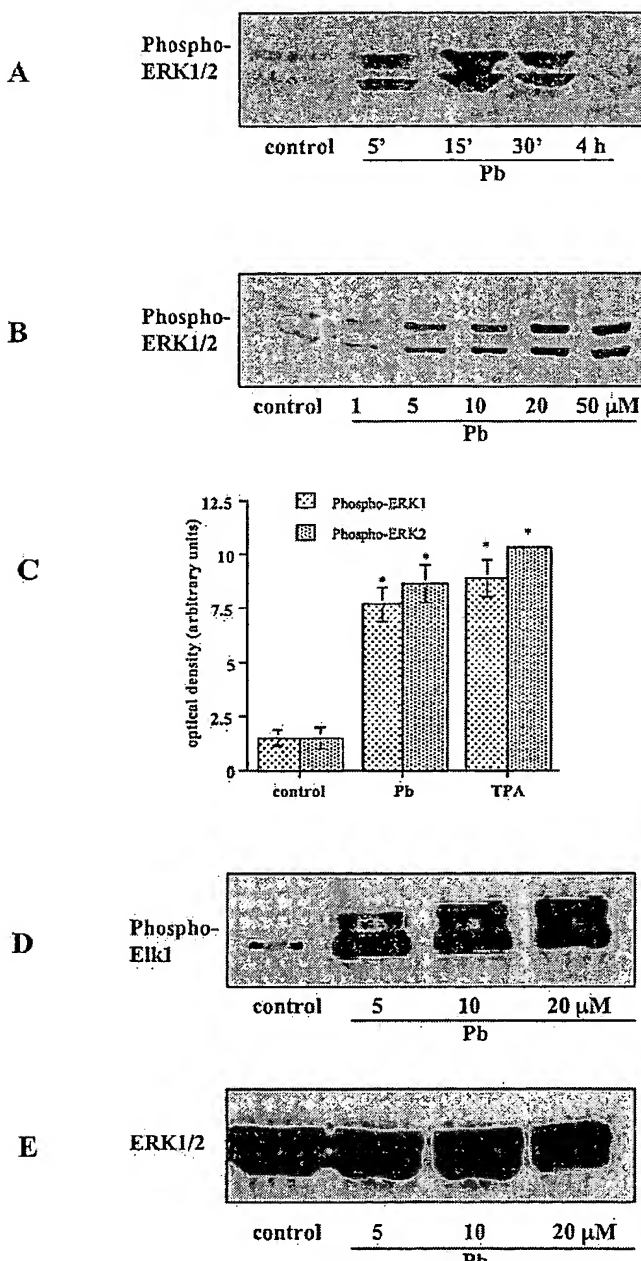


Fig. 1. Activation of MAPK by lead acetate. **A**, time course of lead (5 μ M Pb)-induced phosphorylation of ERK1/2. **B**, concentration-dependent phosphorylation of ERK1/2 by lead (Pb, 5 min). **C**, quantitation of the effect of lead (10 μ M Pb) and TPA (200 ng/ml), both at 15 min, on ERK1/2 phosphorylation (mean \pm S.E.; $n = 3$). **D**, lead (Pb; 15 min) increases MAPK activity, measured by an immunoassay using GST-Elk-1 as substrate. **E**, ERK1/2 protein levels did not change after lead (Pb) treatment (15 min). Blots shown are from one experiment, which was repeated three times with similar results. *, significantly different from control, $p < 0.05$.

trations (1–50 μ M), lead did not have any cytotoxic effect and was able to stimulate DNA synthesis and cell cycle progression in astrocytoma cells (Lu et al., 2001).

Role of PKC in Lead-Induced MAPK Activation. To determine the role of PKC in lead-induced MAPK activation, cells were pretreated with GF109203X, which acts as a competitive inhibitor for the ATP-binding site of PKC, for 30 min prior to lead treatment. Lead-induced MAPK activation was

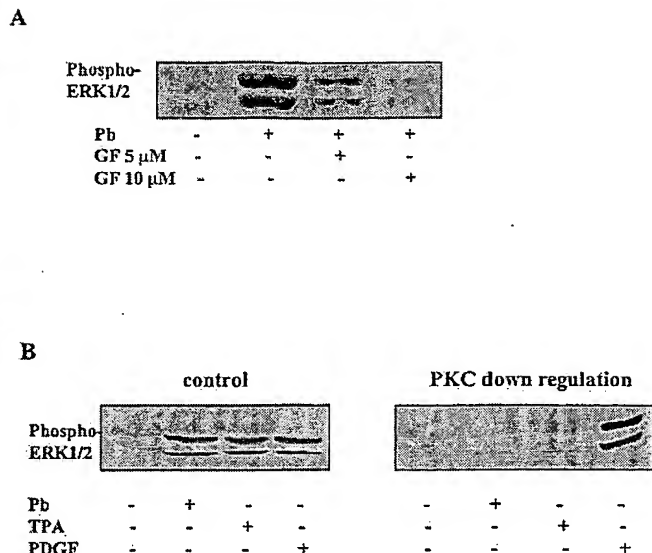


Fig. 2. Role of PKC in lead-induced phosphorylation of ERK1/2. **A**, the PKC inhibitor GF109203X (30 min before lead) inhibits activation of MAPK by lead (10 μ M Pb, 15 min). **B**, lead, lead (10 μ M Pb), TPA (200 ng/ml), and PDGF (25 ng/ml) caused activation of MAPK (left). In cells pretreated with TPA (200 ng/ml, 24 h) to down-regulate PKC, the effects of lead and TPA were inhibited, whereas PDGF still caused MAPK activation. Blots shown are from one experiment, which was repeated three times with similar results.

significantly decreased in the presence of GF109203X (Fig. 2A). Additionally, cells were treated with the phorbol ester TPA (200 ng/ml) for 24 h before lead treatment. Such prolonged treatment of TPA is known to down-regulate PKC α and ϵ in astrocytoma cells (Guizzetti et al., 1998). The ability of lead and TPA to activate MAPK was also inhibited under this condition (Fig. 2B). In contrast, platelet-derived growth factor (PDGF), which has been shown to activate MAPK independently of PKC (Baron et al., 2000), retained its ability to activate MAPK after PKC down-regulation.

To further investigate the specific isozyme of PKC involved in lead-induced MAPK activation, we used a myristoylated PKC peptide inhibitor that is based on the pseudosubstrate region for classical PKC (α and β). Since this astrocytoma cell line only expresses the PKC α isozyme, in addition to the novel PKC ϵ and the atypical PKC ζ and PKC ι (Post et al., 1996; M. Guizzetti and L. G. Costa, unpublished), the pseudosubstrate would be expected to target PKC α . Cells were preincubated with the pseudosubstrate (25 μ M) for 45 min before treatment with lead or other chemicals. This pretreatment inhibited lead-induced activation of MAPK, whereas PDGF retained its ability to activate MAPK (Fig. 3A). Our previous experiments had shown that prolonged treatment with high concentration of lead (100 μ M, 24 h) was able to selectively down-regulate PKC α , without causing any cytotoxicity (Lu et al., 2001). After this pretreatment, lead lost its ability to activate MAPK, whereas the effect of PDGF was unaffected (Fig. 3B). Under this condition, TPA still caused activation of MAPK, suggesting that the other TPA-sensitive isoform of PKC present in these cells (PKC ϵ) is also involved in TPA-induced MAPK activation.

MEK Inhibitors Inhibit Lead-Induced MAPK Activation and DNA Synthesis. MEK1/2, the kinase upstream of ERK1/2, was also activated by lead treatment (10 μ M), as shown by an increase in its phosphorylated form (Fig. 4A).

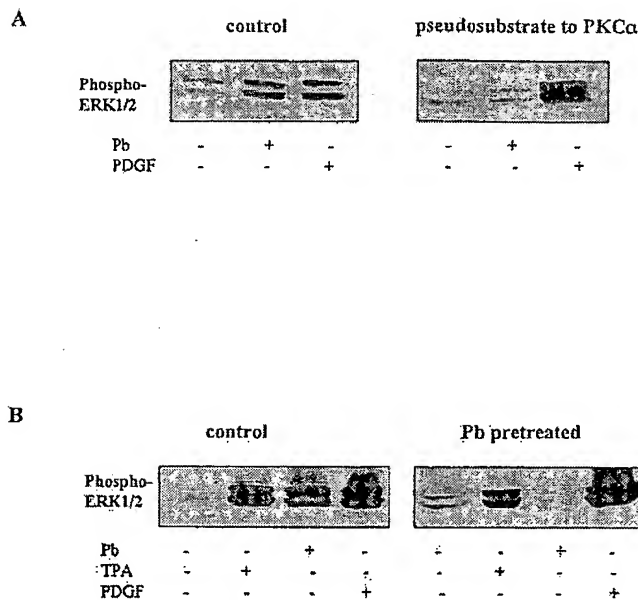


Fig. 3. Activation of MAPK by lead is mediated by PKC α . **A**, the pseudosubstrate to PKC α (25 μ M, 30 min) inhibits MAPK activation by lead (10 μ M Pb, 15 min) but not by PDGF (25 ng/ml). **B**, lead (10 μ M Pb), TPA (200 ng/ml), and PDGF (25 ng/ml) activate MAPK (left). In cells pretreated with lead (100 μ M Pb, 24 h) to selectively down-regulate PKC α (Lu et al., 2001), the effect of lead is inhibited, whereas TPA and PDGF remained effective in activating MAPK. Blots shown are from one experiment, which was repeated three times with similar results.

Activation of MEK1/2 by lead was inhibited by the PKC inhibitor GF109203X and by down-regulation of PKC through prolonged TPA treatment (200 ng/ml, 24 h) (Fig. 4A). Two MEK1/2 inhibitors, PD98059 and UO126, were able to inhibit MAPK activation induced by lead (Fig. 4B). Lead-induced DNA synthesis, as measured by [*methyl-³H*]thymidine incorporation into cell DNA, was also blocked by the two MEK1/2 inhibitors (Fig. 4C). PD98059 and UO126 have been recently found not to be specific for MEK1/2 but to also inhibit MEK5, the kinase that phosphorylates ERK5 (BMK1), a MAPK which may also be involved in the mitogenic response to growth factors (Kamakura et al., 1999; Kato et al., 2000). Lead, however, did not activate ERK5 in astrocytoma cells (Fig. 4D), suggesting that the effects of the two MEK inhibitors on lead-induced DNA synthesis can be ascribed to their action on MEK1/2.

Lead Activates p90^{RSK} in a PKC- and MAPK-Dependent Manner. Lead also induced a concentration-dependent phosphorylation of p90^{RSK}, a target of ERK1/2, which seems to play a role in cell proliferation (Frodin and Gammeltoft, 1999) (Fig. 5A). Pretreatments with TPA (200 ng/ml, 24 h) to down-regulate PKC, or with the PKC inhibitor GF109203X, attenuated the effect of lead on p90^{RSK}, whereas the MEK inhibitor UO126 completely abolished it (Fig. 5B).

Lead Does Not Activate PI3K and p70^{SEK}. The selective activation of PKC α by lead may be due to an interaction of this metal with the C2 domain of the enzyme, which confers calcium/phosphatidylserine binding to classical PKC isozymes (Mellor and Parker, 1998). Such domain is not unique for PKC, as it is found in other calcium- and phospholipid-binding proteins, such as phosphatidylinositol 3-kinase (PI3K), which plays a central role in cell proliferation (Coulonval et al., 2000). We found that lead was unable to

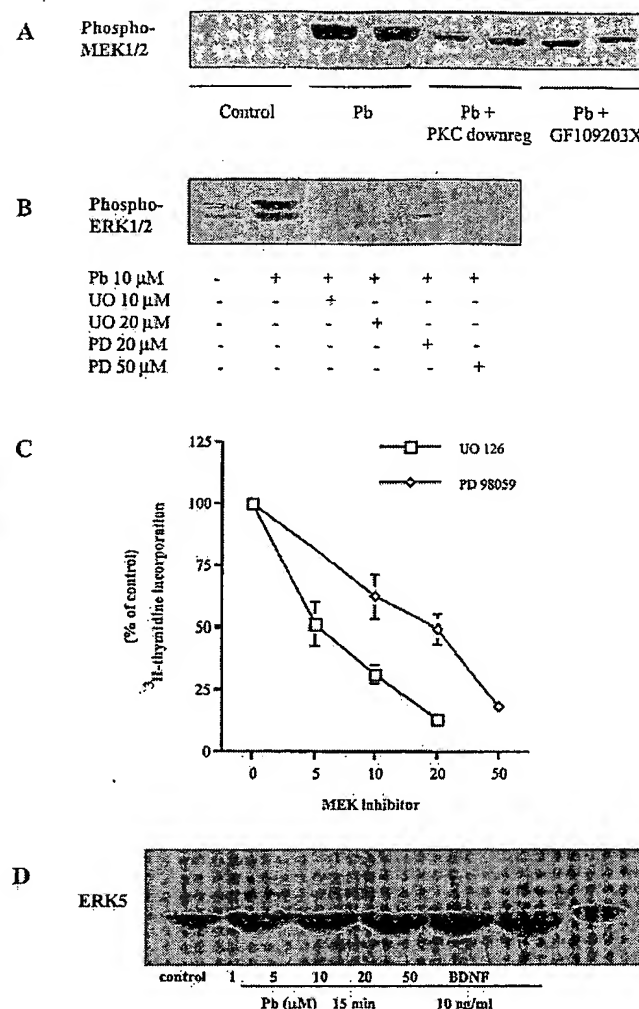


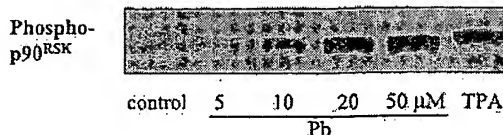
Fig. 4. Effect of lead on MEK1/2. **A**, lead (10 μ M Pb, 15 min) caused MEK1/2 phosphorylation. The effect of lead was inhibited by PKC down-regulation by TPA pretreatment (200 ng/ml, 24 h) and by pretreatment with the PKC inhibitor GF109203X (5 μ M, 30 min). **B**, lead (10 μ M Pb)-induced ERK1/2 phosphorylation is inhibited by the MEK inhibitors UO126 and PD98059 (30 min). **C**, lead-induced DNA synthesis (10 μ M, 24 h) is inhibited by PD98059 and UO126 (mean \pm S.E.; $n = 3$). **D**, lead (Pb) does not activate ERK5 in astrocytoma cells. Blots shown are from one experiment, which was repeated three times with similar results.

cause phosphorylation of Akt/PKB, a major substrate of PI3K (Fig. 6A). Phosphorylation of p70^{SEK}, which is a target for PI3K (Coulonval et al., 2000), was also not affected by lead (Fig. 6B). Furthermore, although in some systems activation of MAPK is regulated by PI3K (Toker, 2000), activation of ERK1/2 by lead was not affected by the PI3K inhibitor LY294002 (Fig. 6C).

Discussion

Although the ability of lead to increase DNA synthesis in different cell types had been previously reported (Choie and Richter, 1974; Liu et al., 1997), the intracellular mechanisms involved in this effect had not been elucidated. We have recently shown that lead causes a concentration-dependent increase in DNA synthesis and cell cycle progression in human astrocytoma cells and that this effect was dependent upon stimulation of PKC α (Lu et al., 2001). In the present

A



B

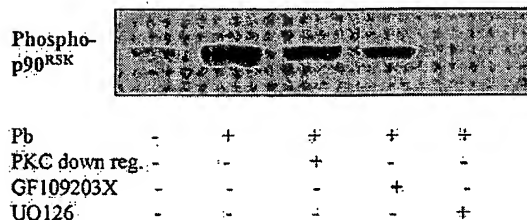
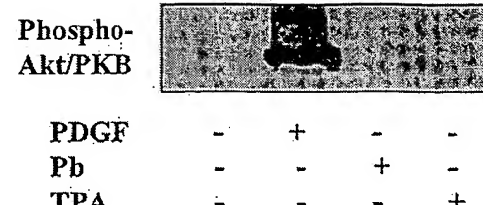


Fig. 5. Activation of $p90^{RSK}$ by lead. **A**, lead (5–50 μ M Pb) and TPA (200 ng/ml) stimulate $p90^{RSK}$ phosphorylation. **B**, lead (10 μ M Pb)-induced phosphorylation of $p90^{RSK}$ is inhibited by down-regulation of PKC with TPA (200 ng/ml, 24 h), by the PKC inhibitor GF109203X (5 μ M) and by the MEK inhibitor UO126 (5 μ M). Blots shown are from one experiment, which was repeated three times with similar results.

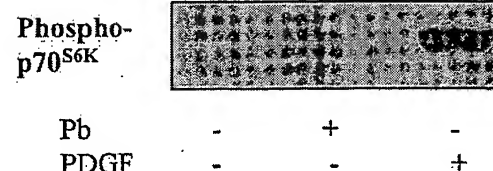
study, we investigated whether lead would activate the MEK-MAPK-RSK cascade in a $PKC\alpha$ -dependent manner, to gain a better understanding of the signal transduction pathway that may be activated by lead and may underlie the increased DNA synthesis. There is evidence that several different stimuli can activate the MEK/MAPK pathway in a PKC -dependent manner (Abe et al., 1998; Axmann et al., 1998). $PKC\alpha$ can activate Raf-1 kinase, either by direct phosphorylation (Kolch et al., 1993) or by modulating its membrane association (Schonwasser et al., 1998); Raf-1, in turn, can phosphorylate MEK, which then activates the ERK1/2 MAPK (McDonald et al., 1993; Derkinderen et al., 1999). Among the substrates of ERK1/2, $p90^{RSK}$ is considered to be relevant for the mitogenic response (Frodin and Gammeltoft, 1999). We found that lead was able to activate ERK1/2 in human astrocytoma cells, as evidenced by an increase in the levels of phosphorylated ERK1/2 and an increase in their activity, without changes in the level of proteins. Experiments with the PKC inhibitor GF109203X and with down-regulation of PKC by prolonged treatment with TPA indicated that activation of MAPK was dependent upon PKC. As human 1321N1 astrocytoma cells express only the $PKC\alpha$ and ϵ TPA-sensitive isozymes, further experiments were carried out, which indicated that $PKC\alpha$ mediates the effect of lead on MAPK. $PKC\alpha$ is also the only PKC isozyme activated by lead in human astrocytoma cells (Lu et al., 2001).

Further experiments were then carried out to elucidate the signaling steps upstream and downstream of MAPK. Lead was able to activate MEK1/2, the kinases that directly phosphorylate ERK1/2, and this effect was also dependent upon PKC. Two inhibitors of MEK, PD98059 and UO126, blocked the ability of lead to activate MAPK, as expected, and, at the same concentrations, they inhibited lead-induced DNA synthesis, thus supporting the main involvement of this signal-

A



B



C

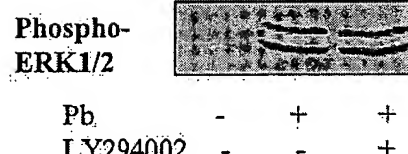


Fig. 6. Effect of lead on PI3K and on $p70^{S6K}$. **A**, lead (10 μ M Pb, 15 min) and TPA (200 ng/ml, 15 min) had no effect on phosphorylation of the PI3K substrate Akt/PKB, whereas the positive control PDGF (25 ng/ml) did. **B**, lead (10 μ M Pb, 15 min) did not induce phosphorylation of $p70^{S6K}$, whereas PDGF (25 ng/ml) did. **C**, lead (10 μ M Pb)-induced phosphorylation of ERK1/2 was not affected by the PI3K inhibitor LY294002 (1 μ M). Blots shown are from one experiment, which was repeated three times with similar results.

ing pathway in the mitogenic effect of this metal. These two MEK1/2 inhibitors have been recently shown to also inhibit MEK5, the kinase that phosphorylates ERK5 (Kamakura et al., 1999), a MAPK that is involved in mitogenic signaling (Kato et al., 2000; Pearson et al., 2000). Lead, however, was unable to induce phosphorylation of ERK5 in astrocytoma cells, suggesting that the inhibitory effect of PD98059 and UO126 on lead-induced DNA synthesis may be ascribed to inhibition of MEK1/2.

The additional link between lead-activated $PKC\alpha$ and MEK1/2 may be represented by Raf-1 kinase (Abe et al., 1998), as $PKC\alpha$ has been shown to activate Raf-1 kinase, either by direct phosphorylation or by modulating its membrane association (Kolch et al., 1993; Schonwasser et al., 1998). In a number of experiments, we attempted measuring activation of Raf-1 kinase by lead. MEK1 was used as a substrate to carry out an immunocomplex kinase assay after immunoprecipitation with an anti-Raf-1 antibody. Although we consistently found an increase in Raf-1 activity upon exposure to lead (10 μ M), the effect of lead was small (30%

above basal), so that experiments with PKC inhibitors were not carried out (data not shown). The finding suggests that Raf-1 may link PKC α to MEK1/2 in the pathway leading to MAPK activation by lead. However, an alternative interpretation of this result (in addition to the possibility of a low sensitivity of the method used to measure Raf-1 activation) is that lead-activated PKC α may in turn activate MEK1/2 through another MEK kinase (Pearson et al., 2000). Downstream of MAPK, we found that lead could activate p90^{RSK}, one of the substrates of ERK1/2, which can activate various transcription factors and seems to play a role in cell proliferation (Zhao et al., 1996; Frodin and Gammeltoft, 1999). Activation of p90^{RSK} also depended on activation of PKC and MEK1/2, as expected.

Selective activation of PKC α by lead in human astrocytoma cells (Lu et al., 2001) may be due to an interaction of this metal with the C2 domain of the enzyme, which confers calcium/phosphatidylserine binding to classical PKC isozymes (Nalefski and Falke, 1996; Mellor and Parker, 1998). Such C2 domain is not unique for PKC, as it is found in several other calcium- and phospholipid-binding proteins, such as synaptotagmin, phospholipase, or PI3K (Nalefski and Falke, 1996; Rizo and Sudhof, 1998). The latter is of interest in the context of an effect of lead on DNA synthesis, as PI3K plays a central role in cell proliferation (Leevers et al., 1999; Coulonval et al., 2000). We found that lead did not stimulate phosphorylation of Akt/PKB, a major substrate of PI3K (Coffer et al., 1998). Lead also did not activate another member of the S6 kinase family, the p70^{S6K}, which is activated by PI3K (Coulonval et al., 2000). Furthermore, although in some systems activation of MAPK is regulated by PI3K (Toker, 2000), this is not the case with lead, as the PI3K inhibitor LY294002 did not affect lead-induced ERK1/2 activation. However, in a preliminary experiment, we have found that LY294002 (1 μ M) inhibited lead-induced DNA synthesis (by 40%), suggesting that activation of other PI3K substrates may be also involved in the mitogenic effect of lead (H. Lu, unpublished).

In summary, the results of this study indicate that the ability of lead to induce DNA synthesis and cell proliferation in human 1321N1 astrocytoma cells is mediated by activation of the MEK1/2 and ERK1/2, signal transduction pathway, via a PKC α -dependent manner. Activation of MEK and MAPK by lead had been previously found in PC12 cells (Ramesh et al., 1999) but was not studied in the context of cell proliferation. Our results suggest that by activating the ERK1/2 pathway, lead may act as a tumor promoter in transformed glial cells, although such findings may not extend to other cell types. In this context, however, our present results are of interest in light of the observed increased risk of lead exposure for brain tumors, most notably astrocytomas (Anttila et al., 1996).

References

Abe MK, Kartha S, Karpova AY, Li J, Liu PT, Kuo WL, and Hershenson MB (1998) Hydrogen peroxide activates extracellular signal-regulated kinase via protein kinase C, Raf-1, and MEK1. *Am J Respir Cell Mol Biol* 18:562–569.

Anttila A, Heikkila P, Nykyri E, Kauppinen T, Pukkala E, Hernberg S, and Hemminki K (1996) Risk of nervous system cancer among workers exposed to lead. *J Occup Environ Med* 38:131–136.

Anttila A, Heikkila P, Pukkala E, Nykyri E, Kauppinen T, Hernberg S, and Hemminki K (1995) Excess lung cancer among workers exposed to lead. *Scand J Work Environ Health* 21:460–469.

ATSDR (Agency for Toxic Substances and Disease Registry) (1999) Toxicological profile for lead, pp 587, US Department of Health and Human Services, Atlanta, GA.

Arxmann A, Seidel D, Reimann T, Hempel U, and Wenzel KW (1998) Transforming growth factor-beta1-induced activation of the Raf-MEK-MAPK signaling pathway in rat lung fibroblasts via a PKC-dependent mechanism. *Biochem Biophys Res Commun* 249:456–460.

Baron W, Metz B, Bansal R, Hoekstra D, and de Vries H (2000) PDGF and FGF-2 signaling in oligodendrocyte progenitor cells: regulation of proliferation and differentiation by multiple intracellular signaling pathways. *Mol Cell Neurosci* 15:314–329.

Bellinger D, Levinton A, Wateraux C, Needleman H, and Rabinowitz P (1987) Longitudinal analysis of environmental exposure to lead and children's intelligence at the age of seven years. *N Engl J Med* 316:1037–1043.

Choie DD and Richter GW (1974) Cell proliferation in mouse kidney induced by lead. I. Synthesis of deoxyribonucleic acid. *Lab Invest* 30:647–651.

Coffer PJ, Jin J, and Woodgett JR (1998) Protein kinase B (c-Akt): a multifunctional mediator of phosphatidylinositol 3-kinase activation. *Biochem J* 335:1–13.

Costa LG (1998) Signal transduction in environmental neurotoxicity. *Annu Rev Pharmacol Toxicol* 38:21–43.

Coulonval K, Vandeput F, Stein RC, Kozma SC, Lamy F, and Dumont JE (2000) Phosphatidylinositol 3-kinase, protein kinase B and ribosomal S6 kinases in the stimulation of thyroid epithelial cell proliferation by cAMP and growth factors in the presence of insulin. *J Biochem (Tokyo)* 348:351–358.

Derkinderen P, Enslen H, and Girault JA (1999) The ERK/MAP-kinases cascade in the nervous system. *Neuroreport* 10:R24–R34.

Ferrell JE Jr (1996) MAP kinases in mitogenesis and development. *Curr Top Dev Biol* 33:1–60.

Frodin M and Gammeltoft S (1999) Role and regulation of 90 kDa ribosomal S6 kinase (RSK) in signal transduction. *Mol Cell Endocrinol* 151:65–77.

Fujiwara Y, Keji T, Yamamoto C, Sakamoto M, and Kozuka H (1995) Stimulatory effect of lead on the proliferation of cultured vascular smooth muscle cells. *Toxicology* 98:105–110.

Guizzetti M, Costa P, Peters J, and Costa LG (1996) Acetylcholine as a mitogen: muscarinic receptor-mediated proliferation of rat astrocytes and human astrocytoma cells. *Eur J Pharmacol* 297:265–273.

Guizzetti M, Wei M, and Costa LG (1998) The role of protein kinase C α and ϵ isozymes in DNA synthesis induced by muscarinic receptors in a glial cell line. *Eur J Pharmacol* 359:223–233.

Hartwig A (1994) Role of DNA repair inhibition in lead- and cadmium-induced genotoxicity: a review. *Environ Health Perspect* 102 (Suppl 3):45–50.

Kamakura S, Moriguchi T, and Nishida E (1999) Activation of the protein kinase ERK5/BMK 1 by receptor tyrosine kinases. *J Biol Chem* 274:26563–26571.

Kato Y, Chao TH, Hayashi M, Topping RL, and Lee JD (2000) Role of BMK1 in regulation of growth factor-induced cellular responses. *Immunol Res* 21:233–237.

Kolch W, Heidecker G, Kochs G, Humel R, Vahidi H, Mischak H, Finkenzeller G, Marne D, and Rapp UR (1993) Protein kinase C α activates Raf-1 by direct phosphorylation. *Nature (Lond)* 364:249–252.

Leevers SJ, Vanhaestertroo B, and Waterfield MD (1999) Signalling through phosphoinositide 3-kinases: the lipids take centre stage. *Curr Opin Cell Biol* 11:219–225.

Liu JY, Lin JK, Liu CC, Chen WK, Liu CP, Wang CJ, Yen CC, and Hsieh YS (1997) Augmentation of protein kinase C activity and liver cell proliferation in lead nitrate-treated rats. *Biochem Mol Biol Int* 43:355–364.

Lu H, Guizzetti M, and Costa LG (2001) Inorganic lead stimulates DNA synthesis in 1321N1 human astrocytoma cells: role of protein kinase C α . *J Neurochem* 78:590–599.

McDonald SG, Crews CM, Wu L, Driller J, Clark R, Erikson RL, and McCormick F (1993) Reconstitution of the Raf-1-MEK-ERK signal transduction pathway in vitro. *Mol Cell Biol* 13:6615–6620.

Mellor H and Parker PJ (1998) The extended protein kinase C superfamily. *Biochem J* 332:281–292.

Nalefski EA and Falke JJ (1996) The C2 domain calcium-binding motif: structural and functional diversity. *Protein Sci* 5:2375–2390.

Pearson G, Robinson F, Gibson TB, Xu BE, Karandikar M, Berman K, and Cobb MH (2000). Mitogen-activated (MAP) kinase pathways: regulation and physiological functions. *Endocr Rev* 22:153–183.

Post GR, Collins LR, Kennedy ED, Moskowitz SA, Aragay AM, Goldstein D, and Brown JH (1996) Coupling of the thrombin receptor to G12 may account for selective effects of thrombin on gene expression and DNA synthesis in 1321N1 astrocytoma cells. *Mol Biol Cell* 7:1679–1690.

Ramesh GT, Manna SK, Aggarwal BB, and Jadhav AL (1999) Lead activates nuclear transcription factor- κ B, activator protein-1, and amino-terminal c-Jun kinase in pheochromocytoma cells. *Toxicol Appl Pharmacol* 155:280–286.

Razani-Boroujerdi S, Edwards B, and Sopori ML (1999) Lead stimulates lymphocyte proliferation through enhanced T cell-B cell interaction. *J Pharmacol Exp Ther* 288:714–719.

Rizo J and Sudhof TC (1998) C2 domains, structure and function of a universal Ca^{2+} -binding domain. *J Biol Chem* 273:15879–15882.

Schonwasser DC, Marais RM, Marshall CJ, and Parker PJ (1998) Activation of the mitogen-activated protein kinase/extracellular signal-regulated kinase pathway by conventional, novel, and atypical protein kinase C isotypes. *Mol Cell Biol* 18:790–798.

Steenland K, Selevan S, and Landrigan P (1992) The mortality of lead smelter workers: an update. *Am J Public Health* 82:1641–1644.

Toker A (2000) Protein kinases as mediators of phosphoinositide 3-kinase signaling. *Mol Pharmacol* 57:652–658.

Zelikoff JT, Li JM, Hartwig A, Wang XW, Costa M, and Rossman TG (1988) Genetic toxicology of lead compounds. *Carcinogenesis* 9:1727–1732.

Zhao Y, Bjorbaek C, and Moller DE (1996) Regulation and interaction of pp90(rsk) isoforms with mitogen-activated protein kinases. *J Biol Chem* 271:29773–29781.

Address correspondence to: Dr. Lucio G. Costa, Department of Environmental Health, University of Washington, 4225 Roosevelt Way NE, Seattle, WA 98105. E-mail: lgcosta@u.washington.edu

In Vivo Identification of the Mitogen-Activated Protein Kinase Cascade as a Central Pathogenic Pathway in Experimental Mesangioproliferative Glomerulonephritis

DIRK BOKEMEYER,* DARIUS PANEK,* HERBERT J. KRAMER,* MARION LINDEMANN,* MASASHI KITAHARA,† PETER BOOR,† DANTSCHO KERJASCHKI,‡ JAMES M. TRZASKOS,§ JÜRGEN FLOEGE,† and TAMMO OSTENDORF†

*Medical Polyclinic, Division of Nephrology, University of Bonn, Bonn, Germany; †Division of Nephrology and Immunology, University of Aachen, Aachen, Germany; ‡Institute for Clinical Pathology, University of Vienna, Vienna, Austria; and §DuPont Pharmaceuticals Research Laboratories, Wilmington, Delaware.

Abstract. Evidence was recently provided for the activation of extracellular signal-regulated kinase (ERK), the best characterized mitogen-activated protein kinase, as an intracellular convergence point for mitogenic stimuli in animal models of glomerulonephritis (GN). In this study, *in vivo* ERK activity was blocked, with a pharmacologic inhibitor (U0126) of the ERK-activating kinase, in rats with mesangioproliferative GN. After injection of the monoclonal anti-Thy1.1 antibody (OX-7), the rats were treated (days 3 to 6) with low (10 mg/kg body wt) or high (100 mg/kg body wt) doses of U0126 administered intraperitoneally twice daily. On day 6 after induction of the disease, whole cortical tissue and isolated glomeruli were examined by using kinase activity assays, Western blot analyses, and immunohistochemical assays. Treatment with U0126

significantly reduced glomerular stimulation of ERK in anti-Thy1 GN. In the high dose-treated group, this downregulation was accompanied by a reduction in the number of glomerular mitotic figures, back to healthy control levels, and significant decreases in the numbers of total ($P < 0.05$) and 5-bromo-2'-deoxyuridine-positive ($P < 0.05$) glomerular cells. Immunohistochemical double-staining of renal sections demonstrated that mesangial cells were the major glomerular targets of U0126 in anti-Thy1 GN. These observations point to ERK as a putative intracellular mediator of the proliferative response in GN and suggest that pharmacologic treatments that interfere with the activation of ERK may be of potential therapeutic interest.

Mitogen-activated protein (MAP) kinases are important mediators involved in the intracellular network of interacting proteins that transduce extracellular stimuli to intracellular responses (1). Extracellular signal-regulated kinases (ERK) were the first reported and are still the best described members of the group of MAP kinases. Two ERK isoforms have been described; ERK1 (or p44 MAP kinase) and ERK2 (or p42 MAP kinase) are serine/threonine kinases that regulate the expression of many genes via the phosphorylation of several transcription factors (1,2). The binding of extracellular stimuli to G protein-coupled receptors or protein tyrosine kinase receptors results in the formation of GTP-Ras, which induces the sequential activation of cytoplasmic protein kinases, leading to their phosphorylation and activation (1,2). MAP kinase/ERK kinase 1 (MEK1) and MEK2 are specific activators of ERK1

and ERK2. MEK are dual-specificity protein kinases that phosphorylate both threonine and tyrosine regulatory sites in ERK (3). Although an extensive body of data describes the pivotal role of this signaling pathway in the control of cellular proliferation *in vitro* (1,2), little is known regarding the roles of ERK1 and ERK2 in physiologic or pathophysiologic conditions or their activation *in vivo*. Other members of the rapidly growing group of MAP kinases include stress-activated protein kinases, p38 MAP kinases (α , β , γ , and δ), ERK3, and ERK5 (1,2,4,5). Compared with ERK1 and ERK2, however, the physiologic function of most of these kinases, even *in vitro*, is less well defined (1,2,4,5).

A major focus of research on the pathogenesis of proliferative glomerulonephritis (GN) has been to define extracellular growth-promoting factors (6). In contrast, little is known regarding the intracellular mediators that contribute to cellular growth in renal diseases. Such intracellular messengers represent likely targets for therapeutic pharmacologic interventions in proliferative glomerular diseases. We recently demonstrated for the first time, in rats with anti-glomerular basement membrane GN (7) or experimental mesangioproliferative GN (8), *in vivo* activation of ERK accompanying glomerular cell proliferation. Those data pointed to ERK as a regulator of cellular growth in proliferative GN. We performed the study described

Received July 27, 2001. Accepted February 1, 2002.

Correspondence to Dr. Dirk Bokemeyer, Medizinische Poliklinik, University of Bonn, Wilhelmstrasse 35-37, 53111 Bonn, Germany. Phone: 49-228-2872263; Fax: 49-228-2872266; E-mail: bokemeyer@uni-bonn.de

1046-6573/1306-1473

Journal of the American Society of Nephrology

Copyright © 2002 by the American Society of Nephrology

DOI: 10.1097/01.ASN.0000017576.50319.AC

here to examine the effects of *in vivo* ERK inhibition on the progression of proliferative glomerular diseases. Therefore, we induced anti-Thy1.1 GN in rats. After the initial mesangiolysis after injection of the anti-Thy1.1 antibody, this form of GN is characterized by an overshooting proliferative phase that resembles human mesangiproliferative GN (9). We used the compound U0126 (10) to block ERK activation *in vivo* and to assess its effect on the development of anti-Thy1.1 GN in rats. U0126 was demonstrated to be a potent and highly specific inhibitor of the ERK-activating kinases MEK1 and MEK2 (10).

Materials and Methods

Cell Culture

Primary rat mesangial cells (MC) were prepared and cultured as described previously (11). Before stimulation with platelet-derived growth factor-BB (PDGF-BB) (Sigma Chemical Co., St. Louis, MO), subconfluent cells were starved in serum-free medium for 24 h.

Cell Counting

For cell counting, MC were seeded in 24-well culture plates (5×10^{-4} cells/well; well diameter, 12 mm) and cultured for 24 h. Under these conditions, a cell confluence of approximately 70% was reached. Cells were serum-starved for 24 h in serum-free medium before stimulation with PDGF (20 ng/ml), in the presence or absence of U0126. After 24 h, the cells were trypsinized and cell counting was performed by using the CASY-1 system (Schärflle, Reutlingen, Germany), which is based on the Coulter counter principle.

Induction of Anti-Thy1.1 GN and Experimental Design

All animal experiments were approved by the local review boards. Anti-Thy1.1 mesangial proliferative GN was induced in male Wistar rats (weighing 150 to 160 g; Charles River, Sulzfeld, Germany) by injection of 1 mg/kg monoclonal anti-Thy1.1 antibody (clone OX-7; European Collection of Animal Cell Cultures, Salisbury, UK). After euthanasia, the rats were nephrectomized and a renal cortical section was obtained for light microscopy. Another cortical section was directly lysed in Triton X-100 buffer (see below), and the rest of the cortical tissue (approximately 80% of the whole cortex) was used to generate a preparation of glomeruli, via standard sieving methods (12), before lysis in Triton X-100 buffer.

Initially, eight healthy rats were studied for evaluation of the effect of a single dose of the MEK inhibitor U0126 on basal glomerular ERK activity. Subsequently, 30 rats were used to examine the effect of U0126 treatment on the progression of mesangiproliferative GN. Rats received twice-daily intraperitoneal injections of U0126 dissolved in DMSO (or vehicle alone), starting on day 3 after the induction of anti-Thy1.1 GN. Healthy control animals either were not treated or received U0126 according to the schedule described above. The animals were nephrectomized on day 6 and received the last dose of U0126 1 h before euthanasia. In addition, the thymidine analogue 5-bromo-2'-deoxyuridine (BrdU) (20 mg/kg body wt; Sigma) was injected intraperitoneally 4 h before euthanasia on day 6. Twenty-four-hour urine collections were performed on day 5 after disease induction.

Renal Morphologic Assessments

Tissue for light microscopy was fixed in methyl Carnoy's solution or formalin and embedded in paraffin (13). Four-micron sections were stained with the periodic acid-Schiff reagent and counterstained with

hematoxylin. In periodic acid-Schiff-stained sections, the number of nuclei per glomerulus and the number of mitoses in 100 glomerular tufts were determined. In addition, cellular death in renal sections was assayed with the terminal deoxynucleotidyl transferase-mediated dUTP-biotin nick-end-labeling method (14).

Immunohistochemical Staining

Four-micrometer sections of methyl Carnoy's solution-fixed tissue were processed by using the indirect immunoperoxidase technique, as described previously (13). Primary antibodies included BU-1 (a monoclonal antibody against BrdU) (Amersham, Braunschweig, Germany), 1A4 (a monoclonal antibody against α -smooth muscle actin) (Dako, Glostrup, Denmark), JG-12 (a monoclonal endothelial cell-specific antiserum) (15), monoclonal anti-ED1 antibody (Camon, Wiesbaden, Germany), and the affinity-purified IgG fraction of a polyclonal rabbit anti-rat fibronectin antibody (Chemicon, Temecula, CA). Double-immunostaining was performed as described previously (16). Fibronectin staining was evaluated by using a point-counting method. For this procedure, a grid composed of 121 dots was superimposed on the glomeruli (range, 30 to 50; magnification, $\times 100$) and the percentages of dots overlying stained areas were counted.

Western Blot Analyses

Whole cortical tissue or isolated glomeruli were homogenized in 2 ml of Triton X-100 lysis buffer [50 mM Hepes, pH 7.5, 150 mM NaCl, 1.5 mM MgCl₂, 1 mM ethylene glycol bis(β -aminoethyl ether)-*N,N,N',N'*-tetraacetic acid, 10% glycerol, 1% Triton X-100, 1 μ g/ml aprotinin, 1 μ g/ml leupeptin, 1 mM phenylmethylsulfonyl fluoride, 0.1 mM sodium orthovanadate] at 4°C. After incubation for 5 min, lysates were centrifuged at 4°C for 15 min at 10,000 \times g. The soluble lysates were mixed 1:4 with 5 \times Laemmli buffer and were heated for 5 min at 95°C. Soluble lysates (80 μ g) were loaded in each lane and separated by sodium dodecyl sulfate-polyacrylamide gel electrophoresis, using 4 and 10% acrylamide for stacking and resolving gels, respectively. Proteins were transferred to nitrocellulose membranes (pore size, 0.45 μ m; Schleicher and Schuell, Keene, NH) and probed with polyclonal antibodies against the carboxy-terminal peptide of p42 ERK (17), as well as polyclonal antibodies against the phosphorylated regulatory sequences of ERK (Calbiochem, Schwalbach, Germany). The primary antibodies (diluted 1:1000) were detected with horseradish peroxidase-conjugated rabbit anti-mouse IgG or horseradish peroxidase-conjugated Protein A and were observed with the Amersham ECL system (Amersham, Braunschweig, Germany), after extensive washing of the membranes. The intensities of the identified bands were quantified by densitometry, using the BioRad Gel Doc 1000 system and Multi-Analyst software (Bio-Rad, Munich, Germany).

ERK Activity Assays

Soluble lysates (400 μ g; prepared as described above) were incubated for 90 min with 2 μ l of polyclonal antibody recognizing p42 ERK (17). Immunocomplexes were adsorbed to Protein A-Sepharose (Pharmacia, Freiburg, Germany), washed twice with lysis buffer and twice with kinase buffer (10 mM MgCl₂, 20 mM Hepes, pH 7.4, containing 200 μ M sodium orthovanadate), and resuspended in 60 μ l of kinase buffer containing 50 μ M ATP. The final reaction buffer also contained 2 μ g of glutathione-S-transferase-Elk1 (Santa Cruz Biotechnology, Santa Cruz, CA). The reaction was initiated by incubation at 30°C for 45 min. Then, 20 μ l of 4 \times Laemmli buffer was added to terminate the reaction, and samples were subjected to sodium dodecyl sulfate-polyacrylamide gel electrophoresis. Proteins were then analyzed by Western blot analysis, as described above, with a polyclonal

anti-phospho-Elk1 antibody (New England Biolabs, Beverly, MA) that recognized only the phosphorylated forms of Elk1.

Statistical Analyses

Values are expressed as means \pm SEM. Statistical analyses were performed with the Bonferroni *t* test. $P < 0.05$ was considered statistically significant.

Results

MEK Inhibition Blocks the Mitotic Activity of Cultured MC

To establish an effect of ERK signaling cascade inhibition on the proliferation of MC, we first examined the effect of the MEK inhibitor U0126 on PDGF-BB-induced mitotic activity of cultured rat MC. As demonstrated by anti-phospho-ERK Western blot analysis, which identified only active ERK forms phosphorylated within the regulatory sequence, U0126 demonstrated dose-dependent inhibition of PDGF-induced ERK activation in MC (Figure 1A). As expected, incubation of MC with PDGF stimulated cellular proliferation. U0126 dose-dependently led to a complete inhibition of this proliferative response to PDGF (Figure 1B). In this experimental setting, U0126 did not induce apoptosis or reduce the cellular viability of cultured MC in the presence of PDGF, as measured with nucleosome assays and cellular lactate dehydrogenase release, respectively (data not shown).

U0126 Inhibits Glomerular ERK Activity In Vivo

Next, we evaluated whether an intraperitoneal injection of U0126 would inhibit renal glomerular ERK activity *in vivo*. Healthy male Wistar rats received a single intraperitoneal injection of U0126, 1 h before nephrectomy and isolation of the glomeruli. As demonstrated by anti-phospho-ERK Western blot analysis (Figure 2A, upper), U0126 dose-dependently blocked the basal phosphorylation of ERK. Equal loading of glomerular proteins was confirmed by reprobing of immunoblots with a polyclonal antiserum that detected total ERK2 (Figure 2A, middle). The results of the anti-phospho-ERK Western blot analysis were confirmed with an immunocomplex ERK activity assay using a glutathione-S-transferase fusion protein of the transcription factor Elk1 as the substrate in the kinase reaction. The extent of Elk1 phosphorylation was determined by anti-phospho-Elk1 Western blot analysis (Figure 2A, lower). Collectively, these results established that U0126 could inhibit glomerular ERK activity *in vivo*.

On the basis of these findings, rats with mesangioproliferative GN were treated with a low (10 mg/kg body wt, twice daily) or high (100 mg/kg body wt, twice daily) dose of U0126 or received vehicle (DMSO) alone. It is known that the rapid mesangiolysis that occurs within 24 h after injection of the anti-Thy1.1 antibody is critical for the overshooting glomerular proliferation. Therefore, treatment with U0126 was initiated 48 h after induction of the disease, *i.e.*, at a time point when the nephritis was well established. Rats were euthanized on day 6, the time point with maximal glomerular ERK activation and glomerular proliferation (8). We evaluated the *in vivo* activity of ERK both in the renal cortex and in isolated glomeruli. As

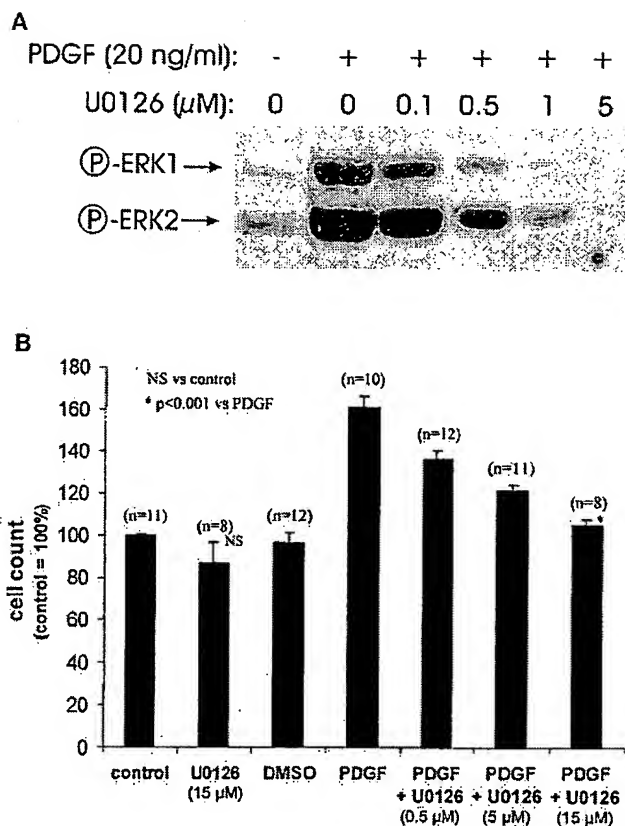


Figure 1. U0126 inhibition of the proliferation of cultured rat mesangial cells (MC). (A) Quiescent MC were incubated with platelet-derived growth factor-BB (PDGF-BB) for 10 min, in the presence or absence of various concentrations of U0126. U0126 was added to the culture medium 10 min before stimulation with PDGF. Cell lysates were examined by Western blot analysis, using an anti-phospho-extracellular signal-regulated kinase (ERK) antiserum that recognizes only ERK forms phosphorylated within the regulatory sequence. (B) For cell counting, serum-starved MC were incubated with PDGF (20 ng/ml), U0126, or vehicle (DMSO) for 24 h.

described previously (8), we observed an increase in ERK activity in crude cortical lysates on day 6 of anti-Thy1.1 GN (Figure 2B), with an even more pronounced increase in isolated glomeruli (Figure 2C), indicating that the glomeruli were the major source of the increased cortical ERK activity in anti-Thy1.1 GN. Renal phosphorylation of ERK was reduced, in a dose-dependent manner, in rats treated with U0126 (Figure 2, B and C, upper). Equal loading of glomerular lysates was confirmed by reprobing of immunoblots with an antiserum that detected total ERK (Figure 2, B and C, middle). In addition, immunocomplex ERK activity assays demonstrated a similar pattern of U0126 effects on ERK activity (Figure 2, B and C, lower). Densitometric analysis of the ERK activity assays in isolated glomeruli of rats with anti-Thy1 GN demonstrated statistically significant effects of the MEK inhibitor U0126 on ERK activity at a dose of 100 mg/kg body wt, administered twice daily (Figure 2D). These analyses also suggested that U0126 reduced basal ERK activity in healthy rats, although this finding was not statistically significant (Figure 2D).

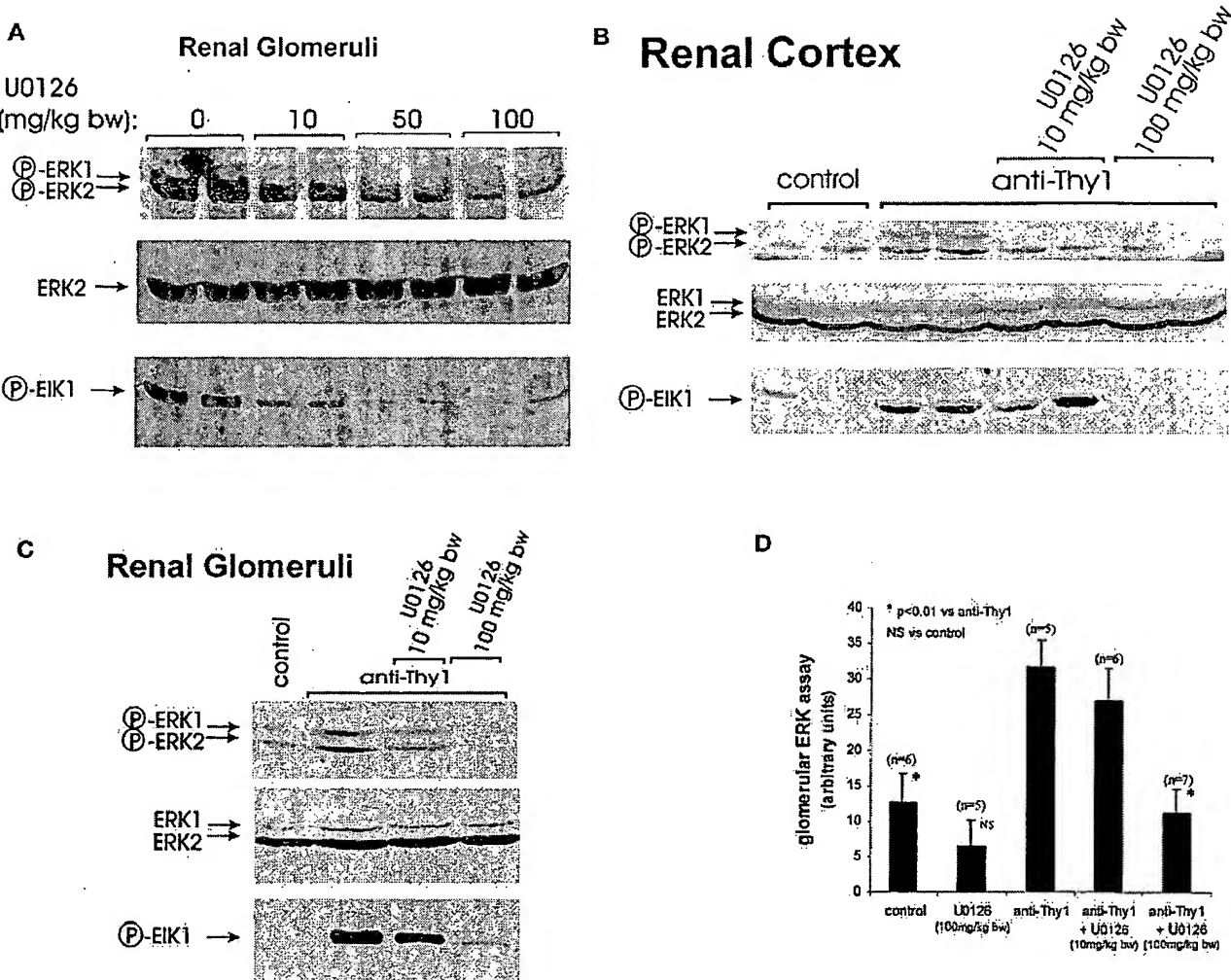


Figure 2. Pharmacologic inhibition of renal ERK activity. (A) Dose-dependent effects of U0126 on basal glomerular ERK activity in healthy rats. Each slot represents one animal. One hour after a single intraperitoneal injection of U0126 or an equivalent volume of vehicle (DMSO), the rats were nephrectomized and renal glomeruli were isolated. (Upper) Western blot analysis using an anti-phospho-ERK antiserum that identifies only ERK forms phosphorylated within the regulatory sequence. (Middle) Confirmation of equal loading by reprobing of immunoblots with a polyclonal anti-ERK2 antiserum. (Lower) ERK activity assayed by the ability of immunoprecipitated ERK to phosphorylate a glutathione-S-transferase fusion protein of the transcription factor Elk1. The kinase reaction was monitored by Western blot analysis with a polyclonal anti-phospho-Elk1 antiserum that recognizes only protein phosphorylated at position 383, the site of Elk1 phosphorylation by ERK. (B) Inhibition of cortical ERK activity in rats with anti-Thy1.1 glomerulonephritis (GN). Each slot represents one animal. Rats were euthanized on day 6 after injection of the anti-Thy1.1 antibody. Animals were treated twice daily, from day 3 to day 6, with U0126 or vehicle. (Upper) Phosphorylated and thus activated ERK detected in glomerular lysates by anti-phospho-ERK Western blot analysis. (Middle) Confirmation of equal loading by reprobing of immunoblots with a polyclonal anti-ERK2 antiserum. (Lower) ERK immunocomplex activity assayed as described above. (C) Inhibition of glomerular ERK activity in anti-Thy1.1 GN. As indicated above, after treatment with U0126 or vehicle from day 3 to day 6, rats were euthanized on day 6 after induction of anti-Thy1.1 GN. (Upper) Western blot analysis using an anti-phospho-ERK antiserum. (Middle) Confirmation of equal loading by reprobing of immunoblots with a polyclonal anti-ERK2 antiserum. (Lower) ERK immunocomplex activity assay. (D) Densitometric analysis of independent assessments of Elk1 phosphorylation in the ERK assays with glomerular tissues.

ERK Inhibition Blunts Glomerular Proliferation in Anti-Thy1.1 GN

The renal morphologic features in the proliferative phase of anti-Thy1.1 GN are characterized by pronounced glomerular hypercellularity (Figure 3, A and B). In the group receiving high-dose U0126, these histologic changes were potently

blunted in most glomeruli (Figure 3C). In accordance with the glomerular histologic features demonstrated in Figure 3, we detected an increase in the number of glomerular cells (assessed as the number of glomerular nuclei) in rats with anti-Thy1 GN, compared with control animals (Figure 4A). Treatment with U0126 induced a significant reduction of glomerular

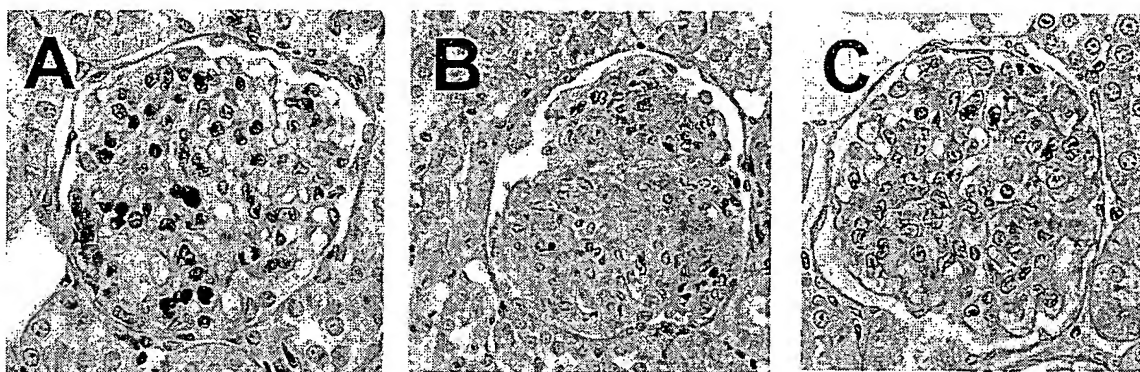


Figure 3. Light microscopic analyses of renal cortical sections stained with periodic acid-Schiff stain. Magnification, $\times 600$. (A) Glomerulus from a healthy control rat. (B) Representative glomerulus from a rat 6 d after induction of anti-Thy1.1 GN. The rats received intraperitoneal injections of the vehicle (DMSO) twice daily. (C) Representative glomerulus from a rat treated twice daily with 100 mg/kg body wt U0126, 6 d after induction of anti-Thy1.1 GN.

cells in rats with anti-Thy1 GN. The changes in glomerular cell proliferation were further examined with assessments of the number of glomerular mitotic figures and BrdU-positive nuclei. In rats with anti-Thy1 GN that were treated with the MEK inhibitor at 100 mg/kg body wt, we observed a significant reduction in mitoses (Figure 4B). This effect of U0126 was also demonstrated by quantification of BrdU-positive nuclei (Figure 4C). In addition to the action of U0126 in proliferative GN, we observed significant reductions in the numbers of glomerular mitotic figures and BrdU-positive cells in healthy control animals (Figure 4, B and C). However, this effect did not induce a significant reduction in the number of glomerular cells in healthy rats treated with U0126 (Figure 4A). We previously described a massive induction of apoptosis within hours and a slight increase in glomerular apoptosis up to 10 d after the induction of anti-Thy1 GN (8). In the study presented here, treatment with U0126 did not affect the level of glomerular apoptosis (Figure 4D). Considering the link between MC proliferation and MC matrix expansion, we quantified glomerular staining for fibronectin by grid-counting. The data support this link (Figure 4E), but the reduction in glomerular fibronectin staining in rats treated with U0126 was not statistically significant. Anti-Thy1.1 GN is not a model of severe proteinuria. However, compared with control rats, a moderate increase in albuminuria in rats with GN and an even smaller increase in healthy rats receiving U0126 were observed (Figure 4F). In nephritic rats, U0126 induced a dose-dependent, statistically nonsignificant reduction in albuminuria (Figure 4F).

To identify the type of proliferating glomerular cells targeted by inhibition of the MEK-ERK module in anti-Thy1.1 GN, immunohistochemical double-staining was performed. Staining with BrdU was combined with cell type-specific immunohistochemical marker staining. The number of proliferating MC was significantly reduced in rats treated with high-dose U0126 (100 mg/kg body wt, twice daily), compared with untreated rats with anti-Thy1.1 GN (Figure 5A). Compared with proliferating MC, the total number of proliferating glomerular monocytes/macrophages was much lower (Figure 5B). Furthermore, the number of double-positive (BrdU- and ED1-

positive) cells in rats with mesangiproliferative GN was not affected by U0126 (Figure 5B). Double-staining for proliferating glomerular endothelial cells demonstrated no effect of treatment with the MEK inhibitor in nephritic animals (data not shown).

Discussion

In this study, we demonstrate for the first time that pharmacologic compounds can inhibit renal ERK activity *in vivo* and, more importantly, that such interventions can prevent overshooting cellular proliferation in mesangiproliferative GN. These data provide strong evidence for ERK being a putative regulator of the proliferative response to renal immune injury *in vivo*.

Most of our current knowledge regarding the physiologic relevance of MAP kinases is based on *in vitro* studies with cultured cells. The MAP kinase ERK plays a pivotal role in the regulation of important cellular functions such as proliferation, differentiation, and apoptosis (1). In cultured cell lines, mitogenic stimulation by various extracellular agonists is correlated with ERK activation (1). More importantly, dominant-negative interfering mutants of Ras or Raf-1 (components upstream of MEK in the ERK signaling cascade) have been demonstrated to inhibit growth factor-induced cell proliferation (18,19), whereas constitutively activated Raf-1 induces cell proliferation (18). Furthermore, dominant-negative or constitutively active mutants of MEK inhibit or accelerate NIH3T3 cell proliferation, respectively (20,21), and constitutively active MEK has been demonstrated to induce cellular transformation (22). Finally, catalytically inactive mutants of ERK and its antisense cDNA inhibit proliferation (23). These *in vitro* data indicate an essential role for the ERK cascade in the control of cellular proliferation. Recently, we were able to describe the *in vivo* activation of ERK in renal proliferative inflammatory glomerular diseases in rats, namely anti-glomerular basement membrane GN (7) and experimental mesangiproliferative GN (8). During the course of anti-Thy1.1 GN, we demonstrated that maximal activation of ERK was detectable in phases of the disease characterized by augmented glomerular cell prolifera-

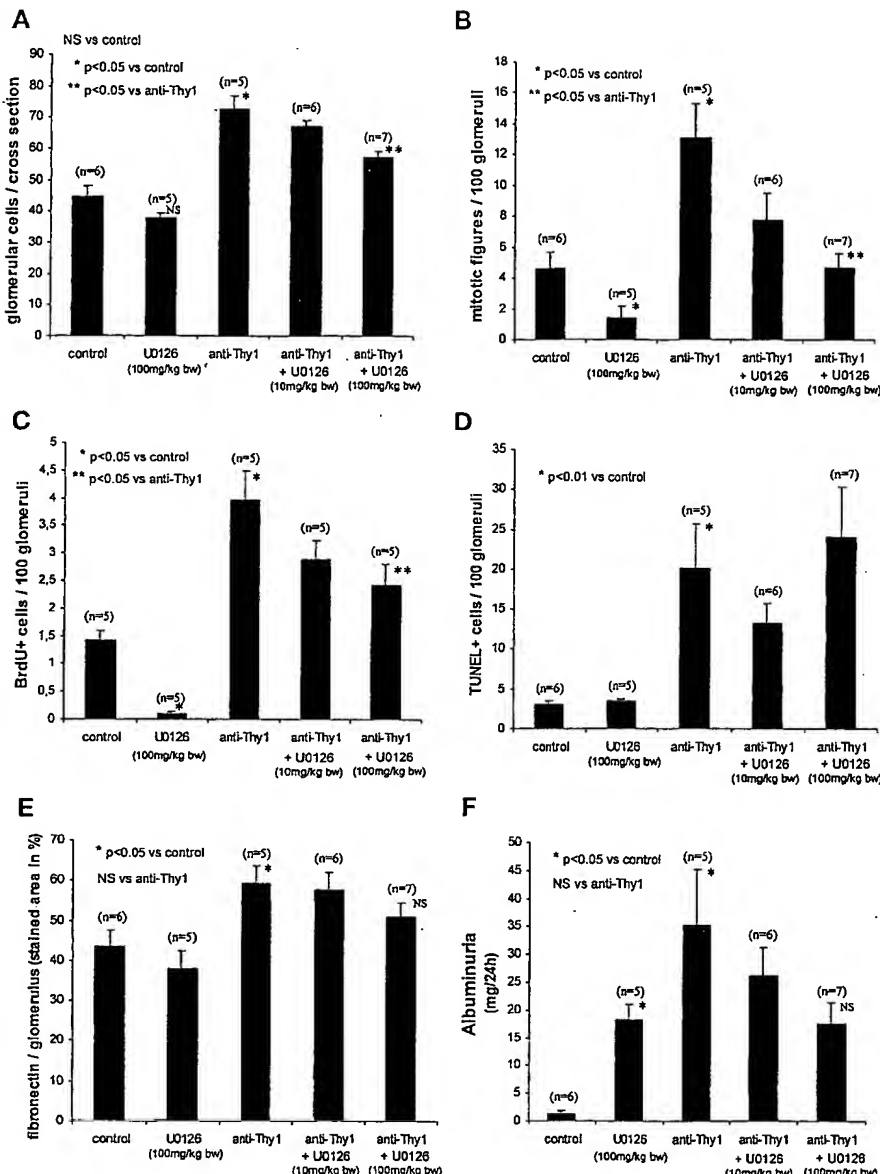


Figure 4. U0126 inhibition of glomerular cell proliferation in anti-Thy1.1 GN. The rats received injections of U0126 or vehicle as described above. (A) Number of glomerular cells per glomerulus, estimated as the number of nuclei per glomerular cross-section, after staining with periodic acid-Schiff stain. (B) Glomerular cell proliferation assayed in rats 6 d after induction of anti-Thy1.1 GN, as the number of mitotic figures in 100 glomerular cross-sections. (C) Glomerular cell proliferation assayed in rats 6 d after induction of anti-Thy1.1 GN, as the number of 5-bromo-2'-deoxyuridine (BrdU)-positive cells in 100 glomerular cross-sections. (D) Glomerular apoptosis and cell death assessed with the terminal deoxynucleotidyl transferase-mediated dUTP-biotin nick-end-labeling (TUNEL) assay. (E) Immunohistochemical staining for fibronectin, for assessment of extracellular matrix production in rats given injections of U0126 or vehicle, as described above. The stained area per glomerulus was measured by grid counting. (F) Urinary albumin excretion assayed 6 d after induction of anti-Thy1.1 GN.

tion (8). Although our data suggested that ERK contributed to glomerular proliferation *in vivo*, no interventional studies were available that examined whether inhibition of ERK activation could prevent cellular proliferation in inflammatory diseases, especially with respect to the kidney. Because we demonstrated the induction of MEK protein expression in anti-Thy1.1 GN (8), a pharmacologic inhibitor of MEK (U0126) seemed to be an attractive tool to prevent activation of the MEK-ERK module. In this study, U0126, when administered intraperitoneally

twice daily, dose-dependently prevented glomerular ERK activation in anti-Thy1.1 GN. Furthermore, treatment with the MEK inhibitor reduced glomerular cell proliferation (the characteristic feature of experimental mesangioproliferative GN) and seemed to decrease pathologic proteinuria in this disease model. In accordance with our findings, another group recently demonstrated *in vivo* that inhibition of the ERK signaling cascade could reduce the growth of colon cancer in mice (24).

As observed previously (8), the kinetics of ERK activation

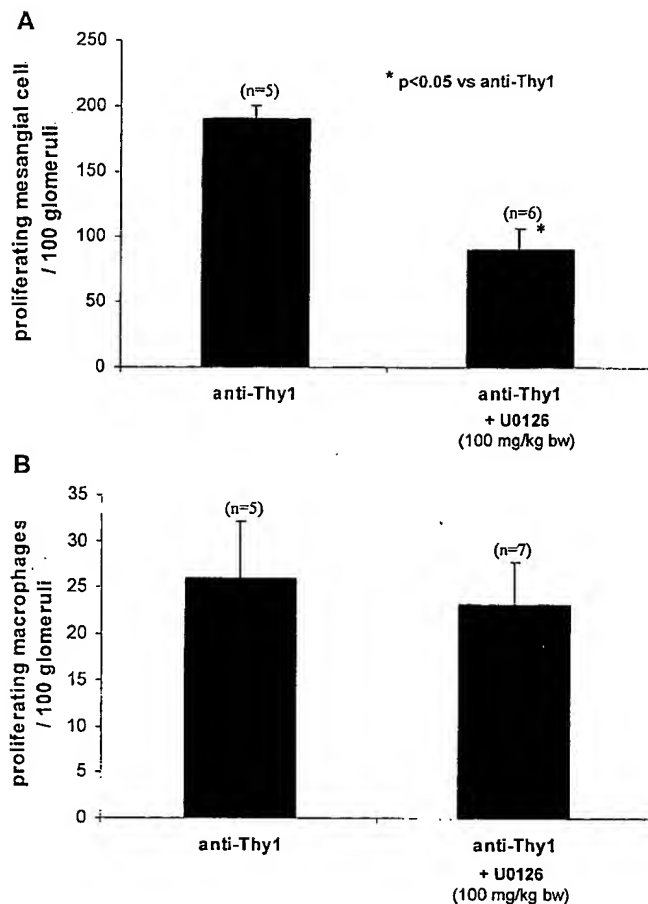


Figure 5. U0126 inhibition of the proliferation of glomerular MC *in vivo*. Immunohistochemical double-staining was performed with rats given injections of U0126 or vehicle, as described above. (A) Effect of treatment with U0126 on the number of glomerular proliferating MC. Sections from animals given injections of the anti-Thy1.1 antibody were stained for BrdU and α -smooth muscle actin. (B) Effect of treatment with U0126 on the number of glomerular cells double-positive for BrdU and the monocyte/macrophage marker ED1.

during the course of anti-Thy1.1 GN suggested that resident glomerular cells, rather than infiltrating cells, are the sites of altered intracellular MAP kinase signaling. The study presented here supports that conclusion, because our data demonstrated that MC, rather than infiltrating monocytes/macrophages, were the main glomerular targets of MEK-ERK inhibition in mesangiproliferative GN. Cellular proliferation of intrinsic glomerular cells is thought to be essential for the progression of proliferative GN to end-stage renal disease (16). The proliferative response to injury in GN may be augmented by a convergence of multiple cytokines at ERK, inducing its activation. We previously demonstrated that PDGF is a major extracellular factor in the progression of anti-Thy1.1 GN (25). Because we demonstrated here that inhibition of ERK in cultured MC potently decreased PDGF-induced proliferation, it is tempting to speculate that the demonstrated effect of ERK inhibition on glomerular proliferation in mesangiproliferative

GN might be attributable, in part, to inhibition of PDGF-induced intracellular signaling events *in vivo*.

The use of the MEK inhibitor U0126 allowed us to establish that inhibition of intracellular ERK activity substantially decreased glomerular cell proliferation in experimental mesangiproliferative GN, thus providing a novel strategy for the treatment of proliferative responses to immune injury. Such a mechanism-based therapy might be a potential approach not only in mesangiproliferative GN but also in other renal or extrarenal immune diseases associated with increased cellular proliferation. However, it is essential to establish the pathophysiological relevance of the MEK-ERK module in each form of immune injury, to identify the diseases that are most likely to benefit from treatment with a MEK inhibitor. Such studies, other than this study, have not been performed. In healthy control rats, inhibition of basal glomerular proliferation, in association with mild albuminuria, was observed. These changes were not correlated with detectable pathologic features in renal histologic assessments. No side effects of treatment with U0126 were observed in rats with anti-Thy1 GN during the course of this study. However, on the basis of knowledge regarding the ERK signaling cascade, the question of whether other proliferating cells, *e.g.*, hematopoietic cells, may be affected by long-term systemic suppression of the MEK-ERK signaling module must be explored.

In conclusion, this study provides new insights into the pathogenesis of glomerular proliferation in response to immune injury, with compelling support for the pivotal role of the ERK signaling cascade in mesangiproliferative GN. Furthermore, our data point to a new therapeutic strategy for the treatment of proliferative GN, *i.e.*, inhibition of MEK as part of a mechanism-based therapeutic concept.

Acknowledgments

We gratefully acknowledge the assistance of Jennifer Zimmer, Gabriele Dietzel, Gertrud Minartz, Kerstin Schenk, and Andrea Cosler. This work was supported by Grants Bo 1288/13-1 (to Dr. Bokemeyer) and SFB 542/C7 (to Drs. Floege and Ostendorf) from the Deutsche Forschungsgemeinschaft and in part by a BONFOR research grant from the Faculty of Medicine, University of Bonn. We thank A. Christine Tabakka, Jia-Sheng Yan, and Dr. Christopher A. Teleha for the synthesis of U0126.

References

1. Bokemeyer D, Sorokin A, Dunn MJ: Multiple intracellular MAP kinase signaling cascades. *Kidney Int* 49: 1187–1198, 1996
2. Hill CS, Treisman R: Transcriptional regulation by extracellular signals: Mechanisms and specificity. *Cell* 80: 199–211, 1995
3. Payne DM, Rossomando HJ, Martino P, Erickson AK, Her JH, Schbanowitz J, Hunt DF, Weber MJ, Sturgill TW: Identification of the regulatory phosphorylation sites in pp42/mitogen-activated protein kinase (MAP kinase). *EMBO J* 10: 885–892, 1991
4. Ono K, Han J: The p38 signal transduction pathway: Activation and function. *Cell Signal* 12: 1–13, 2000
5. Lee JD, Ulevitch RJ, Han J: Primary structure of BMK1: A new mammalian MAP kinase. *Biochem Biophys Res Commun* 213: 715–724, 1995

6. Abboud HE: Growth factors in glomerulonephritis. *Kidney Int* 43: 252–267, 1992
7. Bokemeyer D, Guglielmi KE, McGinty A, Sorokin A, Lianos EA, Dunn MJ: Activation of extracellular signal-regulated kinase in proliferative glomerulonephritis in rats. *J Clin Invest* 100: 582–588, 1997
8. Bokemeyer D, Ostendorf T, Kunter U, Lindemann M, Kramer HJ, Floege J: Differential activation of mitogen-activated protein kinases in experimental mesangiproliferative glomerulonephritis. *J Am Soc Nephrol* 11: 232–240, 2000
9. Floege J, Eng E, Young BA, Johnson RJ: Factors involved in the regulation of glomerular mesangial cell proliferation *in vitro* and *in vivo*. *Kidney Int* 43: S47–S54, 1993
10. Favata MF, Horiuchi KY, Manos EJ, Daulerio AJ, Stradley DA, Feeser WS, Van Dyk DE, Pitts WJ, Earl RA, Hobbs F, Copeland RA, Magolda RL, Scherle PA, Trzaskos JM: Identification of a novel inhibitor of mitogen-activated protein kinase kinase. *J Biol Chem* 273: 18623–18632, 1998
11. Bokemeyer D, Sorokin A, Dunn MJ: Differential regulation of the dual-specificity protein-tyrosine phosphatases CL100, B23 and PAC1 in mesangial cells. *J Am Soc Nephrol* 8: 40–50, 1997
12. Misra RP: Isolation of glomeruli from mammalian kidney by graded sieving. *Am J Clin Pathol* 58: 135–139, 1972
13. Johnson RJ, Garcia RL, Pritzl P, Alpers CE: Platelets mediate glomerular cell proliferation in immune complex nephritis induced by anti-mesangial cell antibodies in the rat. *Am J Pathol* 136: 369–374, 1990
14. Gavrieli Y, Sherman Y, Ben-Sasson SA: Identification of programmed cell death *in situ* via specific labeling of nuclear DNA fragmentation. *J Cell Biol* 119: 493–501, 1992
15. Kim YG, Suga SI, Kang DH, Jefferson JA, Mazzali M, Gordon KL, Matsui K, Breiteneder-Geleff S, Shankland SJ, Hughes J, Kerjaschki D, Schreiner GF, Johnson RJ: Vascular endothelial growth factor accelerates renal recovery in experimental thrombotic microangiopathy. *Kidney Int* 58: 2390–2399, 2000
16. Floege J, Ostendorf T, Janssen U, Burg M, Radeke HH, Vargeese C, Gill SC, Green LS, Janjic N: Novel approach to specific growth factor inhibition *in vivo*: Antagonism of platelet-derived growth factor in glomerulonephritis by aptamers. *Am J Pathol* 154: 169–179, 1999
17. Wang Y, Simonson MS, Pouysségur J, Dunn MJ: Endothelin rapidly stimulates mitogen-activated protein kinase activity in rat mesangial cells. *Biochem J* 287: 589–594, 1992
18. Miltenerger RJ, Cortner J, Farnham PJ: An inhibitory Raf-1 mutant suppresses expression of a subset of v-Raf-activated genes. *J Biol Chem* 268: 15674–15680, 1993
19. Pronk GJ, Bos JL: The role of p21^{ras} in receptor tyrosine kinase signaling. *Biochem Biophys Acta* 1198: 131–147, 1994
20. Seger R, Seger D, Reszka AA, Munar ES, Eldar-Finkelman H, Dobrowolska G, Jensen AM, Campbell JS, Fischer EH, Krebs EG: Overexpression of mitogen-activated protein kinase kinase (MAPKK) and its mutants in NIH 3T3 cells. *J Biol Chem* 269: 25699–25709, 1994
21. Brunet A, Pages G, Pouysségur J: Constitutively active mutants of MAP kinase kinase (MEK1) induce growth factor-relaxation and oncogenicity when expressed in fibroblasts. *Oncogene* 9: 3379–3387, 1994
22. Mansour SJ, Matten WT, Hermann AS, Candia JM, Rong S, Fukasawa K, Vande Woude GF, Ahn NG: Transformation of mammalian cells by constitutively active MAP kinase kinase. *Science (Washington DC)* 265: 966–970, 1994
23. Pages G, Lenormand P, L'Allemand G, Chambard JC, Meloche S, Pouysségur J: Mitogen-activated protein kinase p42^{mapk} and p44^{mapk} are required for fibroblast proliferation. *Proc Natl Acad Sci USA* 90: 8319–8323, 1993
24. Sebolt-Leopold JS, Dudley DT, Herrera R, Van Beclaere K, Wiland A, Gowan RC, Tecle H, Barrett SD, Bridges A, Przybranowski S, Leopold WR, Saltiel AR: Blockade of the MAP kinase pathway suppresses growth of colon tumors *in vivo*. *Nature Med* 5: 810–816, 1999
25. Ostendorf T, Kunter U, Grone HJ, Bahlmann F, Kawachi H, Shimizu F, Koch KM, Janjic N, Floege J: Specific antagonism of PDGF prevents renal scarring in experimental glomerulonephritis. *J Am Soc Nephrol* 12: 909–918, 2001

Sustained extracellular signal-regulated kinase activation by 6-hydroxydopamine: implications for Parkinson's disease

Scott M. Kulich and Charleen T. Chu

Department of Pathology, Division of Neuropathology, University of Pittsburgh School of Medicine, Pittsburgh, Pennsylvania, USA

Abstract

Although the toxin 6-hydroxydopamine (6-OHDA) is utilized extensively in animal models of Parkinson's disease, the underlying mechanism of its toxic effects on dopaminergic neurons is not completely understood. We examined the effects of 6-OHDA on the CNS-derived tyrosine hydroxylase expressing B65 cell line, with particular attention to the regulation of the extracellular signal-regulated protein kinases (ERK). 6-OHDA elicited a dose-dependent cytotoxicity in B65 cells. Toxic doses of 6-OHDA also elicited a biphasic pattern of ERK phosphorylation with a prominent sustained phase, a pattern that differed from that observed with hydrogen peroxide (H_2O_2) treatment. 6-OHDA-elicited ERK

phosphorylation was blocked by PD98059, an inhibitor of the upstream mitogen activated protein kinase kinase (MEK) that phosphorylates and activates ERK. PD98059 also conferred protection against 6-OHDA cytotoxicity, but did not affect H_2O_2 toxicity in B65 cells. These results suggest that ERK activation plays a direct mechanistic role in 6-OHDA toxicity, rather than representing a protective compensatory response, and raise the possibility that abnormal patterns of ERK activation may contribute to dopaminergic neuronal cell death.

Keywords: dopaminergic cell death, mitogen-activated protein kinases, oxidative stress.

J. Neurochem. (2001) 77, 1058–1066.

Parkinson's disease, defined clinically by the triad of tremor, bradykinesia, and rigidity, is a common neurodegenerative disease. Although Parkinson's disease may affect younger individuals with specific genetic susceptibilities, the majority of cases occur sporadically in the aging population and lack a well-defined etiology (Moghal *et al.* 1994). The neuropathologic findings of Parkinson's disease are characterized by selective neuronal death affecting the locus ceruleus, dorsal motor nucleus of vagus, nucleus basalis of Meynert and, most importantly, the dopaminergic neurons of the substantia nigra pars compacta (SNpc) (reviewed in (Lang and Lozano 1998). It is the loss of the striatal projections from the SNpc neurons that is believed to result in the majority of symptoms in Parkinson's disease. The mechanisms leading to neuronal cell death in Parkinson's disease remain unclear.

Insight into potential mechanisms contributing to neurodegeneration in Parkinson's disease has been gained from animal models of Parkinson's disease. One such model involves the neurotoxin 6-hydroxydopamine (6-OHDA). 6-OHDA is a dopamine analog that readily undergoes non-enzymatic oxidation producing hydrogen peroxide (H_2O_2), superoxide, and hydroxyl radical at physiologic pH (Cohen and Heikkila 1974). Moreover, intrastriatal injections of

6-OHDA result in a parkinsonian pattern of neuronal loss in rats (Ungerstedt 1968). Although used as an exogenous neurotoxin in this model, there is evidence suggesting that 6-OHDA can be formed from dopamine *in vivo*. The neurons within the SNpc contain increased iron in Parkinson's disease (Hirsch *et al.* 1991). In addition, the activities of catalase and glutathione peroxidase, the major enzymes responsible for the elimination of H_2O_2 , are reduced in Parkinson's disease brains (Ambani *et al.* 1975;

Received November 22, 2000; revised manuscript received February 13, 2001; accepted February 14, 2001.

Address correspondence and reprint requests to C. T. Chu, Room A-516, UPMC Presbyterian, 200 Lothrop St., Pittsburgh, PA 15213, USA. E-mail: chu@np.awing.upmc.edu

Abbreviations used: DH10, DME media with 10 mM HEPES, 2 mM L-glutamine, 10% fetal calf serum; ECL, enhanced chemiluminescence; ERK, extracellular signal-regulated protein kinase; HRP, horseradish peroxidase; JNK, c-Jun N-terminal kinase/stress activated protein kinase; LDH, lactate dehydrogenase; MAP, mitogen activated protein; MEK, kinase that phosphorylates and activates ERK (also known as MAP kinase kinase); MTS, [3-(4,5-dimethylthiazol-2-yl)-5-(3-carboxymethoxyphenyl)-2-(4-sulfophenyl)-2H-tetrazolium, inner salt]; 6-OHDA, 6-hydroxydopamine; PBST, phosphate buffered saline with 0.3% (w/v) Tween-20; PMS, phanazine methsulfate; SNpc, substantia nigra pars compacta.

Kish *et al.* 1985). In the presence of free ferric iron and H_2O_2 , the major product of dopamine oxidation has been reported to be 6-OHDA (Jameson and Linert 2000). Indeed, 6-OHDA is elevated in the urine of Parkinson's disease patients treated with levodopa (Andrew *et al.* 1993), suggesting that 6-OHDA may play a role in parkinsonian disease progression.

Although many lines of data support the role of oxidative mediators in 6-OHDA-induced neurotoxicity, the exact mechanisms by which 6-OHDA elicits its neurotoxic effects have yet to be fully elucidated. Mice that overexpress superoxide dismutase show protection from intraventricular injections of 6-OHDA (Asanuma *et al.* 1998). 6-OHDA can inhibit mitochondrial complex I activity (Glinka and Youdim 1995), potentially contributing to increased mitochondrial superoxide generation. In addition, other non-mitochondrial mechanisms may also contribute to 6-OHDA toxicity. Activation of c-Jun N-terminal kinase (JNK) occurs in response to 6-OHDA in the dopaminergic MN9D cell line (Choi *et al.* 1999). JNK is a member of the mitogen-activated protein (MAP) kinase family, protein serine/threonine kinases that play critical roles in cellular responses to a wide range of extracellular stimuli. JNK, p38 MAP kinase, and extracellular signal-regulated kinases (ERK) comprise the three major classes of MAP kinases. The dynamic balance between branches of the MAP kinase family is believed to regulate neuronal decisions to live or die in response to stressors (Xia *et al.* 1995). In particular, ERK activation may play a pivotal role.

Many neuroprotective/neurotrophic factors activate receptor tyrosine kinases. A major mechanism by which these kinases transmit signals is through ERK, which undergoes a dual phosphorylation event leading to its activation (reviewed in Segal and Greenberg 1996). ERK activation appears to antagonize apoptotic pathways in some cell systems (Xia *et al.* 1995; Holmström *et al.* 1998). Several recent studies, however, indicate that ERK activation may also play a pathologic role in neurons exposed to increased oxidative stress (Oh-hashi *et al.* 1999; Stanciu *et al.* 2000). The effects of 6-OHDA upon ERK signaling pathways are unknown.

This study was designed to investigate the role of ERK activation in neuronal cell responses to 6-OHDA. The rat CNS-derived B65 cell line exhibits electrically excitable membranes that can produce regenerative action potentials, expresses tyrosine hydroxylase and neuronal markers, binds α -neurotoxin, and extends neurites in response to low serum or dibutyryl cAMP (Schubert *et al.* 1974). 6-OHDA elicited sustained ERK phosphorylation in B65 cells that could be inhibited by the MEK inhibitor PD98059. PD98059 also conferred significant protection against 6-OHDA cytotoxicity. These effects appeared specific to 6-OHDA, as they could not be recapitulated with comparable doses of H_2O_2 . These results suggest that abnormal patterns of ERK

activation may contribute to mechanisms of dopaminergic neuron death relevant to Parkinson's disease.

Materials and methods

Chemical reagents (except where specified) were purchased from Sigma (St Louis, MO, USA).

Cell culture

Cell culture reagents were purchased from BioWhittaker (Walkerville, MD, USA). Cell culture plates were purchased from Corning (Acton, MD, USA). B65 cells were the kind gift of Dr David Schubert of the Salk Institute (Schubert *et al.* 1974). B65 cells were maintained in Dulbecco's modified Eagle's medium (DMEM) supplemented with 10 mM HEPES, 2 mM L-glutamine, and 10% heat-inactivated fetal calf serum (FCS; DH10). Cells were plated at a density of 140 cells/mm² for all experiments and grown for 2 days prior to use at 37°C in a humidified incubator with 5% CO_2 .

Toxicity assays

6-OHDA was prepared fresh for each assay in ice-cold 0.05% (wt/vol) ascorbate. H_2O_2 was diluted in water. The concentration of the H_2O_2 stock solution was confirmed by measuring the absorbance at 240 nm using the extinction coefficient of 0.0437 cm/mm⁻¹. Cell injury in response to 6-OHDA and H_2O_2 was determined using two independent methodologies:

Lactate dehydrogenase (LDH) release assay

Release of LDH into the culture medium was determined using the Sigma 340-UV LDH detection system. Briefly, B65 cells, grown in a 96-well plate format, were exposed to the varying concentrations of 6-OHDA, H_2O_2 , or vehicle for 18–20 h. Following visual inspection and gentle centrifugation (5 min, 225 g), aliquots were obtained from the supernatant. An equal volume of 2% (v/v) Triton X-100 was added to the wells and cells were lysed using vigorous pipetting. LDH activities in supernatant and lysate were determined by measuring the decrease in absorbance at 340 nm associated with reduction of pyruvate in a linear velocity reaction (Wroblewski and LaDue 1955). Levels of LDH released into the supernatant were expressed as percent of total LDH activity.

MTS assay

The CellTiter 96 Aqueous non-radioactive cell proliferation assay (Promega, Madison, WI, USA), which measures the conversion of the tetrazolium salt [3-(4,5-dimethylthiazol-2-yl)-5-(3-carboxymethoxyphenyl)-2-(4-sulfophenyl)-2H-tetrazolium, inner salt] (MTS), was used as follows: Twenty microliters of a 1:20 mixture of PMS (phanazine methsulfate): MTS was added to each well of a 96-well plate containing treated cells in a final volume of 100 μ L of media. The A_{490} was determined immediately following addition of PMS: MTS, and again following a 4-h incubation of the cells at 37°C, with the change in absorbance representing enzymatic conversion of tetrazolium to formazan. For experiments utilizing 6-OHDA, each concentration of 6-OHDA utilized had its own background control (media plus 6-OHDA in the absence of cells), since superoxide radicals generated by 6-OHDA may react directly with tetrazolium dyes such as MTS (Sutherland and Learmonth 1997). Using these controls, we determined that little to

no further superoxide was generated by 6-OHDA following overnight incubations. Assay conditions were thus selected to minimize this non-enzymatic contribution. All data are expressed as a percentage of control values obtained from cells treated with vehicle alone.

MEK inhibitor experiments

PD98059 (Cell Signaling, Beverly, MA, USA) was prepared as a 50- μ M stock in 100% dimethylsulfoxide (DMSO). Thirty minutes prior to the addition of 6-OHDA or H_2O_2 , cells were exposed to fresh DH10 media containing: (a) 50 μ M PD98059, (b) 0.1% DMSO (concentration of vehicle present in PD98059 treated cells), or (c) no additional additives.

Cell lysates and immunoblotting

Cell lysates were obtained at various time points using lysis buffer containing 0.1% Triton X-100 and a protease/phosphatase inhibitor cocktail as previously described (Chu *et al.* 1997). For pulse-chase experiments, the pulse of 6-OHDA was terminated by aspiration of the media containing 6-OHDA, washing once with the same volume of fresh DH10, and then growing the cells in fresh DH10. Equal amounts of protein, as determined by Coomassie Plus Protein Assay (Pierce, Rockford, IL, USA), were subjected to electrophoresis through 5–15% polyacrylamide gels under reducing conditions (Chu and Pizzo 1993), and transferred to Immobilon-P membranes (Millipore, Bedford, MA, USA). The membranes were blocked for 2 h with 5% non-fat dry milk in 20 mM potassium phosphate, 150 mM potassium chloride, pH 7.4 containing 0.3% (w/v) Tween-20 (PBST) and then probed overnight at room temperature (25°C) with an activation-specific antiphospho-ERK antibody, which only recognizes ERK that is phosphorylated on both Y202 and T204 (Cell Signaling, Beverly, MA, USA; diluted 1 : 2000 in PBST), followed by incubation with HRP-conjugated sheep-anti-mouse IgG (Amersham, Piscataway, NJ, USA). Antibody detection was carried out using an ECL detection kit (Amersham, Piscataway, NJ, USA). Blots were then stripped as previously described (Chu *et al.* 1997), and reprobed with antitotal ERK kinase (Upstate Biotechnology, Lake Placid, NY, USA) (1 : 10 000, 1 h, room temperature, 1% non-fat milk in PBST) followed by incubation with HRP-conjugated donkey anti-rabbit IgG (Amersham, Piscataway, NJ, USA) and ECL detection. Specificity of the antisera were confirmed by substitution of non-immune antisera for the primary antibodies, and by inclusion of control lanes containing lysates from a fibroblast-line treated with known activators of ERK phosphorylation (Chu *et al.* 1997). Densitometric analysis of blots was performed using the electrophoresis documentation and analysis system 120 (Kodak, Rochester, NY, USA).

Results

6-OHDA toxicity in B65 cells

Exposure of B65 cells to 6-OHDA resulted in dose-dependent cell injury. Incubation of B65 cells overnight in the presence of 6-OHDA resulted in cell injury as detected by either increased amounts of LDH released from the cells or decreased ability of the cells to metabolize the tetrazolium dye MTS (Fig. 1a). H_2O_2 , a potential

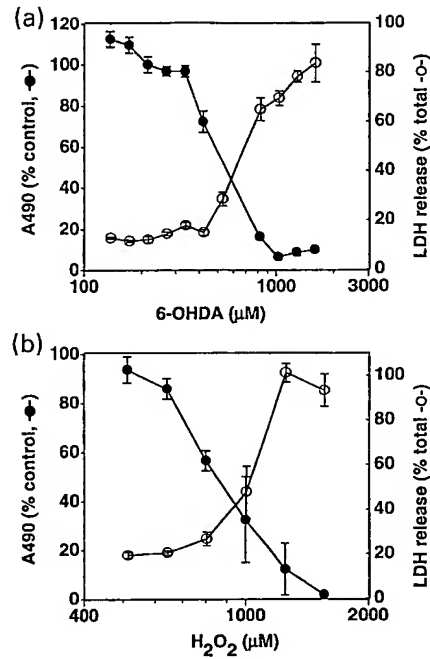


Fig. 1 Cytotoxicity of 6-OHDA and H_2O_2 in B65 cells. B65 cells were exposed to (a) 6-OHDA or (b) H_2O_2 for 18–20 h. Cell injury was determined by measuring LDH activity released into the media (○) or by altered MTS metabolism (●). Values were normalized to total LDH activity or the A₄₉₀ of vehicle treated control cells, respectively, as described in the Materials and methods section. Each value represents the mean of triplicate wells \pm SE. Each experiment was performed independently at least three times. Representative plots are illustrated.

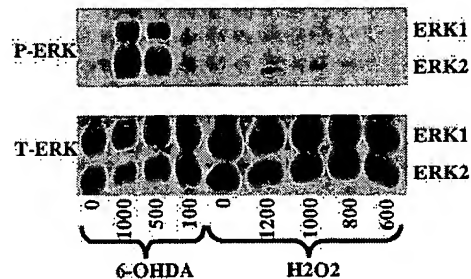


Fig. 2 Dose-response study of ERK activation in B65 cells. Cells were treated with the indicated μ M concentrations of 6-hydroxydopamine (6-OHDA), H_2O_2 (H_2O_2) or vehicle (0.05% ascorbate for 6-OHDA, water for H_2O_2) for 18 h. The cells were then lysed and equal amounts of protein (20 μ g) were subjected to immunoblot analysis using an antibody specific for activated dually phosphorylated ERK (top, P-ERK). The blots were then stripped and reprobed with antibody against total ERK (bottom, T-ERK). Blots depicted are representative of eight independent experiments.

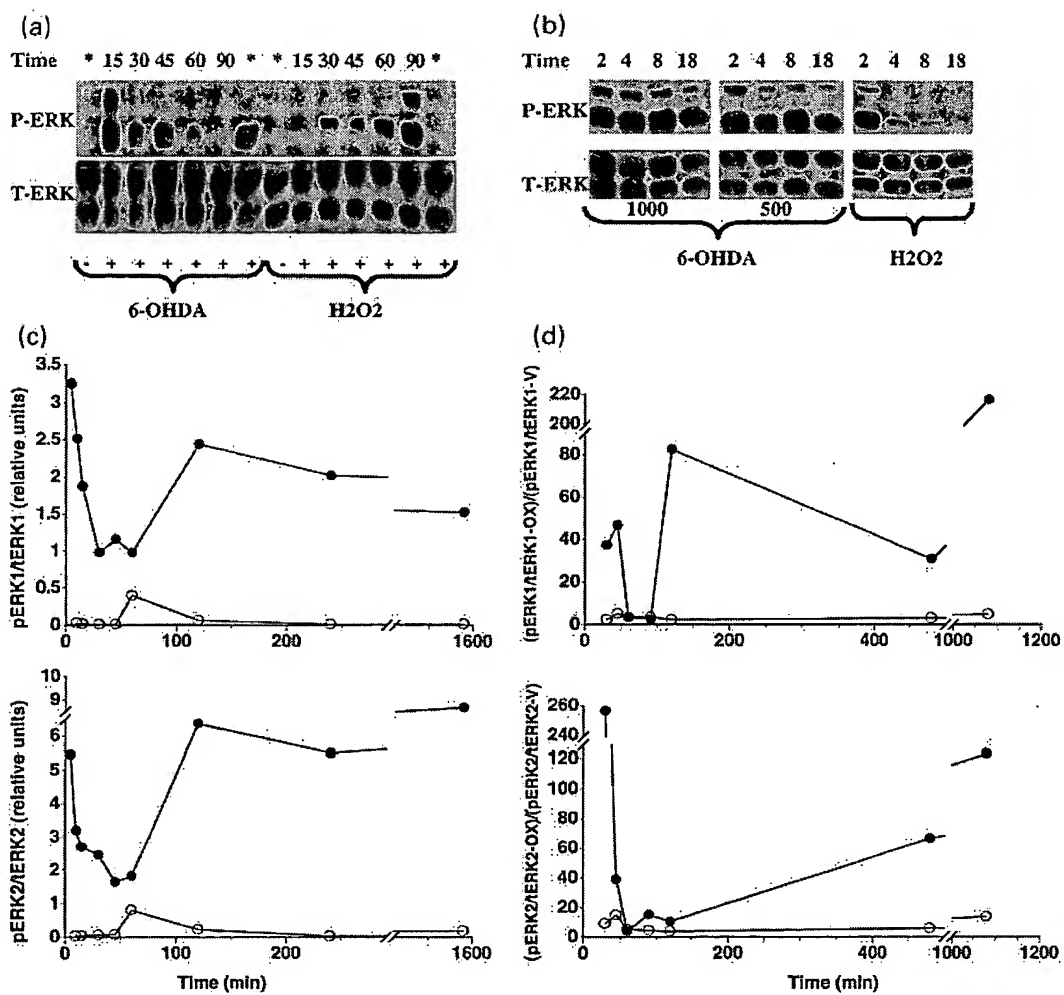


Fig. 3 Kinetics of ERK activation in B65 cells in response to 6-OHDA and H₂O₂. (a) Cells treated with 500 μ M 6-hydroxydopamine (6-OHDA) or 1 mM H₂O₂ (H₂O₂) for the indicated times (minutes) were lysed and equal amounts of protein (50 μ g) were subjected to immunoblot analysis using antibody against the activated form of ERK (top, P-ERK). The blots were then stripped and reprobed with antibody against total ERK (bottom, T-ERK). Lanes designated with * were harvested following an overnight (16 h) incubation. Lanes designated with – were treated with the appropriate vehicle (0.05% ascorbate for 6-OHDA, water for H₂O₂). (b) Cells were treated with either 1000 or 500 μ M 6-OHDA or 1 mM H₂O₂ for the indicated time (hours) then subjected to immunoblot analysis as in (a). (c) Immunoblots from cells treated with 1000 μ M 6-OHDA were subjected to densitometric analysis, and the data for the ERK1 (top panel) and ERK2 (bottom panel) isoforms from a representative time-course is shown. Closed circles (●) represent the

relative band intensity of phosphorylated ERK/total ERK elicited by 6-OHDA; open circles (○) represent the phosphorylated ERK/total ERK ratio observed in vehicle-treated cells. Cells treated with only fresh DH10 exhibited a pattern of ERK phosphorylation similar to that seen with the vehicle controls. (d) Immunoblots from cells treated with 500 μ M 6-OHDA and 1 mM H₂O₂ were subjected to densitometric analysis, and the data for the ERK1 (top panel) and ERK2 (bottom panel) isoforms from a representative time-course is shown. Closed circles represent the relative band intensity elicited by 6-OHDA while open circles represent the relative band intensity elicited by H₂O₂. Data are expressed as the ratio of phosphorylated ERK to total ERK elicited by the oxidizing agents (pERK/tERK-OX) normalized to the ratio of phosphorylated ERK to total ERK elicited in vehicle treated cells (pERK/tERK-V). Data shown in panels A-D are representative compilations of 10 independent time-course experiments.

byproduct of 6-OHDA metabolism (Cohen and Heikkila 1974), also exhibited a dose-dependent toxicity in B65 cells (Fig. 1b). The EC₅₀ for 6-OHDA and H₂O₂ under these conditions were 573 \pm 41 and 880 \pm 35 μ M, respectively

(mean \pm SEM, 10 independent experiments for each reagent). For subsequent experiments, the concentrations of 6-OHDA and H₂O₂ utilized were based upon the dose-response curves for the cell passage used.

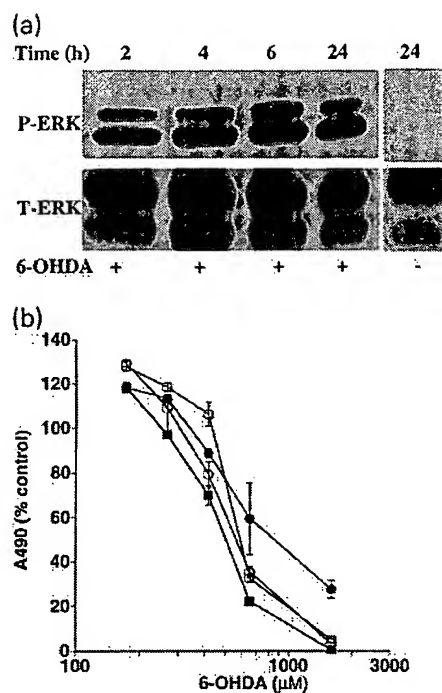


Fig. 4 Pulse-chase studies comparing ERK phosphorylation and cytotoxicity. (a) Cells were pulsed with 1 mM 6-hydroxydopamine (6-OHDA) for the indicated times (hours) at which time 6-OHDA was removed. The cells were washed with DH10 and then incubated in fresh DH10 for a total incubation time of 24 h. Immunoblot analysis of cell lysates was performed as described above. Cells treated with vehicle did not exhibit increased phosphorylation at any time point (24 h time point shown as an example). Data shown are representative of four independent experiments. (b) Cells were pulsed with various concentrations of 6-OHDA for the indicated times (2 h: ●, 4 h: ○, 6 h: ■, 22 h: □), washed and placed in fresh DH10 for a total incubation time of 22 h. Cell injury was determined using the MTS viability assay. Each value represents the mean of triplicate wells \pm SEM. The experiment was performed independently three times, and a representative plot is illustrated.

ERK phosphorylation elicited by 6-OHDA

Immunoblot analysis of cell lysates from B65 cells following an overnight exposure to 6-OHDA revealed strong induction of ERK phosphorylation affecting both the ERK1 (p44) and ERK2 (p42) isoforms (Fig. 2). The level of ERK activation was dose-dependent, with sublethal doses showing little ERK phosphorylation and lethal doses showing the greatest amount of ERK phosphorylation. This pattern of ERK phosphorylation did not appear to be a general response to cell injury or H_2O_2 generation since similar effective concentrations of H_2O_2 were not effective at eliciting ERK phosphorylation following overnight incubation (Fig. 2). Although 6-OHDA has not been reported to bind any known dopamine receptors, D_2 dopamine receptor stimulation may result in ERK activation

(Cai *et al.* 2000). Potential ligation of dopamine receptors by 6-OHDA did not contribute to these observations, however, as concentrations of up to 1 mM dopamine failed to elicit ERK phosphorylation.

Kinetics of 6-OHDA elicited ERK phosphorylation

In an attempt to better define the nature of 6-OHDA-mediated ERK activation in B65 cells, an analysis of the kinetics of ERK phosphorylation was performed. Although the kinetics of ERK phosphorylation following 6-OHDA treatment were slightly variable with different passages of B65 cells, a biphasic response with an intense early phosphorylation by 15 min, a decrease towards baseline levels at 60–90 min, followed by a second, sustained phase of phosphorylation was consistently observed (Fig. 3). Separate studies indicate that the initial phase of ERK activation may occur as early as 5 min after application of 6-OHDA. This phosphorylation response was not observed with vehicle-treated cells (Fig. 3c) or with cells treated with fresh media alone, indicating that this observation was not simply an effect of fresh media. In contrast to 6-OHDA, H_2O_2 , gave a unimodal response that was not sustained (Fig. 3). The sustained phase of 6-OHDA-mediated ERK phosphorylation peaked within 2–4 h of treatment and, unlike that observed following H_2O_2 treatment, remained substantially elevated above that observed in the vehicle control throughout the time course of the experiment (Figs 3c and d).

The continued presence of phosphorylated ERK elicited by 2–26 h exposures to 6-OHDA contrasts strikingly with growth factor receptor-mediated ERK phosphorylation, for which down-regulating systems rapidly terminate the response even in the continued presence of ligand. Because 6-OHDA undergoes fairly rapid auto-oxidation at physiologic pH (Cohen and Heikkila 1974), we wished to define the minimum duration of 6-OHDA exposure that would elicit sustained ERK phosphorylation. Pulse-chase experiments showed that in order to elicit sustained ERK

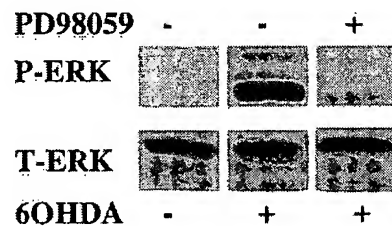


Fig. 5 Effect of the MEK inhibitor PD98059 upon 6-OHDA mediated ERK phosphorylation. B65 cells treated for 20 h with 500 μ M 6-hydroxydopamine (6-OHDA) in the presence (+) or absence (-) of 50 μ M PD98059 were lysed and equal amounts of protein (50 μ g) were subjected to immunoblot analysis using antibody against the activated form of ERK (top, P-ERK). The blots were then stripped and reprobed with antibody against total ERK (bottom, T-ERK).

phosphorylation, B65 cells required the presence of 6-OHDA for at least 2–4 h (Fig. 4a) since shorter exposures did not result in sustained ERK activation. Similarly, a 2-h pulse with 6-OHDA resulted in cytotoxicity, although a 4-h incubation was necessary to elicit dose-response curves identical to longer treatments (Fig. 4b). These experiments suggest that the pulse length that commits the cells to death correlates with the time it takes to achieve induction of the sustained phase of 6-OHDA elicited ERK-phosphorylation.

Inhibition of 6-OHDA-mediated ERK phosphorylation by PD98059

Sustained ERK phosphorylation secondary to 6-OHDA treatment could result from a variety of different mechanisms. Activation of upstream signaling molecules, inhibition of dephosphorylation, and inhibition of protein degradation have been previously observed as mediators of sustained ERK phosphorylation in different cellular contexts (Traverse *et al.* 1992; Runden *et al.* 1998; Hashimoto *et al.* 2000). In an attempt to better define the role of upstream activators of ERK in 6-OHDA-mediated sustained ERK phosphorylation, B65 cells were exposed to PD98059, an inhibitor of MEK 1/2, a dual potential protein kinase that is capable of directly activating ERK. As illustrated in Fig. 5, the presence of 50 μ M PD98059 substantially inhibited 6-OHDA-mediated sustained ERK phosphorylation, suggesting that 6-OHDA affects the signal transduction machinery upstream of MEK 1/2. The presence of PD98059 also inhibited the H_2O_2 -induced activation of ERK (data not shown).

Inhibition of 6-OHDA-mediated cytotoxicity by PD98059

Although traditionally associated with responses such as differentiation or proliferation, recent reports have implicated sustained ERK activation in oxidative toxicity to primary cortical neurons and the hippocampal neuronal cell line HT22 (Stanciu *et al.* 2000). In addition, compensatory up-regulation of neurotrophic factors or their receptors is a hypothetical possibility. In order to assess the role of ERK phosphorylation in 6-OHDA-mediated toxicity, B65 cells were exposed to 6-OHDA in the presence of PD98059. The presence of 50 μ M PD98059 resulted in decreased B65 injury in response to 6-OHDA as determined by both MTS and LDH release assays (Figs 6a and b). PD98059 had no effect on H_2O_2 -mediated cell injury as determined by MTS (Fig. 6c) or LDH release assays (data not shown). These results support a role for sustained ERK phosphorylation in 6-OHDA cytotoxicity in this tyrosine hydroxylase-expressing CNS neuronal cell line.

Discussion

Although the toxin 6-OHDA is utilized extensively in animal models of Parkinson's disease, the underlying mechanism of its toxic effects on dopaminergic neurons is

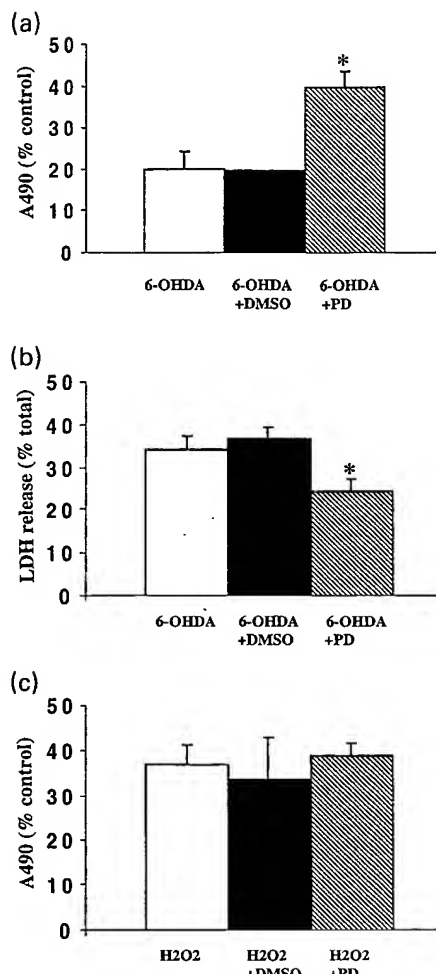


Fig. 6 Effect of PD98059 on 6-OHDA-mediated cytotoxicity. Following overnight exposure of B65 cells to 655 μ M 6-OHDA in the absence (white bar) or presence (hatched bar) of 50 μ M PD98059, cytotoxicity was determined utilizing MTS (a) and LDH release (b) assays. Cells treated with 6-OHDA in the presence of 0.1% DMSO, the vehicle in which the inhibitor was dissolved (black bar), showed values similar to those lacking DMSO. PD98059 treatment had no effect upon the A_{490} or total LDH values of ascorbate-treated control wells against which the other treatment conditions were normalized (A_{490} values: 2.26 ± 0.06 , untreated; 2.23 ± 0.08 PD98059 treated; total LDH values: 129 ± 27 IU/mL, untreated; 132 ± 23 IU/mL, PD 98059 treated). MTS data is a compilation of five independent experiments and LDH release data is a compilation of three independent experiments. Data are expressed as the mean \pm SEM. Analysis by two-tailed Student's *t*-tests yielded *p*-values of <0.05 (*). (c) Following overnight exposure of B65 cells to 1 μ M H_2O_2 in the absence (white bar) or presence (hatched bar) of 50 μ M PD98059, cytotoxicity was determined utilizing a MTS assay. Cells treated with H_2O_2 in the presence of 0.1% DMSO (black bar), showed values similar to those lacking DMSO. MTS data is a compilation of five independent experiments, and is expressed as the mean \pm SEM ($p = 0.75$, two-tailed Student's *t*-test).

not completely understood. As MAP kinase signaling cascades play important roles in neuronal survival and differentiation, this study was designed to investigate the effects of 6-OHDA upon activation of the ERK branch of the MAP kinase superfamily. A CNS-derived neuronal cell line was selected to generate a uniform population of tyrosine hydroxylase-expressing cells for cytotoxicity and immunoblot analysis. Using this model, two significant findings regarding potential mechanisms underlying 6-OHDA-mediated toxicity were observed. First, 6-OHDA, but not H_2O_2 , elicits a dose-dependent sustained activation of ERK. Second, PD98059, inhibits 6-OHDA-elicited ERK phosphorylation, and confers protection from 6-OHDA-mediated toxicity, but not H_2O_2 toxicity. These results suggest a specific detrimental role of ERK phosphorylation in 6-OHDA-mediated toxicity.

ERK isoforms are activated by neurotrophic factors such as brain-derived neurotrophic factor or glial cell line-derived neurotrophic factor, both of which are neuroprotective for dopaminergic neurons (Frim *et al.* 1994; Choi-Lundberg *et al.* 1997). While it has been well documented that ERK activation leads to favorable responses such as differentiation and neuroprotection, recent evidence has also implicated ERK in detrimental responses to oxidative stress. In neuroblastoma SH-SY5Y cells, sequential activation of both p38 and ERK contributes to peroxynitrite-induced apoptosis (Oh-hashi *et al.* 1999). An abnormal immunohistochemical staining pattern for phosphorylated ERK has also been observed in susceptible neurons from the brains of patients with Alzheimer's disease (Perry *et al.* 1999). In several non-neuronal cell types, apoptosis and inhibition of DNA synthesis are associated with ERK activation (Tombes *et al.* 1998; Bhat and Zhang 1999; Ishikawa and Kitamura 1999). In addition, recent studies in cell lines and primary cortical neurons suggest ERK activation may play a direct role in neuronal cytotoxicity (Stanciu *et al.* 2000). Although kinase inhibitor studies must always be interpreted with caution as the compound may have effects on unrecognized signaling pathways, PD98059 exhibits strong *in vitro* selectivity for inhibiting MEK 1/2 (Alessi *et al.* 1995). Since the development of sustained ERK phosphorylation correlates with commitment to death (Fig. 4), and PD98059, which effectively blocks 6-OHDA-mediated ERK phosphorylation (Fig. 5) confers protection (Fig. 6), this study offers additional support for the concept that sustained ERK phosphorylation can contribute to oxidative neuronal injury.

Two general patterns of ERK activation have been observed, transient and sustained (reviewed in Marshall 1995). The divergent roles of ERK phosphorylation patterns are well illustrated in PC12 cells, where transient ERK activation by epidermal growth factor leads to cell proliferation but sustained ERK activation by nerve growth factor leads to nuclear translocation of ERK and differentiation (Traverse *et al.* 1992). It is important to point out that,

in these physiologic patterns of ERK activation, the transient component peaks at 2 min and returns to baseline by ~60 min, whereas the 'sustained' component refers to elevation of ERK phosphorylation for 1.5–3 h. Much longer periods of ERK activation, as seen in this study, may prove detrimental, particularly in the setting of neuronal responses to oxidative stressors. For example, elevated ERK phosphorylation was reported in cortical neurons and a hippocampal cell line for 3–15 h in response to oxidative glutamate toxicity associated with glutathione depletion (Stanciu *et al.* 2000). Sustained ERK phosphorylation secondary to phosphatase inhibition appears to selectively target certain susceptible neuronal populations (Runden *et al.* 1998). This report is the first to demonstrate an association between the redox cycling 6-OHDA and sustained ERK activation that is not down-regulated >20 h following removal of the neurotoxin (Fig. 4a).

A second interesting observation is that B65 cells demonstrate a biphasic response to 6-OHDA (Fig. 3) with an initial robust ERK activation followed by a return towards baseline and a subsequent delayed, sustained ERK activation. The decrease in ERK phosphorylation at ~60–90 min is most prominent with lower doses of 6-OHDA, and this period of time may be associated with refractoriness to ERK activation by neurotrophic factors (CTC, unpublished observations). The previous reports of detrimental sustained ERK phosphorylation have not reported this early activation phase. Additional studies to define the contributions of these phases of ERK phosphorylation to the detrimental effect observed in B65 cells are currently being pursued.

While the concentrations of 6-OHDA utilized in the present study are higher than the doses reported in recent reports of 6-OHDA-mediated toxicity in primary cultures (Eggert *et al.* 1999; Lotharius *et al.* 1999), it is difficult to make direct comparisons between the experimental systems. Although highly enriched for neurons, primary cultures contain additional cell populations that may influence the responsiveness of the target neuron population, which often comprises only 5% of the cells (Lotharius *et al.* 1999). In addition, there are differences in the length of exposure to the toxin and the methodology used to assess cell injury. Finally, our preliminary studies utilizing differentiated B65 cells suggest that cell cycle status may also influence susceptibility to toxins.

Metabolism of 6-OHDA is complex and may generate several different reactive species. H_2O_2 and superoxide have both been shown to modulate the activities of protein kinases and protein phosphatases in multiple systems (reviewed in Suzuki *et al.* 1997; Klann and Thiels 1999). Although the kinetics of ERK phosphorylation in B65 differs between 6-OHDA, H_2O_2 (Fig. 3) and xanthine/xanthine oxidase-treated cells (unpublished observation), we cannot rule out a potential role for H_2O_2 and superoxide in

6-OHDA-mediated ERK activation based on the present studies. It is possible that intracellularly generated superoxide or interactions between H_2O_2 and superoxide are important. Another potential 6-OHDA metabolite, dopamine quinone, is an electron-deficient intermediate of dopamine metabolism that is capable of covalently modifying free or protein bound thiol groups. Modification of cys118 of ras has been associated with direct ras activation (Lander *et al.* 1997). Activation of a signaling molecule such as ras that lies upstream of ERK would be consistent with our findings that PD98059, an inhibitor of MEK 1/2, is capable of attenuating 6-OHDA-mediated sustained ERK activation. Additional studies will be required to further evaluate the potential contributions of these metabolic intermediates and to better define which members of the signal transduction cascade are responsible for 6-OHDA-mediated ERK activation.

Oxidative stress has been postulated to play a role in many neurodegenerative diseases (reviewed in Beal 1995). Our study lends further support to other studies indicating an association between oxidative stressors and sustained ERK activation in neuronal cells (Runden *et al.* 1998; Stanciu *et al.* 2000). While the relevance of these *in vitro* observations to *in vivo* situations is unclear, recent reports have described an abnormal pattern of activated ERK staining in pathologic states linked to increased oxidative stress. Increased levels of both total and activated ERK has been observed within atherosclerotic lesions of cholesterol-fed rabbits (Hu *et al.* 2000). An abnormal punctate staining pattern of activated ERK has also been described in susceptible neurons in the brains of patients with Alzheimer's disease (Perry *et al.* 1999). While the status of ERK activation in patients with Parkinson's disease is currently unknown, the involvement of ERK in 6-OHDA toxicity suggests that abnormal ERK activation could contribute to mechanisms of neuronal cell death relevant to Parkinson's disease.

Only recently has it been appreciated that oxidative species such as H_2O_2 and superoxide may play important roles in modulating signal transduction pathways (reviewed in Suzuki *et al.* 1997). This study links the redox cycling neurotoxin 6-OHDA, which is commonly used in parkinsonian models, to an unusual biphasic pattern of sustained ERK phosphorylation. As dopamine itself can also undergo redox cycling, and high doses of dopamine can contribute to oxidative toxicity both *in vivo* and *in vitro* (Hastings *et al.* 1996; Luo *et al.* 1998), similar mechanisms may contribute to enhanced susceptibility of dopaminergic neurons. As 6-OHDA can be identified in the urine of both control and Parkinson's disease patients, and it is elevated in patients that have received levodopa (Andrew *et al.* 1993), it is possible that these patterns of abnormal ERK activation can contribute to ongoing neuron loss and progression of Parkinson's disease. Identification of the oxidative

mechanisms involved and the members of the signal transduction cascade that are affected by 6-OHDA to yield sustained ERK activation would be important for understanding the molecular pathogenesis of neuronal loss relevant to Parkinson's disease and related neurodegenerative diseases.

Acknowledgements

We thank Dr Tim Oury for helpful discussions. Dr Chu is a Charles E. Culpeper Scholar in Medical Science, and this work was supported in part by the Rockefeller Brothers Fund, grant RO1 NS40817 from the National Institutes of Health, and grants from the Scaife Family Foundation of Pittsburgh, the American Parkinson Disease Association, and the National Parkinson Foundation.

References

- Alessi D. R., Cuenda A., Cohen P., Dudley D. T. and Saltiel A. R. (1995) PD 098059 is a specific inhibitor of the activation of mitogen-activated protein kinase kinase in vitro and in vivo. *J. Biol. Chem.* **270**, 27489–27494.
- Ambani L. M., Van Woert M. H. and Murphy S. (1975) Brain peroxidase and catalase in Parkinson disease. *Arch. Neurol.* **32**, 114–118.
- Andrew R., Watson D. G., Best S. A., Midgley J. M., Wenlong H. and Petty R. K. H. (1993) The determination of hydroxydopamines and other trace amines in the urine of Parkinsonian patients and normal controls. *Neurochem. Res.* **18**, 1175–1177.
- Asanuma M., Hirata H. and Cadet J. L. (1998) Attenuation of 6-hydroxydopamine-induced dopaminergic nigrostriatal lesions in superoxide dismutase transgenic mice. *Neuroscience* **85**, 907–917.
- Beal M. F. (1995) Aging, energy, and oxidative stress in neurodegenerative diseases. *Ann. Neurol.* **38**, 357–366.
- Bhat N. R. and Zhang P. (1999) H_2O_2 activation of multiple mitogen-activated protein kinases in an oligodendrocyte cell line: role of extracellular signal-regulated kinase in hydrogen peroxide-induced cell death. *J. Neurochem.* **72**, 112–119.
- Cai G., Zhen X., Uryu K. and Friedman E. (2000) Activation of extracellular signal-regulated protein kinases is associated with a sensitized locomotor response to D_2 dopamine receptor stimulation in unilateral 6-hydroxydopamine-lesioned rats. *J. Neurosci.* **20**, 1849–1857.
- Choi W. S., Yoon S. Y., Oh T. H., Choi E. J., O'Malley K. L. and Oh Y. J. (1999) Two distinct mechanisms are involved in 6-hydroxydopamine- and MPP⁺-induced dopaminergic neuronal cell death: role of caspases, ROS, and JNK. *J. Neurosci. Res.* **57**, 86–94.
- Choi-Lundberg D., Lin Q., Chang Y., Chiang Y., Hay C., Mohajeri H., Davidson B. and Bohn M. (1997) Dopaminergic neurons protected from degeneration by GDNF gene therapy. *Science* **275**, 838–841.
- Chu C. T. and Pizzo S. V. (1993) Receptor-mediated antigen delivery into macrophages: Complexing antigen to α_2 -macroglobulin enhances presentation to T-cells. *J. Immunol.* **150**, 48–58.
- Chu C. T., Everiss K. D., Batra S., Wikstrand C. J., Kung H.-J. and Bigner D. D. (1997) Receptor dimerization is not a factor in the signalling activity of a transforming variant epidermal growth factor receptor (EGFRvIII). *Biochem. J.* **324**, 855–861.
- Cohen G. and Heikkila R. E. (1974) The generation of hydrogen peroxide, superoxide radical, and hydroxyl radical by 6-hydroxydopamine,

dialuric acid, and related cytotoxic agents. *J. Biol. Chem.* **249**, 2447–2452.

Eggert K., Schlegel J., Oertel W., Wurz C., Krieg J. C. and Vedder H. (1999) Glial cell line-derived neurotrophic factor protects dopaminergic neurons from 6-hydroxydopamine toxicity in vitro. *Neurosci. Lett.* **269**, 178–182.

Frim D., Uhler T., Galpern W., Beal M., Breakefield X. and Isacson O. (1994) Implanted fibroblasts genetically engineered to produce brain-derived neurotrophic factor prevent 1-methyl-4-phenylpyridinium toxicity to dopaminergic neurons in the rat. *Proc. Natl. Acad. Sci. USA* **91**, 5104–5108.

Glinka Y. Y. and Youdim M. B. (1995) Inhibition of mitochondrial complexes I and IV by 6-hydroxydopamine. *Eur. J. Pharmacol.* **292**, 329–332.

Hashimoto K., Guroff G. and Katagiri Y. (2000) Delayed and sustained activation of p42/p44 mitogen-activated protein kinase induced by proteasome inhibitors through p21 (ras) in PC12 cells. *J. Neurochem.* **74**, 92–98.

Hastings T. G., Lewis D. A. and Zigmond M. J. (1996) Role of oxidation in the neurotoxic effects of intrastriatal dopamine injections. *Proc. Natl. Acad. Sci. USA* **93**, 1956–1961.

Hirsch E. C., Brandel J. P., Galle P., Javoy-Agid F. and Agid Y. (1991) Iron and aluminum increase in the substantia nigra of patients with Parkinson's disease: an X-ray microanalysis. *J. Neurochem.* **56**, 446–451.

Holmström T. H., Chow S. C., Elo I., Coffey E. T., Orrenius S., Sistonen L. and Eriksson J. E. (1998) Suppression of Fas/APO-1-mediated apoptosis by mitogen-activated kinase signaling. *J. Immunol.* **160**, 2626–2636.

Hu Y., Dietrich H., Metzler B., Wick G. and Xu Q. (2000) Hyperexpression and activation of extracellular signal-regulated kinases (ERK1/2) in atherosclerotic lesions of cholesterol-fed rabbits. *Arterioscler. Thromb. Vasc. Biol.* **20**, 18–26.

Ishikawa Y. and Kitamura M. (1999) Dual potential of extracellular signal-regulated kinase for the control of cell survival. *Biochem. Biophys. Res. Commun.* **264**, 696–701.

Jameson, G. N. L. and Linert, W. (2000) 6-Hydroxydopamine, dopamine, and ferritin: a cycle of reactions sustaining parkinson's disease?, in *Free Radicals in Brain Pathophysiology* (Poli G., Cadena E. and Packer L., eds), pp. 247–272. Marcel Dekker, Inc., New York.

Kish S. J., Morito C. and Hornykiewicz O. (1985) Glutathione peroxidase activity in Parkinson's disease brain. *Neurosci. Lett.* **58**, 343–346.

Klann E. and Thiel E. (1999) Modulation of protein kinases and protein phosphatases by reactive oxygen species: implications for hippocampal synaptic plasticity. *Prog. Neuropsychopharmacol. Biol. Psychiatry* **23**, 359–376.

Lander H. M., Hajjar D. P., Hempstead B. L., Mirza U. A., Chait B. T., Campbell S. and Quilliam L. A. (1997) A molecular redox switch on p21 (ras). Structural basis for the nitric oxide-p21 (ras) interaction. *J. Biol. Chem.* **272**, 4323–4326.

Lang A. E. and Lozano A. M. (1998) Parkinson's disease. First of two parts. *N. Engl. J. Med.* **339**, 1044–1053.

Lotharius J., Dugan L. L. and O'Malley K. L. (1999) Distinct mechanisms underlie neurotoxin-mediated cell death in cultured dopaminergic neurons. *J. Neurosci.* **19**, 1284–1293.

Luo Y., Umegaki H., Xiantao W., Abe R. and Roth G. S. (1998) Dopamine induces apoptosis through an oxidation-involved SAPK/JNK activation pathway. *J. Biol. Chem.* **273**, 3756–3764.

Marshall C. J. (1995) Specificity of receptor tyrosine kinase signaling: transient versus sustained extracellular signal-regulated kinase activation. *Cell* **80**, 179–185.

Moghal S., Rajput A. H., D'Arcy C. and Rajput R. (1994) Prevalence of movement disorders in elderly community residents. *Neuroepidemiology* **13**, 175–178.

Oh-hashi K., Maruyama W., Yi H., Takahashi T., Naoi M. and Isobe K. (1999) Mitogen-activated protein kinase pathway mediates peroxynitrite-induced apoptosis in human dopaminergic neuroblastoma SH-SY5Y cells. *Biochem. Biophys. Res. Commun.* **263**, 504–509.

Perry G., Roder H., Nunomura A., Takeda A., Friedlich A. L., Zhu X., Raina A. K., Holbrook N., Siedlak S. L., Harris P. L. and Smith M. A. (1999) Activation of neuronal extracellular receptor kinase (ERK) in Alzheimer disease links oxidative stress to abnormal phosphorylation. *Neuroreport* **10**, 2411–2415.

Runden E., Seglen P. O., Haug F. M., Ottersen O. P., Wieloch T., Shamloo M. and Laake J. H. (1998) Regional selective neuronal degeneration after protein phosphatase inhibition in hippocampal slice cultures: evidence for a MAP kinase-dependent mechanism. *J. Neurosci.* **18**, 7296–7305.

Schubert D., Heinemann S., Carlisle W., Tarikas H., Kimes B., Patrick J. and Steinback J. H. (1974) Clonal cell lines from the rat central nervous system. *Nature* **249**, 224–227.

Segal R. A. and Greenberg M. E. (1996) Intracellular signaling pathways activated by neurotrophic factors. *Ann. Rev. Neurosci.* **19**, 463–489.

Stanciu M., Wang Y., Kentor R., Burke N., Watkins S., Kress G., Reynolds I., Klann E., Angiolieri M., Johnson J. and Defranco D. B. (2000) Persistent activation of ERK contributes to glutamate-induced oxidative toxicity in a neuronal cell line and primary cortical neuron cultures. *J. Biol. Chem.* **275**, 12200–12206.

Sutherland M. W. and Learmonth B. A. (1997) The tetrazolium dyes MTS and XTT provide new quantitative assays for superoxide and superoxide dismutase. *Free Radic. Res.* **27**, 283–289.

Suzuki Y. J., Forman H. J. and Sevanian A. (1997) Oxidants as stimulators of signal transduction. *Free Radic. Biol. Med.* **22**, 269–285.

Tombes R. M., Auer K. L., Mikkelsen R., Valerie K., Wymann M. P., Marshall C. J., McMahon M. and Dent P. (1998) The mitogen-activated protein (MAP) kinase cascade can either stimulate or inhibit DNA synthesis in primary cultures of rat hepatocytes depending upon whether its activation is acute/phasic or chronic. *Biochem. J.* **330**, 1451–1460.

Traverse S., Gomez N., Paterson H., Marshall C. and Cohen P. (1992) Sustained activation of the mitogen-activated protein (MAP) kinase cascade may be required for differentiation of PC12 cells. Comparison of the effects of nerve growth factor and epidermal growth factor. *Biochem. J.* **288**, 351–355.

Ungerstedt U. (1968) 6-Hydroxy-dopamine induced degeneration of central monoamine neurons. *Eur. J. Pharmacol.* **5**, 107–110.

Wroblewski F. and Ladue J. (1955) Lactic dehydrogenase activity in blood. *Proc. Soc. Exp. Biol. Med.* **90**, 210.

Xia Z., Dickens M., Raingeaud J., Davis R. J. and Greenberg M. E. (1995) Opposing effects of ERK and JNK-p38 MAP kinases on apoptosis. *Science* **270**, 1326–1331.

Research report

MPP⁺ increases α -synuclein expression and ERK/MAP-kinase phosphorylation in human neuroblastoma SH-SY5Y cells

Cristina Gómez-Santos^a, Isidre Ferrer^b, Julia Reiriz^c, Francesc Viñals^a, Marta Barrachina^b, Santiago Ambrosio^{a,*}

^aUnitat de Bioquímica, Departament Ciències Fisiològiques II, Campus Bellvitge, Universitat de Barcelona, c/ Feixa Llarga s/n, L'Hospitalet del Llobregat E-08907, Barcelona, Spain

^bUnitat de Neuropatologia, Departament Biologia Cellular i Anatomia Patològica, Universitat de Barcelona, Barcelona, Spain

^cDepartament d'Infermeria Fonamental i Medicoquirúrgica, Escola Universitària d'Infermeria, Universitat de Barcelona, Barcelona, Spain

Accepted 15 January 2002

Abstract

α -Synuclein is a brain presynaptic protein that is linked to familiar early onset Parkinson's disease and it is also a major component of Lewy bodies in sporadic Parkinson's disease and other neurodegenerative disorders. α -Synuclein expression increases in substantia nigra of both MPTP-treated rodents and non-human primates, used as animal models of parkinsonism. Here we describe an increase in α -synuclein expression in a human neuroblastoma cell line, SH-SY5Y, caused by 5–100 μ M MPP⁺, the active metabolite of MPTP, which induces apoptosis in SH-SY5Y cells after a 4-day treatment. We also analysed the activation of the MAPK family, which is involved in several cellular responses to toxins and stressing conditions. Parallel to the increase in α -synuclein expression we observed activation of MEK1,2 and ERK/MAPK but not of SAPK/JNK or p38 kinase. The inhibition of the ERK/MAPK pathway with U0126, however, did not affect the increase in α -synuclein. The highest increase in α -synuclein (more than threefold) in 4-day cultures was found in adherent cells treated with low concentrations of MPP⁺ (5 μ M). Inhibition of ERK/MAPK reduced the damage caused by MPP⁺. We suggest that α -synuclein increase and ERK/MAPK activation have a prominent role in the cell mechanisms of rescue and damage, respectively, after MPP⁺-treatment. © 2002 Elsevier Science B.V. All rights reserved.

Theme: Disorders of the nervous system

Topic: Degenerative disease: Parkinson's

Keywords: Parkinson's disease; MPP⁺; α -Synuclein MAP kinase; SH-SY5Y

1. Introduction

α -Synuclein is a major component of Lewy bodies in sporadic Parkinson's disease and dementia of Lewy bodies, and also of inclusions found in both glial and neuronal cells in multiple system atrophy [8,17,31,36]. In Alzheimer's disease a 35-sequence of α -synuclein has been identified as the non-A β component (NAC) of amyloid plaques [51]. The aggregation of synucleins seems to be associated with neurodegenerative processes in α -synucleinopathies [38], but the physiological role of α -

synuclein and whether it has a role in inclusion body formation or neuronal degeneration remain unknown.

α -Synuclein has been found in association with vesicles and also free in the cytosol of neurons and non-neuronal cells [55]. It is an inhibitor of phospholipase D [22,40], it interacts with dopamine transporters [33], it also interacts with both the proteasomal complex [16] and the cytoskeleton proteins [10], mainly with tau, stimulating tau phosphorylation by PKA and consequently inhibiting its binding to microtubules [24], and it shares some properties with chaperones [44]. Moreover, α -synuclein binds ERK2/MAPK and forms a complex with the ERK2-activated transcriptional factor Elk-1 [21], indicating a relationship between α -synuclein and the MAP kinase pathways. The three members of the mitogen-activated protein kinase family (MAPK): extracellular signal-regulated kinase

*Corresponding author. Tel.: +34-93-402-9094; fax: +34-93-402-4268.

E-mail address: ambrosio@bellvitge.bvg.ub.es (S. Ambrosio).

(ERK/MAPK), stress activated c-Jun N-terminal kinase (SAPK/JNK) and p38 kinase, have been implicated in apoptosis underlying several neurodegenerative processes [4,39,41].

Interest in α -synuclein increased when mutant isoforms, A53T and A30P, were identified in some familiar parkinsonisms [30,44]. A53T forms discrete spherical assemblies and fibrils more rapidly than the wild-type or other mutant isoforms [9], and A30P sensitizes neuronal cells to oxidative damage [28]. An aggregation of α -synuclein has also been found in the substantia nigra of baboons [29] and mice [53] treated with MPTP, used as animal models of Parkinson's disease. MPP⁺, the active metabolite of MPTP, has been extensively described as a mitochondrial inhibitor. We found little or no effect on mitochondrial activity at a low concentration (5 μ M) of MPP⁺ [5], although long exposure (4 days) of human neuroblastoma SH-SY5Y cells to this concentration causes apoptosis in about 20% of the cells, and exposure to higher concentrations (100–1000 μ M) causes both apoptosis and necrosis, with a dose-dependent increase in necrosis [19].

Here we analyse the effect of a range of concentrations of MPP⁺ on the expression of α -synuclein and the activation of the kinase pathways in SH-SY5Y cells. Both the expression of α -synuclein and the activation of ERK/MAPK increased after a 4-day exposure to 5 μ M MPP⁺. Although a causal relationship between these processes has not been established, they suggest that an intracellular transduction mechanism involving these proteins contributes to MPP⁺-induced neurodegeneration.

2. Materials and methods

2.1. Reagents

MPP⁺ iodide was purchased from RBI (Natick, MA) and added to the medium to a final concentration of 5, 100 or 1000 μ M. Cells were exposed to MPP⁺ for 24 h or 4 days. One hundred μ M of *N*-benzyloxycarbonyl-Val-Ala-Asp(OMe)-fluoromethylketone (zVAD.fmk, Enzyme Systems, Dublin, CA) was used as a broad-specificity irreversible caspase inhibitor. U0126 (Calbiochem, Darmstadt, Germany) was used at 1 μ M as a specific inhibitor of MEK1 and MEK2, to reduce the activation of ERK/MAPK. Anisomycin (1 μ g/ml, Sigma RBI, St. Louis) was used as an inducer of both JNK and p38 phosphorylation. One hundred nM staurosporine (Calbiochem) was used as a non-specific apoptosis inducer in neuroblastoma cells.

The following antibodies were used: anti- α -Synuclein-1 (mouse monoclonal from Transduction Labs., Lexington, KY, 1:1000 dilution); anti-phospho-MEK1,2 (rabbit polyclonal from New England BioLabs, Beverly, MA, 1:500 dilution); anti-ERK/MAP kinase phospho-specific (ERK/MAPK-P) (Calbiochem), rabbit polyclonal antibody, 1:100 dilution, which detects phosphorylated Tyr204 of p44 and

p42 MAP kinases (phosphorylated ERK1 and ERK2); purified phospho-p38 MAP kinase (Thr189/Tyr182) (p38-P) rabbit polyclonal antibody (New England BioLabs, 1:200 dilution); anti- τ (Tau) clone Tau-2 (monoclonal antibody from Sigma, 1:1000 dilution); anti- α -tubulin (monoclonal antibody from Sigma, 1:5000 dilution); anti-Ras-Ab3 (mice monoclonal from Calbiochem, 1:200 dilution); anti-phospho-tyrosine (mice monoclonal from Santa Cruz Biotechnology, Santa Cruz, CA, 1:1000 dilution); anti-phospho-Akt (Ser 473) (rabbit polyclonal from New England BioLabs, 1:1000 dilution).

2.2. Cell culture

SH-SY5Y cells (kindly supplied by Dr. J. Comella, University of Lleida, Spain) were grown in Dulbecco's Modified Eagle Medium (DMEM, Gibco BRL, Paisley, UK) supplemented with 10% fetal bovine serum (Gibco BRL), 100 U/ml penicillin and 100 μ g/ml streptomycin. Cells were maintained in a humidified 10% CO₂ atmosphere at 37 °C.

Experiments were performed in 6- or 12-well culture plates at ~80% cell confluence. Cells (2 \times 10⁶) were washed twice in PBS and gently lysed in 100 μ l of buffer (50 mM Tris-HCl pH 6.8, 10% glycerol, 2% SDS). Lysates were stirred for 10 s and boiled at 95 °C for 10 min.

2.3. Western blotting

Protein concentration was determined by the Bradford assay. Equal amounts of protein were loaded on each lane, and electrophoresed on SDS-polyacrylamide gels with Tris-glycine running buffer. They were then transferred to nitrocellulose membranes by semi-dry electrotransfer for 50 min at 40 V. Membranes were incubated with antibodies to the various compounds analysed. After washing, the membranes were incubated with biotinylated secondary antibody labeled with horseradish peroxidase (Amersham, diluted 1:1000), for 1 h at room temperature, washed again and developed with the chemiluminescence ECL Western blotting system followed by apposition of the membranes to autoradiographic films (Hyperfilm ECL, Amersham).

2.4. Ras activation

A pull-down assay to measure the activity status of p21ras was used as described previously [54]. After homogenization, proteins were extracted by addition of 1% Triton X-100 and 1% *N*-octylglucoside. Proteins from lysates were incubated for 2 h at 4 °C with 30 μ g of glutathione S-transferase (GST)-RBD fusion protein (where RBD includes amino acids 51 to 131 of Raf-1 and is the minimal domain required for the binding of Ras-GTP) preadsorbed to glutathione-Sepharose beads. Precipitates were washed and p21ras was detected by resuspend-

ing the final pellet and doing Western-blot with a Ras-antibody. Serum deprived cells, 5 min stimulated with 20% fetal calf serum, were used as controls of Ras activation.

2.5. Cell death

In living cells 3-(4,5-dimethylthiazol-2-yl)-2,5-diphenyltetrazolium bromide, MTT (RBI), is converted into insoluble formazan in proportion to the number of viable cells. A total of 5×10^5 cells were incubated for 2 h at 37 °C with 0.5 mg/ml MTT. The cells were then washed and lysed with an equal volume of isopropanol/1 M HCl (24:1). Reduced-MTT was measured at 550 nm in a 96-microtiter plate [19]. In order to assess the degree of cell death, cells were simultaneously stained with propidium iodide (Sigma, 0.75 µg/ml for 1 min) and Hoechst-33342 (bisbenzimide, Sigma, 2 µg/ml).

3. Results

3.1. Increased α -synuclein protein expression after MPP^+ exposure

α -Synuclein expression increased in human SH-SY5Y cells after 4 days of exposure to 5 or 100 µM MPP^+ . In these conditions, cell viability decreased by about 15% and 40% after 4 days, respectively [19]. Fig. 1 shows the Western blot and the densitometry of a 19-kDa band, corresponding to α -synuclein, which increased after a 4-day exposure to 5 or 100 µM MPP^+ . The increase was higher at 5 µM MPP^+ (a dose previously described to cause apoptosis in about 15% of the cells without significant mitochondrial damage or free radical production [11,19]). After 24 h, a significant increase in α -synuclein was seen with 1 mM MPP^+ , but not with 5 or 100 µM MPP^+ . Experiments were performed using both the whole contents of the well and after eliminating floating cells. α -Synuclein increase was observed in both cases, indicating that this result is not due to α -synuclein accumulation in dead cells. Fig. 1 shows the increase in α -synuclein in adherent cells after washing.

3.2. Effect of MPP^+ on the activation of different kinases

In Fig. 2, the Western blot shows the increase in MEK1,2 (45 kDa) and ERK/MAPK (42–44 kDa) phosphorylated forms after a 4-day-exposure to 5 or 100 µM MPP^+ , with no changes in active forms of JNK (40 kDa), p38 (38 kDa) or Akt (60 kDa). α -Tubulin and tau expression were measured as a control of protein loading. Cells were treated with 1 µg/ml anisomycin to assess the increase in phosphorylation of both SAPK/JNK and p38 [50]. In control SH-SY5Y neuroblastoma cells ERK/MAPK and p38 were already active before treatment. After

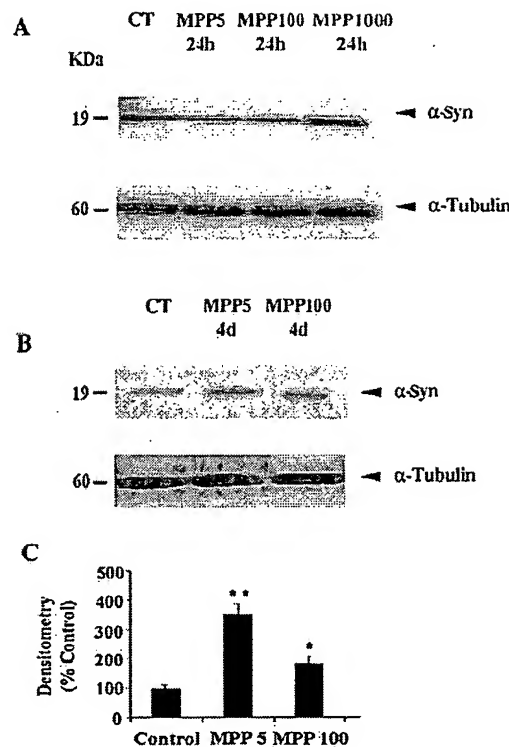


Fig. 1. Expression by Western blot of α -synuclein (α -Syn) and α -tubulin in the control and MPP^+ -incubated SH-SY5Y cells, (A) after 24 h, and (B) after 4 days. Quantitative results (C) were obtained by measurement of the optical density of each band and expressed as the relation between α -synuclein and α -tubulin densities. Results in (C) are shown for 4-day incubations and are the mean \pm S.E.M. of six separate experiments. * P < 0.05; ** P < 0.01 (Mann–Whitney U -test).

4 days, but not at 24 h, MPP^+ activated MEK1,2 and ERK/MAPK (Fig. 2A), by increasing their phosphorylation, in a concentration-dependent way. In contrast, p38-kinase activation decreased after 4 days. Similarly to α -synuclein, MEK1,2 and ERK/MAPK activation increased at 24 h with 1 mM but not with 5 or 100 µM MPP^+ (not shown). Akt was not modified by this treatment. Fig. 3 shows activation of Ras in basal SH-SY5Y cells consistent with the basal activation of ERK/MAPK, and a lack of effect of MPP^+ on Ras activation. The relative amount of total phospho-tyrosines (in a protein molecular mass range between 50 and 172 kDa) was not significantly modified by MPP^+ treatment, as assessed by Western blot with anti-phospho-Tyr antibodies (result not shown), which indicates that a Ras-linked receptor does not participate in MPP^+ toxicity.

3.3. Effect of staurosporine on both α -synuclein expression and activation of MAP kinases

Cells were treated with staurosporine as a control of damage (Fig. 4). Both ERK/MAPK and SAPK/JNK were activated, with no change in p38 kinase, after a 12-h

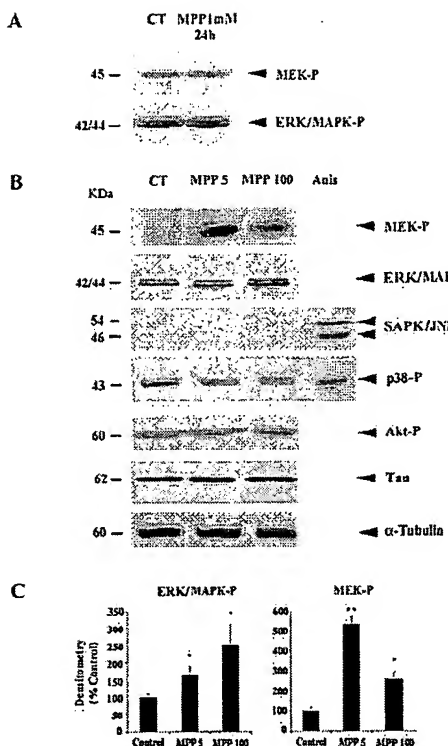


Fig. 2. Expression of MEK-P and ERK/MAPK-P 24 h after 1 mM MPP⁺ (A). Expression of MAP kinase family activated kinases, Akt, Tau and α -Tubulin in SH-SY5Y cells after 4 days of 5 and 100 μ M MPP⁺ exposure by Western blot (B). Activation of JNK and p38 by 1 μ g/ml anisomycin (Anis) is also shown. Results in (C) show the densitometries of ERK/MAPK-P and MEK1,2-P related to α -tubulin and are the mean \pm S.E.M. of five and three different experiments, respectively ($^*P < 0.05$ by Mann–Whitney *U*-test). The Western blot shown is indicative of two (Tau, Akt), three (MEK, JNK, p38) or five (ERK/MAPK) different experiments.

treatment with 100 nM staurosporine. However α -synuclein expression was not modified by staurosporine.

3.4. Attempts to counteract the α -synuclein increase

We had previously shown that the treatment with 100 μ M zVAD.fmk completely prevented the 5 μ M MPP⁺-induced apoptosis [19]. However, this treatment did not modify the increase in α -synuclein (Fig. 5), indicating that this effect is not a consequence of the activation of

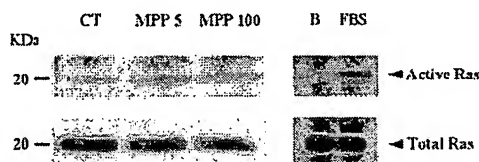


Fig. 3. Western blot of total and active Ras 4 days after MPP⁺ treatment. These results were reproduced in three different experiments. Serum deprived cells (B) and 5 min fetal bovine serum stimulated cells (FBS) were used as control of Ras activation.

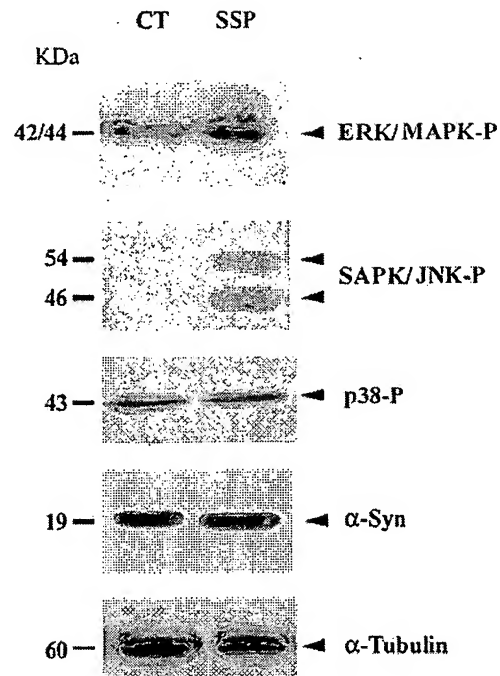


Fig. 4. Western blots of control (CT) and staurosporine-treated (SSP) SH-SY5Y neuroblastoma cells after 12 h of drug exposure. SAPK/JNK and ERK/MAPK were activated, but no changes were seen in p38 or α -synuclein (α -Syn) expression. The results shown are representative of three different experiments.

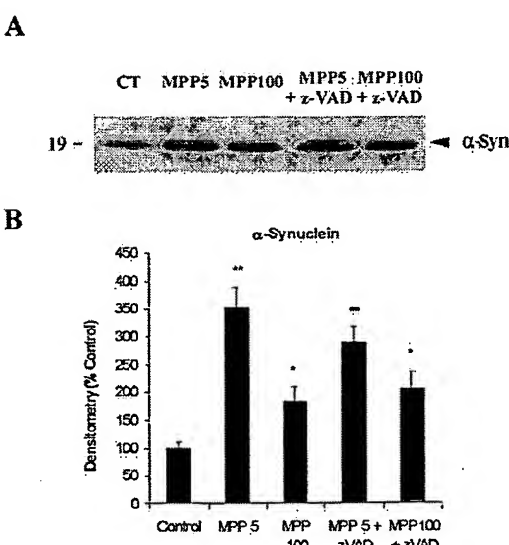


Fig. 5. (A) Western blot showing the α -synuclein (α -Syn) expression in control SH-SY5Y cells (CT) and after treatment with MPP⁺ alone or in combination with 100 μ M zVAD.fmk. The increase induced by MPP⁺ persists after caspase inhibition. (B) Densitometry of the Western blot analysis (related to respective α -tubulin densities). Results are the mean \pm S.E.M. of three separate experiments; $^{**}P < 0.01$ (Mann–Whitney *U*-test).

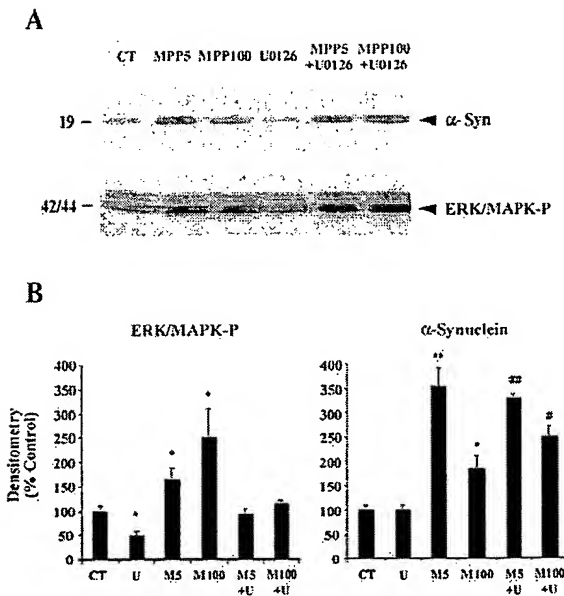


Fig. 6. (A) Western blot of α -synuclein and phosphorylated ERK/MAPK after treatment for 4 days with MPP^+ and the MEK inhibitor U0126. (B) Mean of densitometries of α -synuclein and ERK/MAPK-P related to respective α -tubulin densities, showing a reduction to 50% in ERK/MAPK-P by U0126 (U) counteracted by MPP^+ (M5, 5 μ M MPP^+ ; M100, 100 μ M MPP^+). In the presence of U0126 no significant increase by MPP^+ in ERK/MAPK activation was detected. An increase in α -synuclein expression caused by MPP^+ of nearly threefold was detected even with U0126. Results are the mean of three separate experiments. * $P<0.05$, ** $P<0.01$ compared with control; * $P<0.05$, ** $P<0.01$ compared with U (Mann–Whitney U -test).

caspases. ERK/MAPK phosphorylation was decreased by a daily treatment with the MEK1,2-P inhibitor U0126 for 4 days (Fig. 6). The inhibition of ERK/MAPK-P did not alter the increase in α -synuclein expression. On the other hand U0126, alone or in combination with MPP^+ , decreased cell viability by about 20%, as measured by the number of propidium iodide positive cells, supporting the role of ERK/MAPK activation in cell survival.

3.5. Cell viability

The study with MTT revealed that ERK/MAPK-P inhibition or 5 μ M MPP^+ administration decreased cell viability by 15% after 4 days, whereas 100 μ M MPP^+ reduced viability by 40%. The presence of the MEK1,2 inhibitor U0126 (Table 1) diminished the effect of MPP^+

on cell viability, with no effect at 5 μ M and only an 18% decrease at 100 μ M. Similar results were observed by fluorescence microscopy with propidium iodide. On the other hand, 100 nM staurosporine for 12 h reduced cell viability by 40% and the MEK1,2 inhibition did not modify this effect.

4. Discussion

We verified the presence of α -synuclein in the human neuroblastoma cell line SH-SY5Y, and found that its expression increases after 4 days exposure to MPP^+ over a wide range of concentrations. The clearest effect was seen at 5 μ M, which is close to that achieved in brains of animals given MPTP [45,48]. Previously we showed that 5 μ M MPP^+ does not cause significant mitochondrial damage or oxidative stress [5], although it induces DNA-damage and apoptosis in SH-SY5Y cells [19], suggesting the involvement of an intracellular transduction machinery triggered by low concentrations of MPP^+ .

The role of α -synuclein in neurodegenerative processes is controversial. The overexpression of the A53T form in SH-SY5Y cells enhances their susceptibility to oxidative damage [26]. The overexpression of wild and mutant (A30P or A53T) forms in neurons of mouse nodose ganglia [46] or in human embryonic kidney cells (HEK-293) [44] decreases cell survival without signs of apoptosis. On the other hand, the overexpression of wild-type α -synuclein (but not of the A53 mutated form) in SK-N-MC cells delays cell death induced by serum withdrawal or H_2O_2 [34]. Further, in TSM1 cells, a neocortical cell line, such overexpression protects these cells from apoptotic stimuli, including staurosporine and etoposide [1]. This suggests an antiapoptotic action of α -synuclein as well as a lack of this protective effect with the mutated forms linked to familiar Parkinson's disease. α -Synuclein could be expressed in response to aggression, but when this overexpression is too high or α -synuclein is mutated, it aggregates and precipitates inside the cell, reducing cell viability. Therefore these aggregates of α -synuclein may be considered as death-inducers in both their wild and their mutated form [13,15]. Both oxidative and nitritative damage seem to occur after α -synuclein aggregation [18,50].

α -Synuclein aggregation has been described in nigral neurons of mice and monkeys treated with MPTP [29,53], and in rats chronically treated with rotenone at doses that

Table 1
Cell viability

		Control	MPP^+ (5 μ M)	MPP^+ (100 μ M)	Staurosporine (100 nM)
U0126	–	100 \pm 4	85 \pm 2*	60 \pm 2*	60 \pm 2*
	+	86 \pm 2**	88 \pm 2	68 \pm 2*	45 \pm 1**

Effect of MEK-ERK/MAPK inhibition with U0126 on MPP^+ (4 days) and staurosporine (12 h) treatment measured colorimetrically with MTT at 550 nm. The results are expressed as % and are the mean \pm S.E.M. for six different samples. * $P<0.05$ compared to controls, ** $P<0.05$ compared to the correspondent treatment without U0126 (ANOVA with Duncan's test).

partially inhibit complex I activity (20–30 nM in brain) without impairing whole brain mitochondrial respiration [3], but not in rats treated with 6-hydroxydopamine [27]. So, it seems that α -synuclein aggregation is not a direct consequence of the destruction of the nigrostriatal pathway, but it is linked to both idiopathic and drug-induced parkinsonism.

The binding of α -synuclein to vesicles is abolished by the A30P mutation [23] and by 1 mM MPP⁺ [25]. One mM MPP⁺ releases cytochrome *c* from mitochondria, which associates with α -synuclein and enhances the formation of intracellular aggregates [20,25]. However, although 5 μ M MPP⁺ does not cause mitochondrial cytochrome *c* release [19], it significantly increased α -synuclein expression after 4 days, indicating a slow response to a slight but constant insult. This period of time and this dose correspond to those described for a significant induction of apoptosis in ~20% of SH-SY5Y cells [19]. The increase in α -synuclein expression persisted when caspase activation was blocked by zVAD.fmk, a broad spectrum caspase inhibitor that prevents DNA-leakage and, partially, cell death [19], indicating that α -synuclein induction must be up-stream of caspase activation.

α -Synuclein is constitutively phosphorylated in human HEK-293 and rat PC-12 cells [42]. The physiological and pathological significance of α -synuclein phosphorylation is not yet known. Although binding between α -synuclein and ERK/MAPK seems well demonstrated [21], we cannot conclude that α -synuclein expression increases by ERK/MAPK. Nor is it clear whether MAP kinases play a role in α -synuclein phosphorylation.

We found a significant increase in MEK1,2 and ERK/MAPK phosphorylated forms after 4-days treatment with 5 μ M MPP⁺, but not in stress-activated protein kinases SAPK/JNK or p38 phosphorylated forms, the other members of the MAPK protein family involved in signal transduction of stress-induced apoptosis. The SAPK/JNK and p38 signalling pathways participate in the cellular response to toxins, physical stresses and inflammatory cytokines [49]. JNK and the upstream regulatory kinase, MKK-4, are activated in the midbrain shortly and acutely after MPTP treatment in mice [48], and the neuronal damage is slightly attenuated by JNK inhibition [47]. Both 5 mM MPP⁺ and 500 μ M dopamine cause apoptosis in different cell lines involving SAPK/JNK [6,37]. However, 5 mM MPP⁺ (in contrast to 5 μ M MPP⁺) increases free radical production and oxidative stress [2]. Other authors describe JNK activation by 6-hydroxydopamine but not by 100 μ M MPP⁺ in the murine dopaminergic neuronal cell line MN9D [7]. Our results indicate that neither 5 nor 100 μ M MPP⁺ activates SAPK/JNK or p38 kinases.

The activity of ERK/MAPK is usually triggered by the intracellular pathway that involves Ras–Raf–MEK–MEK-P activation with further transactivation of transcription factors, promoting growth, differentiation, mitosis and survival [32]. The increase in MEK phosphorylation

reported here may be interpreted as a consequence of Raf activation. However, according to our results, Raf does not seem to be activated by Ras, so an alternative mechanism may lead to Raf activation. α -Synuclein shares functional homology with the chaperon protein 14-3-3 [43], since it binds 14-3-3 itself and ligands of 14-3-3. Among these ligands there are protein kinase C [52] and the kinase suppressor of Ras [56], that could be alternative pathways for Raf activation.

The inhibition of the ERK/MAPK pathway by a MEK-P inhibitor decreased cell viability, which is consistent with the protective role of ERK/MAPK activation in cell survival. However, the inhibition of ERK/MAPK pathway prevented the cell viability decrease caused by low concentrations of MPP⁺. Although the ERK/MAPK pathway is usually triggered by plasma receptor activation and promotes cell survival, ERK/MAPK activation has been associated with early tau deposition [14] and with cell damage caused by NO or H₂O₂ [4,41]. Our present results show that ERK/MAPK activation could also be involved in the mechanisms of damage induced by MPP⁺.

The treatment of SH-SY5Y cells with 100 nM staurosporine for 12 h induces oxidative stress and a loss of cell viability of about 40% in SH-SY5Y cells [35]. Staurosporine and MPP⁺ both induce apoptosis through caspase-2 and -3 activation in SH-SY5Y cells [19,35]. Staurosporine increased ERK/MAPK and JNK phosphorylation, consistently with previous results [12], but not α -synuclein expression. This corroborates that α -synuclein increase is not directly linked to MAPK activation. On the other hand the inhibition of ERK/MAPK pathway increases the loss of viability caused by staurosporine but blocks the apoptotic effect of MPP⁺.

In conclusion, MPP⁺ increases both α -synuclein expression and ERK/MAPK phosphorylation in human neuroblastoma SH-SY5Y cells by independent mechanisms. Our results indicate that these mechanisms could be cellular responses to specific chemical insults and may be involved in cell rescue and damage, respectively. The mechanism by which MPP⁺ increases α -synuclein expression in SH-SY5Y cells remains to be elucidated, but it may be related to the intracellular events involved in α -synuclein aggregation found in Parkinson's disease and also in MPTP-treated animals.

Acknowledgements

We are grateful to all the members of the Biochemistry and Neuropathology Units (Campus Bellvitge) of the University of Barcelona, especially Dr. Francesc Ventura and Dr. Jordi Llorens for their many valuable suggestions. We thank Dr. Neus Agell for providing the MEK1,2 antibody. We are also grateful to Robin Rycroft for help with the English. This work was supported by a grant from the Spanish Government, FIS 00/1127.

References

- [1] C. Alves da Costa, K. Ancolio, F. Checler, Wild-type but not Parkinson's disease-related Ala-53-Thr mutant α -synuclein protects neuronal cells from apoptotic stimuli, *J. Biol. Chem.* 275 (2000) 24065–24069.
- [2] S. Ambrosio, A. Espino, B. Cutillas, R. Bartrons, MPP⁺ toxicity in rat striatal slices: relationship between non-selective effects and free radical production, *Neurochem. Res.* 21 (1996) 73–78.
- [3] R. Betarbet, T.B. Sherer, G. McKenzie, M. García-Osuna, A.V. Panov, J.T. Greenamyre, Chronic systemic pesticide exposure reproduces features of Parkinson's disease, *Nat. Neurosci.* 3 (2000) 1301–1306.
- [4] N.R. Bhat, P. Zhang, Hydrogen peroxide activation of multiple mitogen-activated protein kinases in an oligodendrocyte cell line: role of extracellular signal-regulated kinase in hydrogen peroxide-induced cell death, *J. Neurochem.* 72 (1999) 112–119.
- [5] J. Boada, B. Cutillas, T. Roig, J. Bermúdez, S. Ambrosio, MPP⁺-induced mitochondrial dysfunction is potentiated by dopamine, *Biochem. Biophys. Res. Commun.* 268 (2000) 916–920.
- [6] D.S. Cassarino, E.M. Halvorsen, R.H. Swerdlow, N.N. Abramova, W.D. Parker, T.W. Sturgill, J.P. Bennett, Interaction among mitochondria, mitogen-activated protein kinases, and nuclear factor- κ B in cellular models of Parkinson's disease, *J. Neurochem.* 74 (2000) 1384–1392.
- [7] W.-S. Choi, S.-Y. Yoon, T.H. Oh, E.-J. Choi, K.L. O'Malley, Y.J. Oh, Two distinct mechanisms are involved in 6-hydroxydopamine- and MPP⁺-induced dopaminergic neuronal cell death: role of caspases, ROS, and JNK, *J. Neurosci. Res.* 57 (1999) 86–94.
- [8] D.F. Clayton, J.M. George, Synucleins in synaptic plasticity and neurodegenerative disorders, *J. Neurosci. Res.* 58 (1999) 120–129.
- [9] K.A. Conway, J.D. Harper, P.T. Lansbury, Accelerated in vitro fibril formation by a mutant α -synuclein linked to early-onset Parkinson disease, *Nat. Med.* 4 (1998) 1318–1320.
- [10] R.A. Crowther, S.E. Daniel, M. Goedert, Characterisation of isolated α -synuclein filaments from substantia nigra of Parkinson's disease brain, *Neurosci. Lett.* 292 (2000) 128–130.
- [11] B. Cutillas, M. Espejo, S. Ambrosio, 7-Nitroindazole prevents dopamine depletion caused by low concentrations of MPP⁺ in rat striatal slices, *Neurochem. Int.* 33 (1998) 35–40.
- [12] X. Deng, P. Ruvo, B. Carr, W.S. May, Survival function of ERK1/2 as IL-3-activated, staurosporine-resistant Bcl-2 kinases, *Proc. Natl. Acad. Sci. USA* 97 (2000) 1578–1583.
- [13] O.M.A. El-Agnaf, R. Jakes, M.D. Curran, D. Middleton, R. Ingenito, R. Bianchi, A. Pessi, D. Neill, A. Wallace, Aggregates from mutant and wild-type α -synuclein proteins and NAC peptide induce apoptotic cell death in human neuroblastoma cells by formation of beta-sheet and amyloid-like filaments, *FEBS Lett.* 440 (1998) 71–75.
- [14] I. Ferrer, R. Blanco, M. Carmona, R. Ribera, E. Goutan, B. Puig, M.J. Rey, A. Cardozo, F. Viñals, T. Ribalta, Phosphorylated MAP kinase (ERK1, ERK2) expression is associated with early tau deposition in neurones and glial cells, but not with increased nuclear DNA vulnerability and cell death, in Alzheimer disease, Pick's disease, progressive supranuclear palsy and corticobasal degeneration, *Brain Pathol.* 11 (2001) 144–158.
- [15] G. Forloni, M. Bertani, A.M. Calella, F. Thaler, R. Invernizzi, α -Synuclein and Parkinson's disease: selective neurodegenerative effect of α -synuclein fragment on dopaminergic neurons in vitro and in vivo, *Ann. Neurol.* 47 (2000) 632–640.
- [16] M. Ghee, A. Fournier, J. Mallet, Rat α -synuclein interacts with Tat binding protein 1, a component of the 26S proteasomal complex, *J. Neurochem.* 75 (2000) 2221–2224.
- [17] B.I. Giasson, K. Uryu, J.Q. Trojanowski, V.M.Y. Lee, Mutant and wild type human α -synucleins assemble into elongated filaments with distinct morphologies in vitro, *J. Biol. Chem.* 274 (1999) 7619–7622.
- [18] B.I. Giasson, J.E. Duda, I.V. Murray, Q. Chen, J.M. Souza, H.I. Hurtig, H. Ischiropoulos, J.Q. Trojanowski, V.M.Y. Lee, Oxidative damage linked to neurodegeneration by selective α -synuclein nitration in synucleinopathy lesions, *Science* 290 (2000) 985–989.
- [19] C. Gómez, J. Reiriz, M. Piqué, J. Gil, I. Ferrer, S. Ambrosio, Low concentrations of 1-methyl-4-phenylpyridinium ion induce caspase-mediated apoptosis in human SH-SY5Y neuroblastoma cells, *J. Neurosci. Res.* 63 (2001) 421–428.
- [20] M. Hashimoto, A. Takeda, L.J. Hsu, T. Takenouchi, E. Masliah, Role of cytochrome c as a stimulator of α -synuclein aggregation in Lewy body disease, *J. Biol. Chem.* 274 (1999) 28849–28852.
- [21] A. Iwata, S. Miura, I. Kanazawa, M. Sawada, N. Nukina, α -Synuclein forms a complex with transcriptional factor Elk-1, *J. Neurochem.* 77 (2001) 239–252.
- [22] J.M. Jenco, A. Rawlingson, B. Daniels, A.J. Morris, Regulation of phospholipase D2: selective inhibition of mammalian phospholipase D isoenzymes by α - and β -synucleins, *Biochemistry* 37 (1998) 4901–4909.
- [23] P.H. Jensen, M.S. Nielsen, R. Jakes, C.G. Dotti, M. Goedert, Binding of α -synuclein to brain vesicles is abolished by familial Parkinson's disease mutation, *J. Biol. Chem.* 273 (1998) 26292–26294.
- [24] P.H. Jensen, H. Hager, M.S. Nielsen, J. Højrup, J. Gliemann, R. Jakes, α -Synuclein binds to tau and stimulates the protein kinase A-catalyzed tau phosphorylation of serine residues 262 and 356, *J. Biol. Chem.* 274 (1999) 25481–25489.
- [25] J.-i. Kakimura, Y. Kitamura, K. Takata, Y. Kohno, Y. Nomura, T. Taniguchi, Release and aggregation of cytochrome c and α -synuclein are inhibited by the antiparkinsonian drugs, talipexole and pramipexole, *Eur. J. Pharmacol.* 417 (2001) 59–67.
- [26] S. Kanda, J.F. Bishop, M.A. Eglitis, Y. Yang, M.M. Mouradian, Enhanced vulnerability to oxidative stress by α -synuclein mutations and C-terminal truncation, *Neuroscience* 97 (2000) 279–284.
- [27] N.G. Kholodilov, T.F. Oo, R.E. Burke, Synuclein expression is decreased in rat substantia nigra following induction of apoptosis by intrastriatal 6-hydroxydopamine, *Neurosci. Lett.* 275 (1999) 105–108.
- [28] L.-w. Ko, N.D. Mehta, M. Farrer, C. Easson, J. Hussey, S. Yen, J. Hardy, S.-H.C. Yen, Sensitization of neuronal cells to oxidative stress with mutated human α -synuclein, *J. Neurochem.* 75 (2000) 2546–2554.
- [29] N.W. Kowall, P. Hantraye, E. Brouillet, M.F. Beal, A.C. McKee, R.J. Ferrante, MPTP induces α -synuclein aggregation in the substantia nigra of baboons, *Neuroreport* 11 (2000) 211–213.
- [30] R. Kruger, W. Kuhn, T. Müller, D. Woitalla, M. Gruber, S. Kosel, H. Przuntek, J.T. Eppler, L. Schols, O. Reiss, Ala30Pro mutation in the gene encoding α -synuclein in parkinson's disease, *Nat. Genet.* 18 (1998) 106–108.
- [31] J.W. Langston, S. Sastry, P. Chan, L.S. Forno, L.M. Bolin, D.A. Di Monte, Novel α -synuclein-immunoreactive proteins in brain samples from the Contursi kindred Parkinson's, and Alzheimer disease, *Exp. Neurol.* 154 (1998) 684–690.
- [32] M. Le Gall, J.C. Chambard, J.P. Breitmayer, D. Grall, J. Pouyssegur, E. Van Obberghen-Schilling, The p42/p44 MAP kinase pathway prevents apoptosis induced by anchorage and serum removal, *Mol. Biol. Cell* 11 (2000) 1103–1112.
- [33] F.J.S. Lee, F. Liu, Z.B. Pristupa, H.B. Niznik, Direct binding and functional coupling of α -synuclein to the dopamine transporters accelerate dopamine-induced apoptosis, *FASEB J.* 15 (2001) 916–926.
- [34] M.H. Lee, D.-H. Hyun, B. Halliwell, P. Jenner, Effect of the overexpression of wild-type or mutant α -synuclein on cell susceptibility to insult, *J. Neurochem.* 76 (2001) 998–1009.
- [35] E. Lopez, I. Ferrer, Staurosporine- and H-7-induced cell death in SH-SY5Y neuroblastoma cells is associated with caspase-2 and caspase-3 activation, but not with activation of the FAS/FAS-L-caspase-8 signaling pathway, *Mol. Brain Res.* 85 (2000) 61–67.

- [36] C.B. Lücking, A. Brice, Alpha-synuclein and Parkinson's disease, *Cell. Mol. Life Sci.* 57 (2000) 1894–1908.
- [37] Y. Luo, H. Umegaki, X. Wang, R. Abe, G.S. Roth, Dopamine induces apoptosis through an oxidation-involved SAPK/JNK activation pathway, *J. Biol. Chem.* 273 (1997) 3756–3764.
- [38] E. Mezey, A. Dehejia, G. Harta, M.I. Papp, M.H. Polymeropoulos, M.J. Brownstein, Alpha synuclein in neurodegenerative disorders: murderer or accomplice?, *Nat. Med.* 5 (1998) 755–757.
- [39] K. Mielke, T. Herdegen, JNK and p38 stress kinases—degenerative effectors of signal-transduction-cascades in the nervous system, *Prog. Neurobiol.* 61 (2000) 45–60.
- [40] S.-O. Oh, J.-H. Hong, Y.-R. Kim, H.-S. Yoo, S.-H. Lee, K. Lim, B.-D. Hwang, J.H. Exton, S.-K. Park, Regulation of phospholipase D2 by H₂O₂ in PC12 cells, *J. Neurochem.* 75 (2000) 2445–2454.
- [41] K. Oh-hashi, W. Maruyama, H. Yi, T. Takahashi, M. Naoi, K. Isobe, Mitogen-activated protein kinase pathways mediates peroxynitrite-induced apoptosis in human dopaminergic neuroblastoma SH-SY5Y cells, *Biochem. Biophys. Res. Commun.* 263 (1999) 504–509.
- [42] M. Okochi, J. Walter, A. Koyama, S. Nakajo, M. Baba, T. Iwatsubo, L. Meijer, P.J. Kahle, C. Haass, Constitutive phosphorylation of the Parkinson's disease associated α -synuclein, *J. Biol. Chem.* 275 (2000) 390–397.
- [43] N. Ostrerova, L. Petrucelli, M. Farrer, N. Mehta, P. Choi, J. Hardy, B. Wolozin, α -Synuclein shares physical and functional homology with 14-3-3 proteins, *J. Neurosci.* 19 (1999) 5782–5791.
- [44] M.H. Polymeropoulos, C. Lavedant, E. Leroy, S.E. Ide, A. Dehejia, A. Dutra, B. Pike, H. Root, J. Rubenstein, R. Boyer, E.S. Stenroos, S. Chandrasekharappa, A. Athanassiadou, T. Papapetropoulos, W.G. Johnson, A.M. Lazzarini, R.C. Duvoisin, G. Di Iorio, L.I. Golbe, R.L. Nussbaum, Mutation in the α -synuclein gene identified in families with Parkinson's disease, *Science* 276 (1997) 2045–2047.
- [45] S. Przedborski, V. Jackson-Lewis, R. Yokoyama, T. Shibata, V.L. Dawson, T.M. Dawson, Role of neuronal nitric oxide in 1-methyl-4-phenyl-1,2,3,6-tetrahydropyridine (MPTP)-induced dopaminergic neurotoxicity, *Proc. Acad. Sci. USA* 93 (1996) 4565–4571.
- [46] A.R. Saha, N.N. Ninkina, D.P. Hanger, B.H. Anderton, A.M. Davies, V.L. Buchman, Induction of neuronal death by α -synuclein, *Eur. J. Neurosci.* 12 (2000) 3073–3077.
- [47] M.S. Saporito, E.M. Brown, M.S. Miller, S. Carswell, CEO-1347/ KT-7515, an inhibitor of c-jun N-terminal kinase activation, attenuates the 1-methyl-4-phenyltetrahydropyridine-mediated loss of nigrostriatal dopaminergic neurons in vivo, *J. Pharmacol. Exp. Ther.* 288 (1999) 421–427.
- [48] M.S. Saporito, B.A. Thomas, R.W. Scott, MPTP activates c-Jun NH₂-terminal kinase (JNK) and its upstream regulatory kinase MKK4 in nigrostriatal neurons in vivo, *J. Neurochem.* 75 (2000) 1200–1208.
- [49] L.A. Tibbles, J.R. Woodgett, The stress-activated protein kinase pathways, *Cell. Mol. Life Sci.* 55 (1999) 1230–1254.
- [50] B. Torocsik, J. Szeberenyi, Anisomycin affects both pro- and antiapoptotic mechanisms in PC12 cells, *Biochem. Biophys. Res. Commun.* 278 (2000) 550–556.
- [51] K. Uéda, H. Fukushima, E. Maslia, Y. Xia, A. Iwai, M. Yoshimoto, D.A.C. Otero, J. Kondo, Y. Ihara, T. Saitoh, Molecular cloning of cDNA encoding an unrecognized component of amyloid in Alzheimer disease, *Proc. Natl. Acad. Sci. USA* 90 (1993) 11282–11286.
- [52] P.C. Van der Hoeven, J.C. Van der Wal, P. Ruurs, W.J. Van Blitterswijk, Protein kinase C activation by acidic proteins including 14-3-3, *Biochem. J.* 347 (2000) 781–785.
- [53] M. Vila, S. Vukosavic, L.V. Jackson, M. Neystat, M. Jakowec, S. Przedborski, α -Synuclein up-regulation in substantia nigra dopaminergic neurons following administration of the parkinsonian toxin MPTP, *J. Neurochem.* 74 (2000) 721–729.
- [54] F. Viñals, J. Pouyssegur, Confluence of vascular endothelial cells induces cell cycle exit by inhibiting p42/p44 mitogen activated protein kinase activity, *Mol. Cell. Biol.* 19 (1999) 2763–2772.
- [55] K. Wakabayashi, M. Yoshimoto, S. Tsuji, H. Takahashi, Alpha-synuclein immunoreactivity in glial cytoplasmic inclusions in multiple system atrophy, *Neurosci. Lett.* 249 (1998) 180–182.
- [56] Y. Zhang, B. Yao, S. Delikat, S. Bayoumy, X.-H. Lin, S. Basu, M. McGinley, P.-Y. Chan-Hui, H. Lichenstein, R. Kolesnick, Kinase suppressor of Ras is ceramide-activated protein kinase, *Cell* 89 (1997) 63–72.



ACADEMIC
PRESS

Biochemical and Biophysical Research Communications 294 (2002) 220–224

BBRC

www.academicpress.com

Disruption in gastric mucin synthesis by *Helicobacter pylori* lipopolysaccharide involves ERK and p38 mitogen-activated protein kinase participation

Bronislaw L. Slomiany* and Amalia Slomiany

Research Center, University of Medicine and Dentistry of New Jersey, New Jersey Dental School, 110 Bergen Street, Newark, NJ 07103-2400, USA

Received 26 April 2002

Abstract

Helicobacter pylori is a primary factor in the etiology of gastric disease, and its early pathogenic effects are manifested by upregulation of inflammatory processes and the loss of mucus coat continuity. We investigated the role of extracellular signal-regulated kinase (ERK) and p38 mitogen activated protein kinase (MAPK) in the disturbances in gastric mucin synthesis and apoptotic processes evoked by *H. pylori* lipopolysaccharide (LPS). Exposure of gastric mucosal cells to the LPS led to a dose-dependent decrease (up to 59.5%) in mucin synthesis, accompanied by a marked increase in caspase-3 activity and apoptosis. Inhibition of ERK with PD98059 accelerated (up to 36.1%) the LPS-induced decrease in mucin synthesis, and caused further enhancement in caspase-3 activity and apoptosis. Blockade of p38 kinase with SB203580 produced reversal in the LPS-induced reduction in mucin synthesis, and substantially countered the LPS-induced increases in caspase-3 activity and apoptosis. Moreover, inhibition of caspase-3 blocked the LPS-induced increase in caspase-3 activity and produced an increase in mucin synthesis. Thus the detrimental influence of *H. pylori* LPS on gastric mucin synthesis is closely linked to caspase-3 activation and apoptosis, and involves ERK and p38 kinase participation. © 2002 Elsevier Science (USA). All rights reserved.

Keywords: *H. pylori* LPS; Mucin synthesis; ERK and p38 MAPK; Caspase-3 activation

A unique property of gastric epithelium is its ability to withstand the variety of insults by luminal contents. While the nature of this protective mechanism appears to be multicomponential, the major defensive role is assigned to the viscous layer of mucus that tenaciously adheres to the epithelial surfaces [1,2]. The functional performance of the mucus coat depends mainly upon a balance of factors controlling the synthesis and secretion of its mucin component. The importance of mucin in the maintenance of gastric mucosal integrity is evident from data showing that a decrease in the synthesis of sulfated mucus glycoprotein and an increase in mucin degradation are prominent features in the etiology of peptic ulcer [2,3]. Moreover, the loss of mucus coat continuity, its patchy appearance, and the disturbances in mucin synthesis are the prominent markers in the etiology of

gastric disease associated with *Helicobacter pylori* infection [4,5]. Furthermore, it has been shown that *H. pylori* exerts inhibitory effect on the synthesis and secretion of gastric mucin through its cell wall lipopolysaccharide (LPS) [5]. Interestingly, studies with *H. pylori* virulence factors demonstrated that *H. pylori* LPS is also capable of inducing mucosal inflammatory responses that characterize gastritis. These include enhancement in proinflammatory cytokine expression, excessive nitric oxide generation, and a massive epithelial cell apoptosis triggered by the mucosal rise in soluble TNF- α [6,7].

Evidence obtained with several cell culture systems indicates that the regulation of cellular responses to LPS leading to the release of TNF- α occurs mainly through selective activation of p38 and ERK (extracellular signal-regulated kinase) mitogen-activated protein kinase (MAPK) pathways [8,9]. Moreover, these data indicate that activation of p38 kinase cascade appears to be coupled with apoptosis, and the ERK activation is as-

* Corresponding author. Fax: +1-973-972-7020.
E-mail address: slomiabr@umdnj.edu (B.L. Slomiany).

sociated with cell survival [8,10]. Indeed, studies with chondrocytes indicate that LPS-induced inhibition in proteoglycan synthesis and caspase-3 activation can be blocked by a specific inhibitor of p38 MAPK, while the inhibition of ERK results in upregulation of apoptosis and a decrease in proteoglycan synthesis [8–10].

In this study, using rat gastric mucosal cells in culture, we investigated the role of p38 and ERK MAPK in the disturbances in mucin synthesis and apoptotic events evoked by *H. pylori* LPS.

Materials and methods

Mucosal cell incubation. The study was conducted with Sprague-Dawley rats in compliance with the experimental protocol approved by the institutional Animal Care and Use Committee. Gastric mucosal cells were collected by scraping the mucosa with a blunt spatula on ice-cold glass plate, and suspended in 5 volumes of ice-cold Dulbecco's modified (Gibco) Eagle's minimal essential medium (DMEM), supplemented with fungizone (50 µg/ml), penicillin (50 U/ml), streptomycin (50 µg/ml), and 10% fetal calf serum [11]. The cells were gently dispersed by trituration with a syringe, settled by centrifugation at 300g for 5 min and, following three consecutive rinses with DMEM, resuspended in the medium to a concentration of 3×10^6 cell/ml. Aliquots of the cell suspension (1 ml) were transferred to DMEM in culture dishes containing [3 H]glucosamine (110 µCi), and incubated under 95% O₂–5% CO₂ atmosphere at 37°C for various periods of time up to 20 h in the presence of 0–800 µM of *H. pylori* LPS. In the experiments on the effect of caspase-3 inhibitor, Ac-DEVD-CHO (Biomol), and MAPK inhibitors (Calbiochem), PD98059 (ERK1/2) and SB203580 (p38), the cells prior to addition of the LPS were first incubated for 30 min with the inhibitor. At the end of the specified incubation period, the cells were centrifuged at 300g for 5 min, washed three times with phosphate-buffered saline, and the combined supernatants used for [3 H]glucosamine labeled mucus glycoprotein assay [12].

***H. pylori* LPS.** *H. pylori* ATCC No. 4350 clinical isolate was used for LPS preparation [3]. The bacterium was washed with water, treated with ethanol and acetone, dried, and homogenized with liquid phenol-chloroform–petroleum ether. The resulting suspension was centrifuged, and the LPS contained in the supernatant was precipitated with water, washed with 80% phenol solution, and dried with ether. The dry residue was dissolved in a small volume of water at 45°C, centrifuged at 100,000g for 4 h, and the resulting LPS sediment subjected to lyophilization.

Caspase-3 activity assay. Caspase-3 activity assays were conducted using Quanti Zyme assay system (Biomol). The assay is based on the ability of active enzyme to cleave a synthetic substrate, DEVD-pNA (Asp-Glu-Val-Asp-p-anilide). The cells, settled by centrifugation, were rinsed in phosphate-buffered saline, incubated at 4°C with the lysis buffer, and the lysates were centrifuged at 10,000g for 10 min. The aliquots of the resulting cytosolic fraction, diluted with the reaction buffer to contain 30 µg of protein, were incubated in the microtiter wells with 50 µM of DEVD-pNA for 1 h at 37°C, and the caspase-3 activity was measured spectrophotometrically [7].

Apoptosis assay. For quantitative measurements of apoptosis, the gastric mucosal cells were settled by centrifugation, rinsed with phosphate buffered saline, and incubated in the lysis buffer (Boehringer Mannheim). Following centrifugation, the supernatant containing the cytoplasmic histone-associated DNA fragments was diluted and reacted with immobilized anti-histone antibody. After washing, the retained complex was reacted with anti-DNA peroxidase and probed with ABTS reagent for spectrophotometric quantification [7].

Cell viability. Cell preparations before and during the experimentation were assessed for viability and cellular integrity using Trypan

blue dye exclusion assay and the determination of lactate dehydrogenase released into the medium [11].

Mucin analysis. The combined cell wash and incubation medium containing [3 H]-labeled mucin were treated at 4°C with 10 volumes of 2% phosphotungstic acid in 20% trichloroacetic acid for 4 h. The formed crude glycoprotein precipitates were dissolved in 6 M urea and chromatographed on Bio-Gel A-1.5 column (0.9 × 110 cm²). The eluted fractions were monitored spectrophotometrically for protein and for radioactivity by liquid scintillation spectrometry. The mucus glycoprotein fractions eluted in the excluded volume were pooled, dialyzed, lyophilized, and subjected to analysis for total incorporation of radiolabel and for protein content [12].

Data analysis. All experiments were carried out in duplicate, and the results are expressed as means ± SD. The significance level was set at $P < 0.05$. The tests were performed using Stat Soft, STATISTICA, software. The protein content of samples was measured with BCA protein assay kit (Pierce).

Results

The mechanism of the detrimental influence of *H. pylori* colonization on gastric mucin synthesis was investigated using rat gastric mucosal cells exposed to *H. pylori* LPS, and incubated in the presence of a marker of mucin synthesis, [3 H]glucosamine. Under the incubation conditions, the viability of the mucosal cells in culture monitored by Trypan blue uptake remained over 97% for up to 20 h, and the lactate dehydrogenase assays indicated only marginal (0.7–0.9%) cellular damage. In absence of the LPS, the incorporation of [3 H]glucosamine to mucus glycoprotein increased steadily with time of incubation for at least 16 h (Fig. 1A). Introduction of the LPS to the incubation medium led to a dose-dependent decrease in mucin synthesis, which attained a 57.4% reduction at 400 ng/ml (Fig. 1B).

The results of apoptotic assays revealed that in the controls by 16–20 h of incubation the rate of DNA fragmentation increased only about 2.7-folds, while a 19.1-fold increase in apoptosis occurred with the cells incubated with the LPS at 400 ng/ml for 20 h. (Fig. 2). Moreover, the LPS-induced mucosal cell apoptosis was subject to the interference by the inhibitors of ERK and p38 MAPK pathways. The inhibitor of ERK pathway, PD98059, produced a dose-dependent enhancement (up to 2-fold) in apoptosis, while the inhibition of p38 kinase with SB203580 led to a dose-dependent reduction (up to 66.7%) in the LPS-induced mucosal cell apoptosis (Fig. 3).

The data on the effect of ERK and p38 MAPK inhibitors on the synthesis of mucin by gastric mucosal cells incubated in the presence of *H. pylori* LPS are summarized in Fig. 4. The addition of ERK inhibitor, PD98059, led to a dose-dependent acceleration of the LPS-induced decrease (up to 36.1%) in mucin synthesis, whereas blockade of p38 kinase with SB203580 caused the reduction in the severity of the LPS-induced decrease in the glycoprotein synthesis. The effect of SB203580

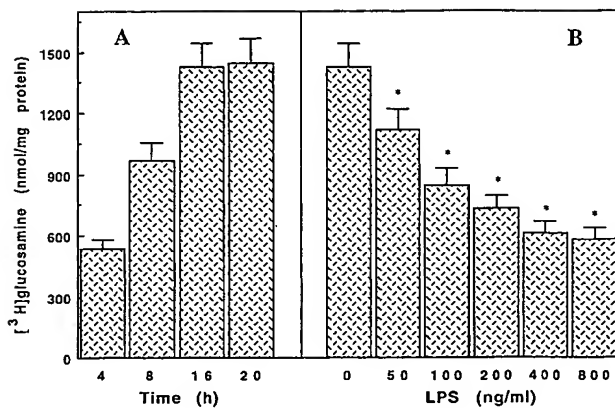


Fig. 1. Effect of *H. pylori* LPS on the synthesis of mucin by rat gastric mucosal cells in culture. A, mucosal cells incubated for the specified time periods in the presence of [³H]glucosamine. B, mucosal cells treated with indicated concentrations of the LPS and incubated for 16 h in the presence of [³H]glucosamine. Values represent the means \pm SD of five experiments performed in duplicate. B, $*P < 0.05$ compared with that of LPS-0.

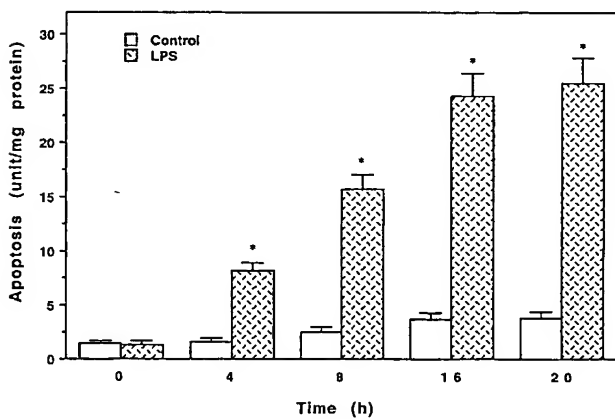


Fig. 2. Effect of *H. pylori* LPS on mucosal cell apoptosis. Gastric mucosal cells were incubated for the specified time periods in the absence and the presence of LPS at 400 ng/ml. Values represent the means \pm SD of five experiments performed in duplicate. $*P < 0.05$ compared with that of control.

was dose-dependent, and at 60 μ M elicited a 91% reversal in the LPS-induced inhibitory effect (Fig. 4).

The expression of caspase-3 activity in gastric mucosal cells incubated in the presence of *H. pylori* is presented in Fig. 5. The mean value for caspase-3 activity in the controls by 16 h of incubation was 6.5 pmol/mg protein, while that in the mucosal cell incubated in the presence of 400 ng/ml LPS reached the mean value of 151.6 pmol/mg protein. Inhibition of ERK pathway with PD98059 potentiated (by 18.5%) the LPS-induced caspase-3 activity, while the p38 kinase inhibitor, SB203580, caused a 68.1% decline in the LPS-induced expression of caspase-3 activity. Moreover, in all cases, addition to the mucosal cell incubates of

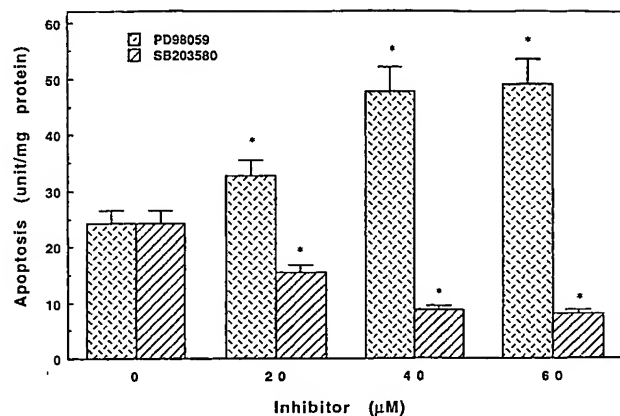


Fig. 3. Effect of MAPK inhibitors on the LPS-induced mucosal cells apoptosis. Gastric mucosal cells were treated with the LPS at 400 ng/ml and incubated for 16 h in the presence of indicated concentrations of ERK (PD98059) and p38 kinase (SB203580) inhibitors. Values represent the means \pm SD of five experiments performed in duplicate. $*P < 0.05$ compared with that of LPS alone.

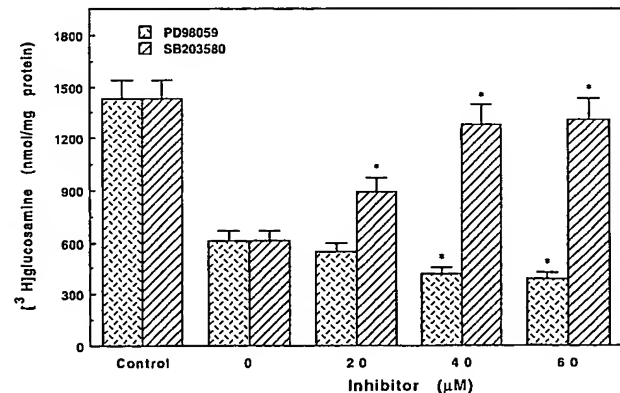


Fig. 4. Effect of MAPK inhibitors on the synthesis of mucin by gastric mucosal cells treated with *H. pylori* LPS. The cells were treated with the LPS at 400 ng/ml and incubated for 16 h, in the presence of [³H]glucosamine, with the indicated concentrations of ERK (PD98059) and p38 kinase (SB203580) inhibitors. Values represent the means \pm SD of five experiments performed in duplicate. $*P < 0.05$ compared with that of LPS alone.

caspase-3 inhibitor, Ac-DEVD-CHO, led to a significant reduction in the LPS-induced caspase-3 activity, and was reflected in the increased synthesis of mucin.

Discussion

Lipopolysaccharide, a component of the outer membrane of *H. pylori* bacterium colonizing the gastric mucosa, is recognized as a potent virulence factor responsible for eliciting acute mucosal inflammatory responses that characterize gastritis and duodenal ulcers [5,7,13,14]. Aside from upregulation of nitric oxide and

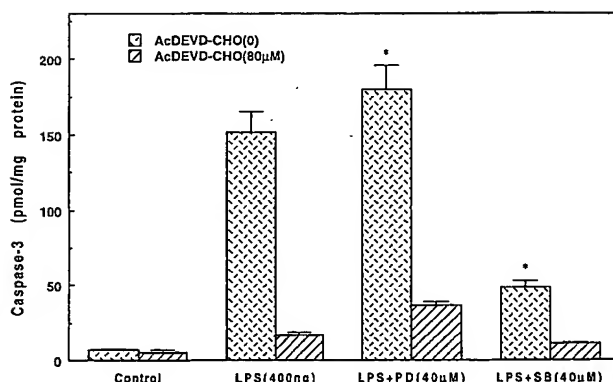


Fig. 5. Effect of *H. pylori* LPS and MAPK inhibitors on the activity of caspase-3. Gastric mucosal cells were treated with the LPS at 400 ng/ml and incubated for 16 h, in the presence of 80 μ M Ac-DEVD-CHO, with the indicated concentrations of ERK (PD98059) and p38 kinase (SB203580) inhibitors. Values represent the means \pm SD of five experiments performed in duplicate. * P < 0.05 compared with that of LPS alone.

prostaglandin production, enhancement in epithelial cell apoptosis, and induction of TNF- α the untoward effects of *H. pylori* LPS are manifested by the inhibition of mucus glycoprotein synthesis [3,5–7]. As the regulation of cellular responses to LPS leading to the release of TNF- α and activation of transcriptional factor NF κ B occur mainly through selective activation of ERK and p38 MAPK, in this study we assessed the role of ERK and p38 MAPK-signaling pathways in the disturbances in gastric mucin synthesis and apoptotic events evoked by *H. pylori* LPS.

The results revealed that exposure of gastric mucosal cells to *H. pylori* LPS led to a dose-dependent inhibition in mucin synthesis, and this effect was accompanied by a marked increase in caspase-3 activity and apoptosis. Inhibition of ERK with PD98059 accelerated the LPS-induced decrease in mucin synthesis and caused further enhancement in apoptosis and caspase-3 activity, whereas blockade of p38 kinase with SB203580 was associated with the reversal in the LPS-induced reduction in the glycoprotein synthesis, and a decrease in caspase-3 activity and apoptosis. Our findings thus provide primary evidence for the participation of ERK and p38 MAPK pathways in the regulation of gastric mucin synthesis in response to *H. pylori*, and show that the effects of ERK and p38 on the glycoprotein synthesis are closely linked to the events caspase-3 activation and apoptosis. Interestingly, we have found earlier that while both p38 and ERK are involved in the mucosal production of TNF- α , it is activation of p38 pathway that also exerts a major influence on the mucosal level of ET-1 and the severity of gastric mucosal inflammatory reaction to *H. pylori* LPS [15]. The p38 MAPK requirement in the apoptotic processes and the regulation of mucin synthesis is supported further by the reports

showing that activation of the p38 leads to the inhibition of proteoglycan synthesis and caspase-3 activation, while the ERK activation leads to the inhibition of caspase-3 activation and upregulation of proteoglycan synthesis and [8,9,16–18].

To gain additional insight into the mechanism of the detrimental influence of *H. pylori* on gastric mucin synthesis, we focused on the role of caspase-3. The inhibition of caspase-3 by Ac-DEVD-CHO not only blocked the *H. pylori* LPS-induced apoptosis but also was reflected in the increased synthesis of mucin. These results, along with the findings that inhibition of ERK with PD98059 potentiated the LPS-induced caspase-3 activity while p38 kinase inhibition with SB203580 blocked caspase-3 activation, are thus consistent with the prevailing view that the activities of proapoptotic p38 and antiapoptotic ERK depend on the modulation of caspase-3 [8,18,19].

Taken together, our findings suggest that the detrimental influence of *H. pylori* LPS on gastric mucin synthesis is closely linked to caspase-3 activation and apoptosis, and involves ERK and p38 kinase participation. Activation of p38 kinase by the LPS leads to the upregulation of proapoptotic signal and is reflected in a decreased mucin synthesis, while ERK functions in gastric mucosal cells as an antiapoptotic signal and its activation leads to upregulation in mucin synthesis. As mucins are recognized as an essential constituent of mucus perimeter of gastric mucosal defense, our results provide an important new insight into the mechanism by which *H. pylori* disrupts the gastric mucosal mucus coat continuity, and hence its functional performance.

References

- [1] W. Silen, Gastric mucosal defense and repair, in: L.R. Johnson (Ed.), *Physiology of the Gastrointestinal Tract*, Raven Press, New York, 1987, pp. 1055–1069.
- [2] B.L. Slomiany, A. Slomiany, Mucus and gastric mucosal protection, in: W. Domschke, S.J. Konturek (Eds.), *The Stomach*, Springer, Berlin, 1993, pp. 116–143.
- [3] Y.H. Liau, R.A. Lopez, A. Slomiany, B.L. Slomiany, *Helicobacter pylori* lipopolysaccharide effect on the synthesis and secretion of sulfated gastric mucin, *Biochem. Biophys. Res. Commun.* 184 (1992) 1411–1417.
- [4] B.J. Marshall, *Helicobacter pylori*, *Am. J. Gastroenterol.* 89 (1994) S116–S128.
- [5] B.L. Slomiany, J. Piotrowski, A. Slomiany, Anti-*Helicobacter pylori* activities of ebrotidine, *Arzneim. Forsch. Drug Res.* 47 (1997) 475–482.
- [6] J. Piotrowski, E. Piotrowski, D. Skrodzka, A. Slomiany, B.L. Slomiany, Induction of acute gastritis and epithelial cell apoptosis by *Helicobacter pylori* lipopolysaccharide, *Scand. J. Gastroenterol.* 32 (1997) 203–211.
- [7] B.L. Slomiany, J. Piotrowski, A. Slomiany, Gastric mucosal inflammatory responses to *Helicobacter pylori* lipopolysaccharide: down-regulation of nitric oxide synthase-2 and caspase-3 by sulglycotide, *Biochem. Biophys. Res. Commun.* 261 (1999) 15–20.

- [8] S.J. Kim, J.W. Ju, C.D. Oh, Y.M. Yoon, W.K. Song, J.H. Kim, Y.J. Yoo, O.K. Bang, J.S. Chun, ERK1/2 and p38 kinase oppositely regulate nitric oxide-induced apoptosis of chondrocytes in association with p53, caspase-3, and differentiation status, *J. Biol. Chem.* 277 (2002) 1332–1339.
- [9] M. Shakibaei, G. Schulze-Tanzil, P. deSouza, T. John, M. Rahmazadeh, R. Rahmazadeh, H.J. Merker, Inhibition of mitogen-activated protein kinase induces apoptosis of human chondrocytes, *J. Biol. Chem.* 276 (2001) 1389–1394.
- [10] H.J. Schaeffer, M.J. Weber, Mitogen-activated protein kinase: specific messages from ubiquitous messengers, *Mol. Cell. Biol.* 19 (1999) 2435–2444.
- [11] B.L. Slomiany, V.L.N. Murty, E. Piotrowski, M. Morita, J. Piotrowski, A. Slomiany, Activation of arachidonoyl phospholipase A2 in prostaglandin-mediated action of sucralfate, *Gen. Pharmacol.* 25 (1994) 261–266.
- [12] B.L. Slomiany, Y.H. Liau, R.A. Lopez, A. Slomiany, Nitcapone effect on the synthesis and secretion of gastric sulfomucin, *Gen. Pharmacol.* 24 (1993) 69–73.
- [13] P.C. Konturek, W. Bielanski, S.J. Konturek, E.G. Hahn, *Helicobacter pylori* associated pathology, *J. Physiol. Pharmacol.* 50 (1999) 695–710.
- [14] W.A. de Boer, Topics in *Helicobacter pylori* infection: focus on a 'search-and-treatment strategy' for ulcer disease, *Scand. J. Gastroenterol.* 35 (Suppl. 232) (2000) 4–9.
- [15] B.L. Slomiany, A. Slomiany, Role of ERK and p38 Mitogen-activated protein kinase cascades in gastric mucosal inflammatory responses to *Helicobacter pylori* lipopolysaccharide, *IUBMB Life* 51 (2001) 315–320.
- [16] K. Ono, J. Han, The p38 signal transduction pathway activation and function, *Cell Signal.* 12 (2000) 1–13.
- [17] S. Yamagishi, M. Yamada, Y. Ishikawa, T. Matsumoto, T. Ikeuchi, H. Hatanaka, p38 Mitogen-activated protein kinase regulates low potassium-induced c-Jun phosphorylation and apoptosis in cultured cerebellar granule neurons, *J. Biol. Chem.* 276 (2001) 5129–5133.
- [18] J.T. Watters, J.A. Sommer, Z.A. Pfeiffer, U. Prabhu, A.N. Guerra, P.J. Bertics, A differential role for mitogen-activated protein kinase in lipopolysaccharide signaling, *J. Biol. Chem.* 277 (2002) 9077–9087.
- [19] D.D. Bannerman, J.C. Tupper, R.D. Erwet, R.K. Winn, J.M. Harlan, Divergence of bacterial lipopolysaccharide pro-apoptotic signaling downstream of IRAK-1, *J. Biol. Chem.* 277 (2002) 8048–8053.

Enhanced ERK-1/2 activation in mice susceptible to coxsackievirus-induced myocarditis

Mary Anne Opavsky,^{1,2} Tami Martino,¹ Marlene Rabinovitch,² Josef Penninger,³ Chris Richardson,³ Martin Petric,² Cathy Trinidad,^{1,2} Lisa Butcher,¹ Janice Chan,¹ and Peter P. Liu¹

¹The Heart and Stroke/Richard Lewar Centre of Excellence, The University of Toronto, and The University Health Network, Toronto, Ontario, Canada

²The Hospital for Sick Children, Toronto, Ontario, Canada

³The Amgen Institute and the Departments of Immunology and Medical Biophysics, The University of Toronto, Ontario, Canada

Address correspondence to: Anne Opavsky, The Hospital for Sick Children, The Department of Pediatrics, Division of Infectious Diseases, 7313 Black Wing, 555 University Avenue, Toronto, Ontario, Canada, MSG 1X8. Phone: (416) 813-6625; Fax: (416) 813-8404; E-mail: anne.opavsky@sickkids.ca.

Received for publication August 14, 2001, and accepted in revised form May 10, 2002.

Group B coxsackieviral (CVB) infection commonly causes viral myocarditis. Mice are protected from CVB3 myocarditis by gene-targeted knockout of p56^{Lck} (Lck), the Src family kinase (Src) essential for T cell activation. Extracellular signal-regulated kinase 1 and 2 (ERK-1/2) can influence cell function downstream of Lck. Using T cell lines and neonatal cardiac myocytes we investigated the role of ERK-1/2 in CVB3 infection. In Jurkat T cells ERK-1/2 is rapidly activated by CVB3; but, this response is absent in Lck-negative JCaM T cells. Inhibition of ERK-1/2 with UO126 reduced CVB3 titers in Jurkat cells, but not in JCaM cells. In cardiac myocytes CVB3 activation of ERK-1/2 is blocked by the Src inhibitor PP2. In addition, viral production in myocytes is decreased by Src or ERK-1/2 inhibition. In vitro, in both immune and myocardial cells, ERK-1/2 is activated by CVB3 downstream of Lck and other Src's and is necessary for efficient CVB3 replication. In vivo, following CVB3 infection, ERK-1/2 activation is evident in the myocardium. ERK-1/2 activation is intense in the hearts of myocarditis-susceptible A/J mice. In contrast, significantly less ERK-1/2 activation is found in the hearts of myocarditis-resistant C57BL/6 mice. Therefore, the ERK-1/2 response to CVB3 infection may contribute to differential host susceptibility to viral myocarditis.

J. Clin. Invest. 109:1561-1569 (2002). doi:10.1172/JCI200213971.

Introduction

Viral myocarditis is an important cause of acute and chronic heart failure (1). Group B Coxsackieviruses (CVBs), members of the *Enterovirus* genus, are the most common etiologic agents associated with acute viral myocarditis and chronic dilated cardiomyopathy (1, 2). The spectrum of disease spans from a fulminant course including arrhythmias or sudden death to mild symptoms and may later progress to chronic heart failure (1, 3). Investigations using murine models have demonstrated that both the T lymphocyte response to viral infection and direct CVB-mediated injury are important in the development of myocarditis following infection with CVB3 (4, 5). Gene-targeted knockout of both CD4⁺ and CD8⁺ T cells or the T cell receptor β^+ (TCR- β) T cells results in minimal heart pathology following CVB3 infection (6). Because activation of p56^{Lck} (Lck), a member of the Src family (Src) of protein tyrosine kinases, is required for normal T cell responses (7), we examined CVB3 infection in Lck-targeted knockout mice. In the absence of Lck, myocardial inflammation was completely absent, there was 100% survival of mice, and viral replication was impaired (8). The latter was confirmed by the significant diminution of CVB3 replication in

JCaM cells, which are Jurkat cells with no functional Lck (8). T cell stimulation by antigen or anti-TCR Ab's is characterized by a rise of intracellular tyrosine protein phosphorylation, which is dependent upon Lck (9, 10). Downstream pathways include the mitogen-activated protein kinases (MAPKs). Important candidates are the extracellular signal-regulated kinases 1 and 2 (ERK-1/2), which are activated rapidly by MEK-1/2 through threonine and tyrosine phosphorylation following TCR engagement and Lck activation via adapter proteins and Ras (11, 12). ERK-1/2 are important participants in the regulation of cell proliferation and differentiation in response to a wide variety of growth factors and cytokines (13-15).

We have hypothesized that the ERK-1/2 signaling cascade is an important mediator of host susceptibility to CVB3 infection and disease. The role of ERK-1/2 was investigated in T cell lines and isolated neonatal cardiac myocytes, representative of the two cell types central to the pathogenesis of viral myocarditis. We find that in Jurkat T cells CVB3 infection specifically and rapidly activates the ERK-1/2 pathway in an Lck-dependent manner. In addition, optimal CVB3 replication in Jurkat cells and cardiac myocytes is dependent

upon activation of Src's and the ERK-1/2 signaling pathway. Furthermore, in CVB3-susceptible A/J mice we demonstrate that the ERK-1/2 signaling pathway was intensely activated early in the course of infection, associated with severe myocarditis and high cardiac viral titers. In contrast, in myocarditis-resistant C57BL/6 mice the ERK-1/2 response remains lower in association with less severe myocardial disease. Thus, our data support the concept that the ERK-1/2 cascade may be an important determinant of host susceptibility to CVB3 infection and virally induced myocarditis.

Methods

Antibodies and reagents. Phosphoprotein-specific mAbs detecting dual phosphorylated ERK-1/2, anti-ERK-1/2 mAb, horseradish peroxidase-conjugated goat anti-rabbit (HRP-GAR) secondary Ab, and MEK-1 inhibitor PD98059 were purchased from New England Biolabs Inc. (Beverly, Massachusetts, USA). The MEK-1/2 inhibitor UO126 and the Src inhibitor PP2 were obtained from Calbiochem-Novabiochem Corp. (San Diego, California, USA). HRP-conjugated goat anti-mouse secondary (HRP-GAM) Ab was from DAKO Corp. (Carpinteria, California, USA). [³⁵S]-methionine was supplied by Amersham Pharmacia Biotech (Baie d'Urfe, Quebec, Canada). All media, FCS, geneticin, and insulin were obtained from Life Technologies Inc. (Burlington, Ontario, Canada). Hygromycin B was obtained from Roche Diagnostics (Laval, Quebec, Canada), and 5-bromo-2-deoxyuridine (BRDU), transferrin, lithium chloride, selenium oxide, and ascorbic acid were from Sigma-Aldrich Canada Ltd. (Oakville, Ontario, Canada). The protein assay reagent was from Bio-Rad Laboratories Canada Ltd. (Mississauga, Ontario, Canada). An enhanced chemiluminescence detection system (ECL) from Amersham Pharmacia Biotech was used.

Cell culture. Jurkat T cells (E6-1), JCaM T cells, and TCR- β -negative (TCR- β^-) T cells were obtained from the American Type Culture Collection (ATCC) (Manassas, Virginia, USA). Cells were grown at 37°C with 5% CO₂ in RPMI medium supplemented with 10 mM HEPES, 1 mM sodium pyruvate, 0.5% penicillin and streptomycin (P/S), and 10% FCS. Jurkat/Lck cells and Jurkat/vector cells required additional supplementation with hygromycin B and geneticin.

Neonatal mouse cardiac myocyte cultures were prepared as described previously (16), with modifications. Briefly, hearts were removed from newborn C57BL/6 mice (Harlan Sprague-Dawley, Indianapolis, Indiana, USA) within 72 hours of birth. Following trimming, ventricles were mechanically minced and then subjected to stepwise enzymatic digestion with 0.15% trypsin. Isolated cells were washed with DMEM/HAM F-12 (1:1), pH 7.4, with 0.5% P/S (DMEM/F-12) plus 10% FCS. Nonmyocytes were depleted by a 90-minute pre-plating on 10-cm² Primaria tissue culture dishes (Becton-Dickinson, Franklin Lakes, New Jersey, USA). Myocytes were resuspended in media plus 10% FCS with 0.1 mM BRDU (to inhibit growth of nonmyocytes

in the presence of serum) and plated in laminin-coated tissue-culture plates (Biocoat; Becton-Dickinson). After 24 to 48 hours, adherent myocytes were washed three times to remove serum and BRDU-containing media and resuspended in serum-free DMEM/F-12 plus the standard additives (5 μ g/ml transferrin, 1 nM lithium chloride, 1 nM selenium oxide, 25 μ g/ml ascorbic acid, and 1 μ g/ml insulin) to ensure optimal health of the myocytes. Insulin was excluded from the media in signaling experiments to minimize baseline ERK-1/2 activation. The myocytes were incubated an additional 24 hours before use.

Viruses. The cardiovirulent CVB3 strain CVB3-CG (CVB3) was adapted by Woodruff and Woodruff (5) and passaged in the laboratory of Charles Gauntt (Department of Microbiology, University of Texas Health Sciences Center at San Antonio, San Antonio, Texas, USA) (17). CVB3-VR30 (Nancy) was obtained from the ATCC. Stock viruses were prepared by passage once through HeLa cells. Virus was grown in HeLa cells until cytopathic effect was observed, then the cell monolayer was washed three times in serum-free RPMI and cells were collected in serum-free RPMI. Cells were lysed by freezing/thawing three times, clarified by centrifugation, and stored at -80°C, after titers were determined by plaque assay on HeLa cells. [³⁵S]-methionine-labeled CVB3 ([³⁵S]-CVB3) was prepared in HeLa cell monolayers and purified by sucrose gradients as described previously (17).

To prepare purified virus for use in signaling experiments, clarified CVB3 and CVB3-VR30 stocks were separately overlaid on 15–45% (wt/wt) sucrose gradients in collection buffer (0.01 M NaCl, 0.01 M Tris-HCl, 0.05 M MgCl₂). Gradients were then centrifuged at 100,000 g at 25°C for 3 hours in an SW28 rotor (Beckman Coulter Inc., Fullerton, California, USA). Prior to application to the gradients, some virus stocks were spiked with 1,000 cpm of radiolabeled virus. Following centrifugation, fractions with peak radioactivity or peak CVB3 titer were pooled and dialyzed in 10K Slide-A-Lyzer Cassettes (Pierce Chemical Co., Rockford, Illinois, USA) against RPMI medium. Virus titers of pooled and dialyzed peak fractions were determined by plaque assay, and aliquots were stored at -80°C.

CVB3 binding and replication. Binding assays of radio-labeled CVB3 were performed as described previously (17). Briefly, after washing in RPMI, cells (5×10^6 cells/test) were incubated with about 30,000 cpm [³⁵S]-CVB3 for 1 hour at room temperature (RT). Supernatant and two subsequent washes were collected and pooled (free virus) separately from the cell pellet (membrane-bound virus). The [³⁵S]-CVB3 cpm were monitored by scintillation spectroscopy. The percentage of virus binding was calculated as follows: [cpm membrane-bound virus/(cpm membrane-bound + cpm-free virus)].

To determine viral production by T cell lines or cardiac myocytes, cells were washed with PBS, then adsorbed with CVB3 in serum-free media for 1 hour at RT. Cells

were then washed to remove unbound virus, resuspended in RPMI plus 10% FCS (T cell lines) or DMEM/F-12 plus standard additives (cardiac myocytes), and incubated at 37°C. CVB3 titers were quantitated by plaque assay on HeLa cell monolayers.

CVB3 treatment of Jurkat cells and cardiac myocytes. Following incubation in RPMI with reduced serum (0.5% FCS) for 18 hours, Jurkat or JCaM cell aliquots were washed in and resuspended in 200 µl serum-free RPMI and preincubated at RT for 10 minutes. Sucrose-gradient purified CVB3 in serum-free RPMI or control serum-free RPMI was added to aliquots for the indicated times. Cells were incubated at RT for 5 to 10 minutes or at 37°C for 30 minutes or longer, and then cells were washed in PBS containing 400 µM sodium orthovanadate, 5 mM EDTA, and 10 mM sodium fluoride. The cells were solubilized on ice for 15 minutes in lysis buffer containing 0.5% Triton X-100, 50 mM Tris, pH 7.6, 300 mM NaCl, 1 mM sodium orthovanadate, 5 mM EDTA, 10 µg/ml leupeptin, 10 µg/ml aprotinin, and 1 mM PMSF. The lysates were spun at 12,000 g for 10 minutes at 4°C, and protein concentrations of the supernatants were determined with the Bio-Rad Laboratories Canada Ltd. system.

Following incubation for 24 hours in serum-free, insulin-free DMEM/F-12 plus additives, monolayers of isolated neonatal cardiac myocytes were washed in PBS, then adsorbed with CVB3 in serum-free media for 1 hour at RT. Cells were then washed to remove unbound virus, resuspended in serum-free, insulin-free DMEM/F-12, and incubated at 37°C for 48 hours. Then, media was removed and monolayers were solubilized on ice for 15 minutes with lysis buffer.

Analysis of ERK-1/2 activation. Whole cell lysates were mixed with 2× Laemmli sample buffer, boiled, and proteins resolved by SDS-PAGE (8–16% gradient gel; Novex, San Diego, California, USA) and transferred to PVDF. Membranes were blocked for 1 hour at RT with 5% powdered skim milk in TBS with 0.05% Tween (TBST), reacted with anti-phospho-ERK-1/2 (1:2,000) at 4°C overnight, and then incubated with HRP-GAM Ab (1:1,000) for 1 hour at RT. Blots were developed with an ECL detection system. After membranes were incubated in stripping buffer (10 mM β-mercaptoethanol, 2% wt/vol SDS, 62.5 mM Tris, pH 6.7) for 30 minutes at 50°C, they were washed in TBST, blocked, and incubated with anti-ERK-1/2 (1:1,000) at 4°C overnight. After incubation with HRP-GAR Ab (1:4,000) for 30 minutes at RT, total ERK-1/2 was detected with ECL. Ratios of phosphorylated/total ERK-1/2 were compared using densitometry (NIH Image Version 1.62; NIH, Bethesda, Maryland, USA).

CVB3 infection in mice. A/J (The Jackson Laboratories, Bar Harbor Maine, USA) and C57BL/6 mice (Harlan Sprague-Dawley), with documented differential susceptibility to CVB3 myocarditis (18), were inoculated intraperitoneally with 5×10^4 plaque-forming units (pfu) CVB3 at 6 weeks of age ($n = 40$ per group). Animals were sacrificed on days 1, 2, and 4 after infection

($n = 5$ per group). Uninfected controls were sacrificed at day 0. Organs were snap-frozen in liquid nitrogen and stored for later homogenization and tissue lysis, then processed as described above to detect ERK-1/2 activation. Alternatively, day-4 hearts were embedded in OCT for cryosection. For the detection of infectious CVB3, homogenates of cardiac or splenic tissue were analyzed by plaque assay (6). Additional A/J and C57BL/6 mice were infected with 10^4 pfu CVB3 and followed to day 10 after infection to assess severity of myocarditis at the time of peak inflammation. Transverse cryosections (day 4) of paraffin-embedded sections (day 10) of hearts were stained with hematoxylin and eosin and examined histopathologically for evidence of inflammation and necrosis, as described previously (6).

Results

CVB3 infection of Jurkat cells activates the ERK-1/2 signaling pathway. T lymphocytes and T cell lines are known to be permissive to viral infection (19, 20) and are important in the pathogenesis of CVB3 myocarditis (6, 8). We used Jurkat cells, a human T cell leukemia cell line, to examine the effects of CVB3 on intracellular signal transduction pathways. Specifically, to determine the effect of CVB3 on the ERK-1/2 signaling cascade, we first examined phosphorylation of the kinase in whole cell lysates collected from CVB3-treated and control Jurkat cells. Cardiovirulent CVB3 induced rapid ERK-1/2 phosphorylation as early as 5 minutes after treatment (Figure 1a). We have followed the phosphorylation status of ERK-1/2 for up to 4 hours after infection and have found that the response persists to 2 hours after infection (Figure 1b). In dose-response experiments CVB3 treatment at an moi of 25 was the threshold dose, with a moi of 50 consistently resulting in at least a two- to ninefold increase in ERK-1/2 phosphorylation. A minimal number or percentage of viral receptors may need to be bound by virus or cross-linked by the multivalent CVB3 to trigger subsequent signaling events. Activation of the ERK-1/2 cascade was also observed with a second strain of the virus, CVB3-VR30 (Nancy) (Figure 1c). These results indicate that CVB3 exposure triggers activation of the ERK-1/2 signaling in Jurkat cells.

CVB3-triggered ERK-1/2 activation in Jurkat cells is dependent on Lck. We reported previously that CVB3 replication is decreased in Lck knockout mice and also in JCaM cells, a Jurkat cell variant with no functional Lck (8). This led us to hypothesize that Lck controls host susceptibility to CVB3 infection via the ERK-1/2 signaling pathway. To explore a relationship between Lck and CVB3 activation of the ERK-1/2 signaling pathway, the intensity of ERK-1/2 phosphorylation was compared between infected Jurkat and JCaM cells. The dramatic activation of ERK-1/2 in Jurkat cells following exposure to CVB3 is in contrast to the essentially absent response in JCaM cells (Figure 2a). To determine if there may have been delayed activation in JCaM cells, incubation was continued for as long as 60 minutes before processing. This difference in phosphorylation

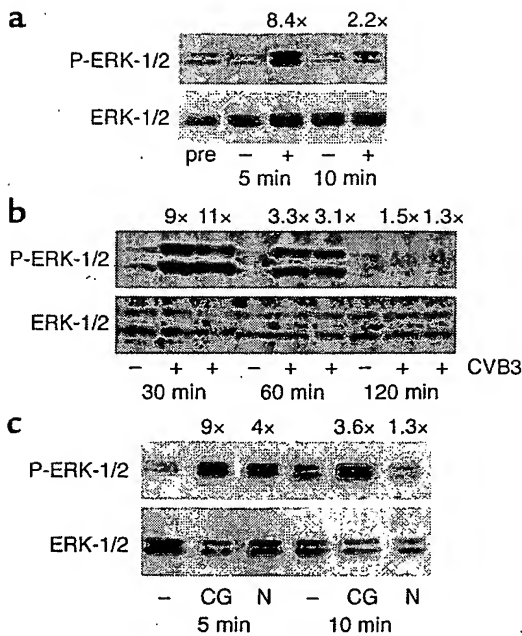


Figure 1

CVB3 infection activates the ERK-1/2 pathway in Jurkat cells. (a) Jurkat cells (10^7) were lysed before (pre) or after treatment with CVB3 (moi = 50; +) or control media (−) for the indicated times. One result represents five experiments. (b) Jurkat cells (10^6) were lysed 30 minutes to 4 hours after infection with CVB3 (moi = 50; +) or control media (−) for the indicated times. The increase in ERK-1/2 phosphorylation evident at 30 minutes to 2 hours after infection did not extend to the 4-hour time point. One result represents two experiments. (c) Five or 10 minutes after treatment with CVB3-CG (CG) or CVB3-VR30 (Nancy; N) (moi = 50), or control media (−), cells (10^7) were lysed. One result represents three experiments. All cell lysates were immunoblotted with anti-phospho-ERK-1/2 (P-ERK-1/2) and anti-total ERK-1/2 Ab's. Fold change in P-ERK-1/2-total ERK-1/2 ratio is indicated.

of ERK-1/2 was not due to a lack of MAPK expression because equivalent levels of total ERK-1/2 are present in both cell lines.

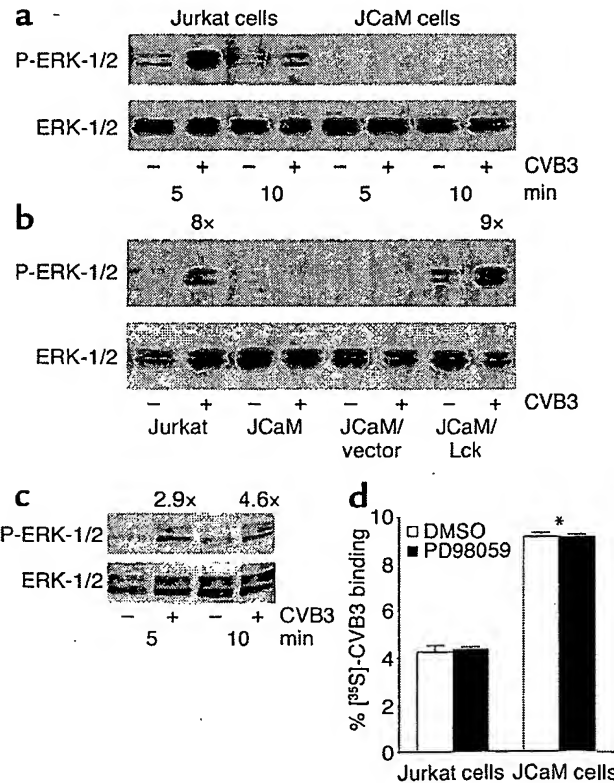
To confirm that Lck has an important role in viral activation of ERK-1/2, JCaM cells expressing Lck constitutively after transfection (JCaM/Lck) or controls transfected with vector alone (JCaM/vector) were exposed to CVB3. Treatment with CVB3 stimulated phosphorylation of ERK-1/2 by eightfold in Jurkat cells and ninefold in JCaM/Lck cells, in contrast to JCaM and JCaM/vector cells, which exhibited no phosphorylation of ERK-1/2 above baseline (Figure 2b). Treatment with the phorbol ester PMA rapidly activates the ERK-1/2 cascade in JCaM cells, indicating that the cell line does have an intact ERK-1/2 response system (not shown), despite low baseline levels of

phosphorylation. We also treated $TCR-\beta^{-/-}$ Jurkat cells with CVB3 and observed ERK-1/2 phosphorylation, similar to wild-type Jurkat cells, indicating that a functional TCR, upstream of Lck, is not required for CVB3-triggered activation of this MAPK (Figure 2c). These findings indicate that ERK-1/2 activation triggered by infection with CVB3 is dependent on the presence of Lck. Exposure to CVB3 did not alter activation of the p38 MAPK or SAPK/JNK cascades in either Jurkat or JCaM cells (not shown).

To investigate the importance of Lck and ERK-1/2 activation in viral attachment, as the first step in infection of cells, we measured binding of radiolabeled CVB3 to T cell lines in the presence and absence of PD98059 (Figure 2d). We found that the absence of ERK-1/2 activation following viral infection in JCaM

Figure 2

Activation of the ERK-1/2 pathway by CVB3 infection is dependent on p56^{Lck} (Lck). (a) Jurkat cells or JCaM cells (10^7) were incubated with CVB3 (moi = 50; +) or control media (−) for 5 or 10 minutes, then lysed. One result represents three experiments. (b) Jurkat, JCaM, and JCaM cells with control vector (JCaM/vector) or Lck restored (JCaM/Lck) (10^7) were incubated with CVB3 (moi = 50; +) or control media (−) for 5 minutes, then lysed. One result represents two experiments. (c) $TCR-\beta$ chain negative Jurkat cells (10^7) were lysed after incubation for 5 or 10 minutes with CVB3 (moi = 50; +) or control media (−), then lysed. One result represents two experiments. All cell lysates were immunoblotted with anti-phospho-ERK-1/2 (P-ERK-1/2) and anti-total ERK-1/2 Ab's. Fold change in P-ERK-1/2-total ERK-1/2 ratio is indicated. (d) CVB3 binding to T cell lines does not require activation of ERK-1/2. Jurkat and JCaM cells (5×10^6) were incubated with [³⁵S]-CVB3 for 1 hour in the presence (PD98059) or absence (DMSO) of MEK-1/2 inhibitor. Binding of virus is expressed as mean percentages (\pm SEM) for triplicate cultures. Viral binding to JCaM cells was twice as high as binding to Jurkat cells (* $P = 0.0001$; Student *t* test).



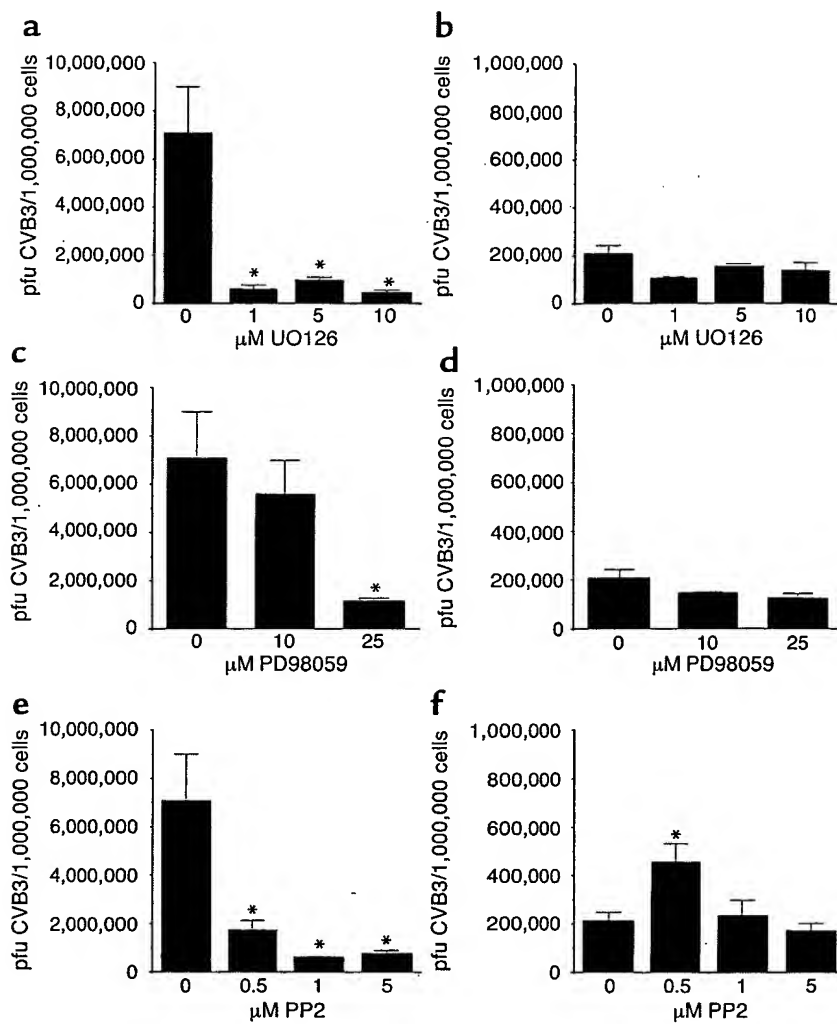


Figure 3

CVB3 replication in Jurkat cells is regulated by Src's and the ERK-1/2 signaling pathway. To assess infectivity, T cell lines (10^6) were treated with kinase inhibitors in DMSO or with DMSO alone (0) for 1 hour at 37°C , and then cells were infected with CVB3 (moi = 1) as described in Methods. Following incubation at 37°C for 48 hours, cells were frozen, then viral titers were determined by plaque assay. Treatment of (a) Jurkat and (b) JCaM cells with the MEK-1/2 inhibitor UO126 decreased CVB3 titers in Jurkat cells, but did not affect viral production in JCaM cells at the same doses of inhibitor. Treatment of (c) Jurkat and (d) JCaM cells with the MEK-1/2 inhibitor PD98059 significantly decreased CVB3 titers in Jurkat cells, but not in JCaM cells. Treatment of (e) Jurkat and (f) JCaM cells with the Src inhibitor PP2 decreased CVB3 titers in Jurkat cells, but not in JCaM cells. Titers were increased in JCaM cells treated with 0.5 μM PP2. Virus titers are expressed as mean pfu/ 10^6 cells (\pm SEM, $n = 3$ per group). * $P < 0.05$ DMSO versus kinase inhibitor for each cell type (ANOVA plus Bonferroni/Dunn post hoc testing).

cells is not due to impaired CVB3 binding. In fact, despite decreased CVB3 yields in cells lacking Lck (JCaM), binding of [³⁵S]-CVB3 was doubled in these cells, as compared with Jurkat cells. This may be due to a threefold increase in expression of the CVB receptor decay accelerating factor (DAF) in JCaM cells (not shown). Furthermore, MEK-1/2 inhibition did not reduce binding of radiolabeled CVB3 to either cell line, indicating that this initial attachment phase proceeds without ERK-1/2 activation.

CVB3 growth is dependent on activation of the ERK-1/2 pathway in Jurkat cells. The activation of ERK-1/2 observed following infection of Jurkat cells with CVB3 led us to investigate the importance of this signaling pathway in the viral replicative process. We found that the specific MEK-1/2 inhibitor UO126 reduced virus yield in Jurkat cells by up to 94% (Figure 3a). In contrast, treatment of Lck-negative JCaM cells with UO126 did not affect the already lower levels of CVB3 produced (Figure 3b). In addition, PD98059, also a MEK-1/2 inhibitor, decreased CVB3 titers in Jurkat cells by 83% (Figure 3c), but did not significantly affect viral production by JCaM cells at the same doses

(Figure 3d). These findings demonstrate a requirement for the activation of the ERK-1/2 signaling pathway for optimal CVB3 replication in Jurkat cells.

The Src (Lck, Hck, Fyn) inhibitor, PP2, decreased CVB3 production by Jurkat cells by 90% (Figure 3e). This is consistent with the impaired replication in the Lck negative T cell line. However, the lower baseline level of viral replication in JCaM cells was not inhibited by PP2 (Figure 3f). In fact, the lowest dose of PP2 increased CVB3 titers in JCaM cells versus control. So, while Lck is the primary Src required for efficient viral replication in T cells, other Src's may influence CVB3 infection as well.

Src and ERK-1/2 participate in the response of cardiac myocytes to CVB3 infection. We extended our investigation of the ERK-1/2 cascade in CVB3 infection to the heart, using isolated neonatal cardiac myocyte cultures. Treatment of cardiac myocytes with the MEK-1/2 inhibitor UO126 decreased the CVB3 titer significantly, as shown in Figure 4a. As well, the specific Src inhibitor, PP2, significantly suppressed CVB3 infection in cardiac myocytes (Figure 4b).

ERK-1/2 phosphorylation increased 2.6-fold 2 days after infection of cardiac myocytes with CVB3 (Figure 4c).

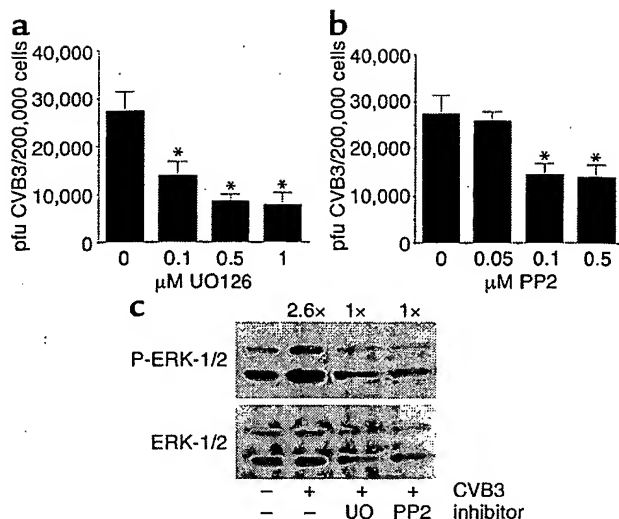


Figure 4

CVB3 replication in neonatal mouse cardiac myocyte cultures is regulated by Src's and the ERK-1/2 signaling pathway. (a) Cardiac myocytes, isolated from neonatal mice, were incubated with DMSO (0) or the MEK-1/2 inhibitor UO126 for 1 hour at 37°C, infected with CVB3 (moi = 5), and then incubated for 48 hours. (b) Cardiac myocytes were incubated with DMSO (0) or the Src's PP2 for 1 hour at 37°C, then infected as above. Virus titers are expressed as mean pfu/2 × 10⁵ cells (± SEM, n = 3 per group). *P < 0.05 DMSO versus kinase inhibitor for each cell type (ANOVA plus Bonferroni/Dunn post hoc testing). (c) ERK-1/2 activation following CVB3 infection in isolated cardiac myocytes was blocked by inhibition of ERK-1/2 and Src activation. The increase in ERK-1/2 phosphorylation observed 48 hours after viral infection was inhibited by treatment with 1 μM UO126 (UO) and 1 μM PP2. One result represents two experiments. Cell lysates were immunoblotted with anti-phospho-ERK-1/2 (P-ERK-1/2) and anti-total ERK-1/2 Ab's. Fold change in P-ERK-1/2-total ERK-1/2 ratio is indicated.

This activation of the ERK-1/2 pathway was inhibited by treatment with both MEK-1/2 and Src inhibitors, suggesting that these protein kinases regulate CVB3 infection of cardiac myocytes. Decreased CVB3 production by cardiac myocytes by MEK-1/2 and Src inhibitors and viral activation by ERK-1/2 are consistent with findings in the T cell model.

The relationship between ERK-1/2 activation and susceptibility to CVB3 myocarditis in mice. We observed that CVB3 activates ERK-1/2 in Jurkat cells and cardiac myocytes and that ERK-1/2 inhibition impairs viral growth in both of these cell types. We subsequently hypothesized that this signaling pathway may also be associated with host susceptibility to myocarditis in vivo. We proceeded to compare two mouse strains with differential susceptibility to myocarditis. CVB3 infection led to an acute and severe myocarditis in A/J mice, but produced minimal myocardial inflammation and necrosis in C57BL/6 mice. Myocytolysis is evident in the myocardium of A/J mice 4 days after infection, in the absence of any accompanying cellular infiltrate (Figure 5a). Cardiac myocytes are healthier and appear more intact in C57BL/6 mice at the same time point (Figure 5b). The peak inflammatory infiltrate

in the myocardium occurs at about day 10 in this model. Large areas of myocyte destruction and infiltrating mononuclear cells are found in the hearts of A/J mice 10 days following CVB3 infection; however, myocardial disease is minimal in C57BL/6 mice (Figure 5c and d). Cardiac viral titers were initially similar between the two strains, but by day 4 viral titers were significantly higher in the hearts of A/J mice compared with C57BL/6 mice (Figure 5e). In contrast, peak viral titers in the spleen were not different between the two strains of mice (not shown).

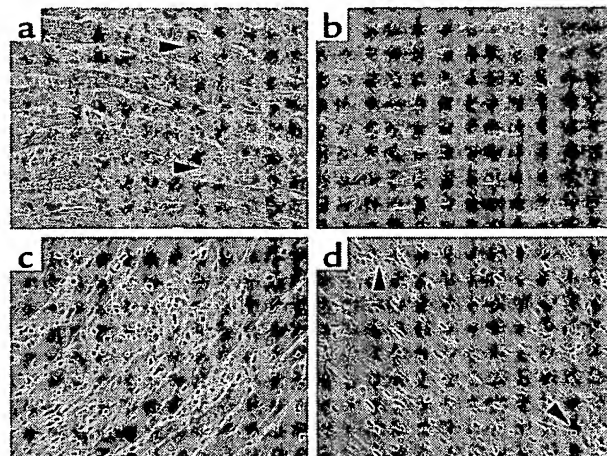


Figure 5

A/J mice are more susceptible to CVB3 myocarditis. At 4 days after infection representative cryosections (10 μm) illustrate that (a) myocyte damage and myocytolysis (arrowheads) in the myocardium of A/J mice are widespread, but (b) in the hearts of C57BL/6 mice cardiac myocytes are generally intact, with cross-striations visible in normal-appearing myocytes. Ten days after infection, representative sections of paraffin-embedded tissue (4 μm) illustrate (c) large areas of myocyte destruction and infiltrating mononuclear cells in the hearts of A/J mice, but (d) only small isolated foci of inflammatory cells (arrowheads) in the myocardium of C57BL/6 mice. All histological sections were stained with hematoxylin and eosin, with original magnification ×400. (e) CVB3 titers were significantly greater in A/J mouse hearts, consistent with the more aggressive heart disease evident on histopathology. *P < 0.05 for A/J mice day-4 titers versus day-1 and -2 titers; **P < 0.05 for day-4 titers in A/J versus C57BL/6 hearts (n = 3 per group; ANOVA plus Bonferroni/Dunn post hoc testing).

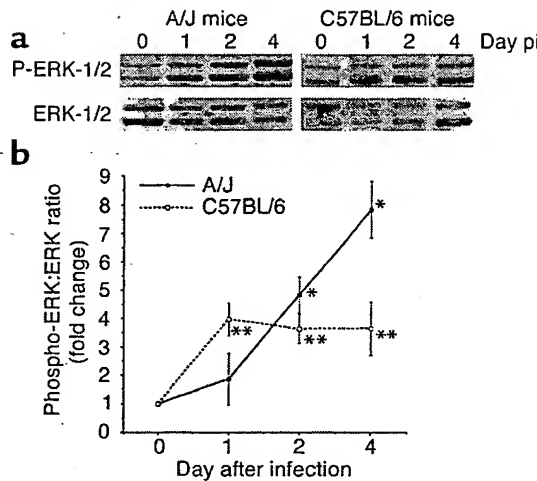


Figure 6

ERK-1/2 activation in the heart is associated with susceptibility to CVB3 myocarditis. (a) ERK-1/2 phosphorylation was increased in the hearts of CVB3-infected mice as early as day 1 postinfection (pi). By day 4, ERK-1/2 activation was more intense in myocarditis-susceptible A/J mice. Levels of phosphorylated ERK-1/2 (P-ERK-1/2) and total ERK-1/2 in the heart were determined by Western blot analysis of tissue homogenates from uninfected controls (0) and days 1, 2, and 4 after CVB3 infection. Results shown are representative of 5 mice per group. (b) The fold change in myocardial P-ERK-1/2:total ERK-1/2 ratios from day 0 (baseline set at 1) was determined following densitometry. By day 2 after infection, ERK-1/2 activation in the myocardium of A/J mice was elevated fivefold above the baseline in uninfected control mice. In A/J mice the intensity of ERK-1/2 phosphorylation continued to increase to eight times baseline by day 4 after infection. ERK-1/2 activation persisted at a lower level in the hearts of myocarditis-resistant C57BL/6 mice. Values are expressed as the mean fold change from baseline (\pm SEM; $n = 5$ per group). * $P < 0.05$ versus day 0 for A/J mice, and on day 4 A/J versus C57BL/6 mice; ** $P < 0.05$ versus day 0 for C57BL/6 mice (ANOVA plus Bonferroni/Dunn post hoc testing).

ERK-1/2 phosphorylation in the myocardium of CVB3-infected A/J mice increased in parallel with high viral titers and severity of myocarditis. ERK-1/2 is activated as early as 24 hours after infection, before peak viral titers are reached (Figure 6a). By day 2 after CVB3 infection of A/J mice, ERK-1/2 activation in the myocardium was elevated fivefold above the baseline in uninfected control mice. In A/J mice the intensity of ERK-1/2 phosphorylation continued to increase to eightfold baseline by day 4 following infection (Figure 6, a and b). ERK-1/2 activation persisted at a significantly lower level in the hearts of myocarditis-resistant C57BL/6 mice. In the spleens no significant change in ERK-1/2 activation was observed (data not shown).

Discussion

We have presented evidence in this study in support of our hypothesis that activation of the ERK-1/2 signaling cascade is a potential determinant of susceptibility to CVB3 infection. To gain insight into the role of ERK-1/2 in the pathogenesis of CVB3 infection we studied both T cells and cardiac myocytes. We have

found that CVB3 infection triggers activation of the ERK-1/2 signaling cascade and that optimal viral replication depends on ERK-1/2 activation. Virus appears to amplify its own replication by enlisting the host cell's signal transduction system, specifically, the ERK-1/2 pathway. The data suggest a Src-dependent activation of ERK-1/2 by CVB3 is common to both T cells and cardiac myocytes and may be significant in the whole animal's response to infection. This concept is supported in a mouse model of host susceptibility to myocarditis. Intense phosphorylation of ERK-1/2 in the myocardium is specifically correlated with high cardiac titers of CVB3 and severe myocarditis. ERK-1/2 activation persists at lower levels in the hearts of mice with relative resistance to CVB3 myocarditis.

Following gene-targeted knockout of Lck, mice are protected from CVB3 myocarditis (8). Our studies in T cell lines suggest that one mechanism by which Lck may influence the myocarditis phenotype is via activation of the ERK-1/2 pathway. Experiments described here demonstrate that CVB3 stimulates rapid phosphorylation of ERK-1/2 in an Lck-dependent manner. In addition, viral production depends on activation of the ERK-1/2 cascade in Jurkat cells. However, Src or ERK-1/2 inhibition does not significantly decrease the already lower level of viral production in JCaM cells. These data suggest that Lck is upstream of ERK-1/2 and is the primary Src required for efficient CVB3 replication in T cells. In cardiac myocytes CVB3 also activates ERK-1/2 in a Src-dependent manner. As with Jurkat cells, ERK-1/2 activation is required for peak susceptibility to viral infection. Thus, the ERK-1/2 signaling cascade is not only activated by CVB3, but is a host cell component essential to productive replication of the virus. This leads to the hypothesis of a self-amplification process, whereby the virus promotes its own growth by activation of the ERK-1/2 cascade.

Findings thus far suggest that Src's in cardiac myocytes may have a comparable role to Lck in the T cell. In mice lacking the Lck gene, viral titers in the heart were decreased 4 days after CVB3 infection (8). This is consistent with the decrease in viral production by isolated cardiac myocytes with inhibition of Src's. Interestingly, we have detected Lck RNA using RT-PCR and Lck protein in the hearts of both A/J and C57BL/6 mice (not shown). In addition, several Src's, including Lck, are expressed in the rabbit heart. In the adult rabbit and isolated cardiac myocytes Lck is activated by ischemic preconditioning, an established cardioprotective technique (21). These observations challenge the traditional concept that Lck is expressed only in T cells, B cells, and natural killer cells (22). While Lck may be a primary upstream kinase that influences ERK-1/2 phosphorylation in response to CVB3 in T cells, the specific contribution of other protein kinases to regulation of the viral life cycle remains to be determined. Interestingly, in Lck-negative JCaM cells, treatment with a low dose of the Src inhibitor PP2

increased CVB3 titers, while higher doses of PP2 had no effect. While Lck appears to be required for optimal viral replication, perhaps other Src's inhibit viral replication in the absence of Lck. The dose-dependent effect of PP2 on viral replication may reflect differential inhibition of Src's. Alternative mechanisms for ERK-1/2 activation, other than through Lck or related Src's, may also influence the viral replicative process and the host cell response to CVB3 infection at different times following infection.

Several viruses have evolved diverse mechanisms to stimulate signal transduction pathways that may promote viral replication, regulate host inflammatory responses to infection, or induce viral oncogenic transformation of cells. Reports of the effects of Enteroviruses on intracellular signal transduction pathways are limited and focus on later stages of infection, at the time of virus-induced host protein synthesis shutoff (23-25). During infection with echovirus 1 and 7, ERK-1/2 activation was shown to be induced by 5 hours after infection, while p38 MAPK was activated by 10 hours after infection (25). CVB3 infection has been shown to induce tyrosine phosphorylation of host proteins in HeLa cells from 3 to 5 hours after infection (23). Sam68, a cellular target of Src's, interacts with the poliovirus RNA-dependent RNA polymerase 3D (26) and associates with RasGAP in response to CVB3 infection (24). RasGAP is cleaved at 6 hours after infection, possibly activating the Ras/MAPK pathway (24). The authors hypothesized that the persistent ERK-1/2 activation observed at this late stage of infection may affect CVB3-induced cytotoxicity or apoptosis. In contrast, by focusing earlier in the viral life cycle, we have demonstrated a requirement for this growth-activated MAPK in efficient CVB3 replication. The potential for a multiplicity of roles for protein kinases in viral infection has been illustrated by the study of signal transduction pathways involved in HIV infection. A Lck activation in HIV-mediated signal transduction is consistent with viral binding to CD4, the major HIV receptor (27). As well, HIV-1 binding to CD4 receptors activates the MEK/ERK signal transduction pathway (28). In addition, ERK-1/2 enhances the infectivity of HIV-1 virions themselves, in part by phosphorylation of the viral proteins Vif, Rev, Tat, Nef, and p17^{Gag} (29). In CVB3-infected cells the downstream effects of ERK-1/2 activation may influence both the function of host cellular proteins and the infectivity of viral proteins, as with HIV-1. Activation of the ERK-1/2 cascade may influence CVB3 replication at any time from viral entry to progeny release. Viral binding appears to proceed independently of ERK-1/2 activation; however, early steps, such as viral entry or uncoating may be dependent on activation of this kinase in the first 2 hours following infection. It is possible that regulation of early events in the viral life cycle may have an impact downstream, affecting total viral yield.

In the hearts of infected mice ERK-1/2 is activated as early as 24 hours following CVB3 inoculation, before peak cardiac viral titers are reached. Interestingly, ERK-1/2 activation is not transient. Perhaps this is due to the presence of ongoing viral stimulation, as it replicates and spreads through the myocardium. Consistent with this is the ERK-1/2 activation present in isolated cardiac myocytes 48 hours following CVB3 infection. ERK-1/2 phosphorylation increases from day 0 to day 4 in the hearts of susceptible A/J mice. In contrast, increased ERK-1/2 phosphorylation persists at a lower level in the hearts of myocarditis-resistant C57BL/6 mice. The higher peak cardiac viral titers in susceptible A/J mice 4 days after infection may stimulate the increased levels of ERK-1/2. Early ERK-1/2 activation may also promote viral replication, to differing degrees, depending on the mouse strain. In vitro observations support both CVB3 activation of ERK-1/2 and the influence of ERK-1/2 on viral production. The absence of inflammatory foci in the myocardium of mice at day 4 after infection, particularly in comparison with infiltrates seen at day 10, suggest that the source of phosphorylated ERK-1/2 is not infiltrating immune cells.

In summary, we have demonstrated that the ERK-1/2 signaling cascade is a potentially novel determinant of susceptibility to CVB3 infection and disease. In T cell lines the ERK-1/2 pathway is specifically and rapidly activated in an Lck-dependent manner. This supports ERK-1/2 activation as a mechanism by which Lck controls susceptibility to CVB3 myocarditis. CVB3 may in this way promote the exuberant T lymphocyte response found in CVB3 myocarditis. As demonstrated by the infection of murine cardiac myocytes with CVB3, the importance of Src and the ERK-1/2 cascade in the establishment of viral infection is not restricted to T cells. The virus may take advantage of one element of the host's signal transduction system to promote its own infectivity. Consistent with observations made in vitro in T cells and cardiac myocytes, activation of the ERK-1/2 pathway in the heart is associated with elevated CVB3 replication and pathogenicity in mice. Moreover, ERK-1/2 activation is increased in the hearts of mice susceptible to severe myocarditis. The discovery of different patterns of ERK-1/2 activation in the hearts of myocarditis-susceptible and -resistant mice highlights a critical juncture downstream of viral receptors, which, with further study, may lead to new strategies in the treatment of severe CVB disease.

Acknowledgments

We greatly appreciate the technical assistance of Fayed Dawood and Wen-Hu Wen with the animal protocols. This research was supported by grants from the Canadian Institutes of Health Research (CIHR) and the Heart and Stroke Foundation of Ontario. M.A. Opavsky was a postdoctoral fellow of the CIHR. P.P. Liu is the Heart and Stroke/Polo Endowed Research Chair at the University of Toronto.

- Opavsky, M.A., Sole, M.J., and Liu, P. 1998. Myocarditis. In *Cardiology*. W. Parmley and K. Chatterjee, editors. Lippincott-Raven. Philadelphia, Pennsylvania, USA.
- Woodruff, J. 1980. Viral myocarditis. A review. *Am. J. Pathol.* 101:427-484.
- Liu, P., Martino, T., Opavsky, M.A., and Penninger, J. 1996. Viral myocarditis: balance between viral infection and immune response. *Can. J. Cardiol.* 12:935-943.
- Chow, L.H., Beisel, K.W., and McManus, B.M. 1992. Enteroviral infection of mice with severe combined immunodeficiency: evidence for direct viral pathogenesis of myocardial injury. *Lab. Invest.* 66:24-31.
- Woodruff, J.F., and Woodruff, J.J. 1974. Involvement of T lymphocytes in the pathogenesis of Coxsackie virus B3 heart disease. *J. Immunol.* 113:1726-1734.
- Opavsky, M.A., et al. 1999. Susceptibility to myocarditis is dependent on the response of $\alpha\beta$ T lymphocytes to coxsackieviral infection. *Circ. Res.* 85:551-558.
- Voronova, A.F., Buss, J.E., Parchinsky, T., Hunter, T., and Sefton, B.M. 1984. Characterization of the protein apparently responsible for the elevated tyrosine protein kinase activity in LSTRA cells. *Mol. Cell Biol.* 4:2705-2713.
- Liu, P., et al. 2000. The tyrosine kinase p56lck is essential in Coxsackievirus B3-mediated heart disease. *Nat. Med.* 6:429-434.
- Hsi, E.D., et al. 1989. T cell activation induces rapid tyrosine phosphorylation of a limited number of cellular substrates. *J. Biol. Chem.* 264:10836-10842.
- Straus, D.B., and Weiss, A. 1992. Genetic evidence for the involvement of the Lck tyrosine kinase in signal transduction through the T cell antigen receptor. *Cell.* 70:585-593.
- Franklin, R., et al. 1994. Ligation of the T cell receptor complex results in activation of the Ras/Raf-1/MEK/MAPK cascade in human T lymphocytes. *J. Clin. Invest.* 93:2134-2140.
- Guckind, J.S. 1998. The pathways connecting G protein-coupled receptors to the nucleus through divergent mitogen-activated protein kinase cascades. *J. Biol. Chem.* 273:1839-1842.
- Sturgill, T.W., Ray, L.B., Erikson, E., and Maller, J.L. 1988. Insulin-stimulated MAP-2 kinase phosphorylates and activates ribosomal proteins S6 kinase II. *Nature.* 334:715-718.
- Boulton, T.G., et al. 1991. ERKs: a family of protein-serine/threonine kinases that are activated and tyrosine phosphorylated in response to insulin and NGF. *Cell.* 65:663-675.
- Davis, R.J. 1993. The mitogen-activated protein kinase signal transduction pathway. *J. Biol. Chem.* 268:14553-14556.
- Parker, T.G., Packer, S.E., and Schneider, M.D. 1990. Peptide growth factors can provoke "fetal" contractile protein gene expression in rat cardiac myocytes. *J. Clin. Invest.* 85:507-514.
- Martino, T.A., et al. 1998. Cardiovirulent Coxsackieviruses and the decay-accelerating factor (CD55) receptor. *Virology.* 244:302-314.
- Chow, L., Gauntt, C., and McManus, B. 1991. Differential effects of myocarditis variants of Coxsackievirus B3 in inbred mice: a pathologic characterization of heart tissue damage. *Lab. Invest.* 64:55-64.
- Vuorinen, T., Vainionpaa, R., Kettinen, H., and Hyypia, T. 1994. Coxsackievirus B3 infection in human leukocytes and lymphoid cell lines. *Blood.* 84:823-829.
- Vuorinen, T., Vainionpaa, R., Vanharanta, R., and Hyypia, T. 1996. Susceptibility of human bone marrow cells and hematopoietic cell lines to Coxsackievirus B3 infection. *J. Virol.* 70:9018-9023.
- Ping, P., et al. 1999. Demonstration of selective protein kinase C-dependent activation of Src and Lck tyrosine kinases during ischemic preconditioning in conscious rabbits. *Circ. Res.* 85:542-550.
- Bolen, J.B., Rowley, R.B., Spana, C., and Tsygankov, A.Y. 1992. The Src family of tyrosine protein kinases in hemopoietic signal transduction. *FASEB J.* 6:3403-3409.
- Huber, M., Selinka, H.-C., and Kandolf, R. 1997. Tyrosine phosphorylation events during Coxsackievirus B3 replication. *J. Virol.* 71:595-600.
- Huber, M., et al. 1999. Cleavage of RasGAP and phosphorylation of mitogen-activated protein kinase in the course of Coxsackievirus B3 replication. *J. Virol.* 73:3587-3594.
- Huttunen, P., Hyypia, T., Vihinen, P., Nissinen, L., and Heino, J. 1998. Echovirus 1 infection induces both stress- and growth-activated mitogen-activated protein kinase pathways and regulates the transcription of cellular immediate-early genes. *Virology.* 250:85-93.
- McBride, A., Schlegel, A., and Kirkegaard, K. 1996. Human protein Sam68 relocalization and interaction with poliovirus RNA polymerase in infected cells. *Proc. Natl. Acad. Sci. USA.* 93:2296-2301.
- Manna, S.K., and Aggarwal, B.B. 2000. Differential requirement for p56lck in HIV-tat versus TNF-induced cellular responses: effects on NF- κ B, activator protein-1, c-jun N-terminal kinase, and apoptosis. *J. Immunol.* 164:5156-5166.
- Popik, W., Hesselgesser, J.E., and Pitha, P.M. 1998. Binding of human immunodeficiency virus type 1 to CD4 and CXCR4 receptors differentially regulates expression of inflammatory genes and activates the MEK/ERK signaling pathway. *J. Virol.* 72:6406-6413.
- Yang, X., and Gabuzda, D. 1999. Regulation of human immunodeficiency virus type 1 infectivity by the ERK mitogen-activated protein kinase signaling pathway. *J. Virol.* 73:3460-3466.

MEK-Specific Inhibitor U0126 Blocks Spread of Borna Disease Virus in Cultured Cells

OLIVER PLANZ,^{1*} STEPHAN PLESCHKA,² AND STEPHAN LUDWIG³

Institut für Immunologie, Bundesforschungsanstalt für Viruskrankheiten der Tiere, Tübingen,¹ Institut für Virologie, Fachbereich Veterinär-Medizin, Justus-Liebig Universität, Giessen,² and Institut für Medizinische Strahlenkunde und Zellforschung (MSZ), Würzburg,³ Germany

Received 17 October 2000/Accepted 21 February 2001

Borna disease virus (BDV) is a highly neurotropic virus that causes Borna disease, a virus-induced immune-mediated encephalomyelitis, in a variety of warm-blooded animals. Recent studies reported that BDV can be detected in patients with psychiatric disorders. BDV is noncytopathic, replicates in the nucleus of infected cells, and spreads intraxonally *in vivo*. Upon infection of susceptible cultured cells, virus can be detected in foci. Little is known about the cellular components required for BDV replication. Here, we show that the cellular Raf/MEK/ERK signaling cascade is activated upon infection with BDV. In the presence of the MEK-specific inhibitor U0126, cells get infected with BDV; however, there is a block in virus spread to neighboring cells. The effect of the inhibitor on virus spread was still observed when the compound was added 2 h postinfection but not if treatment was initiated as late as 4 h after infection. Our results provide new insights into the BDV-host cell interaction and show that virus infection can be controlled with drugs interfering with a cellular signaling pathway. Since concentrations of the MEK inhibitor required to block BDV focus formation are not toxic for the host cells, our finding may be important with respect to antiviral drug development.

Mitogen-activated protein kinase (MAPK) cascades have been implicated in a variety of cellular functions ranging from regulation of the proliferative response to the control of apoptotic cell death. The prototype of the MAPK family of signaling pathways is the Raf/MEK/extracellular signal-regulated kinase (ERK) cascade, which plays a major role in the regulation of cell growth and differentiation. Growth factor-induced signals are transmitted by consecutive phosphorylation from the serine/threonine kinase Raf via the dual-specificity kinase MEK (MAPK kinase/ERK kinase) to ERK. Active ERK subsequently translocates to the nucleus to phosphorylate a variety of substrates and mediate changes in gene expression (33, 44). Specific and selective inhibitors have been used to elucidate the function of this kinase cascade in cellular regulation by extracellular stimuli. These inhibitors block activation of MEK by Raf and thus interfere with signaling at the bottleneck of the cascade (1, 14, 15). The MEK-specific inhibitor U0126 (1,4-diamino-2,3-dicyano-1,4-bis[2-aminophenylthio]butadiene) was first described as a compound that partially blocks AP-1 transactivation (15) and T-cell proliferation (12). Inhibition of MEK is selective as U0126 shows little, if any, effect on the kinase activities of protein kinase C, Abl, Raf, MEKK, ERK, JNK, Cdk2, or Cdk4 and the MEK-related kinases MKK-3, MKK-4/SEK, and MKK-6 (15). Further, U0126 has an approximately 100-fold-higher affinity for active MEK than does the previously identified MEK inhibitor, PD98059 (15).

A variety of DNA and RNA viruses induce signaling via MAPK pathways in infected host cells, suggesting that these kinase cascades may play a functional role in virus replication

(3, 7, 34). Borna disease virus (BDV), a noncytolytic single-stranded RNA virus, is the only known member of *Bornaviridae* in the order of *Mononegavirales*. BDV is highly neurotropic and cell associated. The 8.9-kb-size genome with negative polarity is replicated in the nucleus and encodes at least six different known viral proteins: the nucleoprotein (p40), the phosphoprotein (p24), the X protein (p10), and two glycosylated proteins, the matrixprotein (gp18) and the glycoprotein (gp94). Furthermore, an L-polymerase of 190 kDa has been described (18, 23, 26, 37, 39, 43, 45, 46, 48). The phosphoprotein p24 is phosphorylated at serine residues, suggesting that the function of this protein is controlled by cellular kinases (38, 43). A recent report by Walker et al. shows that the L-polymerase of BDV is also phosphorylated, making this protein a further candidate for BDV-host cell interactions (45). BDV induces Borna disease, a T-cell-mediated encephalomyelitis originally described in horses and sheep (24, 35). In recent years this viral infection of the central nervous system has been diagnosed in a wide variety of animals, including cattle, cats, dogs, and birds (reviewed in reference 42). Furthermore, BDV, nucleic acid, and antibodies were detected in blood of patients with psychiatric diseases (2, 5, 6, 22, 30, 31, 36), although no direct correlation between BDV as the causative agent and a particular mental disorder in humans has been demonstrated yet. To date, amantadine and ribavirin have been described as anti-BDV drugs. The effect of amantadine is controversial, and ribavirin reduces infectivity *in vitro* by only 1 \log_{10} (4, 11, 16, 21, 27, 41).

Here we show that BDV infection of different cell lines leads to activation of the Raf/MEK/ERK signaling cascade. Activity of the cascade appears to be essential for BDV spread, since inhibition of the pathway using the potent MEK-specific inhibitor U0126 efficiently blocks infection of cells with progeny virus without being toxic for the host cell.

* Corresponding author. Mailing address: Institut für Immunologie, Bundesforschungsanstalt für Viruskrankheiten der Tiere, D-72076 Tübingen, Germany. Phone: 49 7071 967 254. Fax: 49 7071 967 105. E-mail: oliver.planz@tue.bfav.de.

MATERIALS AND METHODS

Cell lines and virus. The guinea pig cell line CRL 1405 was subcloned, and cells highly susceptible to BDV were used as a standard laboratory cell line for BDV infection (40). Furthermore, the human oligodendrocyte cell line OL (29), also highly susceptible to BDV infection, was used throughout this study. In addition, persistent BDV-infected and -uninfected F10 (rat astrocytes) (47), C6 (8), Vero (17), and 293T (human embryonal kidney cells, expressing SV40 large T antigen) cells were used. The cells were cultured with Iscove modified Dulbecco's medium (IMDM) supplemented with 5% fetal calf serum (FCS), 2 mM L-glutamine, and 100 U of gentamicin/ml.

The fourth rat passage of the Giessen strain He/80 was used for infection (28). In general, adherent cells were infected with a multiplicity of infection (MOI) of 1 or 0.01 focus-forming units in either 96-well or 6-well plates for 1 h in a volume of 25 μ l (for 96-well plate) or 200 μ l (for 6-well plate) of IMDM-2% FCS. For mock infection, 10% normal rat brain homogenate in IMDM-2% FCS was used. Thereafter, culture medium was added and cells were cultivated for 5 to 7 days.

Treatment of cells with the MEK inhibitor U0126. MEK inhibitor U0126 (Promega, Heidelberg, Germany) was dissolved in dimethyl sulfoxide (DMSO) leading to a 50 mM U0126 stock solution. For experiments, U0126 was used at either 6, 12.5, 25, or 50 μ M concentrations in medium. In parallel, control cells were treated with DMSO alone in the respective concentrations. Full activity of U0126 was still observed after 10 h of cell culture. Nevertheless, activity may decline after longer incubation.

Viability staining. CRL and OL cells were treated with 50, 25, and 12.5 μ M U0126 or with DMSO. One day and 6 days later the cells were trypsinized and washed twice with phosphate-buffered saline (PBS). Cells (5×10^5) were treated with 2 μ l (50 μ g/ml) of propidium iodide for 10 min, and viable cells were counted by flow cytometry (FACS-Scan; Becton Dickinson, Heidelberg, Germany).

Infectivity assay and viral antigen detection by immunocytochemistry. Virus infectivity was determined on CRL 1405 cells by a standard immunocytochemistry assay (40). Briefly, 10^6 BDV-infected cells/ml were lysed by sonification and centrifuged, and titers of the supernatant were determined. Titrations were carried out in flat-bottomed 96-well microtiter plates. CRL 1405 cells were cultured for 7 days. Thereafter, the cells were fixed with 4% formaldehyde-PBS and treated with 1% Triton X-100-PBS and viral antigen was demonstrated in an immunocytochemical reaction using anti-BDV-specific mouse monoclonal antibodies directed against the nucleo- and phosphoprotein. Nonspecific binding of antibodies was blocked by incubation of plates with 10% FCS-PBS. The reaction of monoclonal antibodies with cells was detected by a secondary anti-species biotin-labeled antibody (Dianova, Hamburg, Germany) and by a streptavidin-peroxidase conjugate (Dianova). The reaction was visualized with 0.4% *ortho*-phenylenediamine and 0.5 μ l of H₂O₂ (Sigma, Taufkirchen, Germany)/ml.

ERK2 immune-complex kinase assays. Cells were lysed in Triton lysis buffer (TLB) (20 mM Tris HCl, pH 7.4, 137 mM NaCl, 10% glycerol, 1% Triton X-100, 2 mM EDTA, 50 mM Na glycerophosphate, 20 mM Na pyrophosphate, 5 μ g of aprotinin ml⁻¹, 5 μ g of leupeptin ml⁻¹, 1 mM Na vanadate, 5 mM benzamidine) on ice for 10 to 20 min. Cell lysates were then centrifuged at 13,000 $\times g$ for 10 min at 4°C, and supernatants were incubated with an ERK2-specific antiserum (Santa Cruz, Heidelberg, Germany) and protein A-agarose (Roche, Mannheim, Germany) for 2 h at 4°C. Immune complexes were used for *in vitro* kinase assays with myelin basic protein as a substrate for ERK as previously described (25). Proteins were separated by sodium dodecyl sulfate-polyacrylamide gel electrophoresis and were blotted onto polyvinylidene difluoride membranes. Phosphorylated substrates were detected by a BAS 2000 Bio Imaging Analyzer (Fuji, via Raytest, Staufenhardt, Germany) and by autoradiography. Equal loading of immunoprecipitated ERK2 was analyzed by Western blotting using an ERK2-specific antiserum (Santa Cruz) and peroxidase-coupled protein A followed by a standard enhanced chemiluminescence reaction (Amersham, Freiburg, Germany).

RESULTS

BDV infection results in activation of the classical MAPK ERK. A variety of DNA and RNA viruses induce signaling via MAPK cascades in infected host cells (3, 7, 32, 34). However, it is largely unknown which intracellular signaling processes are induced by BDV to support viral replication. To assess whether BDV infection results in an activation of the classical MAPK pathway, the guinea pig cell line CRL 1405 was infected at an MOI of 1 and cell lysates were analyzed for ERK activity in

immune-complex kinase assays at several time points postinfection (p.i.). As a control, mock-infected cells were assessed at the same time points. Figure 1A shows that BDV infection induces a detectable and sustained increase in ERK2 activation 1, 3, and 6 h p.i. The finding that activation of ERK2 by BDV is only marginal compared to mitogenic stimulation (20% FCS [Fig. 1A, lane 8]) may be due to the fact that only a small portion of cells are infected at an MOI of 1 and the measurable activity is diluted by the ERK activity of uninfected cells. Since it is not possible to prepare BDV stocks that allow acute infection with an MOI higher than 1, we analyzed different cell lines which are persistently infected with BDV, thus carrying virus in almost every cell. As shown in Fig. 1B, ERK2 activity is elevated in four different persistently infected cell lines. These findings clearly indicate that BDV induces a sustained activation of the classical MAPK cascade in infected cells.

BDV spread is blocked upon specific inhibition of the Raf/MEK/ERK cascade. Infection of CRL cells with BDV leads to focus formation visible by immunocytochemistry within 5 to 7 days after infection (40). Since acute BDV infection leads to ERK2 activation of CRL cells, it was assessed whether BDV replication requires activity of the Raf/MEK/ERK pathway. CRL cells were pretreated 30 min prior to infection (MOI = 0.01) with a single dose of different concentrations of the MEK inhibitor U0126 ranging from 6 to 50 μ M. Infected cells were examined daily for morphological alterations and were stained 7 days p.i. for the presence of viral proteins. At concentrations of 6 μ M U0126, no difference in virus distribution was observed compared to cells treated with the solvent alone, whereas at 12.5 μ M U0126 the size of foci was significantly reduced. In contrast to cells treated with DMSO (Fig. 2A) in the presence of 25 μ M U0126 and above, no foci could be observed anymore and only single cells were found positive for viral proteins (Fig. 2B). Essentially the same inhibitory effects on BDV spread were obtained when human oligodendrocytes (OL cells) were used as host cells (Table 1).

We further analyzed whether the inhibitory effect of U0126 on virus spread is dependent on the time of administration of the compound. Infected cells were treated with 25 μ M U0126 starting 2 or 4 h after infection, and infectivity was analyzed 5 days after infection. While the inhibiting effect was still obvious if U0126 was added 2 h p.i., no reduction of focus formation could be observed if the reagent was given 4 h p.i. (Table 1).

These results show that the block of BDV spread is dependent on the concentration of U0126, which appears to target a crucial step in the replication cycle occurring between 2 and 4 h after infection. In contrast, no inhibitory effect of U0126 was observed when persistent BDV-infected CRL cells were treated with the MEK inhibitor (data not shown). This indicates that the spread of the virus from cell to cell rather than the initial infection or the intracellular expression of the nucleo- and phosphoprotein is affected by the drug.

BDV-infected cells harbor infective virus after U0126 treatment. To analyze whether the presence of detectable amounts of viral antigen in cells after U0126 treatment still represents infectious virus, CRL and OL cells were treated with U0126 before BDV infection and were cultured for 5 days in the presence of the inhibitor. Thereafter, cell lysates were analyzed for infectious virus by a standard virus titration assay (33). In cells

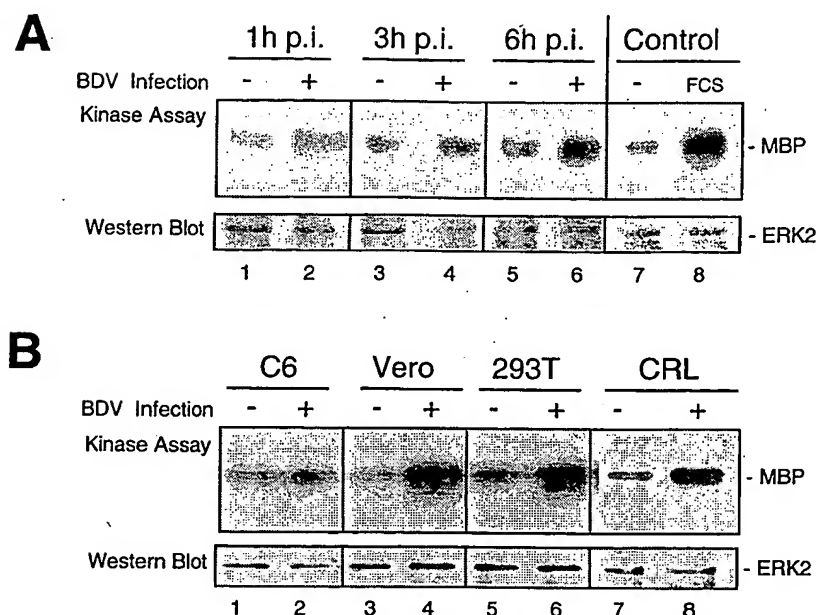


FIG. 1. BDV induces activation of ERK2 in acute and persistently infected cells. (A) CRL cells were either mock infected (lanes 1, 3, and 5) or infected with BDV at an MOI of 1 (lanes 2, 4, and 6) for 1, 3, or 6 h as indicated. In the control reaction, cells were either left untreated (lane 7) or treated with 20% FCS for 1 h as a mitogenic stimulus to activate ERK2 (lane 8). Cell lysates were subjected to ERK2 immune complex kinase assays as described in Materials and Methods by using myelin basic protein as a substrate. Phosphorylated substrates were visualized on X-ray films. ERK2 Western blots were analyzed to confirm equal loading of the kinases. ERK activation upon BDV infection is weak (2- to 4-fold) compared to the control sample stimulated with 20% FCS (13-fold). (B) Cell lysates of parental cells (lanes 1, 3, 5, and 7) or persistently BDV-infected C6 (lane 2), Vero (lane 4), 293T (lane 6), and CRL (lane 8) cells were analyzed for ERK2 activity as described above. ERK activity in persistently infected cell lines ranges roughly from two- to fourfold.

treated with DMSO, a virus titer of $4.7 \log_{10}$ per 10^6 cells was detected, which is the regular level of virus production in these cells (40). In contrast, the virus titer in U0126-treated cells was drastically reduced to $2.3 \log_{10}$ per 10^6 cells, representing a reduction in the virus titer of 99.5%; however, there were still infectious viral particles left. Essentially the same results were observed when OL cells were used as host cells for BDV infection (Tables 2 and 3). This indicates that the positive staining for viral proteins in the single stained cells (Fig. 2B) is not due to aberrantly produced viral proteins; infectious virus particles are formed but appear to be retained in primary infected cells in the presence of the inhibitor.

Next, we questioned if BDV spread is restrained if U0126 is removed from the culture medium. Therefore, CRL and OL cells were treated with 25 μ M U0126 prior to BDV infection and were cultured for five days in the presence of the MEK inhibitor. Thereafter, cells were trypsinized; one part was used for virus titration and the other part was cultured either with or without U0126 for an additional 5 days before they were used for virus titration. As shown in Table 3, the virus titer increased when U0126 was removed from the medium and virus foci were visible (data not shown), indicating that BDV regains its ability to spread in cell culture when the inhibition of the Raf/MEK/ERK signaling cascade is omitted.

U0126 is not toxic for CRL and OL cells. Since U0126 targets an essential signaling pathway for growth regulation, an extended presence of the inhibitor might be toxic for the cell. Confluent CRL or OL cells were incubated for 24 h or 6 days in the presence of different concentrations of U0126 (12.5, 25, and 50 μ M) or the appropriate amount of the solvent alone.

Morphological examination revealed no differences for cells cultured in either condition (Fig. 2C and D). Cells were subsequently stained with propidium iodide, and samples were evaluated by flow cytometry analysis (Fig. 3). Neither the presence of the inhibitor nor of the solvent alone resulted in a decrease of the total cell numbers or in an increased number of dead cells. This indicates that at the concentrations used, U0126 is not toxic for either CRL or OL cells.

DISCUSSION

The cellular factors and processes crucial for BDV replication are poorly defined. Here, we show that the Raf/MEK/ERK signaling pathway is activated upon BDV infection after acute infection. At 1 h after infection, ERK activation is already detected. This very early time point at which ERK activation is detected correlates well with the requirements of the pathway early during infection; however, it would suggest that gene expression is not involved in activation of the kinase cascade. The question remains as to what mechanisms specifically associated with BDV infection are responsible for this activation. In addition, we show that ERK is activated in different persistent BDV-infected cell lines to distinct levels. After this report was submitted, Hans et al. showed that BDV caused constitutive activation of the ERK1/2 pathway and that activated ERKs were not translocated to the nucleus efficiently in persistently infected PC12 cells. That might account for the absence of neuronal differentiation of BDV-infected PC12 cells treated with NGF (20).

Here, we show for the first time that inhibition of the cas-

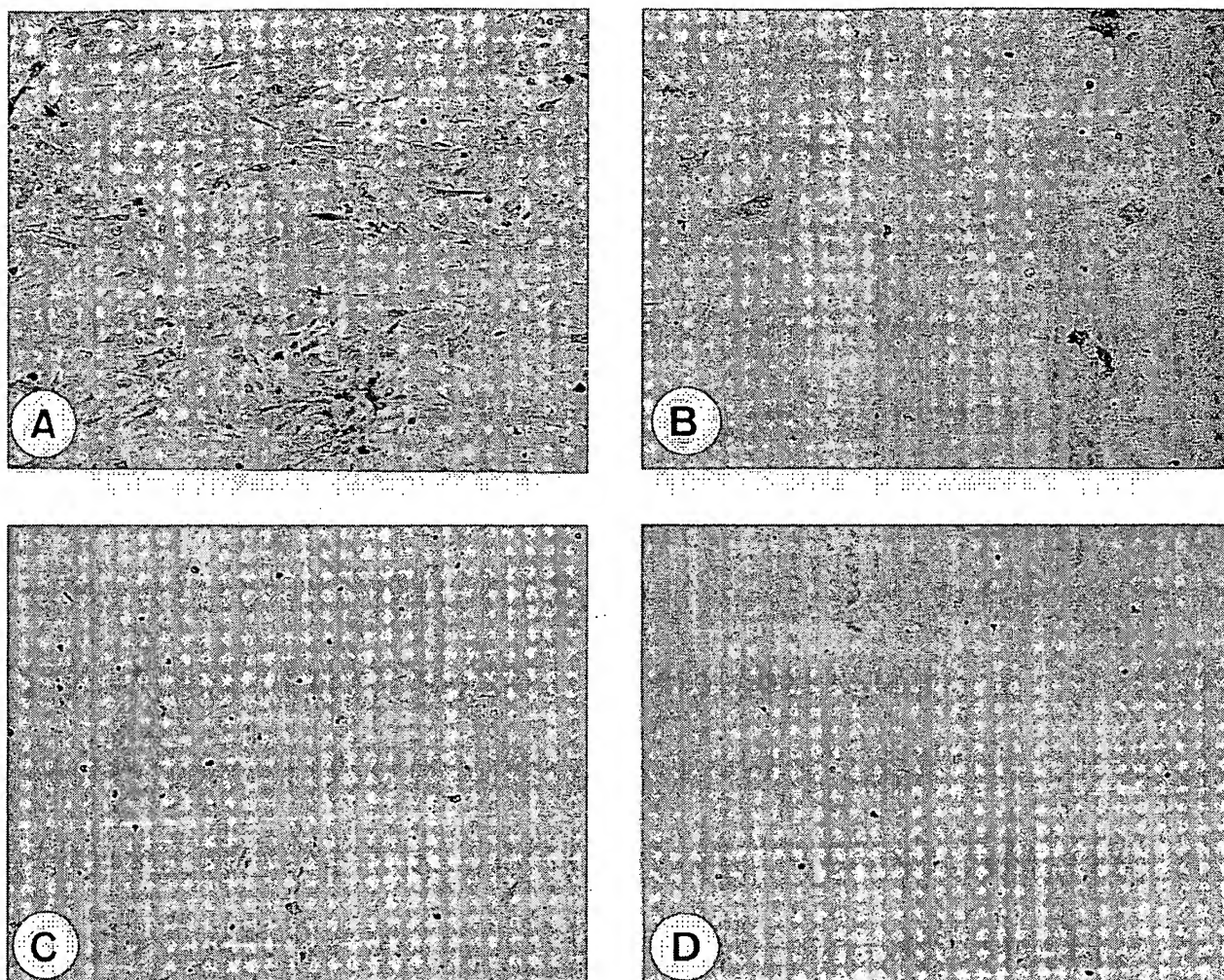


FIG. 2. U0126 inhibits BDV foci formation. BDV-infected (A and B) or mock-infected (C and D) CRL cells were treated with either DMSO (A and C) or 25 μ M U0126 (B and D). Seven days after infection, cells were stained by a standard immunocytochemistry protocol. Magnification, $\times 60$.

cade by the MEK inhibitor U0126 results in a block of BDV spread in cell culture which reduces virus yields up to 99%. Inhibition was observed in two different cell lines highly susceptible to BDV infection, showing that the effect is not restricted to a particular cell type. Moreover, the inhibitory concentrations of U0126 used in this study were not toxic for the

host cells, indicating that inhibition of BDV spread is not an indirect effect due to a loss of cell viability. However, it is known that agents that interfere with cellular functions but are not fatal to the cell can alter cell physiology and, after virus infection, may affect virus replication. Thus, we cannot distinguish at the moment whether the kinase cascade leads to a direct modification of viral proteins or whether the effects are indirectly caused by an altered cell state. Nevertheless, there is an obvious requirement of the Raf/MEK/ERK pathway for the outcome of BDV infection.

Our results show that the Raf/MEK/ERK signaling pathway

TABLE 1. Inhibitory effect of U0126 treatment on BDV spread by the concentration and time of application

Cell line	Inhibitory effect by:						
	Concn of U0126 (μ M)				Time of treatment before or after BDV infection (h)		
	50	25	12.5	6	-0.5	2	4
CRL	+	+	+/−	− ^b	+	+	−
OL	ND ^c	+	−	−	+	+	−

^a +, inhibition of BDV spread; only single infected cells are visible.

^b −, no inhibition of BDV spread to neighboring cells.

^c ND, not done.

TABLE 2. U0126 treatment reduces BDV infectivity

Inhibitor used	Virus titer (\log_{10})/% reduction for cell line:	
	CRL	OL
DMSO	4.7	4.6
U0126	2.3/99.5	2.6/99.0

TABLE 3. BDV infectivity after culture periods in the presence or absence of U0126

Cell line and inhibitor used	Virus titer (\log_{10}) after culture period:	
	First ^a	Second
CRL		
U0126	2.3	2.9
DMSO		4.4
DMSO	4.6	5.0
OL		
U0126	2.6	3.1
DMSO		4.5
DMSO	4.6	4.9

^a Cells were cultured for 5 days (first culture period), one portion was used for virus titration, and the remaining portion was cultured for an additional 5 days (second culture period) in the presence or absence of U0126.

plays an important role in BDV spread from cell to cell. From our data, we conclude that virus entry into the cell and virus replication are not influenced by the inhibitor, since infectious virus is still detected and can be recovered from primarily infected cells treated with the inhibitor. After immunohistochemistry of U0126-treated and BDV-infected cells, it appears that most of the BDV antigen is concentrated in the nucleus. Therefore, one might speculate that viral proteins are located in the cytoplasm to a lesser extent. This could contribute to the inability of the virus to spread beyond the cell, as virus assembly should occur in the late phase of the replication cycle. Furthermore, treatment of persistently BDV-infected cells did not result in a reduction of viral titer, indicating that U0126 treatment does not affect viral replication but rather inhibits the spread of BDV from cell to cell.

Inhibition of virus spread was still achieved when the inhibitor was added to the medium 2 h p.i., indicating that the effect of the drug is not due to an impaired binding of virus to the putative virus receptor or inhibition of virus entry into the cell. Duchala and colleagues have shown that binding and entry of BDV can take up to 4 h (13). Therefore, it is tempting to speculate that virus entry could be limited by the MEK inhibitor. Consequently, this would reduce virus spread and focus formation. Nevertheless, from experiments using UV-inactivated influenza virus, we could show that ERK is not activated and thus virus binding and the uptake of viruses might not be the ERK activating principle (S. Ludwig, unpublished data). Therefore, one might speculate that an early step in the viral replication cycle is affected upon inhibition of the signaling cascade. Inhibition was no longer successful if U0126 was added 4 h p.i. Thus, between 2 and 4 h p.i. the Raf/MEK/ERK signaling pathway is required for secondary infection of neighboring cells. It is puzzling that inhibition of the Raf/MEK/ERK pathway does not result in a loss of infectious virus particle formation, which still can be recovered after 5 days p.i. from primary infected, U0126-treated cells. This observation could be explained by a model in which MEK inhibition results in alteration of a cellular or viral-mediated process which subsequently prevents BDV from spreading from cell to cell but does not interfere with infectivity once the virus is released by cell disruption. Furthermore, the inhibitory effect of U0126 on BDV spread is dependent on the concentration, since doses less than 25 μ M still allow foci formation, demonstrating virus spread.

The efficiency of anti-RNA virus drugs targeting a viral factor is limited as applications of these compounds frequently

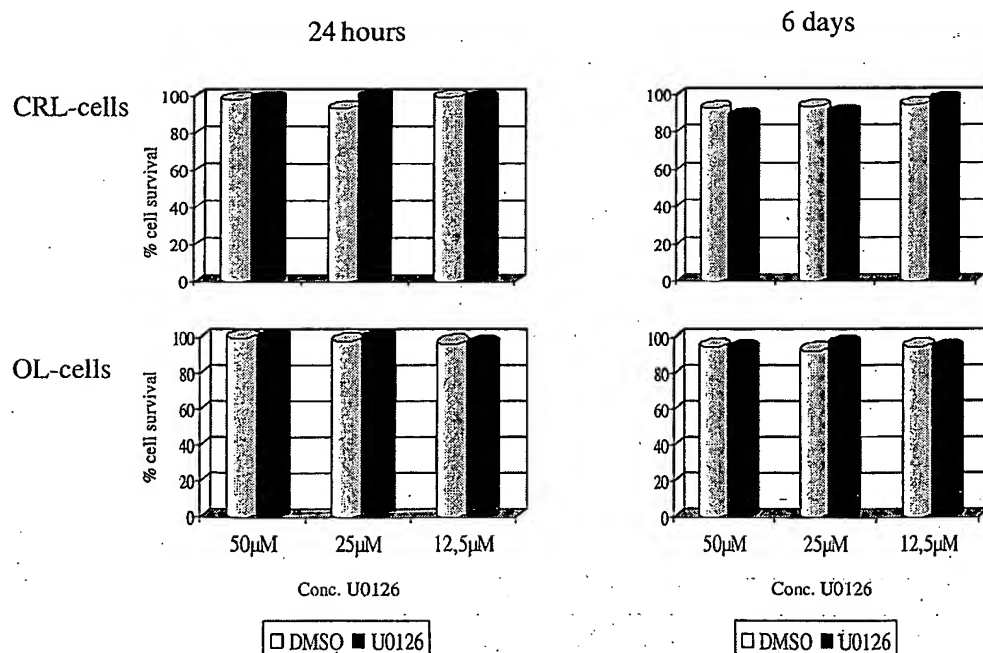


FIG. 3. CRL cells (upper panels) and OL cells (lower panels) were incubated with U0126 or with DMSO alone for either 1 day (left panels) or 6 days (right panels). Cells were treated with propidium iodide and were analyzed by flow cytometry. The percentage of viable cells after treatment with U0126 or DMSO was compared with the viability of untreated cells. Experiments were repeated twice with almost the same results.

result in the rapid selection of drug-resistant virus variants. So far, compounds are very rare that can be used in the antiviral treatment against BDV. Using the nucleoside analog ribavirin, BDV infection could be reduced by 90%, while the effect of amantadine treatment of BDV-infected cells is still controversial (4, 6, 11, 19, 21, 27, 41). As the MEK inhibitor targets a cellular component, it is unlikely that the virus can escape the selection pressure by resistance.

For DNA viruses and in particular for oncogenic viruses, much is known about how these viruses interact with the host cell (3, 7, 32, 34). For RNA viruses little information exists, although interaction of RNA viruses with the Raf/MEK/ERK signaling pathway has been reported. Infection of cells with respiratory syncytial virus results in an increased activity of ERK2. The MEK1 inhibitor PD98059, like U0126, blocks activation of MEK 1 and inhibits the increase in ERK 2 activity after respiratory syncytial virus infection by about 50% (10). Activation of the ERK MAPK pathway also plays a role in human immunodeficiency virus type 1 (HIV-1) replication by enhancing the infectivity of HIV-1 virions through Vif-dependent as well as Vif-independent mechanisms. Inhibition of HIV-1 infectivity could be observed after treatment with a MEK inhibitor (9, 49, 50). Although our present data clearly shows that signaling through MEK is essential for BDV spread, the exact molecular mechanism of how BDV interacts with the cellular Raf/MEK/ERK signaling pathway remains to be elucidated. Since the phosphoprotein p24 is phosphorylated via serine residues, one might speculate that this viral protein could play an important role in BDV-host cell interaction (39, 43).

Our results suggest that BDV-induced early signaling events through the Raf/MEK/ERK cascade are required for BDV spread in cell culture. Leaving important steps of replication to the host is an economic way of reducing the viral genome size and accelerating viral multiplication, but it also clearly creates dependencies that are crucial for the viral life cycle. Thus, the identification of cellular factors which are essential for BDV replication might become an important issue with regard to the understanding of viral biology and for therapeutic intervention.

ACKNOWLEDGMENTS

We thank L. Stitz for critical reading of the manuscript and helpful discussions, Katja Oesterle for expert technical assistance, and Manuela Flüss for providing BDV-293T cells.

The work was supported in part by grants from the Deutsche Forschungsgemeinschaft (to O.P. and S.L.).

REFERENCES

- Alessi, D. R., A. Cuenda, P. Cohen, D. T. Dudley, and A. R. Saltiel. 1995. PD 098059 is a specific inhibitor of the activation of mitogen-activated protein kinase kinase in vitro and in vivo. *J. Biol. Chem.* 270:27489-27494.
- Amsterdam, J. D., A. Winokur, W. Dyson, S. Herzog, F. Gonzalez, R. Rott, and H. Koprowski. 1985. Borna disease virus. A possible etiologic factor in human affective disorders? *Arch. Gen. Psychiatry* 42:1093-1096.
- Benn, J., F. Su, M. Doria, and R. J. Schneider. 1996. Hepatitis B virus HBx protein induces transcription factor AP-1 by activation of extracellular signal-regulated and c-Jun N-terminal mitogen-activated protein kinases. *J. Virol.* 70:4978-4985.
- Bode, L., D. E. Dietrich, R. Stoyloff, H. M. Emrich, and H. Ludwig. 1997. Amantadine and human Borna disease virus in vitro and in vivo in an infected patient with bipolar depression. *Lancet* 349:178-179.
- Bode, L., S. Riegel, H. Ludwig, J. D. Amsterdam, W. Lange, and H. Koprowski. 1988. Borna disease virus-specific antibodies in patients with HIV infection and with mental disorders. *Lancet* 2:689.
- Bode, L., W. Zimmermann, R. Ferszt, F. Steinbach, and H. Ludwig. 1995. Borna disease virus genome transcribed and expressed in psychiatric patients. *Nat. Med.* 1:232-236.
- Bruder, J. T., and I. Kovesdi. 1997. Adenovirus infection stimulates the Raf/MAPK signaling pathway and induces interleukin-8 expression. *J. Virol.* 71:398-404.
- Carbone, K. M., S. A. Rubin, A. M. Sierra-Honigmann, and H. M. Lederman. 1993. Characterization of a glial cell line persistently infected with Borna disease virus (BDV): influence of neurotrophic factors on BDV protein and RNA expression. *J. Virol.* 67:1453-1460.
- Cartier, C., M. Deckert, C. Grangeasse, R. Trauger, F. Jensen, A. Bernard, A. Cozzani, C. Desgranges, and V. Boyer. 1997. Association of ERK2 mitogen-activated protein kinase with human immunodeficiency virus particles. *J. Virol.* 71:4832-4837.
- Chen, W., M. M. Monick, A. B. Carter, and G. W. Hunninghake. 2000. Activation of ERK2 by respiratory syncytial virus in A549 cells is linked to the production of interleukin 8. *Exp. Lung Res.* 26:13-26.
- Cubitt, B., and J. C. de la Torre. 1997. Amantadine does not have antiviral activity against Borna disease virus. *Arch. Virol.* 142:2035-2042.
- DeSilva, D. R., E. A. Jones, M. F. Favata, B. D. Jaffee, R. L. Magolda, J. M. Trzaskos, and P. A. Scherle. 1998. Inhibition of mitogen-activated protein kinase kinase blocks T cell proliferation but does not induce or prevent anergy. *J. Immunol.* 160:4175-4181.
- Duchala, C. S., K. M. Carbone, and O. Narayan. 1989. Preliminary studies on the biology of Borna disease virus. *J. Gen. Virol.* 70:3507-3511.
- Dudley, D. T., L. Pang, S. J. Decker, A. J. Bridges, and A. R. Saltiel. 1995. A synthetic inhibitor of the mitogen-activated protein kinase cascade. *Proc. Natl. Acad. Sci. USA* 92:7686-7689.
- Favata, M. F., K. Y. Horiuchi, E. J. Manos, A. J. Daulerio, D. A. Stradley, W. S. Feeser, D. E. Van Dyk, W. J. Pitts, R. A. Earl, F. Hobbs, R. A. Copeland, R. L. Magolda, P. A. Scherle, and J. M. Trzaskos. 1998. Identification of a novel inhibitor of mitogen-activated protein kinase kinase. *J. Biol. Chem.* 273:18623-18632.
- Ferszt, R., K. P. Kuhl, L. Bode, E. W. Severus, B. Winzer, A. Berghofer, G. Beelitz, B. Brodhun, B. Muller-Oerlinghausen, and H. Ludwig. 1999. Amantadine revisited: an open trial of amantadinesulfate treatment in chronically depressed patients with Borna disease virus infection. *Pharmacopsychiatry* 32:142-147.
- Gonzalez-Dunia, D., B. Cubitt, and J. C. de la Torre. 1998. Mechanism of Borna disease virus entry into cells. *J. Virol.* 72:783-788.
- Gonzalez-Dunia, D., B. Cubitt, F. A. Grasser, and J. C. de la Torre. 1997. Characterization of Borna disease virus p56 protein, a surface glycoprotein involved in virus entry. *J. Virol.* 71:3208-3218.
- Hallensleben, W., M. Zocher, and P. Staeheli. 1997. Borna disease virus is not sensitive to amantadine. *Arch. Virol.* 142:2043-2048.
- Hans, A., S. Syan, C. Crosio, P. Sassone-Corsi, M. Brahim, and D. Gonzalez-Dunia. 2001. Borna disease virus persistent infection activates mitogen-activated protein kinase and blocks neuronal differentiation of PC12 cells. *J. Biol. Chem.* 276:7258-7265.
- Jordan, I., T. Briese, D. R. Averett, and W. I. Lipkin. 1999. Inhibition of Borna disease virus replication by ribavirin. *J. Virol.* 73:7903-7906.
- Kishi, M., Y. Arimura, K. Ikuta, Y. Shoya, P. K. Lai, and M. Kakinuma. 1996. Sequence variability of Borna disease virus open reading frame II found in human peripheral blood mononuclear cells. *J. Virol.* 70:635-640.
- Kliche, S., T. Briese, A. H. Henschen, L. Stitz, and W. I. Lipkin. 1994. Characterization of a Borna disease virus glycoprotein, gp18. *J. Virol.* 68: 6918-6923.
- Ludwig, H., and P. Thein. 1977. Demonstration of specific antibodies in the central nervous system of horses naturally infected with Borna disease virus. *Med. Microbiol. Immunol.* 163:215-226.
- Ludwig, S., K. Engel, A. Hoffmeyer, G. Sithanandam, B. Neufeld, D. Palm, M. Gaestel, and U. R. Rapp. 1996. 3pK, a novel mitogen-activated protein (MAP) kinase-activated protein kinase, is targeted by three MAP kinase pathways. *Mol. Cell. Biol.* 16:6687-6697.
- Malik, T. H., M. Kishi, and P. K. Lai. 2000. Characterization of the P protein-binding domain on the 10-kilodalton protein of Borna disease virus. *J. Virol.* 74:3413-3417.
- Mizutani, T., H. Inagaki, D. Hayasaka, S. Shuto, N. Minakawa, A. Matsuda, H. Kariwa, and I. Takashima. 1999. Transcriptional control of Borna disease virus (BDV) in persistently BDV-infected cells. *Arch. Virol.* 144:1937-1946.
- Narayan, O., S. Herzog, K. Frese, H. Scheefers, and R. Rott. 1983. Pathogenesis of Borna disease in rats: immune-mediated viral ophthalmoneurophthalmopathy causing blindness and behavioral abnormalities. *J. Infect. Dis.* 148: 305-315.
- Pauli, G., and H. Ludwig. 1985. Increase of virus yields and releases of Borna disease virus from persistently infected cells. *Virus Res.* 2:29-33.
- Planz, O., C. Rentzsch, A. Batra, H.-J. Rziba, and L. Stitz. 1998. Persistence of Borna disease virus-specific nucleic acid in the blood of a psychiatric patient. *Lancet* 352:623.
- Planz, O., C. Rentzsch, A. Batra, T. Winkler, M. Buttner, H. J. Rziba, and L. Stitz. 1999. Pathogenesis of Borna disease virus: granulocyte fractions of

psychiatric patients harbor infectious virus in the absence of antiviral antibodies. *J. Virol.* 73:6251–6256.

32. Popik, W., J. E. Hesselgesser, and P. M. Pitha. 1998. Binding of human immunodeficiency virus type 1 to CD4 and CXCR4 receptors differentially regulates expression of inflammatory genes and activates the MEK/ERK signaling pathway. *J. Virol.* 72:6406–6413.
33. Robinson, M. J., and M. H. Cobb. 1997. Mitogen-activated protein kinase pathways. *Curr. Opin. Cell Biol.* 9:180–186.
34. Rodems, S. M., and D. H. Spector. 1998. Extracellular signal-regulated kinase activity is sustained early during human cytomegalovirus infection. *J. Virol.* 72:9173–9180.
35. Rott, R., and H. Becht. 1995. Natural and experimental Borna disease in animals. *Curr. Top. Microbiol. Immunol.* 190:17–30.
36. Rott, R., S. Herzog, B. Fleischer, A. Winokur, J. Amsterdam, W. Dyson, and H. Koprowski. 1985. Detection of serum antibodies to Borna disease virus in patients with psychiatric disorders. *Science* 228:755–756.
37. Schneider, P. A., R. Kim, and W. I. Lipkin. 1997. Evidence for translation of the Borna disease virus G protein by leaky ribosomal scanning and ribosomal reinitiation. *J. Virol.* 71:5614–5619.
38. Schwemmle, M., B. De, L. Shi, A. Banerjee, and W. I. Lipkin. 1997. Borna disease virus P-protein is phosphorylated by protein kinase Cepsilon and casein kinase II. *J. Biol. Chem.* 272:21818–21823.
39. Schwemmle, M., M. Salvatore, L. Shi, J. Richt, C. H. Lee, and W. I. Lipkin. 1998. Interactions of the Borna disease virus P, N, and X proteins and their functional implications. *J. Biol. Chem.* 273:9007–9012.
40. Stitz, L., K. Noske, O. Planz, E. Furrer, W. I. Lipkin, and T. Bilzer. 1998. A functional role for neutralizing antibodies in Borna disease: influence on virus tropism outside the central nervous system. *J. Virol.* 72:8884–8892.
41. Stitz, L., O. Planz, and T. Bilzer. 1998. Lack of antiviral effect of amantadine in Borna disease virus infection. *Med. Microbiol. Immunol.* 186:195–200.
42. Stitz, L., and R. Rott. 1999. Borna disease virus (Bornaviridae), p. 167–173. *In* A. Granoff and R. G. Webster (ed.), *Encyclopedia of virology*. Academic Press, Inc., New York, N.Y.
43. Thiedemann, N., P. Presek, R. Rott, and L. Stitz. 1992. Antigenic relationship and further characterization of two major Borna disease virus-specific proteins. *J. Gen. Virol.* 73:1057–1064.
44. Treisman, R. 1996. Regulation of transcription by MAP kinase cascades. *Curr. Opin. Cell Biol.* 8:205–215.
45. Walker, M. P., I. Jordan, T. Briese, N. Fischer, and W. I. Lipkin. 2000. Expression and characterization of the Borna disease virus polymerase. *J. Virol.* 74:4425–4428.
46. Wehner, T., A. Ruppert, C. Herden, K. Frese, H. Becht, and J. A. Richt. 1997. Detection of a novel Borna disease virus-encoded 10 kDa protein in infected cells and tissues. *J. Gen. Virol.* 78:2459–2466.
47. Wekerle, H., C. Linington, H. Lassmann, and R. Meyermann. 1986. Cellular immune reactivity within the CNS. *Trends Neurosci.* 9:271–277.
48. Wolff, T., R. Pfleger, T. Wehner, J. Reinhardt, and J. A. Richt. 2000. A short leucine-rich sequence in the Borna disease virus p10 protein mediates association with the viral phospho- and nucleoproteins. *J. Gen. Virol.* 81:939–947.
49. Yang, X., and D. Gabuzda. 1998. Mitogen-activated protein kinase phosphorylates and regulates the HIV-1 Vif protein. *J. Biol. Chem.* 273:29879–29887.
50. Yang, X., and D. Gabuzda. 1999. Regulation of human immunodeficiency virus type 1 infectivity by the ERK mitogen-activated protein kinase signaling pathway. *J. Virol.* 73:3460–3466.

LR-3312

Natural Product Letters
Volume 10, pp. 115-118
Reprints available directly from the publisher
Photocopying permitted by license only

© 1997 OPA (Overseas Publishers Association)
Amsterdam B.V. Published in The Netherlands
by Harwood Academic Publishers
Printed in India

ondon) 1988, 238.
14, 154, 273-278.
Am. J. Enol. Vitic.

33.
L.A.; Williams, P.J.

6522.
ol. Vitic. 1990, 41,

rdonner, R.E. J.

41, 1452-1457.
te obtained from a
(, 1992 vintage) an
ac) equipped with
l (solvent system:
tion mode: tail to
further separated
PTFE tubing) and
1.5 mL; elution

anishi, R. *J. Agric.*

x 16 mm; Knauer,
m.
Australia, 1991.

L.A.; Williams, P.J.

429-438.
L.A.; Williams, P.J.

eration-Biotechno-
ubl. Corp.: Carol

phytochemistry 1975,

Food Chem. 1990,

ive, C. In *Progress
ion-Biotechnology*,
Carol Stream, IL,

Phytochem. Anal.

ad Chem. 1994, 42,

ZERUMBONE, AN HIV-INHIBITORY AND CYTOTOXIC SESQUITERPENE OF *Zingiber aromaticum* AND *Z. zerumbet*¹

JIN-RUI DAI, JOHN H. CARDELLINA II*, JAMES B. McMAHON AND
MICHAEL R. BOYD*

Laboratory of Drug Discovery Research and Development, Developmental
Therapeutics Program, Division of Cancer Treatment, Diagnosis and Centers, National
Cancer Institute, Building 1052, Room 121, Frederick, Maryland 21702-1201

(Received 10 January 1997)

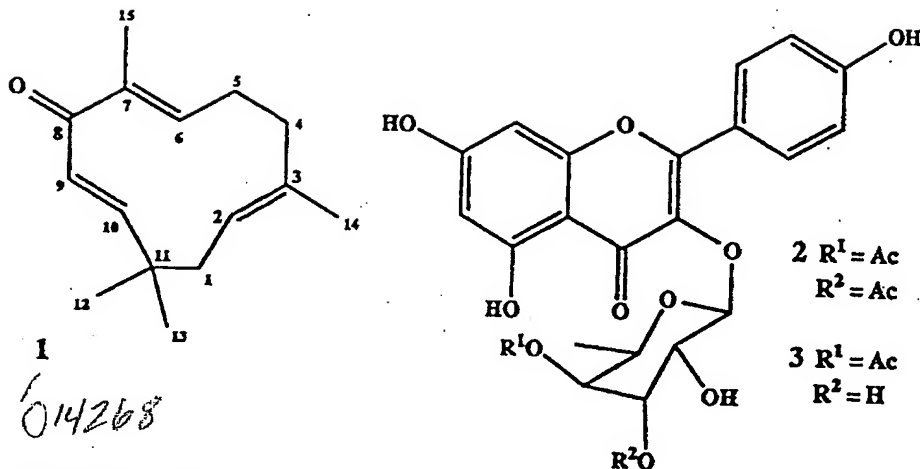
Abstract: Zerumbone and 3",4"-O-diacetylafzelin were isolated from organic extracts of
rhizomes of *Zingiber aromaticum* (Zingiberaceae), and zerumbone and 4"-O-acetylafzelin
were obtained from organic extracts of entire plants of *Z. zerumbet*. Zerumbone exhibited
HIV-inhibitory and cytotoxic activities, while the afzelins were inactive in both assays.

Key Words: HIV-inhibitory, sesquiterpene, zerumbone, *Zingiber*

As part of our screening of natural products extracts for antitumor^{2,3} and anti-HIV⁴
activities, we noted that organic extracts of two species of the genus *Zingiber*, *Z. aromaticum* and *Z. zerumbet*, exhibited similar patterns of both HIV-inhibitory and
cytotoxic activity in the NCI primary screens. While a considerable variety of secondary
metabolites has been reported from this genus,⁵⁻⁹ including reports of cytotoxins,⁸ HIV-
inhibitory activity was heretofore unknown in this genus. Bioassay-guided fractionation
led to isolation of zerumbone 1 as the major antiviral and cytotoxic constituent. Two
known flavonoids (2,3) were also identified and found to be inactive in both assays.

Solvent-solvent partitioning, Sephadex LH-20 gel permeation chromatography and
HPLC, all directed by both the antitumor and anti-HIV primary screens, led to the
isolation of zerumbone, 1, from the hexane and MeOtBu soluble fractions from crude
extracts of both species, while the inactive flavonoids 2 (3,"4"-O-diacetylafzelin) and 3
(4"-O-acetyl afzelin) were obtained from the MeOtBu partition fractions of *Z. aromaticum*
and *Z. zerumbet*, respectively. All three compounds were previously known from *Zingiber*
spp.,⁵⁻⁹ and the spectral data for our compounds matched those in the literature.

— Zerumbone (1) exhibited some anti-HIV cytoprotective activity (EC_{50} 0.04 μ g/mL), as
well as direct cytotoxicity to the host cells (IC_{50} 0.14 μ g/mL) in the National Cancer

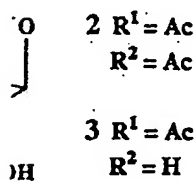
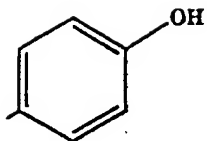


Institute (NCI) primary anti-HIV screen. Cytotoxicity was also reflected in the 60-cell line antitumor screen, with a mean panel GI_{50} of 0.33 $\mu\text{g/mL}$. The volatility of **1** apparently contributed to some inconsistency in assay performance, and its narrow *in vitro* therapeutic index (modest antiviral activity/high cytotoxicity) precluded further consideration as an AIDS-antiviral agent.¹⁰

EXPERIMENTAL:

Collection and Extraction. *Zingiber aromaticum* (Zingiberaceae) was collected in central Java, Indonesia, in November 1988, and *Z. zerumbet* was collected from Panay Island, Philippines, in August 1987. Voucher specimens have been deposited in the Smithsonian Institution, Washington, DC. Dried rhizomes (336 g) of *Z. aromaticum* were ground, then percolated at room temperature in $\text{MeOH}-\text{CH}_2\text{Cl}_2$ (1:1), followed by MeOH . Solvents from the combined organic extracts were removed *in vacuo* to provide a total of 28.24 g (8.4%) of crude organic extract. *Z. zerumbet* (entire plants, 192 g) was extracted using the same procedure to provide a total of 12.10 g (6.3%) of crude organic extract.

Partition and Chromatographic Separation. The organic extract of *Zingiber aromaticum* (5 g) was subjected to a solvent/solvent partitioning protocol to yield hexane



ed in the 60-cell line
ility of **1** apparently
v *in vitro* therapeutic
consideration as an

iceae) was collected
collected from Panay
en deposited in the
Z. aromaticum were
followed by MeOH.
to provide a total of
92 g) was extracted
de organic extract.
extract of *Zingiber*
sol to yield hexane

(2.70 g), MeOtBu (0.968 g), EtOAc (0.687 g) and H₂O (0.595 g) fractions. The HIV-inhibitory hexane fraction (150 mg) was permeated through a Sephadex LH-20 column (2.5 x 85 cm) with CH₂Cl₂-MeOH (2:1); five fractions were obtained. A portion (21 mg) of the HIV-inhibitory fraction C was subjected to HPLC on a C₁₈ column (1 x 25 cm); elution with MeOH-H₂O (4:1) provided **1** (14.1 mg, 23% yield from crude extract, 1.93% from dried rhizome). The HIV-inhibitory MeOtBu fraction (410 mg) was also separated by Sephadex LH-20 gel permeation and C₁₈ HPLC under the same experimental conditions to provide **2** (8.2 mg, 0.49% yield from crude extract, 0.04% from the dried rhizome).

The organic extract of *Z. zerumbet* (2 g) was also subjected to a solvent/solvent partitioning protocol to yield hexane (1.17 g), MeOtBu (0.408 g), EtOAc (0.151 g) and H₂O (0.250 g) fractions. The HIV-inhibitory MeOtBu fraction (220 mg) was permeated through a Sephadex LH-20 column (2.5 x 85 cm) with CH₂Cl₂-MeOH (2:1); seven fractions were obtained. The HIV-inhibitory fraction B (26 mg) was subjected to HPLC on a C₁₈ column (1 x 25 cm); elution with MeOH-H₂O (8:2) provided **1** (12.8 mg, 3% yield from crude extract, 0.19% from entire dried plant). The HIV-inhibitory fraction E (14 mg) was also subjected to HPLC on a cyano-bonded phase column (1 x 25 cm); elution with hexane-*i*-PrOH (3:1) provided **3** (3.8 mg, 0.22% from crude extract, 0.014% from dried entire plant).

Zerumbone (1). HRFABMS *m/z* 219.1741 (calcd for C₁₅H₂₃O, 219.1749); ¹H-NMR (CDCl₃, 500 MHz) δ 6.01 (1H, dd, *J* = 11.5, 2 Hz, H-6), 5.98 (1H, d, 17, H-9), 5.86 (1H, d, 17, H-10), 5.25 (1H, dd, 12, 3, H-2), 2.44 (1H, m, H-5a), 2.34 (2H, m, H-1a, 4a), 2.22 (2H, m, H-4b, 5b), 1.90 (1H, d, 12, H-1b), 1.80 (3H, s, C-13), 1.54 (3H, s, C-12), 1.20 (3H, s, C-15), 1.07 (3H, s, C-14); ¹³C-NMR (CDCl₃, 125 MHz) δ 204.4 (C-8), 160.8 (C-10), 148.8 (C-6), 138.0 (C-7), 136.2 (C-3), 127.2 (C-9), 125.0 (C-2), 42.4 (C-1), 39.5 (C-4), 37.9 (C-11), 29.4 (C-14), 24.4 (C-5), 24.2 (C-15), 15.2 (C-12), 11.8 (C-13); ¹H-NMR (CD₃OD, 500 MHz) δ 6.09 (1H, dd, *J* = 11, 2 Hz, H-6), 5.97 (2H, s, H-9, 10), 5.30 (1H, dd, 12, 3, H-2), 2.51 (1H, m, H-5a), 2.39 (1H, m, H-4a), 2.35 (1H, m, H-1a), 2.25 (2H, m, H-4b, 5b), 1.91 (1H, d, *J* = 12.0 Hz, H-1b), 1.77 (3H, s, C-13),

1.57 (3H, s, C-12), 1.23 (3H, s, C-15), 1.07 (3H, s, C-14); ^{13}C -NMR (CD₃OD, 125 MHz) δ 206.8 (C-8), 163.1 (C-10), 151.1 (C-6), 138.8 (C-7), 137.5 (C-3), 128.0 (C-9), 126.0 (C-2), 43.2 (C-1), 40.2 (C-4), 38.7 (C-11), 29.7 (C-14), 25.3 (C-5), 24.4 (C-15), 15.2 (C-12), 11.7 (C-13).

3",4"-O-Diacetylafzelin (2). $[\alpha]_D$ -217° (c 0.24, MeOH). HRFABMS *m/z* 517.1346 (Calcd for C₂₂H₂₂O₁₂, 517.1346).

4"-O-Acetylafzelin (3). $[\alpha]_D$ -158° (c 0.3, MeOH); HRFABMS *m/z* 475.1245 (Calcd for C₂₁H₂₂O₁₁, 475.1240).

REFERENCES:

1) Part 37 in the series HIV-Inhibitory Natural Products; for part 36, see Hallock, Y.F.; Cardellina II, J.H.; Gulakowski, R.J.; McMahon, J.B.; Schäffer, M.; Stahl, M.; Bringmann, G.; François, G.; Boyd, M. *J. Nat. Prod.*, submitted.

2) Monks, A.; Scudiero, D.; Skehan, P.; Shoemaker, R.; Paull, K.; Vistica, D.; Hose, C.; Langley, J.; Cronise, P.; Vaigro-Wolff, A.; Gray-Goodrich, M.; Campbell, H.; Boyd, M. *J. Natl. Cancer Inst.*, 1991, **83**, 757-766.

3) Boyd, M.R.; Paull, K.D. *Drug Dev. Res.* 1995, **34**, 91-109.

4) Weislow, O.S.; Kiser, R.; Fine, D.L.; Bader, J.; Shoemaker, R.H.; Boyd, M.R. *J. Natl. Cancer Inst.*, 1989, **81**, 577-586.

5) Dev, S. *Tetrahedron Lett.* 1960, **8**, 171-180.

6) Dev., S.; Anderson, J.E.; Cormier, V.; Damodaran, N.P.; Roberts, J.D. *J. Am. Chem. Soc.* 1968, **90**, 1246-1248.

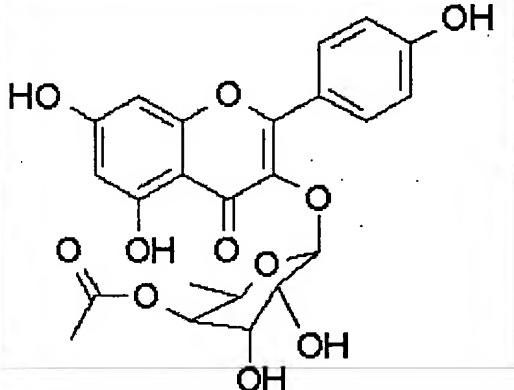
7) Damodaran, N.P.; Dev, S. *Tetrahedron Lett.* 1965, **24**, 1977-1981.

8) Matthes, H.W.; Luu, B.; Ourisson, G. *Phytochemistry* 1980, **19**, 2643-2650.

9) Masuda, T.; Jitoe, A.; Kato, S.; Nakatani, N. *Phytochemistry* 1991, **30**, 2391-2392.

—10) We thank G. Cragg and D.D. Soejarto (collections), T. McCloud (extractions), G. Gray (mass spectral data) and A. Monks and D. Scudiero (primary antitumor screening).

Natural Product without Anti-HIV and Antitumor Activity

	Name 4''-O-Acetylafzelin
Molecular Formula C₂₃H₂₂O₁₁	NSC 703082
Chemical Class Flavonoid glycoside	Source: <i>Zingiber aerumbet</i> [N22189, Q66O7604]]
Discovery Type Known Compound	Reference

Molecular Targets Development Program, CCR, NCI

**This Page is Inserted by IFW Indexing and Scanning
Operations and is not part of the Official Record**

BEST AVAILABLE IMAGES

Defective images within this document are accurate representations of the original documents submitted by the applicant.

Defects in the images include but are not limited to the items checked:

- BLACK BORDERS**
- IMAGE CUT OFF AT TOP, BOTTOM OR SIDES**
- FADED TEXT OR DRAWING**
- BLURRED OR ILLEGIBLE TEXT OR DRAWING**
- SKEWED/SLANTED IMAGES**
- COLOR OR BLACK AND WHITE PHOTOGRAPHS**
- GRAY SCALE DOCUMENTS**
- LINES OR MARKS ON ORIGINAL DOCUMENT**
- REFERENCE(S) OR EXHIBIT(S) SUBMITTED ARE POOR QUALITY**
- OTHER: _____**

IMAGES ARE BEST AVAILABLE COPY.

As rescanning these documents will not correct the image problems checked, please do not report these problems to the IFW Image Problem Mailbox.